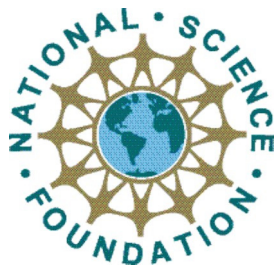




Sonora 2008 Field Campaign



EL SABER DE MIS HIJOS
HARA MI GRANDEZA

A U.S.-Mexico Collaboration on
Hydrological Studies of the North
American Monsoon



TABLE OF CONTENTS

<u>List Of Figures/Illustrations</u>	<u>5</u>
<u>List Of Tables</u>	<u>7</u>
<u>Executive Summary</u>	<u>8</u>
<u>Calendar Of Events</u>	<u>11</u>
<u>Tentative Field Campaign Schedule</u>	<u>12</u>
<u>Study Site: Location And Features</u>	<u>245</u>
<u>Experiments: Overview And Protocol</u>	<u>28</u>
<u>Overview Of Experiments</u>	<u>29</u>
<u>Experiment 1: Isotopic Partitioning Of Evapotranspiration – Rayon Tower</u>	<u>30</u>
<u>Experiment 2: Shrub Sapwood Allometrics And Stand Structural Characteristics – Dry Scrubland, Rayon Tower</u>	<u>39</u>
<u>Experiment 3: Daily Soil Moisture / Temperature Sampling Plots – Rayon Tower</u>	<u>42</u>
<u>Experiment:4 Eddy Covariance Tower Installation/Operation - Cucurpe</u>	<u>48</u>
<u>Experiment 5: Hydrometeorological Station Installation (10) Including Calibration/Soil Sampling - Rio Sonora/San Miguel Basin</u>	<u>73</u>
<u>Static/Dynamic Calibration Of Tipping Bucket Rain Gauges - Rio Sonora/San Miguel</u>	<u>89</u>
<u>Soil Sampling</u>	<u>94</u>
<u>Experiment 6: Flux Measurements Using Df Scintillometer - Installation And Operation – Rio San Miguel</u>	<u>95</u>
<u>Experiment 7: Water Source Characterization Using Major Anions And Isotopes</u>	<u>103</u>
<u>Experiment 8: Soil Surveying</u>	<u>105</u>
<u>Appendix</u>	<u>107</u>
<u>Appendix 1: Ecosystems And Main Plant Species Of The San Miguel Basin</u>	<u>108</u>
<u>Appendix 2: Vegetation Transects Map – Rayon Tower (Data From 2007 Campaign)</u>	<u>117</u>
<u>Appendix 3: Vegetation Cover By Transect (Data From 2007 Campaign)</u>	<u>119</u>
<u>Appendix 4: Photos Of Soil Pit Location (From Sonora Campaign 2007)</u>	<u>121</u>
<u>Appendix 5: Soil Data (From Sonora 2007 Campaign)</u>	<u>130</u>
<u>Appendix 6: Soil Properties Recording Form</u>	<u>135</u>
<u>Appendix 7: Maps Of Sierra Los Locos</u>	<u>137</u>
<u>Appendix 8: Publications</u>	<u>163</u>

<u>Appendix 9: Desert Survival Primer</u>	<u>239</u>
<u>Appendix 10: Medical Care Services</u>	<u>254</u>
<u>Appendix 11: Driving Tips</u>	<u>258</u>
<u>Appendix 12: Safety Considerations When Driving On Rural Roads</u>	<u>259</u>
<u>Appendix 13: CSAT3 Azimuth</u>	<u>264</u>
<u>Appendix 14: Equipment Lists</u>	<u>266</u>
<u>Appendix 15: List Of Participants</u>	<u>274</u>
<u>Appendix 16: Moisture Meter Manual</u>	<u>276</u>
<u>Appendix 17: GPS Start up Manual</u>	<u>279</u>

LIST OF FIGURES/ILLUSTRATIONS

Figure 1: Overall study site map.....	25
Figure 2: Overall land cover map	26
Figure 3: Overall topography/hillshade map	27
Figure 4: Location of the Rayon Eddy Covariance Tower	30
Figure 5: Map of Rayon Tower and Surrounding Sampling Sites.....	31
Figure 6: An example Keeling plot.....	33
Figure 7: Setting Up Vapor Trapping System	34
Figure 8: Moisture Will Be Condensed with an Ethanol/Liquid Nitrogen Mixture.....	35
Figure 9: The vapor collection setup	36
Figure 10: Vials of leaves, stems and soils samples	37
Figure 11: Map of sampling plots.....	42
Figure 12: Some of the equipment used to estimate soil moisture and soil temperature.	44
Figure 13: Example of a sampling plot. Plot dimensions are 1 m x 1 m.....	45
Figure 14: Soil moisture measurements using theta probe.	46
Figure 15: Potential New Tower Location.....	49
Figure 16: Potential New Tower Location.....	50
Figure 17: Tower Base and Anchor Layout.....	54
Figure 18: Tower Base Foundation.....	55
Figure 19: Concrete Mounting Base	56
Figure 20: Anchor Installation	56
Figure 21: Installation of Guy Wires to the Tower.....	57
Figure 22: Turnbuckle Installation.....	57
Figure 23: Tower Crossarm	58
Figure 24: Ground Rod, Clamp & Tower Grounding Installation.....	59
Figure 25: LI-7500 Mounted Under CSAT3	61
Figure 26: LI-7500 Mounted Behind CSAT3.....	61
Figure 27: LI-7500 Electronics Box Mounting Hardware.....	62
Figure 28: CSAT3 Electronics Box	62
Figure 29: CSAT3 & LI-7500 Electronics Box	62
Figure 30: HMP45C Radiation Shield Mounting,	63
Figure 31: Partial emplacement of the HFP01SC, the TCAV and CS616.	63
Figure 32: Texas Electronics Rain Gage Installation	65
Figure 33: CMP3 Pyranometer and Mounting Stand Installation	66
Figure 34: CNR2 and Mount Installed to Mounting Arm	67
Figure 35: Solar Panel Electrical J-Box.....	67
Figure 36: Enclosure Mounting	68
Figure 37: Parallel Solar Panel Wiring.....	68
Figure 38: Parallel Battery Wiring.....	69
Figure 39: Charge Controller Wiring.....	69
Figure 40: Parallel Battery Wiring.....	70
Figure 41: A Neatly Organized Enclosure.....	70
Figure 42: Datalogger Wiring Diagram.....	71
Figure 43: Enclosure Supply Kit.....	72
Figure 44: Map of New Station Points	74

Figure 45: Map of SITE 160.....	75
Figure 46: Map of SITE 161.....	76
Figure 47: Map of SITE 162.....	77
Figure 48: Map of 163 to 165.....	78
Figure 49: Map of SITE 166.....	79
Figure 50: Map of SITE 167.....	80
Figure 51: Map of SITE 168.....	81
Figure 52: Map of SITE 169.....	82
Figure 53: Installation of Metal Pipes in the Field.....	83
Figure 54: Fixation of the enclosure to the post.....	83
Figure 55: Solar panel Installation.....	84
Figure 56: Battery connections.....	84
Figure 57: Solar panel connection in to the datalogger.....	85
Figure 58: Stevens Hydra Probe Model SDI-12.....	85
Figure 59: TR-525 Tipping Bucket Rain Gauge.....	86
Figure 60: Wiring connections for Hydra probe SDI-12.....	87
Figure 61: Wiring connections 6”diameter rain gauge.....	87
Figure 62: Vertical placement of sensors.....	88
Figure 63: Static Calibration for TB using a Burette.....	90
Figure 64: The Texas Electronics model TE525.....	91
Figure 65: The Hydrological Services model TB3-0.01-P.....	91
Figure 66: Allen Wrench adjustment for TB calibration procedure.....	92
Figure 67: Setup and time measurement during the dynamic calibration procedure.....	93
Figure 68: Spatial and temporal scales of satellite remote sensing measurement.....	95
Figure 69: Two Large Aperature Scintillometer.....	96
Figure 70: Graph of sensible heat flux measurements from three LASs.....	96
Figure 71: Footprint weighting function (color) for a LAS transect.....	98
Figure 72: SEBAL-Landsat map of sensible heat fluxes, Rio Grande New Mexico.....	98
Figure 73: Location of Soil Pits.....	105

LIST OF TABLES

Table 1: Rayon Tower Plot coordinates.....	47
Table 2: Coordinates of new stations in Rio Sonora/San Miguel basin	73

EXECUTIVE SUMMARY

The Sonora 2008 field campaign is an essential component of the research program stemming from the funded proposal 'A US-Mexico Collaboration on Hydrological Studies of the North American Monsoon: A Synthesis of Field Experiments, Remote Sensing, and Hydrological Modeling'. This proposal aims to address the pressing need for binational studies that properly characterize the spatial and temporal variability in hydrologic variables such as precipitation, soil moisture, and streamflow around the Sonora region, where the summer monsoon can account for up to 70% of the annual rainfall in the region. This characterization seeks to address an identified gap in our current understanding of monsoon hydrology by integrating ground observations, remote sensing, and hydrologic modeling in a semiarid, mountainous watershed of northern Sonora, México. Hence, the major scientific objectives are to quantify the spatiotemporal variability of hydrologic variables, to estimate the uncertainty of remotely-sensed hydrologic variables such as rainfall and soil moisture through field validation, and to synthesize the observational uncertainty with a hydrologic model. The research program includes various components that are directly addressed by this field campaign: (a) a field program in México for instrument deployment and data collection, (b) research training for undergraduate students prior to and after the field study, and (c) mentoring activities to promote hands-on, team-based learning in a field setting.

The campaign has many participating professors, scientists, and students from different institutions/universities in the United States and Mexico. The 'Tentative Field Campaign Schedule' section provides an overview and detailed glimpse into the experiments and activities planned during this campaign. There are eight experiments that will be done during this campaign. The experimental area includes the Sonora and San Miguel basins. Some of the experiments near Rayón are focused around an eddy covariance tower station located in the San Miguel basin with daily measurements of rain and soil moisture/temperature. Three experiments will be performed in the vicinity of this tower: (a) the daily soil moisture/temperature measurements at multiple depths at the corners and the center of sampling plots located at the 25 grid points of a square grid configuration around the tower, (b) an evapotranspiration flux partitioning experiment at the tower involving isotope measurements on soil and evapotranspiration flux samples, and (c) tree sampling for sapflow allometric relations.

Other experiments taking place in the Rio Sonora/San Miguel basins are: (a) the installation and operation of an eddy covariance tower in an oak forest area, (b) the installation/calibration of 10 new tipping bucket rain gauge stations with soil moisture/temperature sensors in the Rio Sonora/San Miguel basins and surface soil sampling, (c) basin water characterization of water sources in semi-arid regions using major anion and isotope measurements over groundwater, runoff, precipitation and streamflow components, (d) flux measurements using a DF scintillometer, and (e) soil surveying of Sierra Los Locos basin.

EXECUTIVE SUMMARY (CONTINUED)

The Sonora 2008 Campaign has a range of experiments that provide the participating students the benefit of working in different teams. Day-to-day rotation among these teams will give the students a chance to work with different scientists and get a diversely rich exposure to different aspects of field hydrology. This experience is expected to help all the participants in the future to interact inter-culturally (or in any other framework) in a global scientific context.

CALENDAR OF EVENTS

JUNE / JULY 2008						
SUNDAY	MONDAY	TUESDAY	WEDNESDAY	THURSDAY	FRIDAY	SATURDAY
						28 -NMT depart to Hermosillo
29 -NMT depart to Hermosillo	30 Meeting at UNISON - all participants	1 Travel to Rayon	2 Begin Sonora IRES 2008 Campaign	3	4	5 -Enrico Yopez to depart to Hermosillo -Jan Kleissl arrives
6	7	8	9	10	11	12 FREE DAY! 😊
13	14 -Lissette de la Cruz arrives from U of A	15 -Bruce Harrison arrives in Hermosillo -Jan Kleissl departs	16	17	18	19 End of Campaign, depart Rayon

TUESDAY, July 1, 2008

8:00 am - 10:00 am	Breakfast in Hotel Kino and prepare any last details/purchases for departure to Rayon		
10:00 am - 11:00 pm	Meet at Hotel Kino Lobby for departure. <u>(Please be early and ready to leave at 10am)</u> Buy groceries and continue to Rayon		
11:00 pm - 1:30 pm	Travel to Rayon		
1:30 pm - 2:30 pm	Pre-Field Campaign Preparation	Unpack, settle in at house in Rayon	
2:30 pm - 5:30 pm		Tour of Rayon Tower area for students. Explanation of experiments to go on around tower-Enrico Yepez, Enrique Vivoni	
6:00 pm - 8:00 pm		Dinner at Local Rayon Restaurant	
8:00 pm - 10:00 pm		-Prepare equipment/vehicles for field campaign in the morning. -Organize students into experiments to participate in for the next day. -Read over experimental procedure you will do for the next day.	<u>PRESENTATION: LUIS MENDEZ</u>

□ = total number of students working in field each day

WEDNESDAY, July 2, 2008

5:30 am - 6:30 am	Breakfast & prepare, pack, and load vehicles for field experiments.			
6:30 am - 7:30 am	Travel to experiment location			
7:30 am - 6:00 pm	Field Campaign	Field Work		
		<u>Isotopic Condition of Water-</u> Enrico Yepez (+2 students)	<u>Installation of Eddy Covariance Tower in Oak region-</u> -Pick location and begin to dig for base installation Luis Mendez / Agustin Morua Robles / Chris Watts / Julio Rodriguez / (+3 students)	<u>Establish Rayon Tower Sampling Plots - Soil Temperature and Moisture-</u> Enrique Vivoni / Jaime Garatuza / Laura Alvarez (+2 teams of 2) (+3 students) ↓ <u>Input Tower Sampling Data into Laptops at House</u>
7:00 pm - 10:00 pm		Dinner and prepare for field campaign in the morning.	<u>STUDENT ACTIVITY: DATA ANALYSIS 1 - SOIL MOISTURE</u>	
			8	

THURSDAY, July 3, 2008

5:30 am - 6:30 am	Breakfast & prepare, pack, and load vehicles for field experiments.			
6:30 am - 7:30 am	Travel to experiment location			
7:30 am - 6:00 pm	Field Work			
	Field Campaign	<u>Isotopic Condition of Water-</u> Enrico Yopez (+2 students)	<u>Installation of Eddy Covariance Tower in Oak region-</u> -Base construction and concrete fill Luis Mendez / Agustin Morua Robles / Chris Watts / Julio Rodriguez (+3 students)	<u>Tower Sampling Plots - Soil Temperature and Moisture -</u> Enrique Vivoni / Jaime Garatuza / Laura Alvarez (+2 teams of 2) (+3 students)
				↓ <u>Input Tower Sampling Data into Laptops at House</u>
7:00 pm - 10:00 pm		Dinner and prepare for field campaign in the morning.	PRESENTATION: ENRICO YEPEZ STUDENT ACTIVITY: DATA ANALYSIS 1 - SOIL MOISTURE RESULTS	8

FRIDAY, July 4, 2008

5:30 am - 6:30 am	Breakfast & prepare, pack, and load vehicles for field experiments.				
6:30 am - 7:30 am	Travel to experiment location				
7:30 am - 6:00 pm	Field Work				
	Field Campaign	<u>Isotopic Condition of Water-</u> Enrico Yopez (+2 students)	<u>Tree Sampling for Sap flow Allometric Relations-</u> Enrico Yopez (+1 student)	<u>Hydrometeorological Station Installation (10) - Rio Sonora/San Miguel Basins</u> Luis Mendez / Agustin Morua Robles (+2 teams) (+2 students) *NOTE: stay overnight	<u>Tower Sampling Plots - Soil Temperature and Moisture -</u> - Chris Watts / Julio Rodriguez / Enrique Vivoni / Jaime Garatuza / Laura Alvarez (+2 teams of 2) (+3 students)

					<u>Input Tower Sampling Data into Laptops at House</u>		
7:00 pm - 10:00 pm		Dinner and prepare for field campaign in the morning.					8

SATURDAY, July 5, 2008

5:30 am - 6:30 am	Breakfast & prepare, pack, and load vehicles for field experiments.						
6:30 am - 7:30 am	Travel to experiment location						
7:30 am - 6:00 pm		Field Work					
	Field Campaign	<u>Isotopic Condition of Water</u> - Enrico Yepez to depart (+2 students)	<u>Tree Sampling for Sap flow Allometric Relations</u> - Enrico Yepez to depart (+1 student)	<u>Hydrometeorological Station Installation (10) - Rio Sonora/San Miguel Basins</u> Luis Mendez / Agustin Morua Robles (+2 teams) (+2 students) *NOTE: stay overnight	<u>Tower Sampling Plots - Soil Temperature and Moisture</u> - Chris Watts / Julio Rodriguez / Enrique Vivoni / Jaime Garatuza / Laura Alvarez (+2 teams of 2) (+3 students)		
					<u>Input Tower Sampling Data into Laptops at House</u>		
7:00 pm - 10:00 pm		Dinner and prepare for field campaign in the morning.			<u>PRESENTATION: ENRIQUE VIVONI</u>		8

SUNDAY, July 6, 2008

5:30 am - 6:30 am	Breakfast & prepare, pack, and load vehicles for field experiments.						
6:30 am - 7:30 am	Travel to experiment location						
7:30 am - 6:00 pm	Ca mp	Field Work					

		<p><u>Isotopic Condition of Water / Tree Sampling-</u> (+3 students)</p>	<p><u>DF Scintillometer Installation and Operation - Rio San Miguel-</u> Chris Watts / Jan Kliessl (+3 students)</p>	<p><u>Hydrometeorological Station Installation (10) - Rio Sonora/San Miguel Basins</u> Luis Mendez / Agustin Morua Robles (+2 teams) (+2 students) *NOTE: stay overnight</p>	<p><u>Tower Sampling Plots - Soil Temperature and Moisture -</u> Chris Watts / Julio Rodriguez / Enrique Vivoni / Jaime Garatuza / Laura Alvarez (+2 teams of 2) (+3 students)</p> <p>↓</p> <p><u>Input Tower Sampling Data into Laptops at House</u></p>	
7:00 pm - 10:00 pm		Dinner and prepare for field campaign in the morning.				8

MONDAY, July 7, 2008

5:30 am - 6:30 am	Breakfast & prepare, pack, and load vehicles for field experiments.					
6:30 am - 7:30 am	Travel to experiment location					
7:30 am - 6:00 pm		Field Work				
	Field Campaign	<p><u>DF Scintillometer Installation and Operation - Rio San Miguel-</u> Chris Watts / Jan Kliessl (+3 students)</p>	<p><u>Installation of Eddy Covariance Tower in Oak region-</u> -Finish installation Luis Mendez / Agustin Morua Robles (+3 students)</p>	<p><u>Tower Sampling Plots - Soil Temperature and Moisture -</u> Enrique Vivoni / Jaime Garatuza / Laura Alvarez (+2 teams of 2) (+3 students)</p> <p>↓</p> <p><u>Input Tower Sampling Data into Laptops at House</u></p>		
7:00 pm - 10:00 pm		Dinner and prepare for field campaign in the morning.		<u>STUDENT ACTIVITY: DATA ANALYSIS 2 - RAINFALL</u>		9

TUESDAY, July 8, 2008

5:30 am - 6:30 am	Breakfast & prepare, pack, and load vehicles for field experiments.	
6:30 am - 7:30 am	Travel to experiment location	
7:30 am - 6:00 pm	Ca mp	Field Work

		<p><u>DF Scintillometer Installation and Operation - Rio San Miguel-</u> Chris Watts / Jan Kliessl (+3 students)</p>	<p><u>Installation of Eddy Covariance Tower in Oak region-</u> -Finish installation Luis Mendez / Agustin Morua Robles (+3 students)</p>	<p><u>Tower Sampling Plots - Soil Temperature and Moisture -</u> Enrique Vivoni / Jaime Garatuza / Laura Alvarez (+2 teams of 2) (+3 students)</p> <p style="text-align: center;">↓</p> <p><u>Input Tower Sampling Data into Laptops at House</u></p>	
7:00 pm - 10:00 pm		Dinner and prepare for field campaign in the morning.		<p><u>PRESENTATION: Agustin Morua Robles</u></p> <p><u>STUDENT ACTIVITY: DATA ANALYSIS 2- RAINFALL RESULTS</u></p>	9

WEDNESDAY, July 9, 2008

5:30 am - 6:30 am	Breakfast & prepare, pack, and load vehicles for field experiments.				
6:30 am - 7:30 am	Travel to experiment location				
7:30 am - 6:00 pm		Field Work			
	Field Campaign	<p><u>DF Scintillometer Installation and Operation - Rio San Miguel-</u> Chris Watts / Jan Kliessl (+3 students)</p>	<p><u>Hydrometeorological Station Installation (10) - Rio Sonora/San Miguel Basins</u> Luis Mendez / Agustin Morua Robles (+2 teams) (+3 students)</p> <p>*NOTE: may have to stay overnight</p>	<p><u>Tower Sampling Plots - Soil Temperature and Moisture -</u> Enrique Vivoni / Jaime Garatuza / Laura Alvarez (+2 teams of 2) (+3 students)</p> <p style="text-align: center;">↓</p> <p><u>Input Tower Sampling Data into Laptops at House</u></p>	
7:00 pm - 10:00 pm		Dinner and prepare for field campaign in the morning.			9

THURSDAY, July 10, 2008


5:30 am - 6:30 am	Breakfast & prepare, pack, and load vehicles for field experiments.				
6:30 am - 7:30 am	Travel to experiment location				
7:30 am - 6:00 pm	Ca mp	Field Work			

		<p align="center"><u>DF Scintillometer Installation and Operation - Rio San Miguel-</u> Chris Watts / Jan Kliessl (+3 students)</p>	<p align="center"><u>Hydrometeorological Station Installation (10) - Rio Sonora/San Miguel Basins</u> Luis Mendez / Agustin Morua Robles (+2 teams) (+3 students)</p> <p align="center">*NOTE: may have to stay overnight</p>	<p align="center"><u>Tower Sampling Plots - Soil Temperature and Moisture -</u> Enrique Vivoni / Jaime Garatuza / Laura Alvarez (+2 teams of 2) (+3 students)</p> <p align="center">↓</p>	<p align="center"><u>Input Tower Sampling Data into Laptops at House</u></p>	
7:00 pm - 10:00 pm		Dinner and prepare for field campaign in the morning.				9

FRIDAY, JULY 11, 2008

5:30 am - 6:30 am	Breakfast & prepare, pack, and load vehicles for field experiments.						
6:30 am - 7:30 am	Travel to experiment location						
7:30 am - 6:00 pm	Field Campaign	Field Work					
		<p align="center"><u>DF Scintillometer Installation and Operation - Rio San Miguel-</u> Chris Watts / Jan Kliessl (+3 students)</p>	<p align="center"><u>Hydrometeorological Station Installation (10) - Rio Sonora/San Miguel Basins</u> Luis Mendez / Agustin Morua Robles (+2 teams) (+3 students)</p> <p align="center">*NOTE: may have to stay overnight</p>	<p align="center"><u>Tower Sampling Plots - Soil Temperature and Moisture -</u> Enrique Vivoni / Jaime Garatuza / Laura Alvarez (+2 teams of 2) (+3 students)</p> <p align="center">↓</p>	<p align="center"><u>Input Tower Sampling Data into Laptops at House</u></p>		
7:00 pm - 10:00 pm		Dinner and prepare for field campaign in the morning.	<p align="center"><u>PRESENTATION: JAN KLISSL</u></p>			9	

SATURDAY, JULY 12, 2008

9:00 am - 9:00 pm	 <p align="center"><u>FREE DAY!!! TRAVEL TO THE BEACH ~ BAHIA DE KINO ☺</u></p>
-------------------	---

SUNDAY, JULY 13, 2008

5:30 am - 6:30 am	Breakfast & prepare, pack, and load vehicles for field experiments.	
6:30 am - 7:30 am	Travel to experiment location	
7:30 am - 6:00 pm	Ca mp	Field Work

		<p>DF Scintillometer Installation and Operation - Rio San Miguel- Chris Watts / Jan Kliesl (+3 student)</p>	<p>EQUIPMENT ORGANIZATION / DATA RECORDING / STUDENT DATA ACTIVITIES (+3 students)</p>	<p>Tower Sampling Plots - Soil Temperature and Moisture - Enrique Vivoni / Jaime Garatuza / Laura Alvarez (+2 teams of 2) (+3 students)</p> <p>↓</p> <p>Input Tower Sampling Data into Laptops at House</p>	
7:00 pm - 10:00 pm		Dinner and prepare for field campaign in the morning.		<p>STUDENT ACTIVITY: DATA ANALYSIS 3 - TOWER FLUX</p>	9

MONDAY, JULY 14, 2008

5:30 am - 6:30 am	Breakfast & prepare, pack, and load vehicles for field experiments.				
6:30 am - 7:30 am	Travel to experiment location				
7:30 am - 6:00 pm		Field Work			
	Field Campaign	<p>DF Scintillometer Installation and Operation - Rio San Miguel- Chris Watts / Jan Kliesl (+3 students)</p>	<p>EQUIPMENT ORGANIZATION / DATA RECORDING / STUDENT DATA ACTIVITIES (+3 students) Rotate students</p>	<p>Tower Sampling Plots - Soil Temperature and Moisture - Enrique Vivoni / Jaime Garatuza / Laura Alvarez (+2 teams of 2) (+3 students)</p> <p>↓</p> <p>Input Tower Sampling Data into Laptops at House</p>	
7:00 pm - 10:00 pm			Dinner and prepare for field campaign in the morning.		<p>PRESENTATION: ENRIQUE VIVONI</p> <p>STUDENT ACTIVITY: DATA ANALYSIS 3- TOWER FLUX RESULTS</p>

TUESDAY, JULY 15, 2008

5:30 am - 6:30 am	Breakfast & prepare, pack, and load vehicles for field experiments.				
6:30 am - 7:30 am	Travel to experiment location				
7:30 am - 6:00 pm	Ca mp	Field Work			

		<p><u>Set-up Sampler for Streamflow-</u> Lissette de la Cruz -more students only today to observe experimental procedure (+5 students)</p>	<p><u>Tower Sampling Plots - Soil Temperature and Moisture -</u> Enrique Vivoni / Jaime Garatuza / Laura Alvarez (+3 students)</p> <p>↓</p> <p><u>Input Tower Sampling Data into Laptops at House</u></p>		
7:00 pm - 10:00 pm		Dinner and prepare for field campaign in the morning.		<p><u>STUDENT ACTIVITY: DATA ANALYSIS 4 - REMOTE SENSING</u></p>	9

WEDNESDAY, JULY 16, 2008

5:30 am - 6:30 am	Breakfast & prepare, pack, and load vehicles for field experiments.				
6:30 am - 7:30 am	Travel to experiment location				
7:30 am - 6:00 pm		Field Work			
	Field Campaign	<p><u>Set-up Sampler for Streamflow-</u> Lissette de la Cruz (+1 student)</p>	<p><u>Soil Surveying-</u> Bruce Harrison / Jose Luis Zarate (+4 students)</p>	<p><u>Tower Sampling Plots - Soil Temperature and Moisture -</u> Enrique Vivoni / Jaime Garatuza / Laura Alvarez (+2 teams of 2) (+3 students)</p> <p>↓</p> <p><u>Input Tower Sampling Data into Laptops at House</u></p>	
7:00 pm - 10:00 pm		Dinner and prepare for field campaign in the morning.		<p><u>PRESENTATION: CHRIS WATTS</u></p> <p><u>STUDENT ACTIVITY: DATA ANALYSIS 4 - REMOTE SENSING RESULTS</u></p> <p><u>STUDENTS: FINAL PRESENTATION TOPIC/GROUP ASSIGNMENT</u></p>	8

THURSDAY, JULY 17, 2008


5:30 am - 6:30 am	Breakfast & prepare, pack, and load vehicles for field experiments.			
6:30 am - 7:30 am	Travel to experiment location			
7:30 am - 6:00 pm	Field Campaign	Field Work		
		<u>Set-up Sampler for Streamflow</u> Lissette de la Cruz (+1 student)	<u>DF Scintillometer Installation and Operation - Rio San Miguel</u> Chris Watts / Jan Kliessl (+3 students)	<u>Soil Surveying</u> Bruce Harrison / Jose Luis Zarate (+2 students)
			<u>Input Tower Sampling Data into Laptops at House</u>	
7:00 pm - 10:00 pm	Dinner and prepare for field campaign in the morning.		<u>STUDENTS: WORK ON FINAL PRESENTATION</u>	9

FRIDAY, JULY 18, 2008

5:30 am - 6:30 am	Breakfast & prepare, pack, and load vehicles for field experiments.			
6:30 am - 7:30 am	Travel to experiment location			
7:30 am - 6:00 pm	Field Campaign	Field Work		
		<u>Set-up Sampler for Streamflow</u> Lissette de la Cruz (+1 student)	<u>DF Scintillometer Installation and Operation - Rio San Miguel</u> Chris Watts / Jan Kliessl (+3 students)	<u>Soil Surveying</u> Bruce Harrison / Jose Luis Zarate (+2 students)
			<u>Input Tower Sampling Data into Laptops at House</u>	

7:00 pm - 10:00 pm	Dinner and prepare for field campaign in the morning.	PRESENTATION: Lissette de la Cruz STUDENTS: WORK ON FINAL PRESENTATION	9
--------------------	---	---	---

SATURDAY, JULY 19, 2008

5:30 am - 6:30 am	Breakfast & prepare, pack, and load vehicles for field experiments.				
6:30 am - 7:30 am	Travel to experiment location				
7:30 am - 6:00 pm	Field Work				
	Field Campaign	<u>Set-up Sampler for Streamflow-</u> Lissette de la Cruz (+1 student)	<u>DF Scintillometer Installation and Operation - Rio San Miguel-</u> Chris Watts / Jan Kliessl (+3 students)	<u>Soil Surveying-</u> Bruce Harrison / Jose Luis Zarate (+2 students)	<u>Tower Sampling Plots - Soil Temperature and Moisture -</u> Enrique Vivoni / Jaime Garatuza / Laura Alvarez (+2 teams of 2) (+3 students)
		<u>Input Tower Sampling Data into Laptops at House</u>			
7:00 pm - 10:00 pm	<u>-FINAL STUDENT PRESENTATIONS-</u> <u>-COMPLETION OF CAMPAIGN-</u> -Dinner party and prepare for departure from Rayon-				

SUNDAY, JULY 20, 2008

9:00 am - 9:00 pm	<u>End of Campaign</u> -Gather all Equipment -Clean House <u>Leave Rayon, and Return Home</u>
-------------------	--

STUDY SITE:
LOCATION AND FEATURES

1. STUDY SITE

- a) Location of San Miguel and Sonora basins
- b) Regional stations
- c) Sierra de los Locos Basin

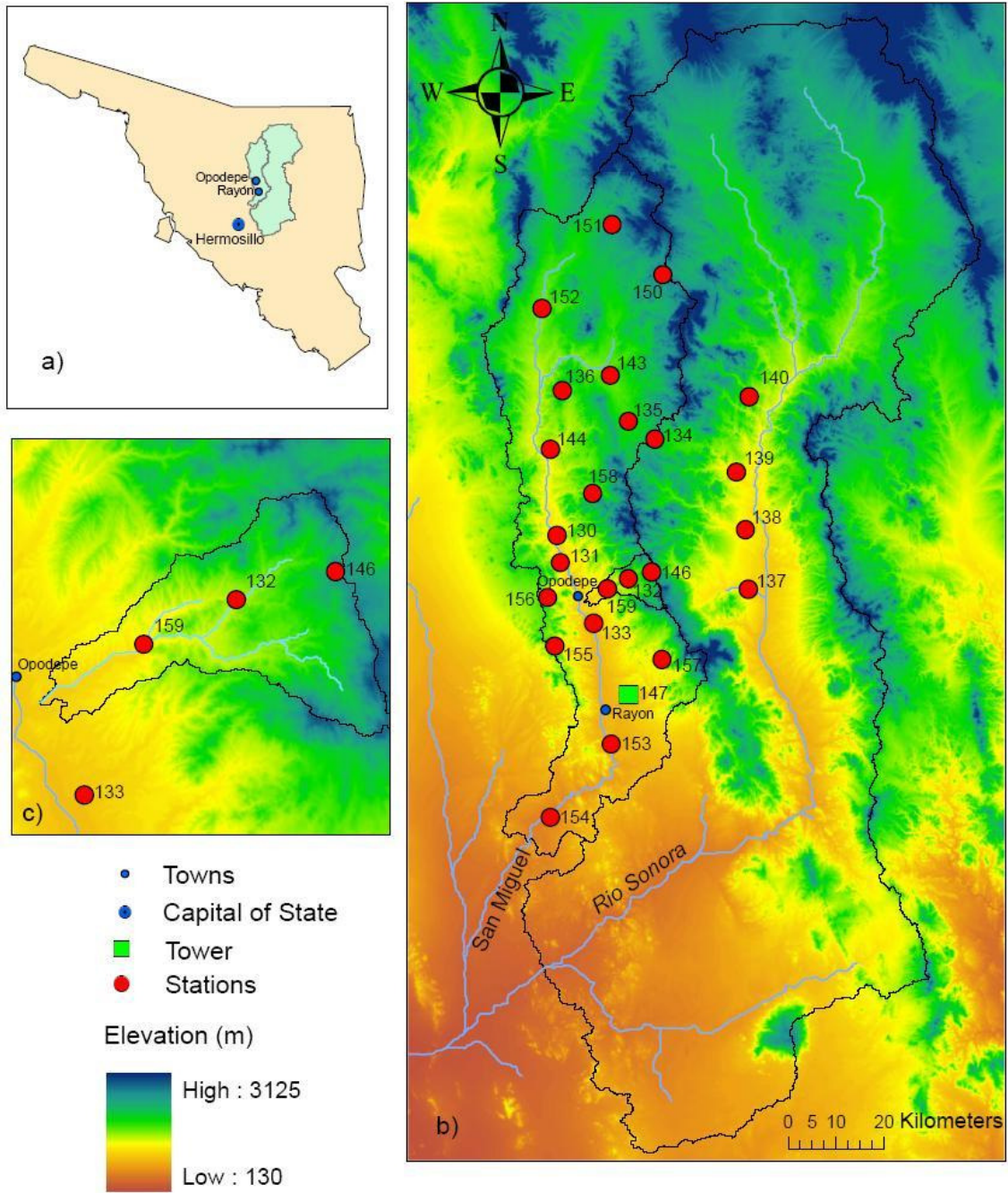
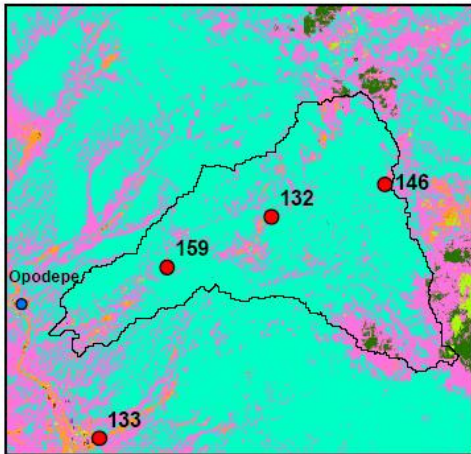


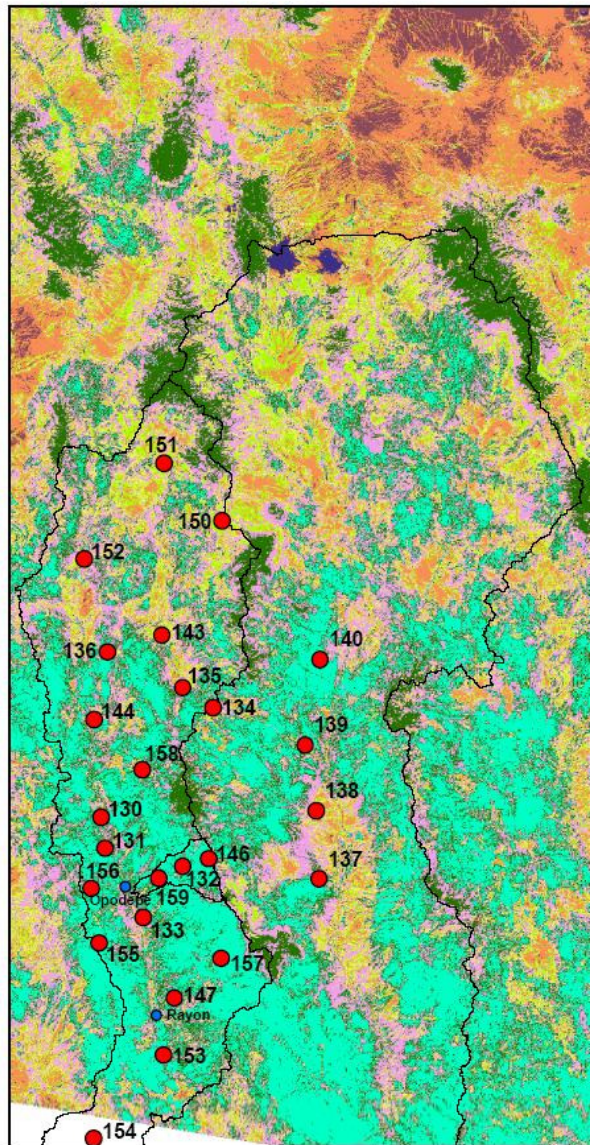
Figure 1: Overall study site map

2. LANDCOVER

Los Locos Basin Landcover



San Miguel and Sonora Basin Landcover



● Stations

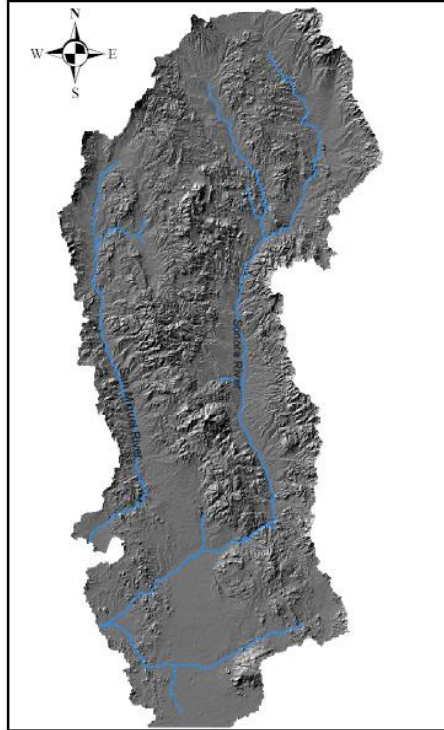
LANDCOVER

- Agriculture
- Evergreen (broad and needle leaf)
- Grassland
- Riparian Mezquite
- Shrubland
- Background
- Bare soil
- Riparian woodland
- Sparse woodland
- Subtropical scrubland
- Water body

Figure 2: Overall land cover map

3. Topography/Hillshade

Sonora and San Miguel Basins



Sierra de los Locos Basin

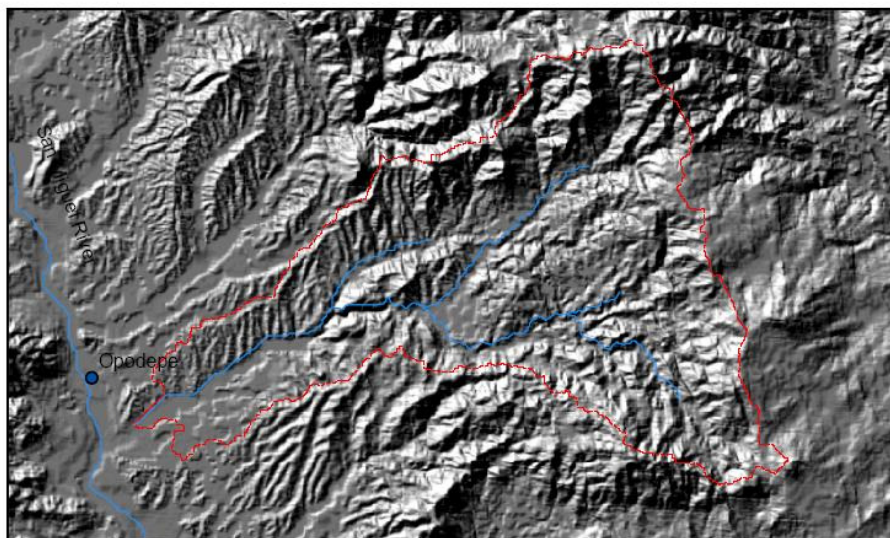


Figure 3: Overall topography/hillshade map

EXPERIMENTS: OVERVIEW AND PROTOCOL

OVERVIEW OF EXPERIMENTS

Introduction

There will be a total of 8 experiments to be conducted in the Sonora and San Miguel Basins. Students will work with professors and graduate students in different locations and will take turns conducting different experiments to provide a vast opportunity for students to develop field and research skills. Students will work in groups which will allow for a multi-cultural and multi-discipline experience.

Goal

To engage in binational studies that properly characterize the spatial and temporal variability in hydrologic variables such as precipitation, soil moisture, and streamflow around the Sonora region, where the summer monsoon can account for a significant amount of the annual rainfall.

EXPERIMENT	LOCATION	PRIMARY INVESTIGATORS	# Days
1. <u>Isotopic Partitioning of Evapotranspiration</u>	Rayon Tower	Enrico Yopez	5
2. <u>Tree Sampling for Sapflow Allometric Relations</u>	Rayon Tower	Enrico Yopez	2
3. <u>Daily Soil Temperature Moisture and Temperature Sampling Plots</u>	Rayon Tower	Chris Watts, Julio Rodriguez, Enrique Vivoni, Laura Alvarez	17
4. <u>Eddy Covariance Tower Installation and Operation</u>	Cucurpe	Luis Mendez, Agustin Morua	3
5. <u>Hydrometeorological Station Installation (10) including Calibration/Soil Sampling</u>	Sonora Basin	Luis Mendez, Agustin Morua	6
6. <u>Flux measurements using DF Scintillometer Installation and Operation</u>	Rio San Miguel Basin	Chris Watts	6
7. <u>Water Source Characterization using Major Anions and Isotopes - Set-up Sampler for Streamflow</u>	Throughout Sonora Basin	Lisette de la Cruz	5
8. <u>Soil Surveying</u>	Sierra Los Locos Basin	Bruce Harrison, Jose Luis Zarate	4

EXPERIMENT 1: ISOTOPIC PARTITIONING OF EVAPOTRANSPIRATION – RAYON TOWER

Goal

The purpose of this experiment is to collect samples of vapor, soils, and transpiring vegetation (stems, leaves) which, through the corresponding isotopic compositions, will help determine the relative proportions of evaporation (E; soil and wet surfaces) and transpiration (T; plant) in the total evapotranspiration flux (ET) measured by eddy covariance in dry shrublands “Matorrales secos” along the Rio San Miguel in Sonora Mexico. The location of this experiment will be at the eddy covariance tower at **station 147** near Rayon:

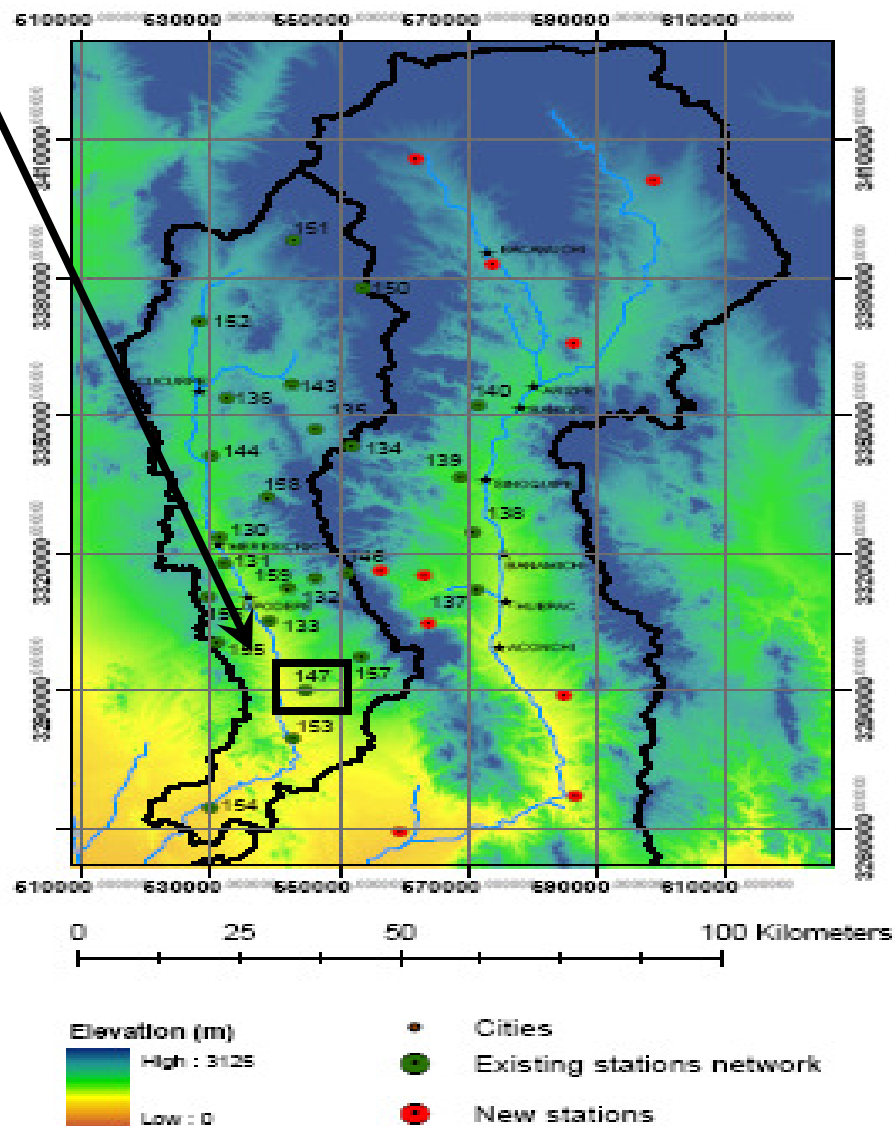


Figure 4: Location of the Rayon Eddy Covariance Tower

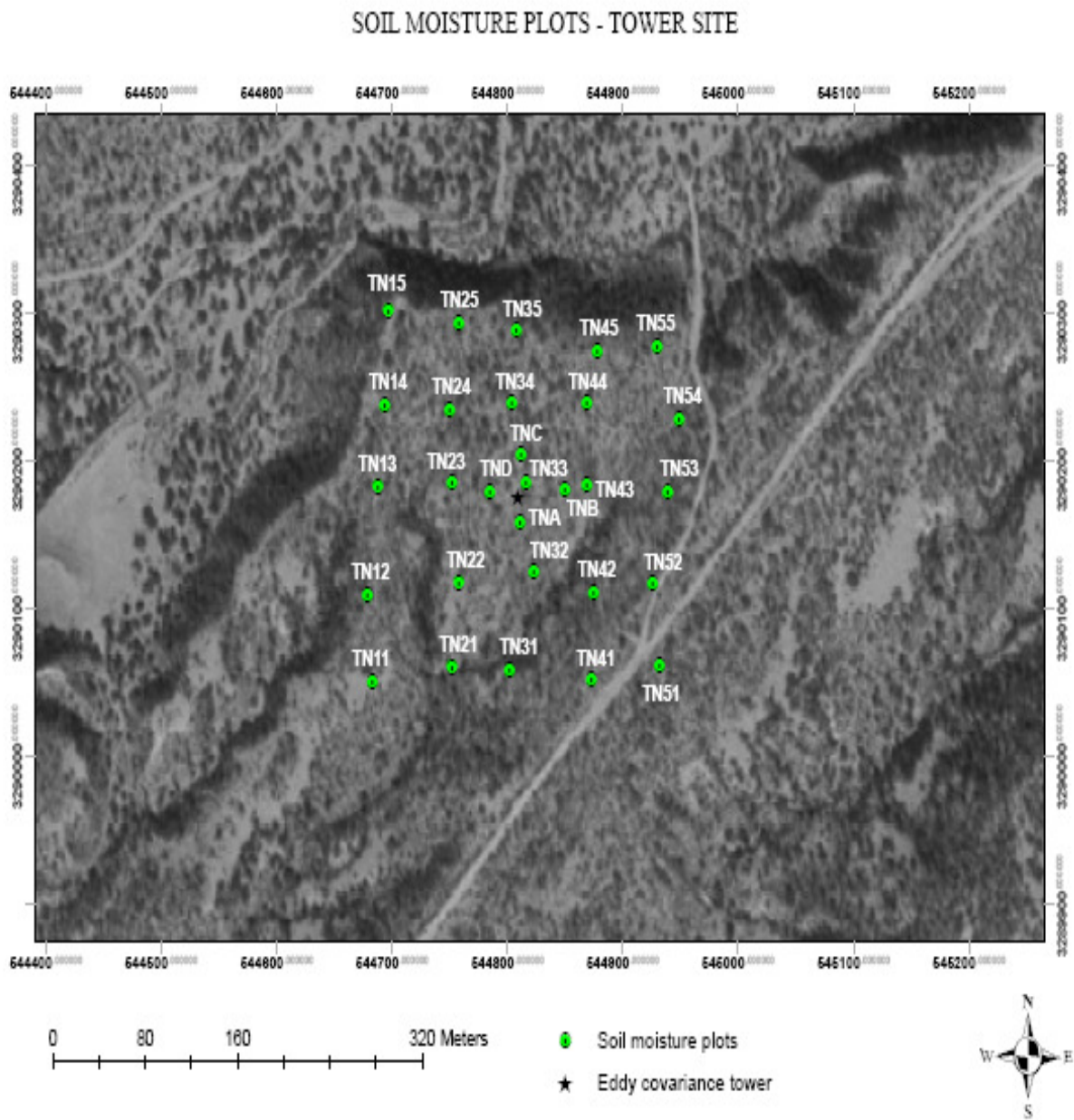


Figure 5: Map of Rayon Tower and Surrounding Sampling Sites

Daily sampling equipment

- Markers/Pens/Pencils (1 pk. ea.)
- GPS Unit (1)
- Chronometer (1)
- Field Notebook (1)
- Soil Auger (1)
- 25 ml Screw-capped Vials (18 or 36 for leaves, 12 for stems, 15 for soils)
- Extra Vegetation Vials (144)
- Labels (a few rolls)
- Hand Pruners (3 in a set)
- Parafilm (1 box)
- Vapor Trapping System (1) *including glassware and liquid nitrogen/alcohol bath
- 12 Volt Batteries (1)
- Aluminum Foil (1 box)
- Cooler (1 medium sized)
- Ziploc Bags (1 box, gal. size)
- Metal File (1)
- Scissors (1)
- Handheld Porometer (1)

For the vapor trapping system:

- Glass Vapor Traps (120)
- Liquid Nitrogen (40 l)
- Ethanol
- Dewar Flask with Lid (1)*item that holds the liquid nitrogen and ethanol
- Thermometer (1)
- Vapor trapping system connected to board and in white plastic container
- Valves (several)
- Tubing

Post-sampling analysis background

Measurements of the stable isotopic compositions of water or water vapor provide a tracer of the sources of ET because water vapor from plant transpiration and soil evaporation each have unique isotopic signatures (Wang and Yakir, 2000). This helps separate the relative contributions of transpiration and evaporation at the ecosystem scale, using a mixing equation:

$$T/ET = \frac{\delta_{ET} - \delta_E}{\delta_T - \delta_E} \quad (\text{Eq. 1})$$

where δ_{ET} is the isotopic composition of evapotranspiration,

δ_E is the isotopic composition of soil evaporation, and
 δ_T is the isotopic composition of transpiration.
 δ_{ET} is estimated using the ‘Keeling plot’ approach (Yakir and Sternberg 2000).

About isotopic composition of evapotranspiration vapor, δ_{ET} :

Determination of the isotopic composition of the evapotranspiration flux (δ_{ET}) is possible using “Keeling plots” (Figure 6) of water vapor. In this model the y-intercept of a simple linear regression between the isotopic composition of several vapor samples and the inverse of the corresponding absolute moisture concentration indicates δ_{ET} .

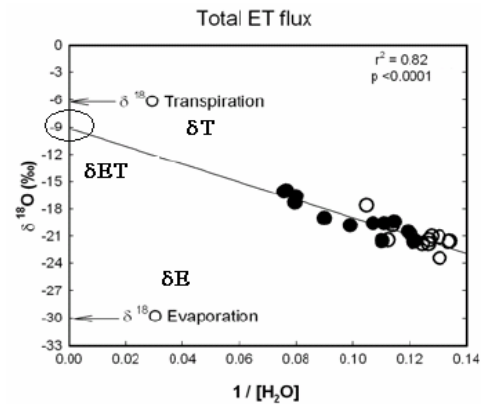


Figure 6: An example Keeling plot

About isotopic composition of vapor from soil evaporation, δ_E :

During the process of evaporation, the isotopic composition of water is modified during the diffusion through boundary layers, where fractionation processes act against the heavy isotopes resulting in an evaporation water flux depleted in heavy isotopes relative to the water at the evaporating surface in the soil. The intensity of such depletion is a function of the isotopic composition of the vapor in the atmosphere and soil water, relative humidity and equilibrium and kinetic fractionations associated with a phase change and diffusion and temperature.

About isotopic composition of the transpiration vapor sources, δ_T :

During transpiration, an isotopic steady state (ISS) can be attained, in which the vapor leaving the leaf has the same isotopic composition of water moving into the leaves from the xylem. This is because of no isotopic fractionation during water uptake by roots and transport to sites of evaporation in leaves, and despite the common enrichment of heavy isotopes in the leaf water as a product of kinetic and equilibrium fractionations. Hence, the isotopic composition of the stem water could be a reliable surrogate for δ_T (Yakir and Sternberg, 2000). However, field and laboratory experiments investigating factors controlling the isotopic composition of leaf water suggest that, during typical diurnal regimes of atmospheric humidity, leaf water is not always at ISS and that transpiration at ISS occurs only after ambient conditions are relatively stable. Thus, a careful consideration of potential deviations from ISS during transpiration is necessary when using the isotopic mass balance depicted in eq. (1) because failure to account for deviations from ISS can translate in significant errors in the final estimates of T/ET under certain circumstances.

Experimental Approach

Initial setup

For the vapor collection, the setup would be done under the supervision of Enrico Yopez on the first 3 days. This setup basically consists of air flow generated with a miniature diaphragm pump to exhaust dry air that has passed through a cryogenic vapor trap resting in a cold bath at $-80\text{ }^{\circ}\text{C}$ (see subplot 2 in Figure 9), where the air flow is regulated with a flow meter to be at 0.5 L min^{-1} . The vapor trap consists of two glass tubes assembled by a gas tight metal tee such that a 6 mm open tube rests inside a 9 mm tube to route the air between the walls of both tubes and then through the inner cavity of the 6mm tube upwards (see subplot 1 in Figure 9; **REMEMBER: when preparing the vapor trap, mark off the radial circumference of the tube with the sharp file so that the tube neatly breaks later along that marking and will not create sharp jagged edges that could cut your hand**).



Figure 7: Setting Up Vapor Trapping System

The air flow aims to simultaneously collect atmospheric vapor from 4 heights within and above the canopy (0.1, 1, 4.5, and 9 m to match the heights where the moisture concentration is being sensed by an infrared gas analyzer) through low-absorption tubing attached to the tower to reach such heights. The cold bath will be maintained at -80°C by periodic additions of liquid nitrogen to a slush of ethanol (**IMPORTANT: In any case, strictly keep the temperature lower than -60°C**). At this temperature, all moisture condenses (freezes) in the glass tubes of the trap and dry air is exhausted towards the pump.



Figure 8: Moisture Will Be Condensed with an Ethanol/Liquid Nitrogen Mixture

For the soil water collection, the setup consists of marking 3 different spots (assign ID labels from 1 to 3) where the soil samples will be extracted at 4 or 5 different depths. Also write down the co-ordinates of these 3 spots into the field notebook using the GPS, along with those assigned IDs.

For the stem and leaves collection, the setup consists of finding 2 plants each from the 3 most representative species (i.e., total of 6 plants) and marking their locations (assign ID labels 1 to 3 from the most representative species to the least if possible, along with the ID suffixes 'a' and 'b' for the 1st and 2nd plant of each species respectively). Also write down into the field notebook the names of these 3 representative species, and the co-ordinates of these 6 plants along with their assigned IDs and ID suffixes. Refer the Appendix on 'Ecosystems and main plant species of the San Miguel basin' for the vegetation classification.

Vapor samples collection (δ_{ET})

IMPORTANT: Periodically check the cold bath temperatures and add liquid nitrogen to a slush of ethanol to maintain them at -80°C . If the temperatures rise to -70°C during each 30-minute experiment and even possibly to -60°C , it's okay, but **DEFINITELY** keep the temperature below -60°C .

The steps for vapor samples collection are:

1. Start the air flow and check if the experimental setup is okay (see subplots 1 and 2 in Figure 9).
2. Vapor will be collected during **six 30-minute periods distributed during the day (each period starts every 2 hours, so there is a 1.5-hour interval between these experimental periods)** to match the averaging periods used by the eddy covariance tower for the ET measurements. Start to time each period and note it in your field notebook.

- Depending on the moisture conditions of the atmosphere, after each 30 minute period of maintaining a constant flow, 30 to 50 μL of water would be collected in each trap. **IMPORTANT: This water collection time should be accurate to within 1 min of this 30-min duration (i.e., 30-min \pm 1 min).** The inner tubes sticking out from the metal tees then have to break to be able to disassemble the vapor trap. The wet portion of the 6mm glass will drop into the 9mm tube, so that we can cap with few layers of parafilm and secure the vapor (the 1st label/wrapping should be securely fastened) for storage and transport to the lab for the isotope analysis (see subplot 3 in Figure 9).

Important: Be quick on breaking the inner tube and capping the samples when the air flow stops. This is to avoid drastic changes in temperature that can evaporate water from the traps, which might then change the isotopic composition of our water samples.

- Repeat the above steps for each 30-minute time period.

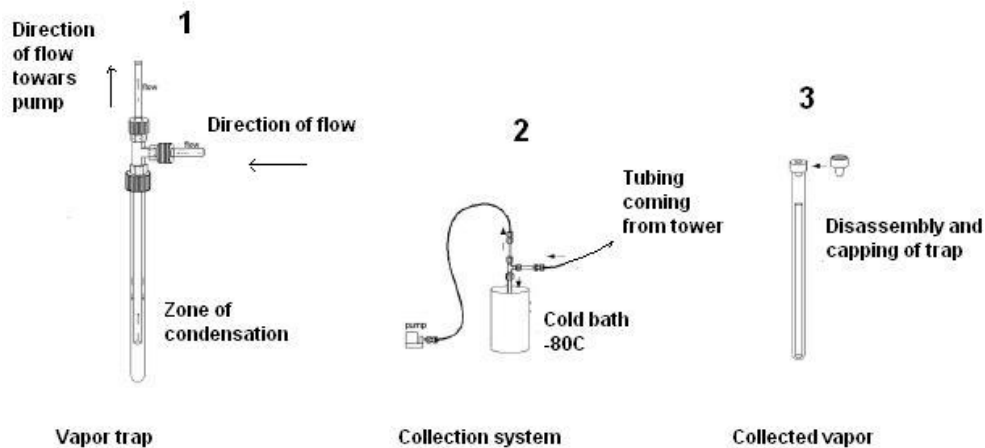


Figure 9: The vapor collection setup

Soil water samples collection (δ_E).

The steps for soil water samples collection (**to be done only once daily**) are:

- For the considered spot, use a hand soil auger as far as possible into the soil to reach the depths needed to obtain the samples. Then, separate the soil sample into sections of 5 cm (should have ideally been 10 cm sections with a deeper soil auger). If the soil sample can not be cut into equal sections of 5 cm, cut the sample so that only the deepest sample is not a full 5 cm. Rapidly put the soil interval sections into separate vials and rapidly cap them to avoid evaporation from the sample (see Figure 10).
- Label the samples using the spot number first, then the date on the next line, and then the sampling interval section number with the sampling interval in parentheses, for example, section 2 (5-10 cm). The section number is one for the topmost and increases with depth.

3. Repeat above steps for each depth at each spot.



Figure 10: Vials of leaves, stems and soils samples

Stems and leaves samples collection (δ_T).

If the stem samples are supposed to be collected on that day, the steps for stem samples collection (**to be done only once daily**) are:

1. For each of the 6 plants, use a set of hand pruners to rapidly cut 6 to 8 pieces (roughly inch-long) of non-green stems and rapidly put all these 6 to 8 pieces into a vial (see Figure 10). Again, rapidly cut another 6 to 8 pieces and put into a duplicate vial. So, we should have 2 vials from each plant.
2. Label with the date, the ID, and the ID suffix (e.g., 'July 22, 2008', followed by '2a' where '2' is the ID and 'a' is the ID suffix).
3. Repeat this for each plant.

The steps for leaves samples collection (**to be done six times daily roughly corresponding to the vapor collection times**) are:

1. For each of the 6 plants, detach several leaves detached from their petioles, and rapidly put into vials (see Figure 6). If we have only 18 vials for the leaves for that day, then mix the leaves from both plants of the representative species sampled into one vial.
2. Label with the date, the ID, and the ID suffix (e.g., 'July 22, 2008', followed by '2a' where '2' is the ID and 'a' is the ID suffix. If only 18 samples are collected, then the ID suffix would be a mix like 'ab').
3. Repeat this for each plant.

References

- Yakir D. and Sternberg, L. da S. (2000) The use of stable isotopes to study ecosystem gas exchange. *Oecologia* 123, 297-311.
- Yepez E.A., Williams D.G., Scott R.L. and Lin G. (2003) Partitioning overstory and understory evapotranspiration in a semi-arid woodland ecosystem from the isotopic composition of water vapor. *Agricultural and Forest Meteorology* 119, 53-68.

Wang X. F. and Yakir, D. (2000) Using stable isotopes of water in evaporation studies. *Hydrological Process* 14, 1407-1421.

EXPERIMENT 2: SHRUB SAPWOOD ALLOMETRICS AND STAND STRUCTURAL CHARACTERISTICS – DRY SCRUBLAND, RAYON TOWER

Objective

The purpose of this survey is to determine the relative canopy cover of the dominant species at the dry scrubland surrounding the Rayon tower and the sapwood area of different size branches from the dominant species to generate allometric relations. Allometric relations will provide information about the suitability of different sap flow methods to measure transpiration in the different species. In combination with projected measurements of transpiration, allometric equations will give predictive power to scale up water fluxes from measurements of individual species.

Proposed Measurements

- 1) Shrub sapwood area (live water-conducting tissues)
- 2) Basal diameter of dominant species per unit of ground area
- 3) Aerial canopy cover

Scope

The structural characteristics of the vegetation influences the surface roughness and creates micro-sites of contrasting energy balances and resource availability for the present species. Furthermore, plant function directly controls the flow of water from the soil to the atmosphere via transpiration.

Measurements of transpiration based on sap flow give us the ability of continuously monitor the physiological stage of the vegetation and estimate the absolute amounts of transpired water per unit of ground area, such advantage is critical to understand the environmental controls of biophysical-driven water exchange between the surface and the atmosphere.

Based on measurements of sap flow and assuming that plant water capacitance is low, stand-level estimates of transpiration (T_{stand}) including several shrub species can be calculated as:

$$T_{stand} = \sum_{i=1}^2 J_{Si} \left(\frac{A_{Si}}{A_g} \right) \quad \text{Eq(1)}$$

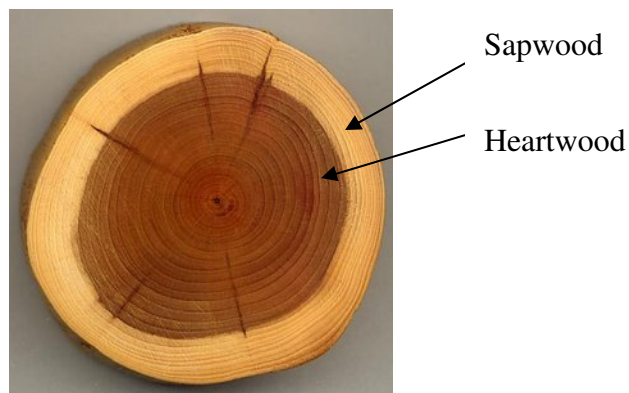
where J_{Si} and (A_{Si}/A_g) are sap flux density ($\text{g m}^{-2} \text{ day}^{-1}$) and sapwood area to ground area ratio ($\text{m}_S^2 \text{ m}_g^{-2}$) of species i . Notice that if a good representation of the relative abundances of the participating species is given estimates of T_{stand} should be robust.

Clearly, to gain knowledge in this area requires a thorough understanding of the mechanistic relations between the vegetation's form and function. Generating tree allometric relations, that is; "assessing the changes in relative dimensions of tree parts that are correlated with changes in overall size", is a practical tool to reach this goal.

Approach

As a preliminary attempt to characterize the physiognomy of the semiarid shrubland near the Rayon tower we will determine the relative cover of the dominant species. Our approach will rely on predictive allometric models rather than extensive surveys or census. Three, 20 by 20 meter plots will be delimited near the vegetation transects used in the 2006 field campaign. On each transect the basal diameter of all present species will be measured with diameter tapes. The area of the plots will be used as A_g in equation 1 while the measurement of basal diameter will be used to predict sap wood areas per unit of ground area based on the approach described below. In a subsample of trees (to be determined based on the densities) the cross section of the aerial canopy cover will be determined with two 50ft measure tapes.

To predict the sap wood area of the present species, the diameter of several branches will be measured and then, each branch will be cut to quantify the sapwood area (live conductive tissue). To determine the sapwood area of each branch and relate it to the branch diameter, we will get a print of the basal cut zone of each branch. To produce the prints we will use overhead transparencies to copy the circumferences of the circles apparent from the cuttings (see figure below). The inner circle is the heartwood (dead tissue) while the clear outer circle is the sapwood. The transparencies will then be scanned to calculate the areas with digital analysis software. By knowing the branch diameter and the sapwood area of several branches of each species we can use the regression line of these parameters to generate a prediction for A_{Si} in equation 1.



We expect our allometric equations to be linear (e.g. simple regressions), however to have robust statistical models (and therefore predictive power) we will need to cover a wide range of branch sizes. To reach this goal easing our sampling efforts and minimizing the impacts to the landscape, we propose to use individual branches of different sizes and extrapolate linearly to the larger or smaller ends. We, therefore, propose to harvest branches from trees of 4 size classes with 2 trees of each size class per species (e.g. branches from a total of 8 trees per species) (See table for expected size classes*).

	Basal Diam. (cm)	Height (m)	Number of trees	Number of Branches/tree
Palo verde				
Class 1	40 to 45	4 to 5	2	3
Class 2	25 to 30	3 to 4	2	3
Class 3	15 to 20	2 to 3	2	3
Class 4	7 to 10	1 to 2	2	3
Ocotillo				
Class 1	80 to 85	4 to 5	2	3
Class 2	40 to 45	2.5 to 3.5	2	3
Class 3	20 to 25	1.5 to 2.5	2	3
Class 4	10 to 15	1 to 1.5	2	3
Acacia				
Class 1	40 to 45	4 to 5	2	3
Class 2	25 to 30	3 to 4	2	3
Class 3	15 to 20	2 to 3	2	3
Class 4	7 to 10	1 to 2	2	3
Mesquite				
Class 1	80 to 85	4 to 5	2	3
Class 2	40 to 45	2.5 to 3.5	2	3
Class 3	20 to 25	1.5 to 2.5	2	3
Class 4	10 to 15	1 to 1.5	2	3

*size classes are expected and may vary after an initial preliminary survey.

We would expect that harvesting branches from individuals from these size classes would provide us with 24 branches per species covering a range of 40 to 200 mm in diameter which would suffice our needs for robust predictive models.

Expected products

The information generated from this study will be primarily used to predict the total canopy cover of the dominate spies present in these shrublands which will be useful to constraint the partial fluxes contributing to ET measured by the tower. Predictions of sapwood area (A_S) will be used to adequately plan the instrumentation of sapflow sensors in future field campaigns.

EXPERIMENT 3: DAILY SOIL MOISTURE / TEMPERATURE SAMPLING PLOTS – RAYON TOWER

Goal

The purpose of this task is to study the variability of soil moisture/temperature within the 1 km² area around the fluxes tower. This will be accomplished by taking daily measurements of soil temperature (at four depths: surface with an infrared thermometer, and 1cm, 5cm, and 10cm using a probe thermometer), soil moisture (using a theta probe), and weather data (provided by the weather station on the tower). The following map provides a view of the overall experimental site around the tower:

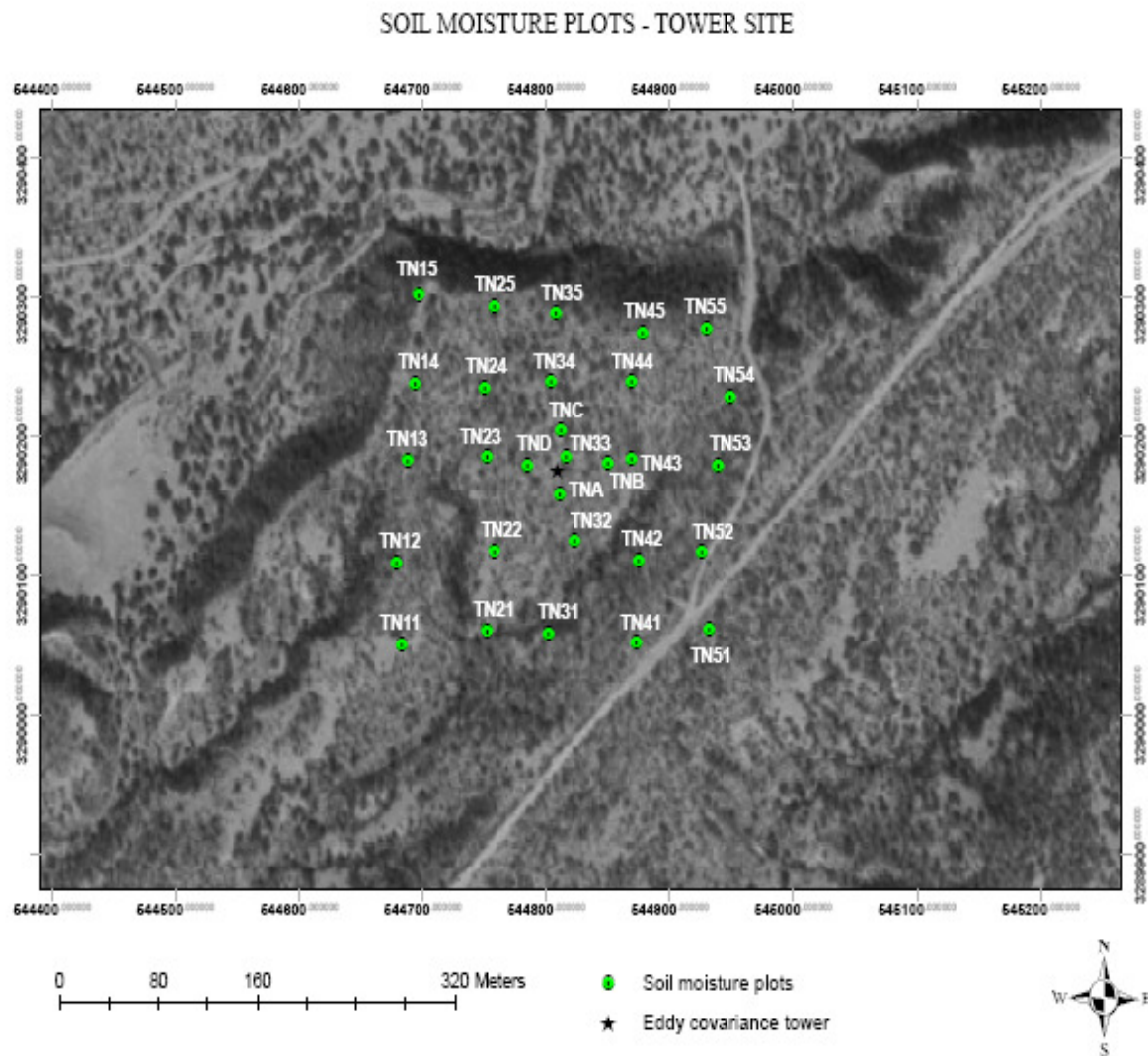


Figure 11: Map of sampling plots

Materials

The first day

- 4 hand held theta probes (soil moisture probe)
- extra tines
- 1 infrared thermometer (surface temperature instrument)
- 3 soil thermometers
- 200 flags
- 100 1' wooden stakes
- 1 GPS unit
- 1 map and coordinates of station locations
- Field notebook
- Writing utensils (permanent marker, pen, pencil)
- Radios
- Digital Camera (when available)
- Handheld compass (2)

Subsequent days

Divide into two groups:

- 4 hand held theta probes
- extra tines
- 2 infrared thermometer (surface temperature instrument)
- 3 soil thermometers
- a few extra flags
- a few extra stakes
- 2 GPS units
- 2 map and coordinates of station locations
- 2 Field notebooks
- Writing utensils (permanent marker, pen, pencil)
- Radios
- Digital Camera (when available)

Procedure

Two groups of two will be needed:

Before departing for the field

1. Gather all necessary equipment (see Figure 12 and the list above).

2. Check that all equipment is working (especially GPS and radios).
3. Double-check your equipment.



Figure 12: Some of the equipment used to estimate soil moisture and soil temperature. This includes theta-probe, thermometers, compass etc.

Plot deployment (first day)

1. Locate sampling location. **(We will be using the same locations as the 2006 campaign.)**
2. Place 4 flags in the ground at this location creating a 1m x 1m square using the flags as corner markers (check figure 13).

IT IS VERY IMPORTANT THAT YOU DO NOT STEP INSIDE THE BOX AS THIS WILL CHANGE THE SOIL COMPACTION AND WILL ALTER THE DATA



Figure 13: Example of a sampling plot. Plot dimensions are 1 m x 1 m

3. Take an exact GPS reading for the location and record in notebook. Also record operators, date, and time in notebook.
4. Mark on the flag the location ID.
5. Take 5 soil moisture measurements; one at each corner of the box and one at the center of the box. Record measurements in notebook. (Figure 14)
6. Note which measurement was taken with which probe.
7. Take surface temperature with the infrared thermometer and record in notebook.
8. Take soil temperatures at 1cm, 5cm, and 10cm, each with different soil thermometers and record in notebook (check Figure 14)
9. Make sure to gather all equipment before departing to the next site.



Figure 14: Soil moisture measurements using theta probe. Soil temperature is measured using thermometers at different depths.

Subsequent Days

1. Record location ID, operators, date, and time in notebook.
2. Take 5 soil moisture measurements; one at each corner of the box and one at the center of the box. Record measurements in notebook.
3. Note which measurement was taken with which probe.
4. Take surface temperature with the infrared thermometer and record in notebook.
5. Take soil temperatures at 1cm, 5cm, and 10cm, each with different soil thermometers and record in notebook.
6. Make sure to gather all equipments before departing to the next site.

Table 1: Rayon Tower Plot coordinates

SITE ID	NORTH	EAST	ELEVATION
TN55	3290277	544930	622
TN45	3290274	544878	626
TN35	3290288	544808	626
TN25	3290293	544758	631
TN15	3290302	544697	627
TN14	3290238	544694	633
TN24	3290235	544750	633
TN34	3290239	544804	637
TN44	3290239	544869	638
TN54	3290228	544949	637
TN53	3290179	544939	641
TN43	3290184	544869	638
TN33	3290185	544816	641
TN23	3290185	544752	638
TN13	3290183	544688	637
TN12	3290110	544679	631
TN22	3290118	544758	633
TN32	3290126	544823	633
TN42	3290111	544875	633
TN52	3290117	544926	640
TN51	3290062	544932	641
TN41	3290052	544873	639
TN31	3290059	544802	628
TN21	3290061	544752	623
TN11	3290051	544683	629
TNA	3290159	544811	634
TNB	3290181	544850	636
TNC	3290204	544812	637
TND	3290179	544785	636

*Projection: UTM-12 N
Datum: WGS84

EXPERIMENT:4 EDDY COVARIANCE TOWER **INSTALLATION/OPERATION - CUCURPE**

Goal

The purpose of this experiment is to properly install, test, and troubleshoot the 30' tower, guy wires with anchors, meteorological & soil sensors, tower grounding, datalogger, enclosure, solar panels, and lead acid batteries.

Background

The Eddy Covariance (aka Eddy Correlation, Eddy Flux) technique is a prime atmospheric flux measurement technique to measure and calculate vertical turbulent fluxes within atmospheric boundary layers. It is a statistical method used in meteorology and other applications that analyzes high-frequency wind and scalar atmospheric data series, and yields values of fluxes of these properties. Such flux measurements are widely used to estimate momentum, heat, water, and carbon dioxide exchange, as well as exchange of methane and other trace gases. The technique is also used extensively for verification and tuning of global climate models, mesoscale and weather models, complex biogeochemical and ecological models, and remote sensing estimates from satellites and aircraft. The technique is mathematically complex, and requires significant care in setting up and processing data.

Potential Installation Locations

When choosing the potential site for the new eddy covariance tower installation, factors such as homogeneity in vegetation and geology were considered. Installation must take place on a relatively level surface and the soil must be suitable to allow for 3 x 3 x 4 pit to be dug for base installation purposes. The tower will be installed in a unique area which will provide valuable information to our current understanding of monsoon hydrology. The ecosystem must be oak savanna.

References

Burba, George (Contributing Author to Background; Steven L. Forman (Topic Editor from Background). 2008. "Eddy Covariance Method." In: Encyclopedia of Earth. Eds. Cutler J. Cleveland (Washington, D.C.: Environmental Information Coalition, National Council for Science and the Environment).

Potential New Tower Location - Sierra Los Locos

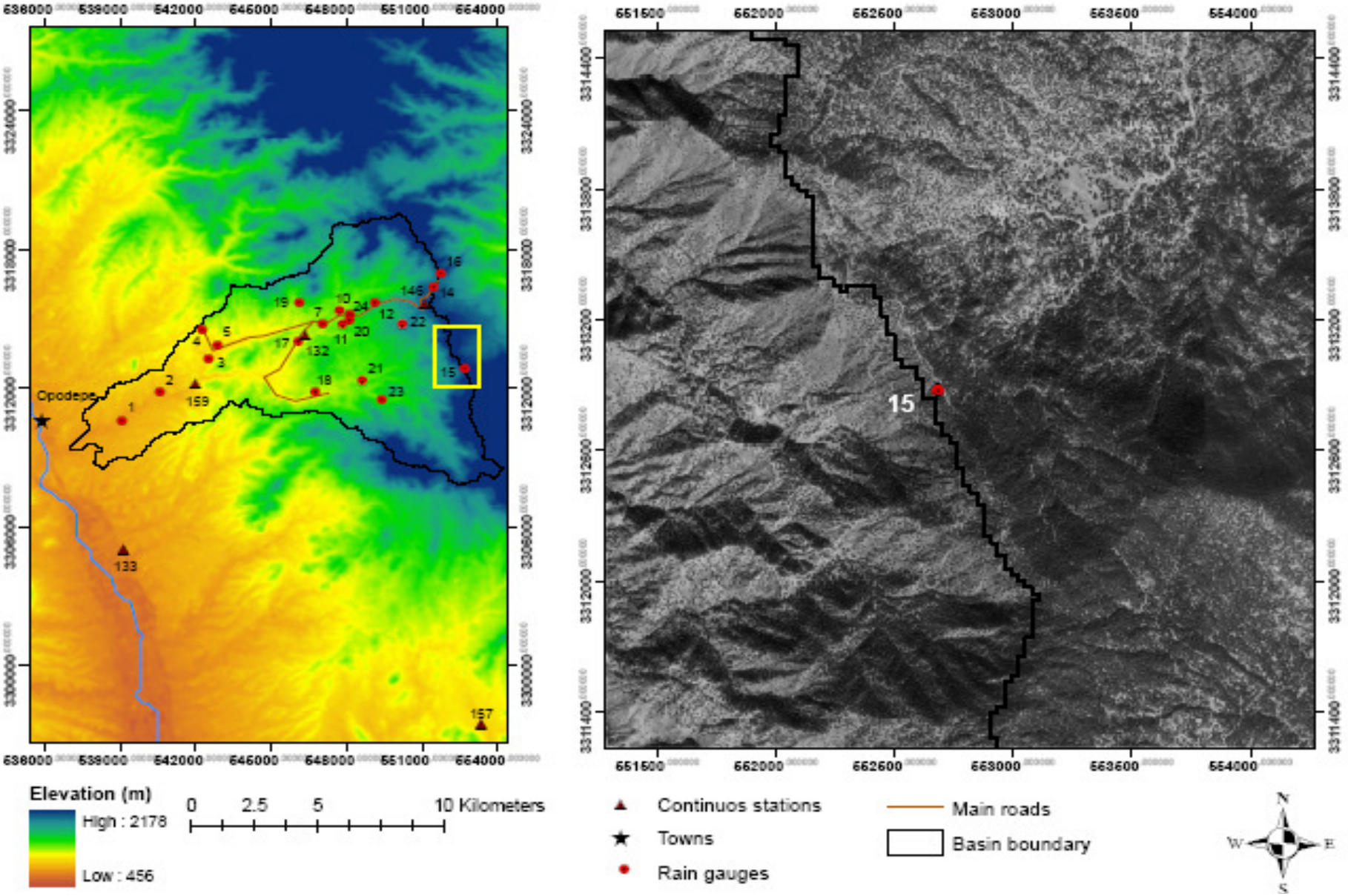


Figure 15: Potential New Tower Location

Potential New Tower Location - Station 134

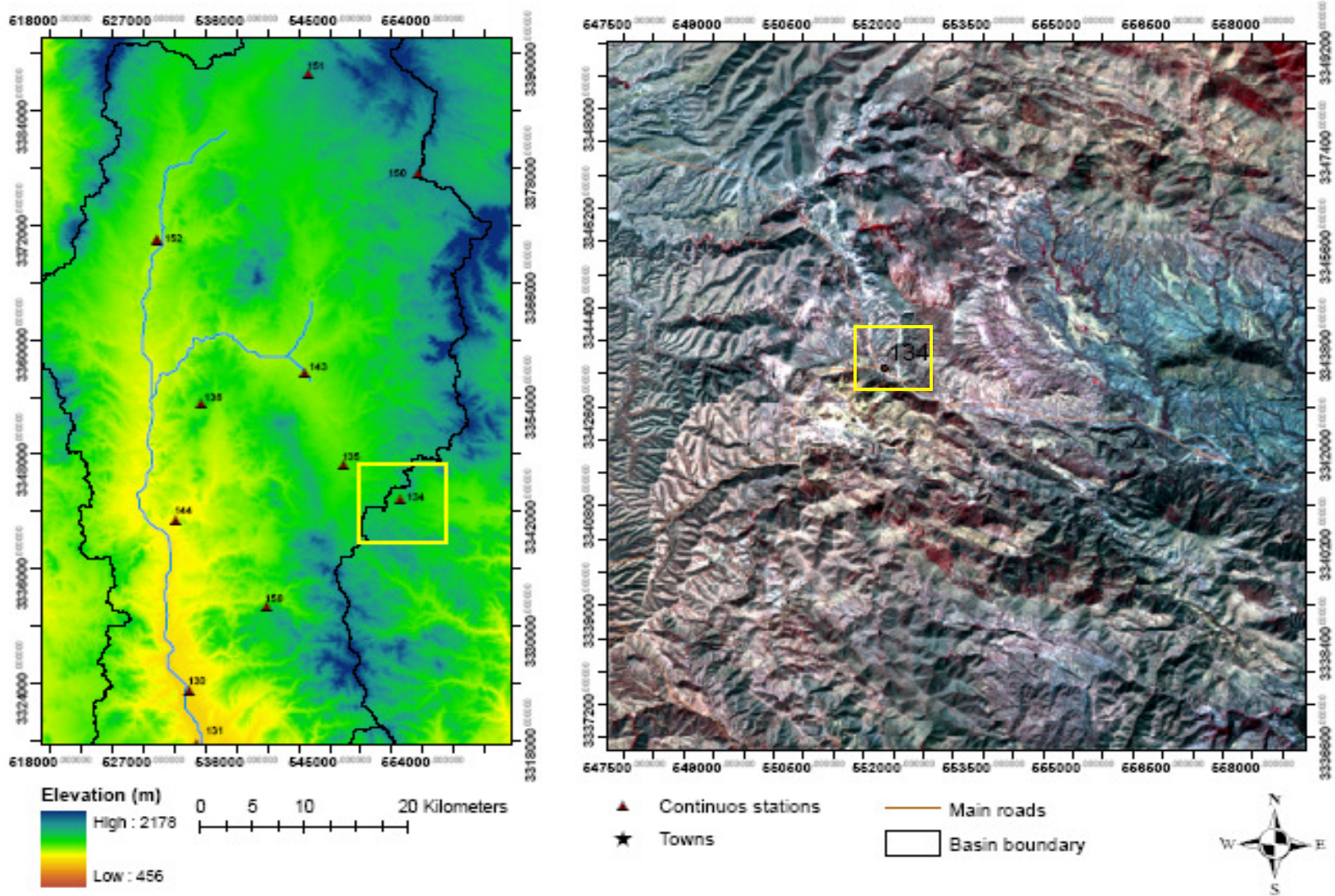


Figure 16: Potential New Tower Location

Installation Tasks

- Located suitable site
- Prepare tower base
 - Install 3 to 10 meter level sensors
 - Raise Tower
 - Install instrumentation enclosures
 - Install 0 to 3 meter level sensors

Tools Required for Tower Installation

- Shovels
- Open end wrenches: 5/16", 3/8", 7/16", 1/2", (2) 9/16", 15/16"
- Adjustable/Crescent wrench
- Magnetic compass
- 6' Step Ladder
- Tape measure (25')
- Nut driver (3/8")
- Level (36" to 48")
- Small Sledgehammer
- Pliers
- Cable Ties
- Climbing harness
- Haul rope (50')
- Non-stretch line
- Wire rope cutters
- Materials for Guy Wires
 - 120' Aircraft Cable 3/16"
 - (3) Turnbuckles 1/2" x 17"
 - (3) Turnbuckles
 - (24) Wire Cable U-bolt Clamps 3/16"
 - (12) Wire Cable Thimbles 3/16"
 - (3) 5/8"-11 x 4" Coarse Hex Cap Bolts
 - (3) 5/8"-11 Coarse Nuts
 - (3) 3/4" x 30" Dbl. Head Earth Auger Anchor
 - Metal bar to screw in anchors
 - Cement (MEX)
- Materials for B18 Base
 - (4) Wood Stakes 12"
 - Pick or digging bar
 - Concrete form materials (optional) (2" x 4" lumber, stakes, saw, hammer, nails, etc.)
 - Cement (MEX)

Additional Tools for Instrumentation Installation

- Lock and key for enclosure
- Magnetic declination angle

- Straight bit (flathead) screwdrivers (small, medium, large)
- Phillips-head screwdrivers (small & medium)
- Small diagonal side-cuts
- Needle-nose pliers
- Wire strippers
- Pocket knife
- Calculator
- Volt/Ohm meter
- Electrical tape
- Datalogger prompt sheet
- Station manuals
- Socket wrench and 7/16" deep well socket
- Pliers
- Felt-tipped marking pens
- Claw hammer
- Channel-lock pliers
- 3/8" nut driver
- 1/4" washers (spacers for U-bolts)
- 5/64" Allen hex wrench
- Enclosure Sealing and Desiccant Kit
- Hose Clamps (2)

Instrumentation Equipment

- CR5000 Measurement and Control System Datalogger
- Datalogger Enclosure and mounting hardware
- CSAT3 3-D Sonic Anemometer and Electrical Box
- LI-7500 Open Path CO₂/H₂O Analyzer and Electrical Box
- HMP45AC Humidity and Temperature Probe with Shield
- (4) CS616 Water Content Reflectometers
- CMP3 Pyranometer, radiation shield and mount
- Setra 278 Barometer
- CNR2 Net Radiometer and mounting arm
- (2) Hukseflux HFP01SC Soil Heat Flux Sensors
- (4) 4 Probe Type-E Averaging Soil Thermocouples
- Crossbars and crossarms (3?)
- Tower Grounding Kit
- Enclosure sealing and desiccant kit

Equipment for EC Tower Power Supply

- (2) 65 watt solar panels
- (2) Solar panel mounts
- Solar panel wiring
- (2) SunXtender deep cycle battery
- SunSaver 10 amp solar charge controller
- Tower Grounding Kit (wire, rod & connectors)

- Battery cables (to datalogger and between both batteries)
- Battery Boxes (2)

Locating a Proper Tower Site

Wind Speed and Direction

Wind sensors should be located over open level terrain. The EPA recommends the wind sensor be a distance of at least ten times the height of nearby buildings, trees, or other obstructions.

Standard measurement heights:

3.0 m \pm 0.1 m recommended (AASC)

2.0 m \pm 0.1 m, 10.0 m \pm 0.5 m optional (AASC)

10.0 m (WMO and EPA)

Temperature and Relative Humidity

The sensor should be housed in a ventilated radiation shield. The EPA recommends the sensor be no closer than four times an obstruction's height, at least 30 m from large paved areas, and located in an open level area that's at least 9 m in diameter. The open areas should be covered by short grass, or where grass does not grow, the natural earth.

Avoid these:

- Large industrial heat sources
- Rooftops
- Steep slopes
- Sheltered hollows
- High vegetation
- Shaded areas
- Swamps
- Areas where snow drifts occur
- Low places holding standing water after rains

Standard measurement heights:

1.5 m \pm 1.0 m (AASC)

1.25 to 2.0 m (WMO)

2.0 m temperature (EPA)

2.0 m and 10.0 m for temperature difference (EPA)

Precipitation

The AASC and EPA suggest tipping buckets be no closer than four times the height of an obstruction. The orifice of the gage must be in a horizontal plane, open to the sky, and above the level of in-splashing and snow accumulation. Typically, tipping buckets are sited on level ground covered with short grass or gravel. Wind shields, such as those used by the National Weather Service, are recommended for open areas.

Standard measurement heights:

1.0 m \pm 1.0 cm (AASC)

30.0 cm minimum (WMO, EPA)

Solar Radiation

Pyranometers should be mounted away from shadows, reflective surfaces, and sources of artificial radiation. Mounting the pyranometer on the southernmost (northern hemisphere)

part (either crossarm or pyranometer mounting arm) of the weather station should minimize shading from the other weather station structures. The height the sensor is mounted is not critical for the accuracy of the measurement. However, pyranometers mounted at heights of 3 m or less are easier to level and clean.

Soil Temperature

The measurement site for soil temperature should be at least 1 m² and typical of the surface of interest. The ground surface should be level with respect to the immediate area (10 m radius).

Standard measurement depths:

10.0 cm ± 1.0 cm (AASC)

5.0 cm, 10.0 cm, 50.0 cm, 100.0 cm (WMO)

Base and Guy Anchor Layout

1. A guyed UT30 tower requires an area approximately 17 feet in diameter. Brush and tall weeds should be removed; otherwise the natural vegetation and ground surface should be disturbed as little as possible.

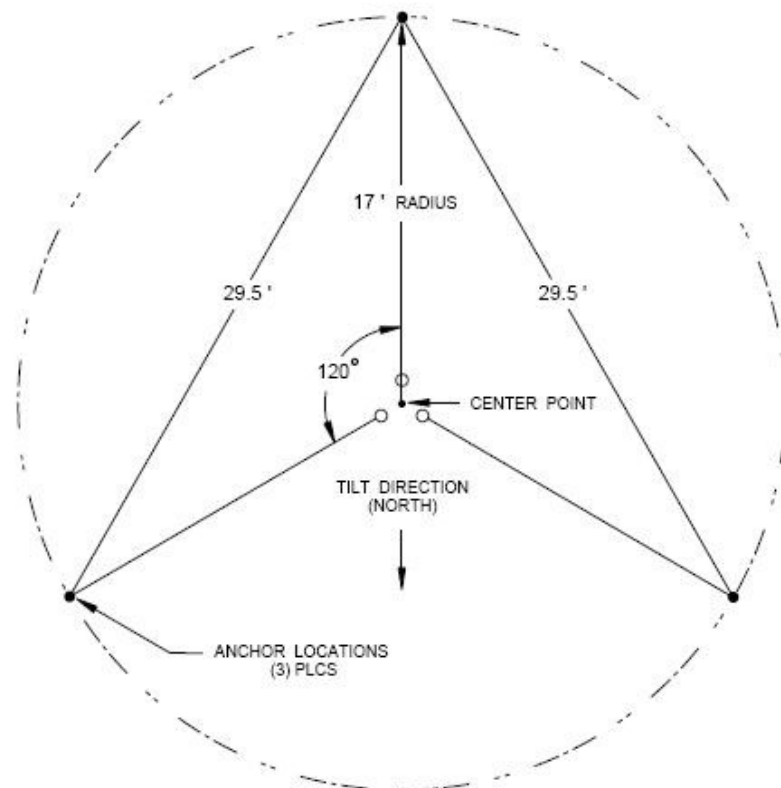


Figure 17: Tower Base and Anchor Layout

2. Drive a stake where the base of the tower will be located. Attach a line to the stake and scribe a circle with a 17 foot radius. Drive a stake on the scribed line, opposite the direction that the tower will hinge, for the first guy anchor location.

MAKE sure that the tower has room to hinge in the direction you choose to orient it.

- a. On level ground, lay out the remaining two anchor locations by measuring 29.5 feet from the first anchor to the scribed line on either side of the base stake (Figure 17).
- b. On unlevel ground, use a compass at the base stake to lay out the remaining two anchor locations 120 degrees from the first. Vary the distance between the tower and each anchor so that the angle between the tower (along the vertical axis) and the guy wire will be approximately 30 degrees.

Tower Base Installation

1. Dig a hole 36" square and 48" deep where the tower base will be located (Figure 18).
2. Attach the bottom section of the tower to the B18 base using one bolt per leg, making sure that the hinge direction is the same for all legs.
3. Center the bottom tower section with the base attached in the hole. **Orient** the tower/base for the proper hinge direction. **Make** sure that the top of the legs will be at least 1/2" above the finished height of the concrete, as in Figure 19.

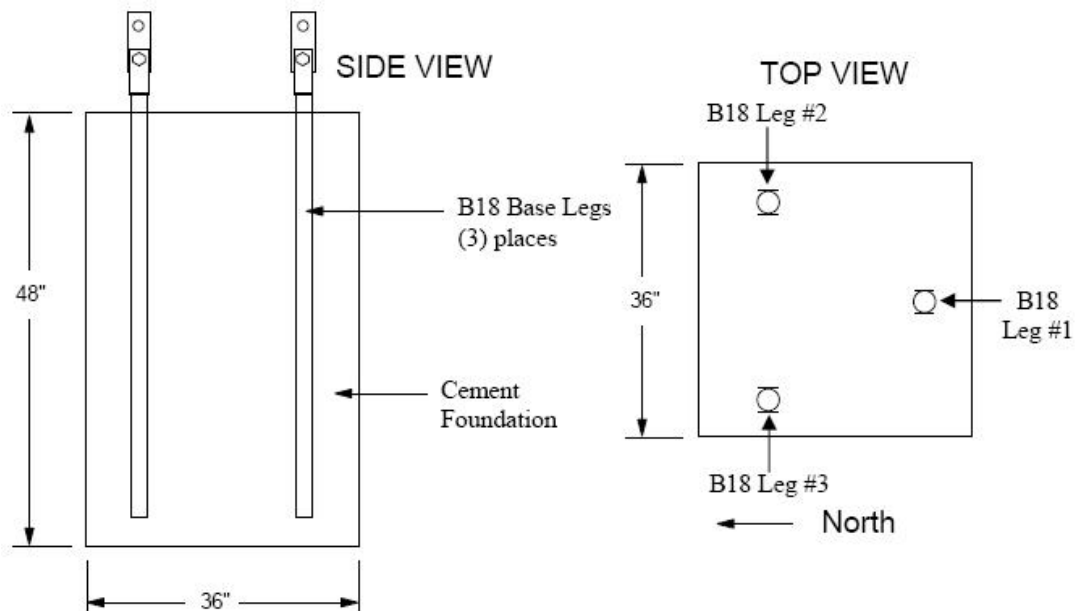


Figure 18: Tower Base Foundation

- Fill the hole with concrete. Getting the bottom tower section plumb is very important. As concrete is poured into the hole, **periodically** check the tower for plumb using a carpenter's level and make adjustments as necessary. Allow three to four days for the concrete to cure.

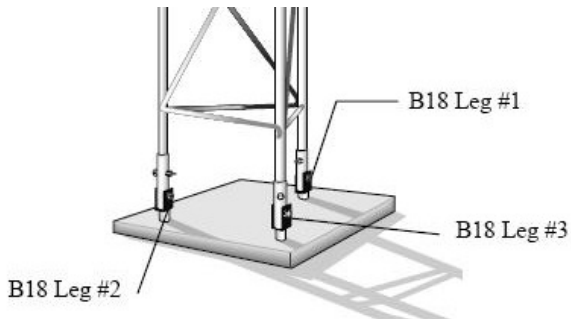


Figure 19: Concrete Mounting Base

Guy Anchor Installation

- Dig a hole approximately 11" in diameter and at least 18" deep at each anchor location.
- Using a piece of rebar or metal rod, screw in an auger soil anchor in each of the anchor locations (in the holes you just dug). The u-channel head of the auger **must** stay above the level of the surrounding earth but the shaft should not protrude from the concrete. You may have to dig deeper and backfill the anchor if the soil is extremely rocky.
- Fill in at least a 18" concrete collar along the upper anchor shaft. This will serve to stabilize the anchor to the lateral loads from the guy cables (Figure 20).

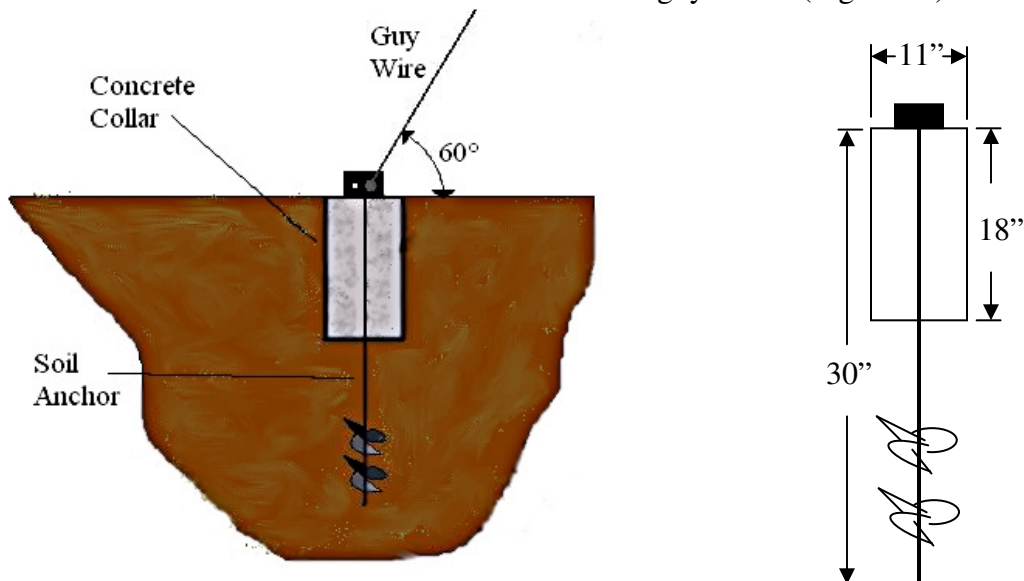


Figure 20: Anchor Installation

UT30 10 M Tower Assembly

1. Having previously installed the base and bottom tower section, remove the bolt from the rear tower leg, and loosen the bolts in the side legs so that bottom tower section is free to hinge. Tilt the tower section to the ground and assemble the remaining sections and mast using the hardware provided with the tower.
2. Install the guy wires to the top of the tower (see Figure 21). Cut from the 250' spool of guy wire: 3-lengths of 3' and 3-lengths of 40'. Attach one end of each of the 40' length cables to the tower using 2 wire clamps on each wire. One wire clamp needs to go as close to the wire thimble as possible without touching it and the other should be a few to several inches away.

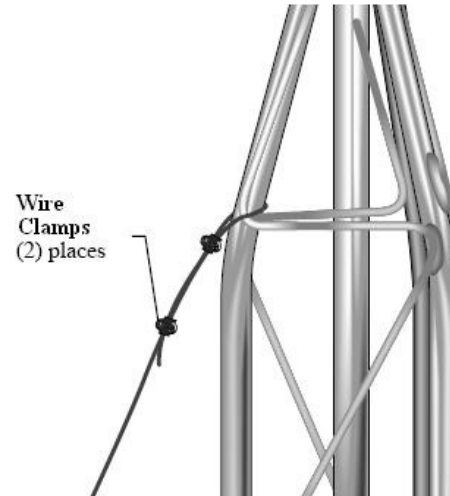


Figure 21: Installation of Guy Wires to the Tower

3. Mount the brackets and sensors that attach to the upper tower sections while the tower is lying on the ground.
4. “Walk” the tower to its upright position and install/tighten the remaining bolts in the tower base.
5. Install the 5/8” hex cap bolts, 5/8” nuts and wire thimbles to the anchors. Make sure to get the wire thimble on the bolt before pushing the bolt all the way through the square hole on the top of the anchor. Tighten with two adjustable wrenches.
6. Using the 3' length wire you cut, make a short length of guy wire between the anchor bolt and the eye of one end of the turnbuckle.

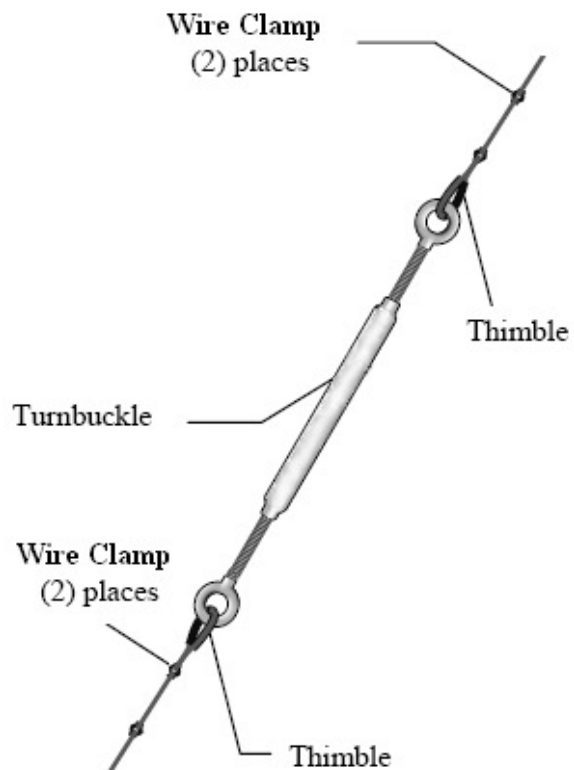


Figure 22: Turnbuckle Installation

7. Use one wire thimble and two wire clamps on each end. One wire clamp needs to go as close to the wire thimble as possible without touching it and the other should be a few inches away.
8. Unscrew the eye bolts from the turnbuckle until at least 1 inch of thread extends into the turnbuckle body. It may help to remove the bolt completely and thread it back in the correct amount. While holding the tower plumb, attach the guy wires to the other eye end of the turnbuckles using a thimble and two wire clamps for each guy wire (see Figure 22). Tighten the turnbuckles until the guy wires are snug and the tower is plumb (use a carpenter's level). **Do not** overtighten the turnbuckles.
9. Attach the crossarms and crossbars at the desired height via the provided u-bolts and nuts (Figure 23). We should have several.



Figure 23: Tower Crossarm

Tower Grounding Kit Installation

1. Drive the ground rod close to the tower using a fence post driver or sledgehammer. Drive the rod at an angle if an impenetrable hardpan layer exists. In hard clay soils, a gallon of gallon can be used to “prime” the soil and hole to make driving the rod easier.
2. Loosen the bolt that attaches the clamp to the ground rod. Insert one end of the 4 AWG wire between the rod and the clamp and tighten the bolt (Figure 24).

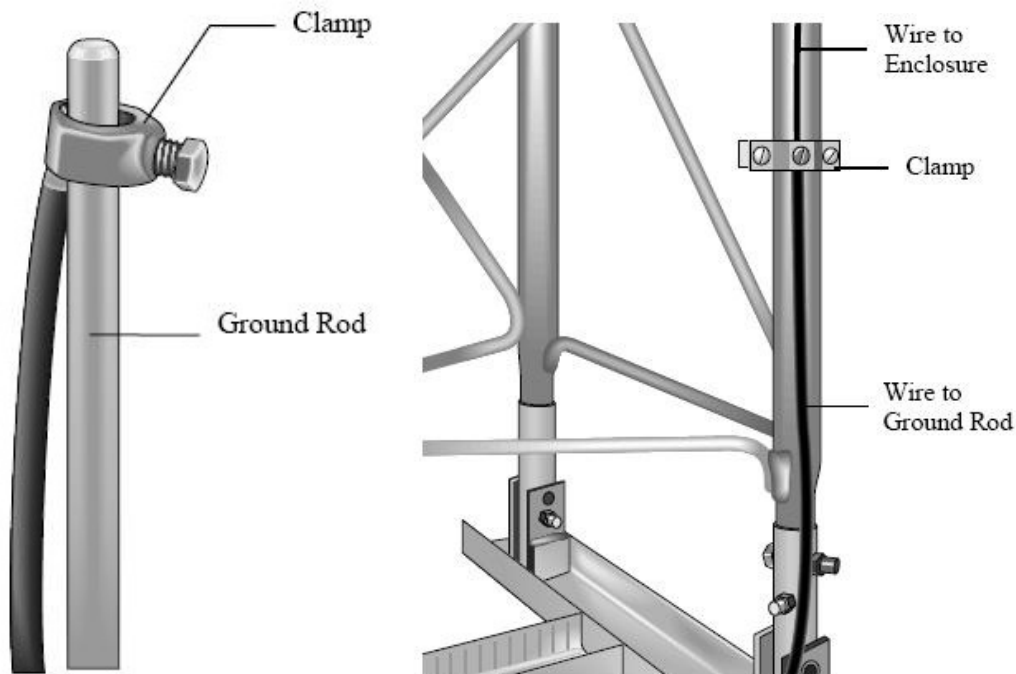


Figure 24: Ground Rod, Clamp & Tower Grounding Installation

3. Attach the tower grounding clamp to the tower leg (Figure 24). Route the 4 AWG wire attached to the ground rod up the tower leg to the grounding clamp. Loosen the set screw and insert the 4 AWG wire and the 24 AWG enclosure ground wire into the hole behind the set screw and tighten the set screw. Route the green wire to where the enclosure will be installed.

Tower Sensor and Instrumentation Installation

Eddy Covariance System

The primary components of the open path eddy covariance system are the CSAT3 three-dimensional sonic anemometer, the LI-7500 open path infrared gas analyzer (IRGA) and the HMP45C temperature and humidity probe. With this configuration, the system can measure carbon dioxide flux, latent heat flux, sonic sensible heat flux, momentum flux, a computed sensible heat flux, temperature, humidity, horizontal wind speed and wind direction. We are going to be installing additional sensors as well, to be detailed in the subsequent subsections.

1. The CSAT3, LI-7500 and HMP45C are mounted to the tower using a horizontal mounting arm and several Nu-Rail crossover fittings and short lengths of pipe.
2. The CSAT3 is attached to a horizontal mounting arm by a 0.75" by 0.75" crossover Nu-Rail, a 1" by 1" crossover Nu-Rail and a 12" length of 0.75" diameter pipe (Figures 25 and 26).
3. The LI-7500 can be mounted two ways, underneath the CSAT3 (Figure 25) or slightly behind the CSAT measurement volume (Figure 26) with a separation of about 15 to 20 cm. The IRGA should be set back from the anemometer to minimize flow distortions. Tilt the IRGA sensor head about 60 degrees from the

horizontal to minimize the amount of precipitation that accumulates on the windows.

The LI-7500 is attached to the horizontal mounting arm by a 1" by 0.75" crossover NU-Rail and the Head Mounting Kit, or a 1" by 0.75" crossover NU-rail, a 0.75" by 0.75" crossover NU-rail, a 10" length of 0.75" diameter pipe and the Head Mounting Kit (Figures 25 and 26).

4. Attach the enclosure mounting hardware to the LI-7500 electronics enclosure (Figures 27). Mount the enclosure hanger kit, and the CSAT electronics as shown in Figures 28 and 29.
5. Make sure to run power cables between the LI-7500 and CSAT3 electronics enclosures and the datalogger enclosure where the charge controller will be.
6. Measure the CSAT3 azimuth. To computer the correct compass wind direction, the station operator must enter the negative x-axis azimuth of the CSAT3 into the datalogger program. If the CSAT3 is installed such that it points into the prevailing wind, the negative x-axis is pointing into the prevailing wind. Take a compass azimuth of the negative x-axis (prevailing wind) and record it into the station log book for later use. Magnetic declination will have to be subtracted from this value when programming the CSAT3 (See Appendix 13). **For the Sierra Los Locos location, the magnetic declination is approximately 10°16' E, and for the Senoquipe location, the magnetic declination is 10°14' E.**
7. Mount the HMP45C radiation shield at the same height as the fast response sensors (CSAT3 and IRGA). The HMP45C radiation shield is mounted either to the tower leg or the end of the horizontal cross arm (Figure 30).

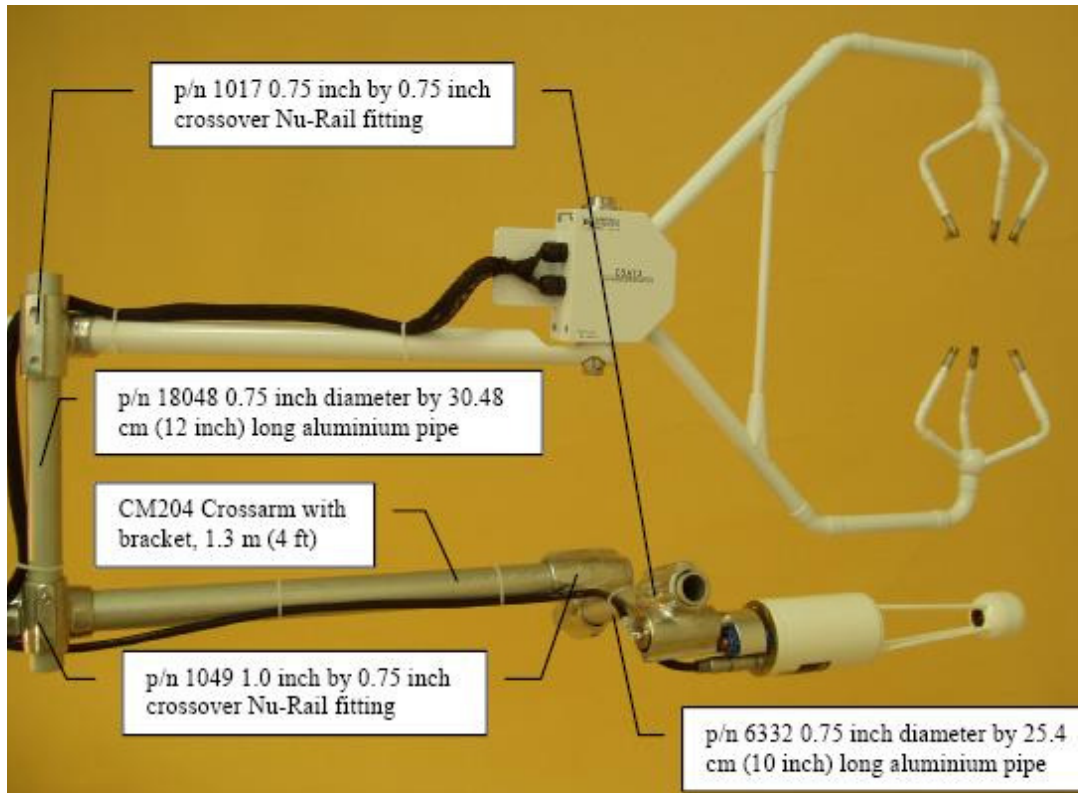


Figure 25: LI-7500 Mounted Under CSAT3

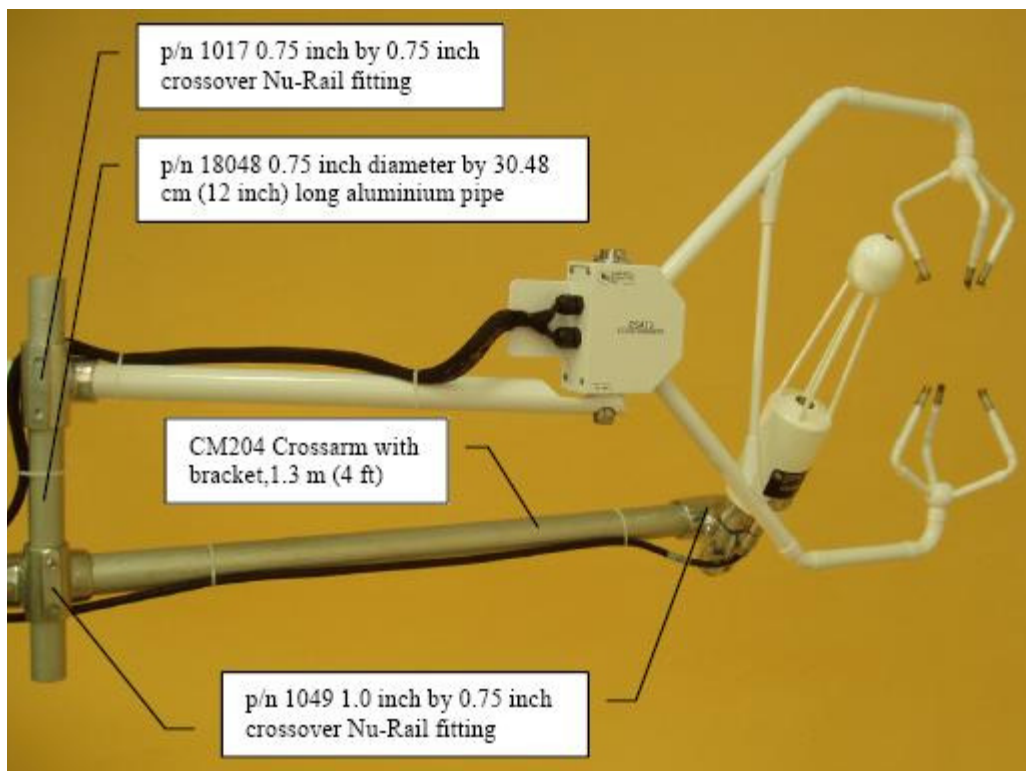


Figure 26: LI-7500 Mounted Behind CSAT3



Figure 27: LI-7500 Electronics Box Mounting Hardware



Figure 28: CSAT3 Electronics Box



Figure 29: CSAT3 & LI-7500 Electronics Box

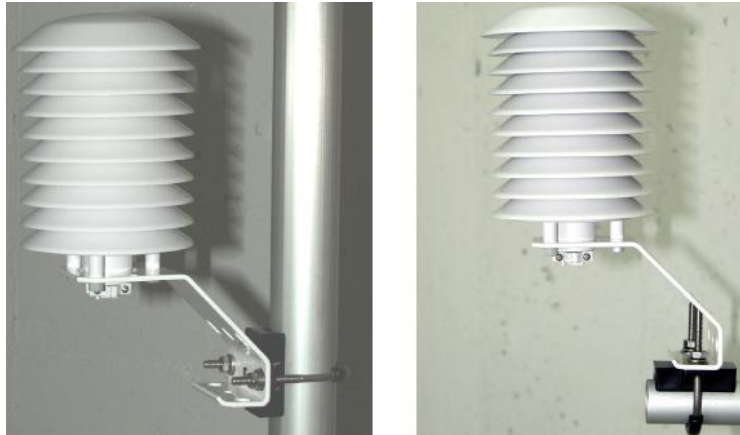


Figure 30: HMP45C Radiation Shield Mounting, left on Tower Leg, right on Horizontal Crossarm

Other Tower Sensors

1. There are two Huskeflux HFP01SC self-calibrating soil heat flux plates. These are setup with a four-probe TCAV (averaging) thermocouple and a CS616 water reflectometer (see Figure 31).

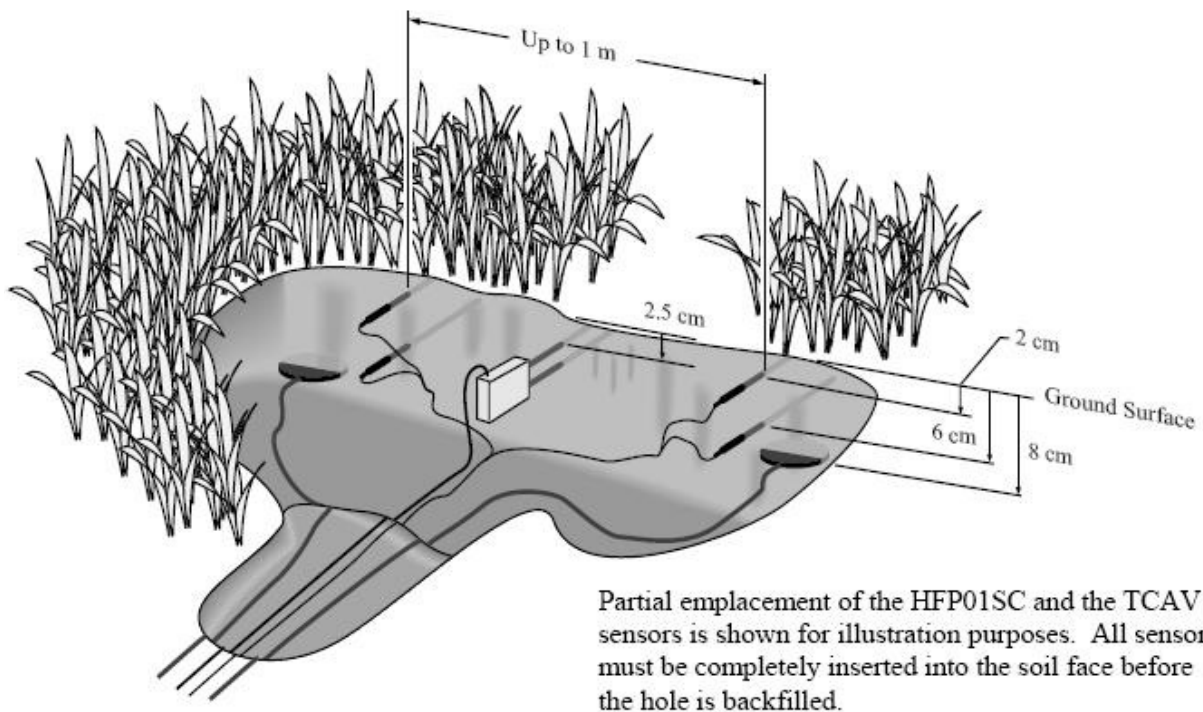


Figure 31: Partial emplacement of the HFP01SC, the TCAV and CS616.

The location of the heat flux plates and thermocouples should be chosen to be representative of the area under study. If the ground cover is extremely varied, it may be necessary to have additional sensors to provide a valid spatial average of soil heat flux.

Use a small shovel to make a vertical slice in the soil. Excavate the soil to one side of the slice. Keep this soil intact so that it can be replaced with minimal disruption.

The sensors are installed in the undisturbed face of the hole. Measure the sensor depths from the top of the hole. With a small knife, make a horizontal cut eight centimeters below the surface into the undisturbed face of the hole. Insert the heat flux plate into the horizontal cut.

NOTE: Install the HFP01SC in the soil such that the side with the text “this side up” is facing the sky.

CAUTION: In order for the HFP01SC to make quality soil heat flux measurements, the plate must be in full contact with the soil.

Never run the sensor leads directly to the surface. Rather, bury the sensor leads a short distance back from the hole to minimize thermal conduction on the lead wire. Replace the excavated soil back into its original position after all the sensors are installed.

2. The 3 remaining water content reflectometers need to be placed in the surrounding soil. Probe rods can be inserted vertically or horizontally into the soil surface, or buried at any orientation to the surface. Ask Luis how to mount these sensors.

The probes must be inserted such that no air voids are created around the rods, and that the rods remain as parallel as possible. A probe insertion guide can be used to minimize errors due to improper insertion.

Standard calibration for the CS616 probe is valid for loamy soils with low organic content. In other types of soils reporting the output in units of period will make it possible to apply your own calibration during the post processing of data.

3. A Texas Instruments tipping bucket rain gauge will be installed near the tower as well. This is the same or a very similar model to what is used in the hydrological stations throughout the Sonora and San Miguel Basins.

Mount the rain gauge to a vertical pipe (see Figure 32 for this install). Mounting the gauge directly to the tower is not recommended.

Dig a 6” diameter hole, 24” deep.

Center a 1 ¼” to 2” IPS pipe in the hole and fill the hole with concrete. Use a level to plumb the pipe as the hole is filled.

- After the concrete has cured, attach the rain gage to the top of the pipe with the hose clamps provided. Route the sensor leads to the datalogger in plastic or metal conduit.
4. The remaining 3 of the four-probe, averaging thermocouples that will need to be buried near the tower. Ask Luis where these need to be placed.
 5. The CMP3 Pyranometer is mounted to the tower; its mounting hardware should already be mounted to it. The CMP3 is usually installed horizontally, but can also be installed at any angle including an inverted position. In all cases it will measure the flux that is incident on the surface that is parallel to the sensor surface.

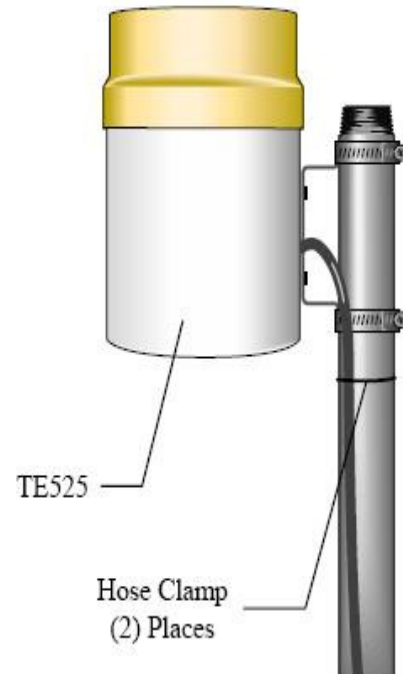


Figure 32: Texas Electronics Rain Gage Installation

Site the CMP3 to allow easy access for maintenance while ideally avoiding any obstructions above the plane of the sensing element. It is important to mount the CMP3 such that a shadow will not be cast on it at any time (the southern side of tower is a good start). Consult Luis on exact location.

If this is not possible, try to choose a site where any obstruction over the azimuth range between earliest sunrise and latest sunset has an elevation not exceeding 5 degrees. Diffuse solar radiation is less influenced by obstructions near the horizon. For instance, an obstruction with an elevation of 5 degrees over the whole azimuth range of 360 degrees decreases the downward diffuse solar radiation by only 0.8%.

The sensor should be mounted with the cable pointing towards the nearest magnetic pole, e.g. in the Northern Hemisphere point the cable towards the Magnetic North Pole.

The CMP3 needs to be installed as follows (consult Figure 33):

Install the pyranometer mounting hardware to the crossarm or horizontal pipe.

Loosely mount the pyranometer on the mounting arm. Do not fully tighten the two mounting screws.

Turn the leveling screws as required to bring the bubble of the spirit level within the ring.

Tighten the mounting screws to secure the assembly in its final position. Check that the pyranometer is still correctly leveled and adjust as necessary.

Attach the white plastic sun screen to the pyranometer.

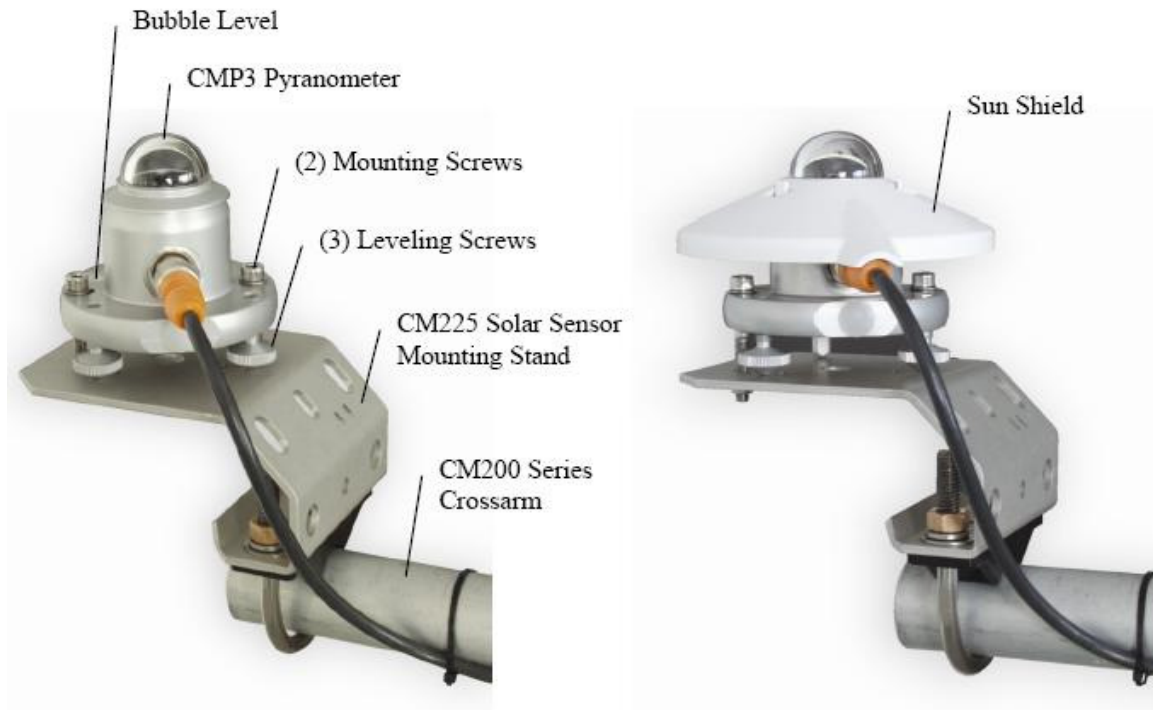


Figure 33: CMP3 Pyranometer and Mounting Stand Installation

6. The CNR2 Net Radiometer also needs to be mounted to the tower. For measurement of the net radiation, it is important that the instrument is located in a place that is representative of the entire region that one wishes to study.

When installed on a mast, the preferred orientation should be such that no shadow is cast on the net radiometer at any time during the day. In the Northern Hemisphere, this implies that the net radiometer should be mounted south of the mast. It is suggested that the CNR2 is mounted at a height of at least 1.5 meters above the surface to avoid the shading effects of the instrument on the soil and to promote spatial averaging of the measurement. If the instrument is H meters above the surface, 99% of the input of the lower sensors comes from a circular area with a radius of $10 H$. Shadows or surface disturbances with radius $<0.1 H$ will affect the measurement by less than 1%.

Installation is simple. Tighten the pipe reducing coupler to a suitably sized mounting arm (see Figure 34).



Figure 34: CNR2 and Mount Installed to Mounting Arm

Solar Panel Wiring

1. Before installing the solar panels to the tower, make sure they are correctly wired. If not, follow the following steps.
2. Using a flat blade screwdriver, remove only the appropriate "KNOCK-OUTS" from the sides of the "G" box. Route wires through the knock-outs and clamps refer to J-Box diagram (see Figure 35).

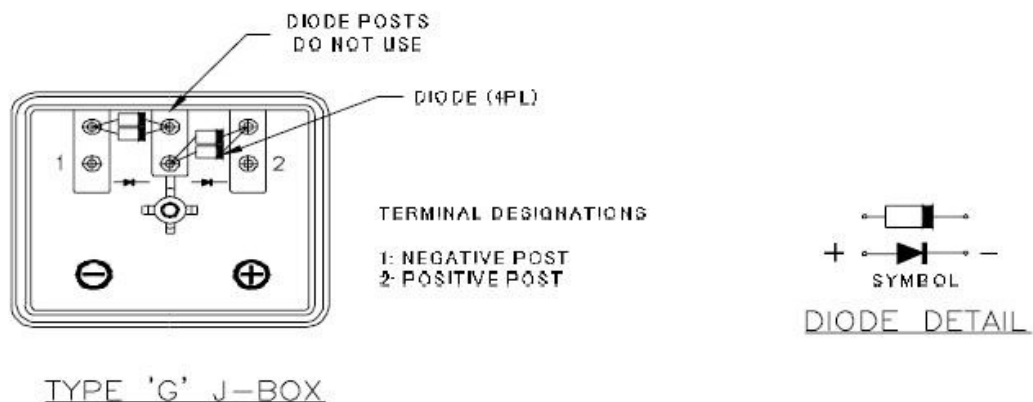


Figure 35: Solar Panel Electrical J-Box

3. Gently hand tighten the terminal screws with cross tip (Phillips head) screwdriver. Do not over tighten, as the terminal can be damaged. The output wiring from the panels are run to a separate enclosure to the next component the charge controller. After checking that module wiring is correct, close and secure all the junction boxes. Use a Phillips head screw driver to secure all screws on the junction box cover to ensure a waterproof seal.

Enclosure Installation

All instrumentation (datalogger, charge controlled and communication peripherals) are mounted in the enclosure. A PVC bulkhead port is installed in the enclosure for routing the sensor and communication cables to the instrumentation.

1. Position the enclosure on the north side of the tower (northern hemisphere) as shown in Figure 36. Attach the enclosure with the U-bolts provided.
2. Route the 14 AWG wire from the brass tripod grounding clamp (Tower Grounding Section) to the enclosure grounding lug. Strip one inch of insulation from each end of the wire and insert the end of the wire into the grounding lugs and tighten the set screws.

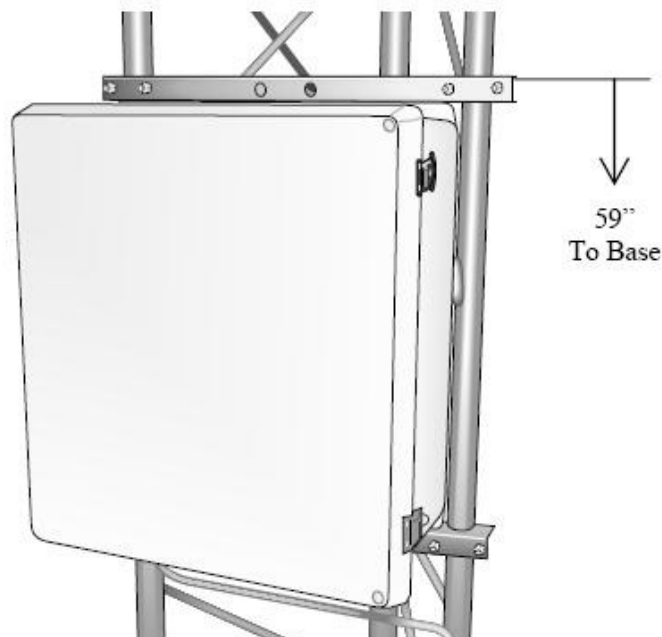


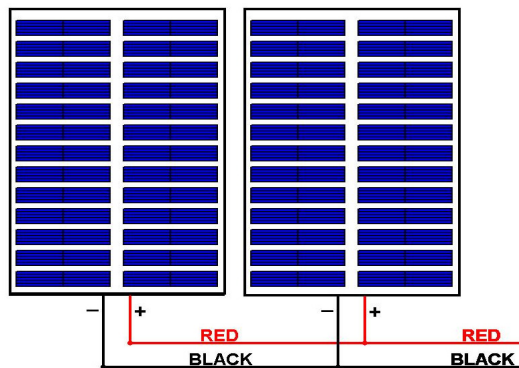
Figure 36: Enclosure Mounting

Enclosure Power Supply Installation

The datalogger and tower instrumentation are powered by a combination of 2 solar panels and 2 deep-cycle batteries. A charge controller must be installed to regulate current and voltage levels to the instrumentation and the batteries.

1. The two SunXtender deep-cycle batteries are 12 volts and therefore must be wired in parallel to maintain a system voltage of 12 V. Wire the batteries as shown in Figure 37 with the gray outdoor 2-conductor wire and the solderless ring terminals. Wire the negative battery terminal to the tower ground either at the enclosure or the rod itself. When you have wired the batteries, place each of them into one of the black battery boxes and tighten the straps.
2. The two 65W solar panels must be wired in parallel as well as shown in Figure 38. Two separate sets of wires from each terminal should go to the charge controller (do not connect them yet).

Solar Panel Parallel
Wiring Diagram



Connect Solar Panel Wires Together
at the Charge Controller

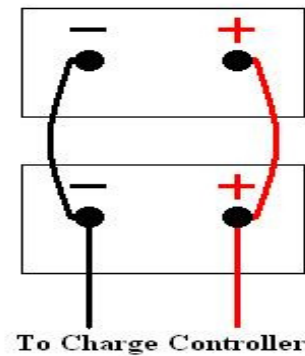


Figure 37: Parallel Solar Panel Wiring

Figure 38: Parallel Battery Wiring

3. The charge controller being used and its appropriate wiring are shown in Figure 39. Wire the terminals in the order indicated in the figure and described below.

Figure 39: Charge Controller Wiring

4. Connect the BATTERIES first. Use care that the bare wires do not touch the metal case of the controller.
5. Connect the SOLAR panel array next. The green LED indicator will light if sunlight is present.
6. Connect the LOAD last. This model includes LVD (low voltage disconnect) and the red LED indicator. If this lights, the battery capacity is low and should be charged before completing the system installation.
7. The controller should have a jumper installed between the negative load terminal and the flooded or sealed connect terminal. We are using sealed batteries, make sure that this jumper is still there, else replace.

8. For most effective surge protection, make sure that the battery negative conductor is properly grounded.

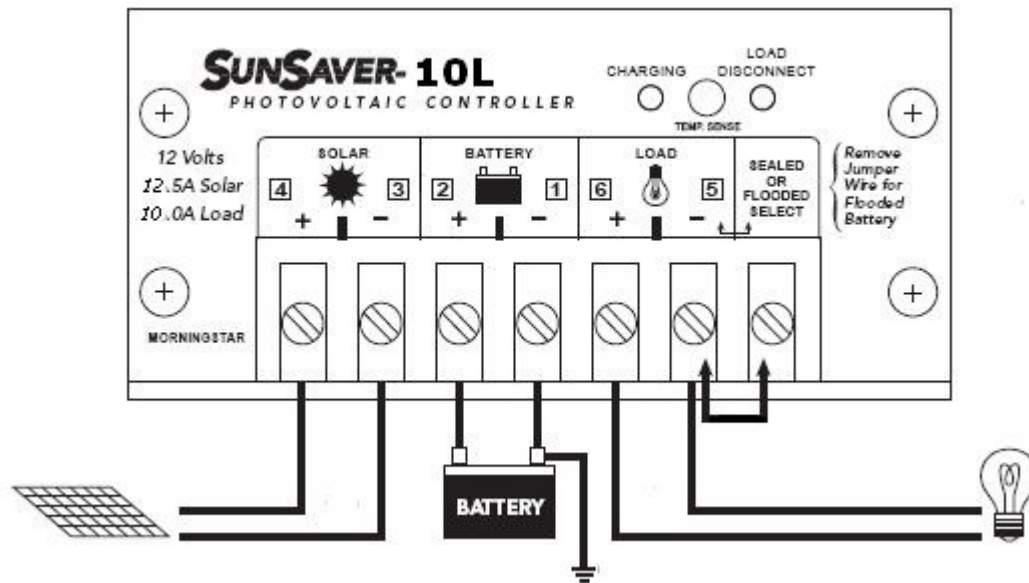


Figure 40: Parallel Battery Wiring

Connecting Sensors

After the sensors have been mounted, route the sensor leads through the entry hole in the bottom of the enclosure and to the datalogger. Secure the leads to the left side of the enclosure using cable ties and tabs (as in Figure 40). These may be found in the enclosure supply kit. Any excess cable should be neatly coiled and secured to the tabs.

To connect a lead wire, loosen the appropriate screw terminal and insert the lead wire (wires should be stripped 5/16"), and tighten the screw using the screwdriver provided with the datalogger. A datalogger program has already been developed; the sensors will have to be wired to specific channels as shown in the wiring diagram in Figure 41.

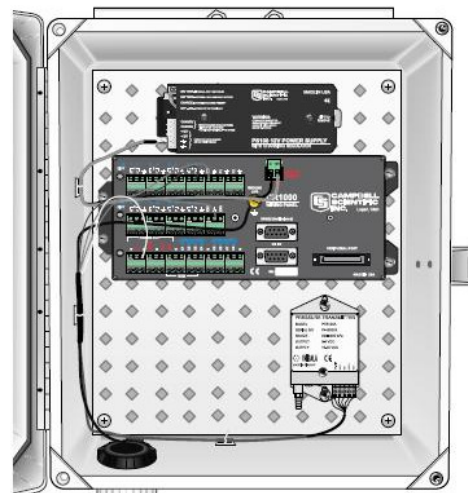


Figure 41: A Neatly Organized Enclosure

DATALOGGER WIRING INFORMATION

CS616 Water Content Reflectometer

(1) Green (G) → 1H Orange (O) → C1 Clear (C) → G Black (B) → G Red (R) → 12V	(2) (G) → 1L (O) → C2 (C) → G (B) → G (R) → 12V	(3) (G) → 2H (O) → C3 (C) → G (B) → G (R) → 12V	(4) (G) → 2L (O) → C4 (C) → G (B) → G (R) → 12V
--	---	---	---

Type 3 (Chromel-Constantan) Thermocouple

(1) Purple (P) → 6H Red (R) → 6L	(2) (P) → 7H (R) → 7L	(3) (P) → 8H (R) → 8L	(4) (P) → 9H (R) → 9L
--	---	---	---

HMP45C Relative Humidity

& Temperature Sensor

White (W) → $\frac{1}{\text{III}}$
Yellow (Y) → 3H
Blue (Bl) → 3L
Black (B) → G
Clear (C) → G
Red (R) → 12V

CM3 Pyranometer

(W) → $\frac{1}{\text{III}}$
(R) → 5H
(Bl) → 5L
(C) → G

Rain Gauge

(B) → $\frac{1}{\text{III}}$
(R) → P1

PTempC

→ Panel Temperature

CSAT3 3D Anemometer and LICOR 7500

CSAT3

Data	Green (G) → SDM-C1
Clock	White (W) → SDM-C2
Enable	Brown (Br) → SDM-C3
Ref.	Black/Clear → G

CS7500

	Gray (Gr) → SDM-C1
	Blue (Bl) → SDM-C2
	Brown (Br) → SDM-C3
	Black/White → G

External Power Supply

CSAT3 Power	(Red) → 12V
CSAT3 Power Ref.	(Black) → G
CS7500 Power	(Red/White) → 12V
CS7500 Power Ref.	(Red/Black) → G
CS7500 Ground	(Green) → G

Figure 42: Datalogger Wiring Diagram

Sealing and Desiccating the Enclosure

When all the sensors and power supply lines have been routed to the enclosure and all have been confirmed to work, the enclosure should be sealed and desiccated. The materials should be included in the kit that came with the enclosure.

Items in the enclosure supply kit are used to strain relief the sensor leads, seal cable entry, and desiccate the enclosure (see Figure 42). This kit should include the following:

- (4) Desiccant packs
- (1) Humidity indicator card
- (6) 4-inch cable ties
- (6) 8-inch cable ties
- (4) Cable tabs
- (1) 4 oz. sealing putty

1. If you have not done so already, secure the sensor leads to the left side of the enclosure and to the datalogger using the cable ties and tabs.

2. Seal around the sensor leads where they enter the enclosure. Place a roll of putty around the sensor leads and press it around the leads and into the coupling to form a tight seal.

3. Remove the RH indicator card and two desiccant packs from the sealed plastic bag. Remove the backing from the

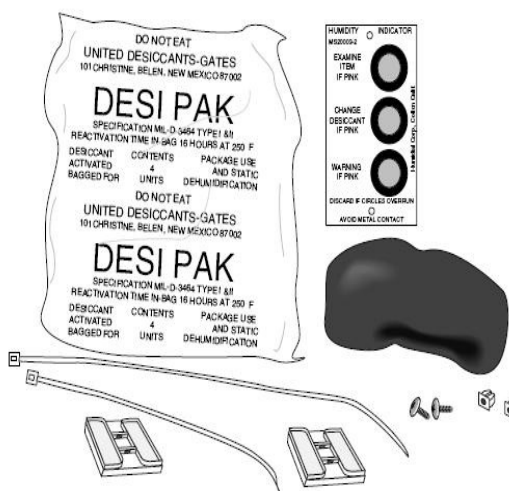


FIGURE 3.4-1. Enclosure Supply Kit

Figure 43: Enclosure Supply Kit

indicator card and attach the card to the right interior wall of the enclosure. The humidity indicator card has three colored circles that indicate the percentage of humidity. Desiccant packs inside the enclosure should be replaced with fresh packs when the upper dot on the indicator begins to turn pink. The indicator card does not need to be replaced unless the colored circles overrun.

**EXPERIMENT 5: HYDROMETEOROLOGICAL STATION
INSTALLATION (10) INCLUDING CALIBRATION/SOIL
SAMPLING - RIO SONORA/SAN MIGUEL BASIN**

Station locations

We will find the station locations using a GPS unit with the station coordinates already uploaded in it. This year locations are listed in Table 2 below and shown on the following maps (Figure 43 - 48). Note: The GPS coordinates are an approximation of the given environmental characteristics sought for analysis; therefore, the characteristics are the main features that should be accounted for during the placement of the new stations.

Table 2: Coordinates of new stations in Rio Sonora/San Miguel basin

Station ID	X	Y	Landuse	Slope (degrees)	Elevation (meters)	Aspect
160	559285	3259488	Subtropical shrub	<1	430	Flat
161	586516	3267023	Sparse woodland	<1	520	Flat
162	584711	3289132	Grassland	<1	620	Flat
163	563696	3304571	Sparse woodland	5	757	Northeast
164	563076	3315262	Sparse woodland	18	808	West
165	556307	3316406	Subtropical shrub	2	879	East
166	586089	3365786	Sparse woodland	19	1106	South
167	573580	3382849	Grassland	<1	1040	Flat
168	598542	3401284	Sparse woodland	3	1188	West
169	561660	3405998	Riparian Mesquite	<1	1260	Flat

*Projection: UTM Zone 12. Datum: WGS-84

San Miguel and Sonora Basin STATIONS NETWORK (NMT) Sierra Los Locos Sub-basin

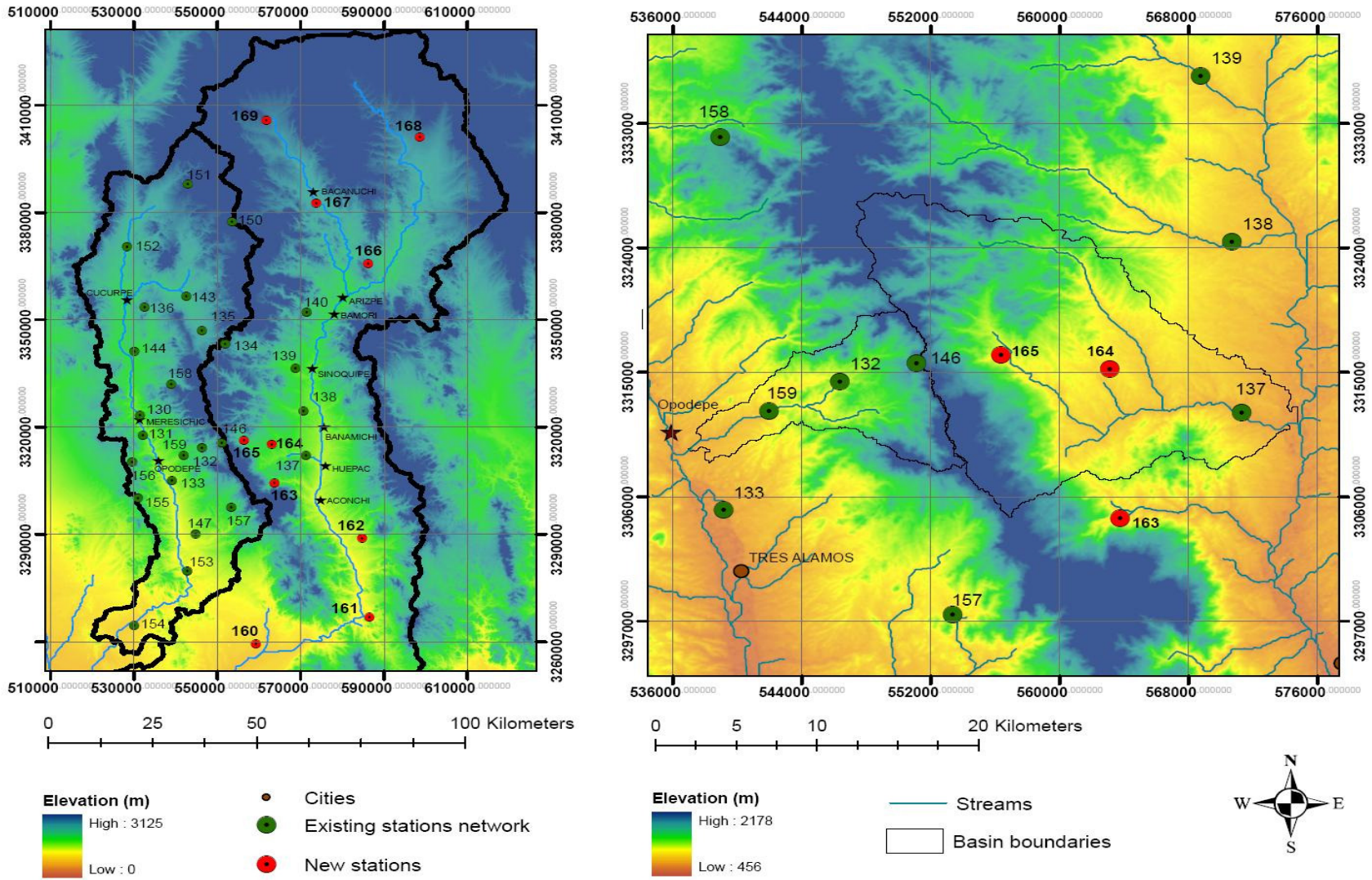


Figure 44: Map of New Station Points

LOCATION OF SITE 160

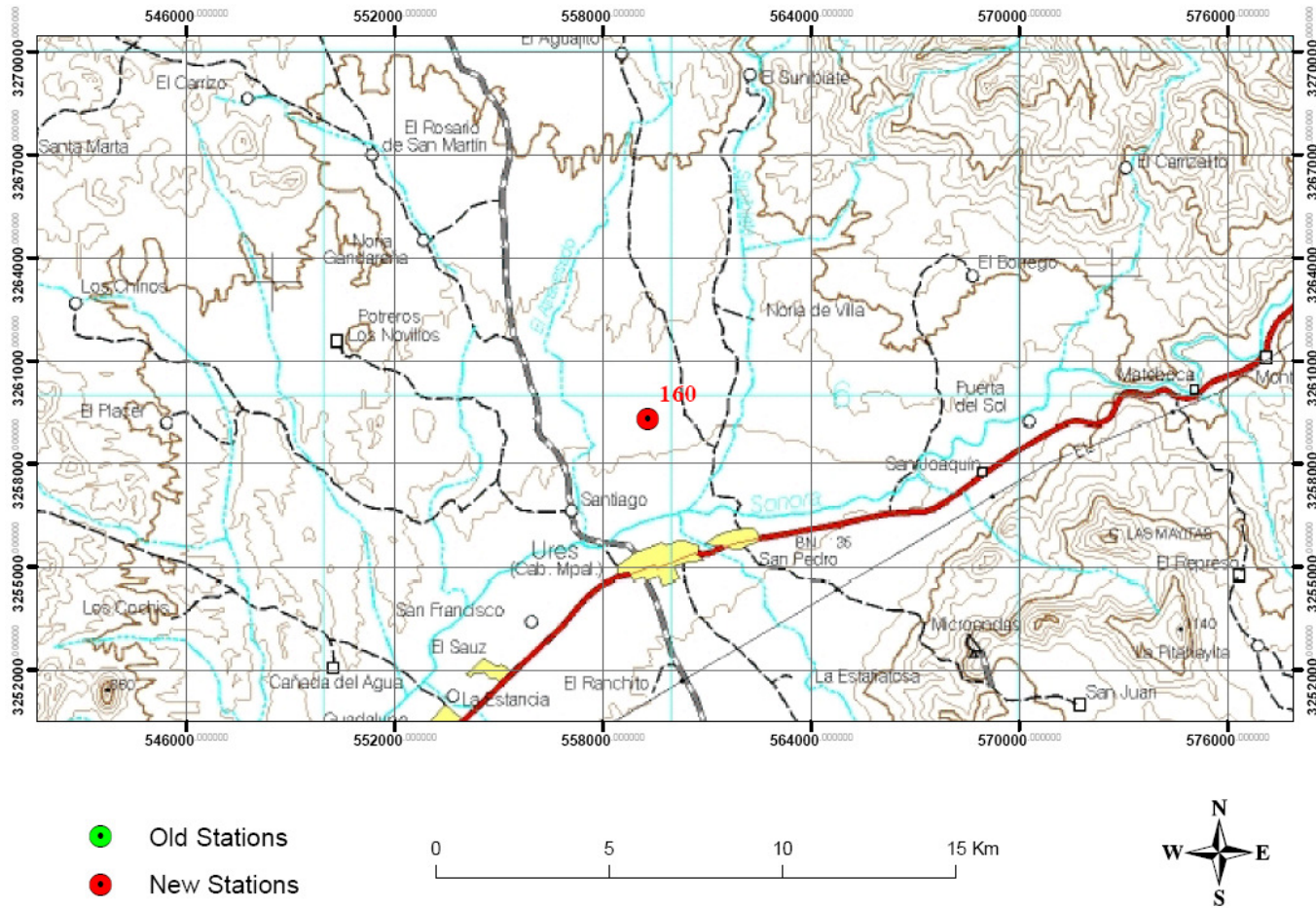
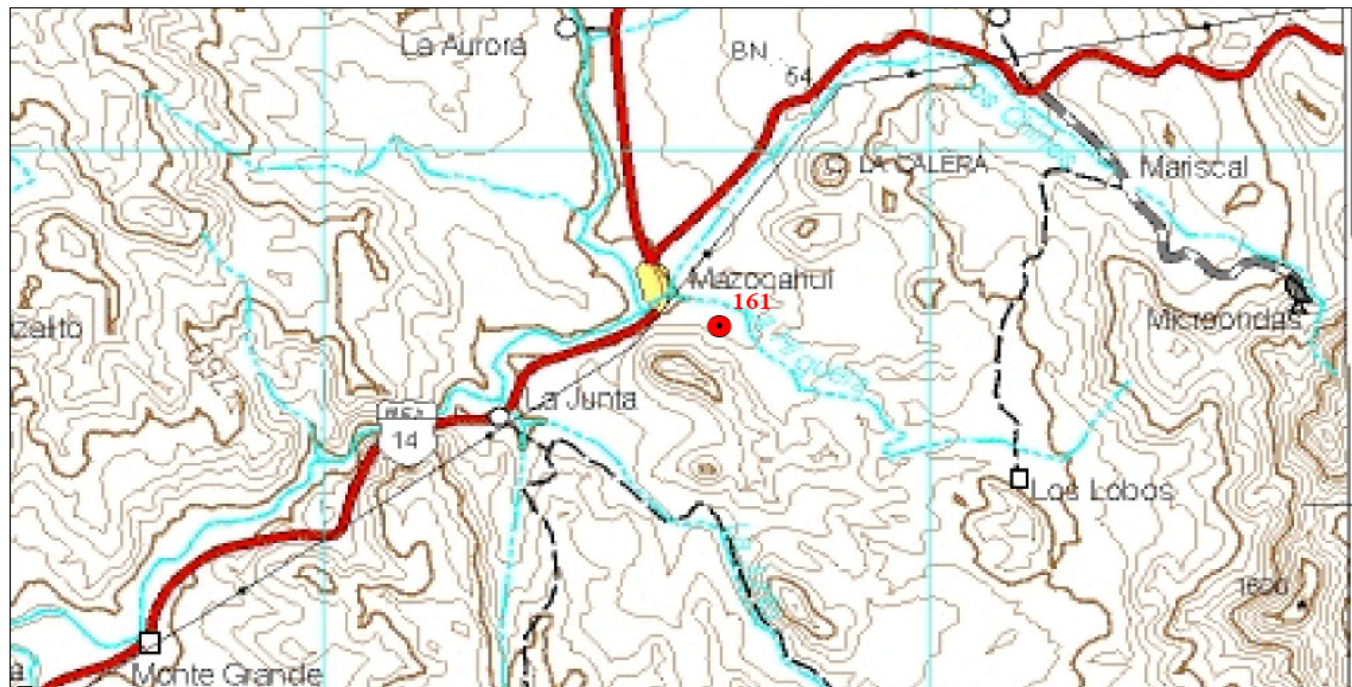


Figure 45: Map of SITE 160

LOCATION OF SITE 161



- Old Stations
- New Stations



Figure 46: Map of SITE 161

LOCATION OF SITE 162



- Old Stations
- New Stations

0 5 10 15 Km



Figure 47: Map of SITE 162

LOCATION OF SITES 163 TO 165

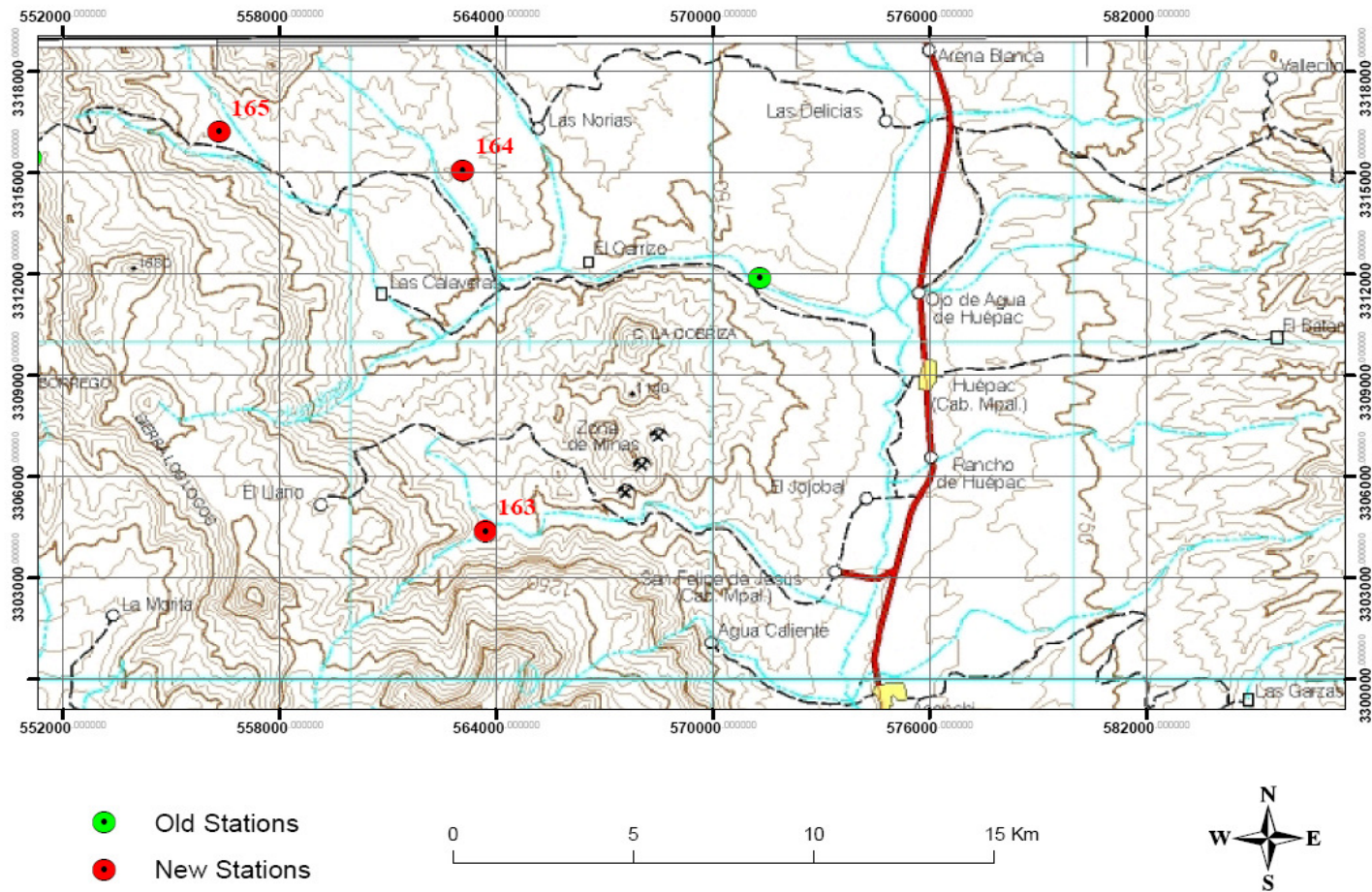


Figure 48: Map of 163 to 165

LOCATION OF SITE 166

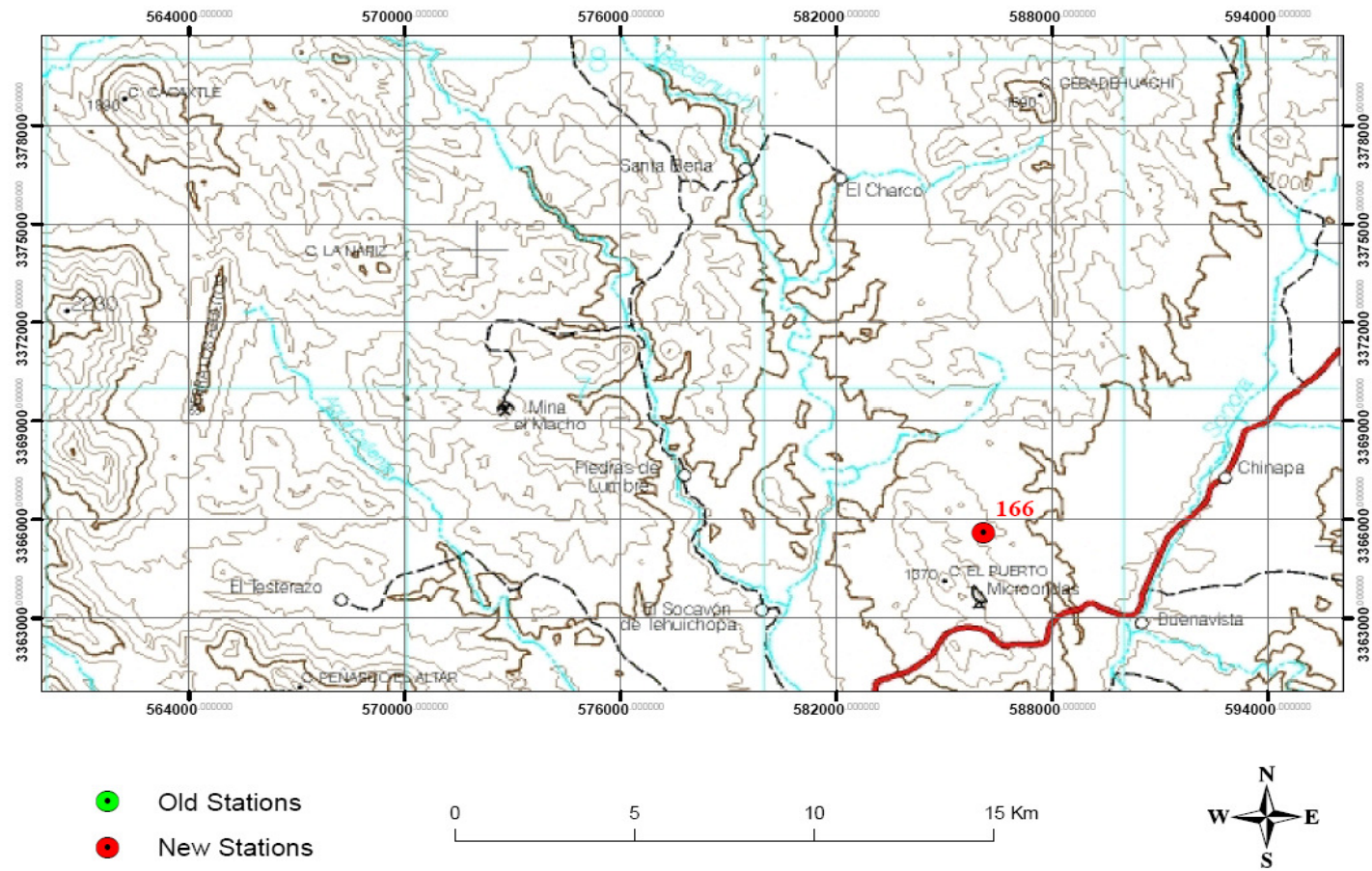


Figure 49: Map of SITE 166

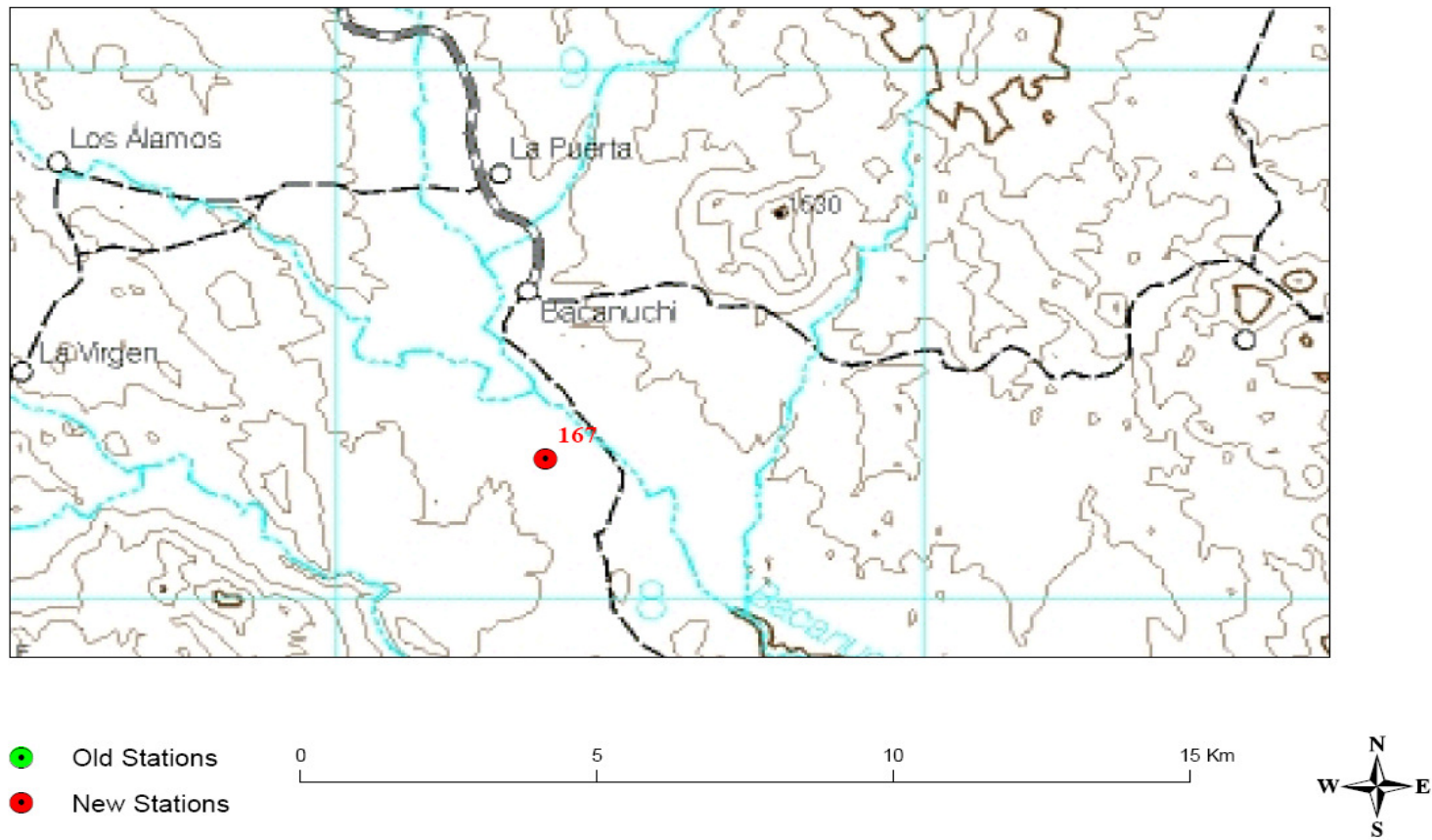
LOCATION OF SITE 167

Figure 50: Map of SITE 167

LOCATION OF SITE 168

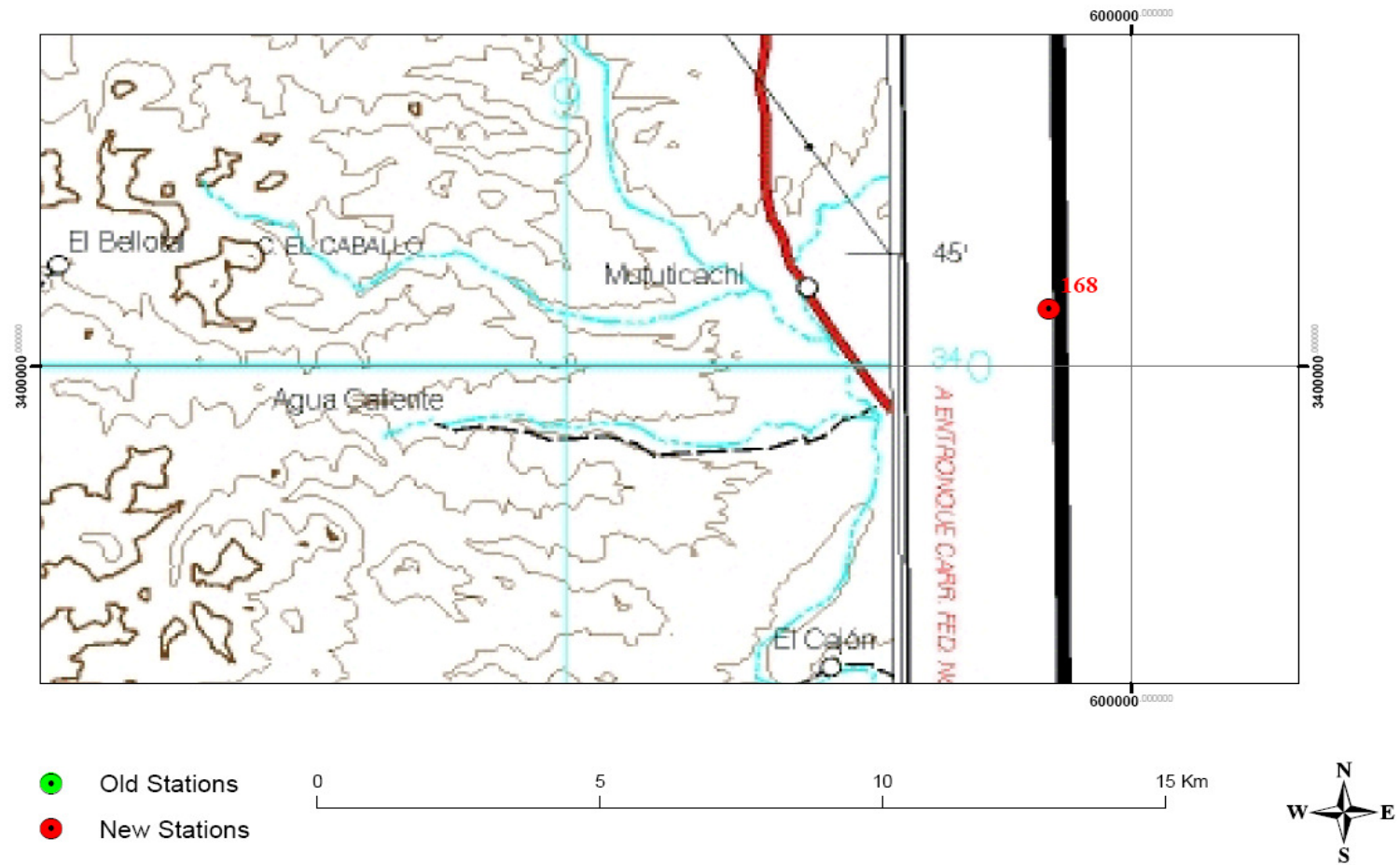


Figure 51: Map of SITE 168

LOCATION OF SITE 169

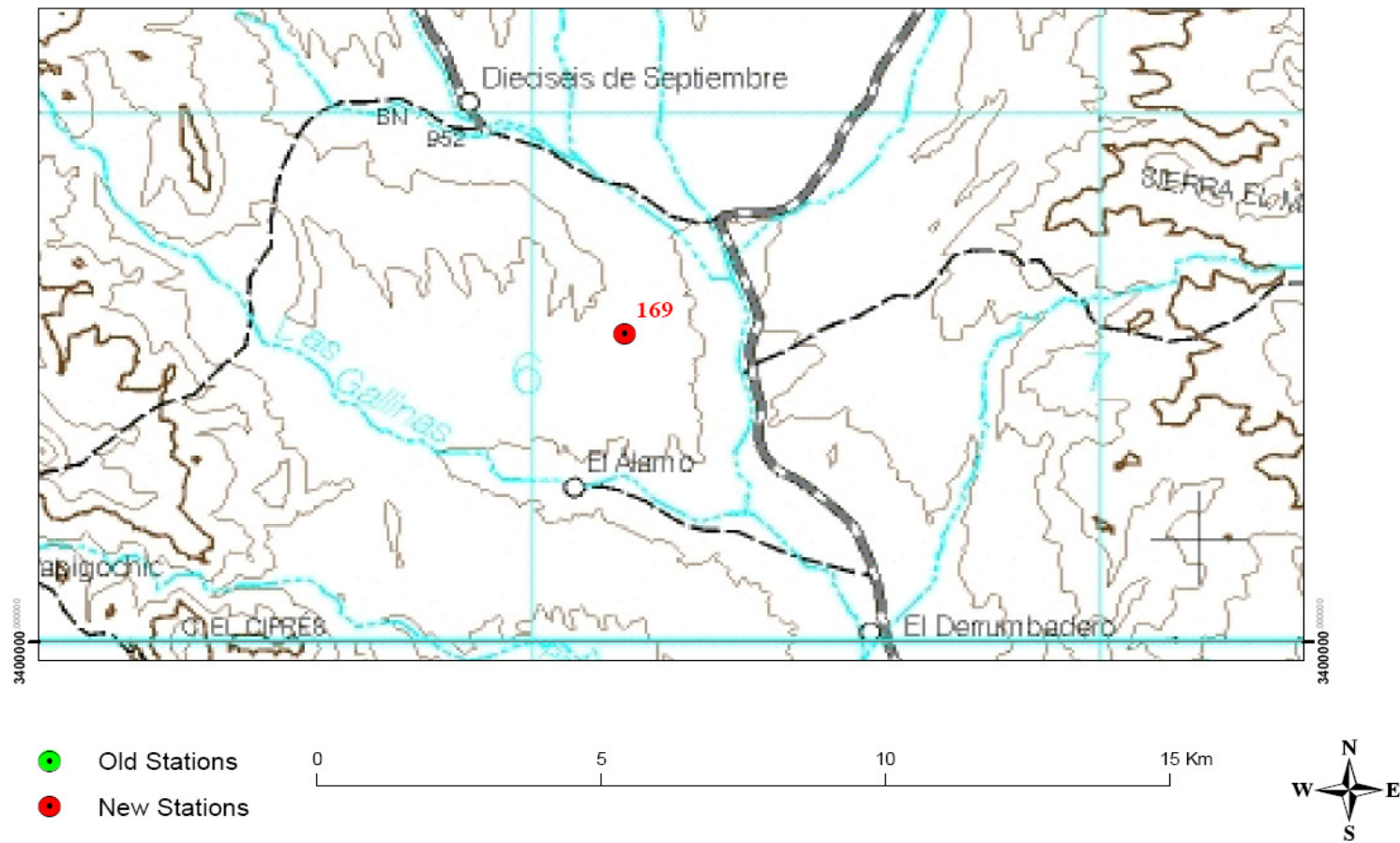


Figure 52: Map of SITE 169

Once the station is located, a 1.5 inches inner diameter galvanized pipe will be inserted in a small soil pit (Figure 44 b,c). For the soil pit we recommend to use a soil digger like the one shown in the figure 1a, shovels and pick will also required. In addition, we need to be sure that the post is properly leveled; we can use a bubble level to reach this. Cement will be needed for appropriate deployment of the station. One extra pole will be inserted in the soil in order to attach the rain gauge. For that reason we will have two posts by site, one for to support the enclosure and the solar panel, and the other for the tipping bucket rain gauge.



Figure 53: a) Soil digger recommend for post installation .b) Installation of metal pipes in the field .c) Final result.

Next step consist in attaching the enclosure to the post. For this purpose we need brackets and 1/2" wrench. Insert the bracket in to enclosure holes as it is shown in figure 45 and use the wrench to fix it.



Figure 54: a) Fixation of the enclosure to the post. b) Final result

When enclosure installation is done, the solar panel should be installed in the upper part of the post, ½” wrench is required to fix it. The panel must pointing south with 43 degrees of inclination as shown in Figure 46.



Figure 55: Solar panel Installation

Solar panel connection to data logger:

The Solar panel needs to be plugged in to the PS100 12V battery. Both cables will be inserted in the CHARGE terminal of the battery (Figure 47), **IMPORTANT!!** Be sure that the battery is **TURNED OFF** when you are connecting the cables. Once connected, then turn it on. The red light will led in approximately 1 hour.

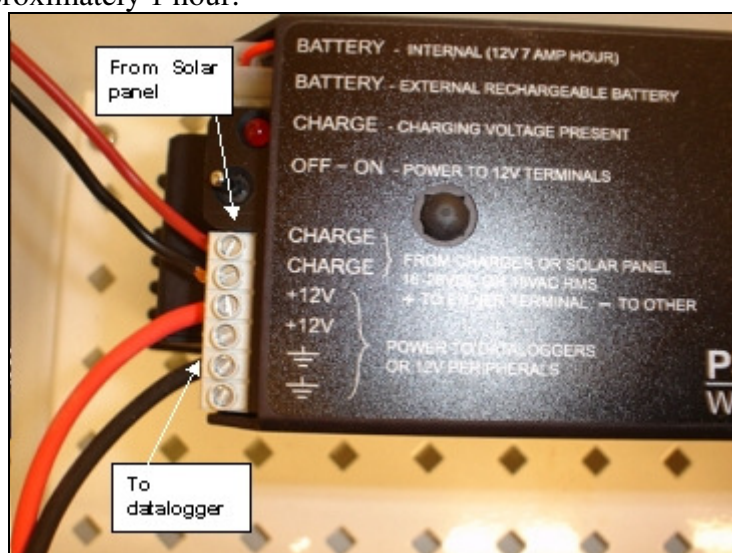


Figure 56: Battery connections

Next step consists on plug the battery to the datalogger. The datalogger model is a CR1000 from Campbell scientific. Figure 4a shows the connections from the battery 12V and ground terminals to the datalogger. Figure 48 shows the appropriate connection of the datalogger with the cables coming from the battery (Remember: red color cable is 12V and black cable is ground).



Figure 57: Solar panel connection in to the datalogger

Sensors:

The sensors that will be connected to the CR1000 datalogger will be:



- 1) Stevens Hydra probe model SDI-12: Two sensors will be connected to the datalogger. One sensor will be installed at 5cm depth in the soil. The other one will be inserted at 10 cm depth.

Figure 58: Stevens Hydra Probe Model SDI-12

- 2) TR-525 typing bucket rain gauges.



Figure 59: TR-525 Tipping Bucket Rain Gauge

Connections:

The sensors must be connected to the datalogger ports according to the following table:

Sensor	Characteristic	Wiring	Datalogger Port
Hydra probe SDI-12	Depth 0-5 cm	Blue Black Red Clear	C5 Ground (G) 12V Ground
Hydra probe SDI-12	Depth 5-10 cm	Blue Black Red Clear	C6 Ground (G) 12V Ground
Rain gauge TE525	Tipping bucket rain gauge	Black	P1 (pulse port)
		White	Ground
		Clear	Ground

Hydra probe connection: As showed before Hydra probe at depth 0-5 cm. should be connected in with the sequence: Blue wire, port C5. Black and clear wires on ground ports (G), and finally red wire must be inserted in 12V port. Check figure 51 to see the location of the datalogger ports.

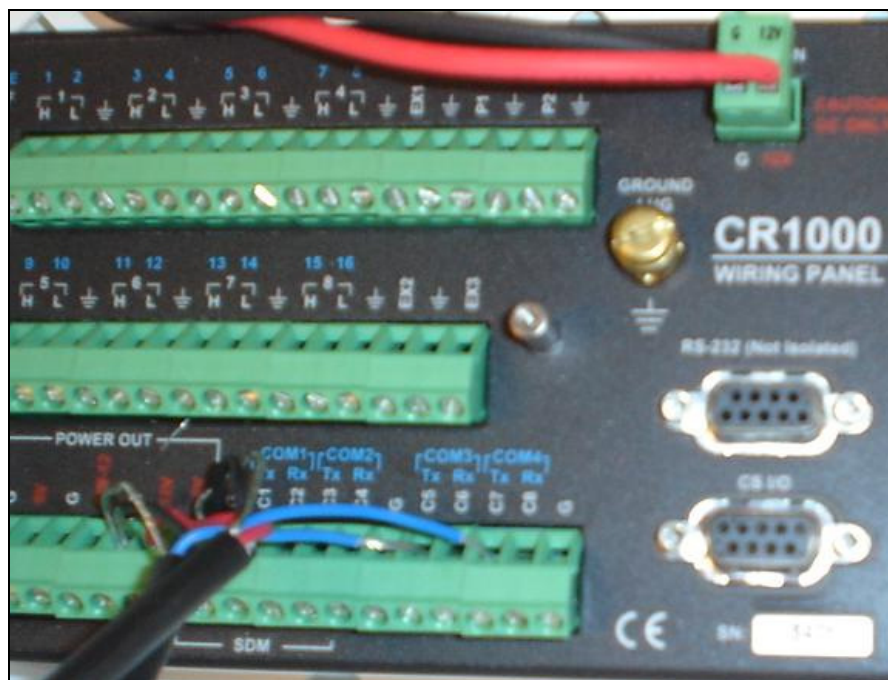


Figure 60: Wiring connections for Hydra probe SDI-12 at 5cm depth. Remember that blue wire sends the sensor signal to the datalogger, black and clear are ground and red is the source of power for the sensor.

For Hydra probe at depth 5-10 cm. should be connected in with the sequence: Blue wire, port C6. Black and clear wires on ground ports (G), and finally red wire must be inserted in 12V port. In addition, 6" rain gauge must be inserted with the following sequence: Black, Port P1, white and clear wires, ground (G) as it is shown in the following Figure 52.

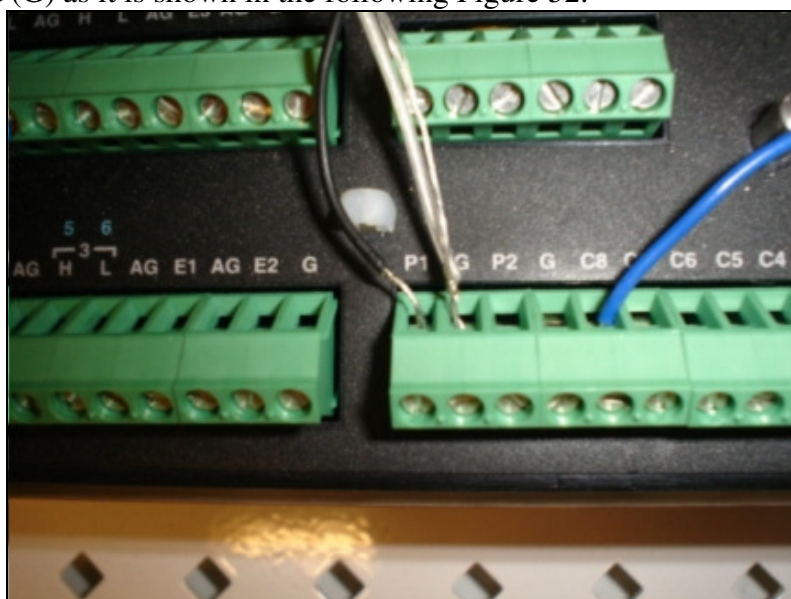


Figure 61: Wiring connections 6" diameter rain gauge. Remember that black wire sends the sensor signal to the datalogger, white and clear, are ground.

Deployment of the soil moisture/soil temperature sensors in the field:

You need to dig a hole of approximately 20 cm depth and 50 cm long with a shovel. Use a measuring tape to place the sensors in the vertical face of the soil pit. Check the Figure 53 in order to put the sensors in the soil pit.



Figure 62: Vertical placement of sensors

STATIC / DYNAMIC CALIBRATION OF TIPPING BUCKET RAIN GAUGES - RIO SONORA/SAN MIGUEL

Introduction

The static calibration approach simply uses a burette to check the water volume that causes the bucket of the tipping bucket (TB) rain gauge to tip. This approach is thus primarily concerned with the accuracy of an individual tip volume in the sense of consistency of the tip volumes between the two buckets of an individual rain gauge.

The dynamic calibration approach employs a calibration kit by Hydrological Services, Inc., which uses a constant flow-constant head-measuring device that dispenses prespecified flow rates to the rain gauge. The dispenser delivers water at five nominal flow rates (50, 100, 200, 300, or 500 mm h⁻¹) using five corresponding calibrated nozzles. This approach is thus concerned with the accuracy of the rain measured over a range of rainfall intensities, particularly for the higher intensities where the fast operation of the tipping mechanism may not be accurately capturing the rain volume.

Goal

To statically and dynamically calibrate tipping bucket rain gauges using a burette and a calibration kit from Hydrological Services, Inc respectively.

Materials

- Calibration kit
- Burette
- Enough water for calibration
- Chronometer
- Field notebook
- Allen wrench
- Laptop with appropriate software for downloading data.

Procedure

IMPORTANT:

- This experiment should not be done during a rainfall event.

Datalogger data download:

- Switch off the datalogger. This will be switched on later after the entire static/dynamic calibration procedures.

Download the data: the procedure is similar to that in the Appendix on 'Collecting data from datalogger to PC for the continuous soil moisture / temperature measurements'.

Static calibration:

At a rain gauge location where static calibration is required, the steps to be followed are:

1. Check if the buckets are empty. Fill the burette with water and release this water into an empty bucket (Figure 54). Write down the volume that causes the bucket to tip. Do at least 5 such readings for each bucket (enter into the field notebook), remembering to make sure that the bucket is empty before it is filled with water each time by the burette. Calculate an average of these 5 readings for each bucket, and enter into the field notebook.



Figure 63: Burette filling a TB rain gauge bucket with water during the static calibration procedure

2. There are two models of rain gauges installed in the Sierra Los Locos Basin: the Texas Electronics model TE525 (Figure 55), and the Hydrological Services model TB3-0.01-P (Figure 56). For the TB3-0.01-P model, the static calibration procedure is complete at this point, please proceed to the dynamic calibration procedure section. For the TE525 model, continue to step 3 in this static calibration procedure.



Figure 64: The Texas Electronics model TE525



Figure 65: The Hydrological Services model TB3-0.01-P

3. If the average tipping volumes from above step 1 for each of the two buckets are different by more than a chosen value of 0.2 mm, then the Allen wrench must be inserted on the underside of the tipping bucket to raise the pole (raising or lowering the pole would decrease or increase the tip volume respectively of that individual bucket). See Figure 57.



Figure 66: Adjusting the height of the pole under the bucket using an Allen wrench during the static calibration procedure

4. Repeat steps 1 & 3 till the difference between the average tipping volumes for each of the two buckets in the Texas Electronics model TE525 is less than a chosen value of 0.2 mm, recording all the values into your field notebook.

Dynamic Calibration:

First, the flow rates of the dispenser are required to be tested in timed tests using a graduated accumulation in the rain gauge. The actual flow rates measured during this procedure may differ from the design flow rates of the nozzles (50, 100, 200, 300, or 500 mm h⁻¹). These measured flow rates from the flow device calibration tests can then be used for subsequent calibration of the TB rain gauges. These flow rate values have already been obtained in the lab, and would be used in the analysis after the field dynamic calibration. The dynamic calibration steps in the field are:

1. Place the holding plate so that it sits on the catch of the TB rain gauge, and the central hollow of this holding plate is right above the bucket (refer Figure 58 where it sits on the rain gauge and would hold the column of the calibration kit to be described in the next few steps).
2. Start with the lowest nozzle size of 50 mm h⁻¹.
3. Ensure that the valve at the top of the column of the calibration kit is closed.
4. Remove (by unscrewing) the base cap or the nozzle (whichever is present) at the base of the column.

5. If this is the first nozzle used, invert and fill the column with water (This filled volume is approximately 653 ml). Otherwise, the remaining water from the previous nozzle uses should be sufficient for this nozzle size used.
6. Screw the selected nozzle size at the same location from where the base cap or the earlier nozzle was removed, invert the column to its earlier upright position, and place it so that its base fits into the central hollow of on the holding plate.
7. The earlier closed position of the valve entrapped some air inside the cylinder. Open this valve so that the created vacuum maintains constant head while releasing water through the nozzle and into the TB rain gauge.
8. Calculate the time taken using the chronometer (see Figure 58) for a prespecified number of total bucket tips: 10, 20, 40, 40 and 50 tips for the 50, 100, 200, 300, and 500 mm h⁻¹ nozzles respectively)..

Note: It is very important that the nozzle is *very clean* to allow for a constant flow



Figure 67: Setup and time measurement during the dynamic calibration procedure.

9. Repeat step 8 to confirm the value obtained in step 8. Enter this value into the field notebook.
10. Repeat steps 3-9 for each increasing nozzle size.

REMINDER: Switch on the datalogger before leaving the location!

SOIL SAMPLING

Goal

To capture the spatial distribution of soil properties at the new station installation sites which are important for hydrologic modeling purposes.

Materials

- Picks
- Shovels
- Measuring tapes or ruler
- Sieves
- Soil notebook or field spreadsheets
- Digital camera
- GPS device
- 4 mil thick soil sample storage bags (1 for each location)
- Clinometer and compass

Procedure

The location for this soil sampling will be done around the site of the new rain gauge installation:

Start with the first location. For each location, follow the steps below:

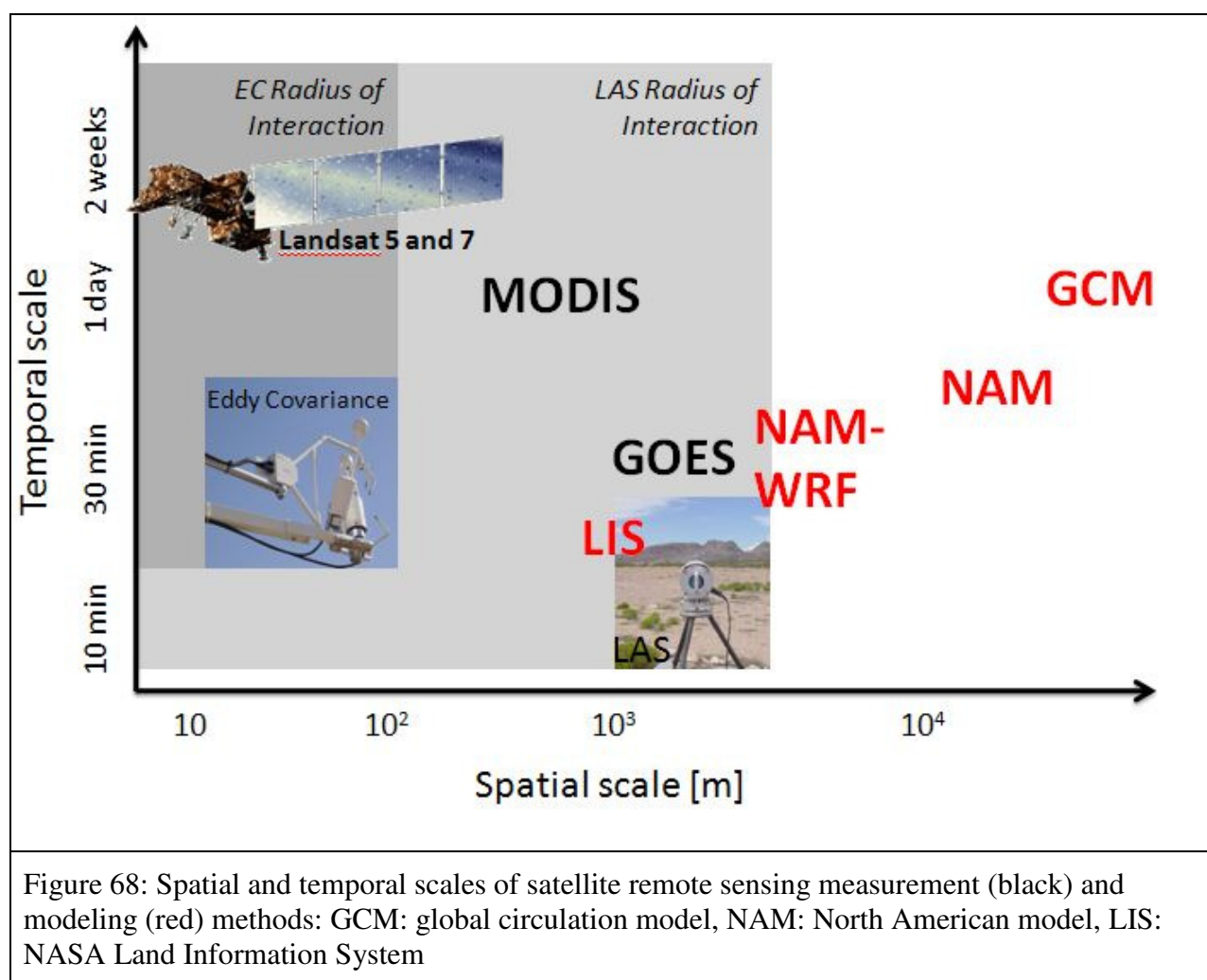
1. Use the co-ordinates stored in the GPS to determine the location. If for some reason a different location is decided upon, list that reason and the new co-ordinates against the surface soil sample site number into the soil notebook.
2. Enter a quick description the sampling location into the soil notebook: The site number (Refer the Appendix or GPS), coordinates, location (i.e. qualitative information: e.g., southwest of ranch, etc.), type of vegetation (prominent and others), elevation, slope, and aspect. For describing the type of vegetation, follow the information given in Appendix 1. For the slope, use the clinometer. For the aspect, use the compass.
3. Take about a kilo of the soil surface sample (0-10 cm depth), including stones. Note down into the soil notebook if there is any bedrock within this top 10 cm. Sieve the kilo of this soil surface sample with 2mm sieve, and see if you have a min of 500 grams of < 2mm for the lab analysis. Store the sample in a sample bag and label the bag with the location number, date and the depth interval, for example, '0-10 cm'. If by any chance you do not have a sieve in the field, remember to sieve the sample in the house in Rayon and put the sample back to its original bag.

EXPERIMENT 6: FLUX MEASUREMENTS USING DF SCINTILLOMETER - INSTALLATION AND OPERATION – RIO SAN MIGUEL

Goal

The purpose of this experiment to install and operate a transect of scintillometers to record sensible heat flux. These readings will be compared to the results of other measurements of sensible heat flux:

Principal Investigators: Jan Kleissl and Christopher J. Watts



Background

A scintillometer transect consists of a transmitter and a receiver (Figure 60). As an active remote sensor, the receiver measures intensity fluctuations (“scintillations”) in the radiation emitted by the transmitter caused by refractive scattering by temperature variations in turbulent eddies. The variance of the beam intensity is proportional to the structure parameter of the refractive index, C_n^2 , a measure of “seeing” in the atmosphere. Since at optical wavelengths temperature fluctuations along the path are the primary cause of refractive scattering, the structure parameter of temperature C_T^2 can be deduced from C_n^2 . For radio wavelengths (> 1 mm) on the other hand, water vapor fluctuations also contribute significantly to beam intensity fluctuations, i.e. the structure parameter of water vapor C_q^2 can be deduced from C_n^2 .



Figure 69: Two LASs (one receiver and one transmitters of two separate transects) during the LAS intercomparison study in northern New Mexico (Kleissl et al., 2008). The corresponding transmitter and receiver are 2 km away.

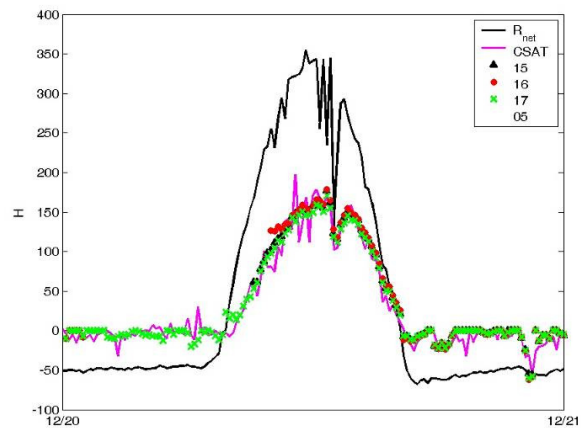


Figure 70: Intercomparison of sensible heat flux measurements from three LASs (symbols), EC (purple line), and net radiation (black line) in December 2005. The LAS measurements agree well with EC and provide a much smoother time series.

Since the radio wave scintillometer is still in a development stage and is not part of our proposed measurement network the rest of this discussion focuses on the optical (sensible heat flux) large aperture scintillometer (LAS, wavelength~880nm). Once C_T^2 is obtained, the sensible heat flux is obtained iteratively from the following equations assuming Monin-Obukhov (1954) similarity theory in the atmospheric surface layer

$$\frac{C_T^2 (z_{LAS} - d)^{2/3}}{T_*^2} = f_T \left(\frac{z_{LAS} - d}{L} \right) = f_T (\zeta)$$

$$T_* = -H / \rho c_p u_* \quad (1)$$

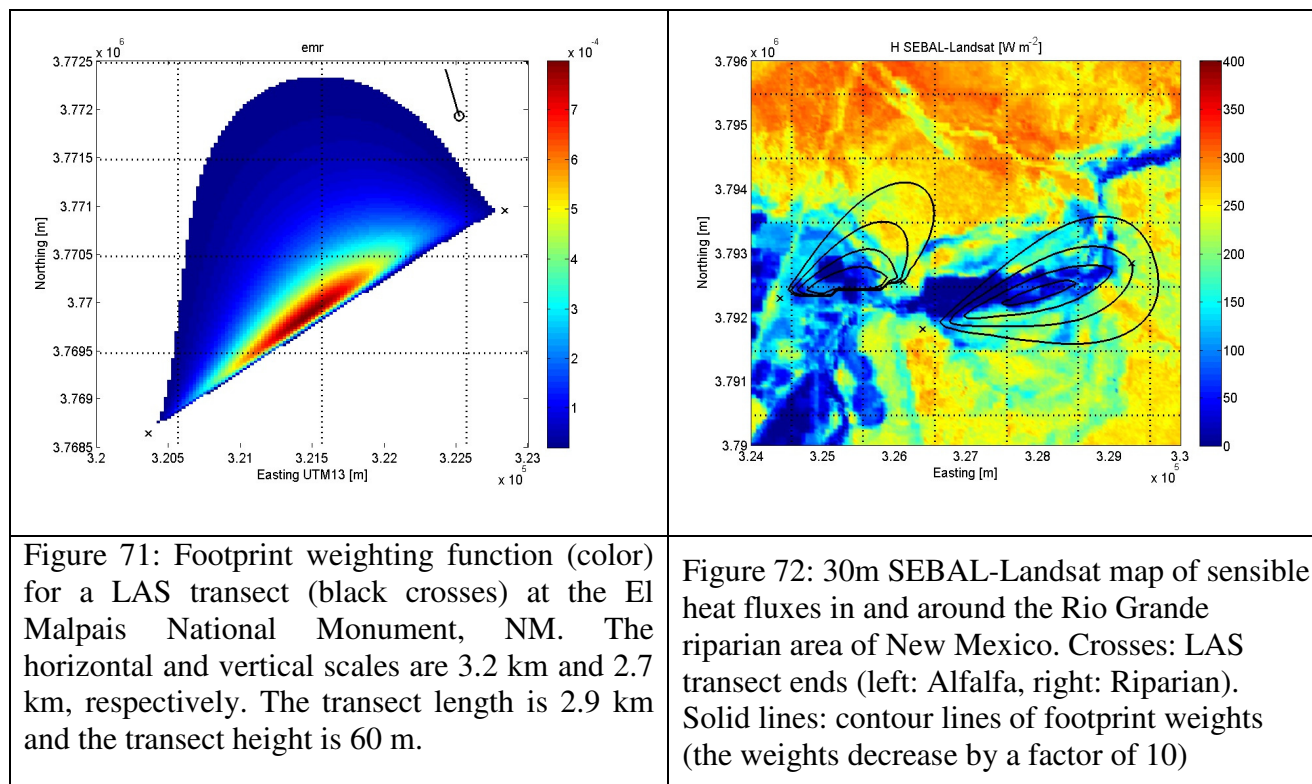
$$L_{MO} = \frac{u_*^2 T}{g \kappa T_*}$$

$f_T = c_{T1}(1 - c_{T2} \zeta)^{-2/3}$ and $f_T = c_{T1}(1 + c_{T3} \zeta^{2/3})$ are the universal stability function for unstable and stable conditions, respectively (Wyngaard et al. 1971; deBruin et al. 1993; Andreas 1988), $\kappa = 0.4$ is the von Karman constant, $c_{T1} = 4.9$, $c_{T2} = 6.1$, $c_{T3} = 2.2$, and L_{MO} is the Obukhov length. The friction velocity u_* is derived from estimates of roughness length z_0 , zero displacement height d , integrated flux profile relationships (Panofsky and Dutton 1984), and measurements of the mean horizontal wind speed. Accurate determination of the effective height z_{LAS} is critical since a relative error in z_{LAS} will result in at least half that relative error in H . The effective height z_{LAS} depends on atmospheric stability, and thus needs to be solved together with Eq. 1, resulting in a different z_{LAS} for each averaging interval (Hartogensis et al. 2003).

At first, it seems like a large number of parameters are required to derive H from C_T^2 which if they needed to be determined averaged over the LAS transect would require a lot of additional measurements and introduce uncertainty. However, Hartogensis et al. (2003) showed that a single measurement of wind speed, temperature, and pressure near the transect center is sufficient to reduce the error to 10% or less. This is especially true for free convective conditions often encountered in the southwestern US and Mexico. In these conditions u_* (and thus wind speed and roughness length) are no longer needed to calculate H . For a full description of the theory behind scintillometry we refer to the October issue of *Boundary-Layer Meteorology* (2002; vol. 105-1) on Recent Developments in Scintillometry Research.

Loescher et al. (2005) and Kleissl et al. (2008), respectively, examined EC and scintillometer flux measurement uncertainties in detail using instrument intercomparisons in laboratory and field. Linear regressions for sensible heat fluxes of eight EC instruments in neutral and unstable stability conditions revealed differences of up to 30%, while typical uncertainties (measured by the standard deviations of the slopes) were 7-11% depending on atmospheric stability. A study with five LASs under ideal conditions showed differences in the regression slopes of up to 21% with typical differences of 5-6%. A comparison of measurements from five collocated LAS transects and an eddy covariance station reveal that LAS measurements agree well with EC and provide a much smoother time series (Figure 61). Moreover, in spite of the complex physics on which scintillometers are based, their operation and data analysis is relatively simple compared to that of EC systems. Therefore, LAS systems have the potential to become a standard hydrologic and meteorological instrument just as a rain gauge or thermometer.

Whereas typical EC footprints are on the order of 100s of m^2 and cover completely different areas when the wind direction changes more than 90 degrees, the footprint areas of LASs are typically on the order of km^2 and cover –at least partly– the same area when the wind direction changes. Since the LAS measurements represents a line-averaged measurements, which is weighted towards the center of the transect, the footprint typically takes the shape of an ellipsoid whose extent is ~30% less than the actual transect length (Figure 62).



Materials

Site Setup Equipment:

- Scintillometer set (1 transmitter, 1 receiver, 2 sun shields, 2 telescopes, and 2 cables)
- Data logger / Data logger container
- Laptop (data logger cables)
- 2 Radios
- 2 GPS units
- 2 Tool kits (including the following: Flathead screwdriver, Phillips screwdriver, Allen set(metric and standard) , 2 adjustable wrenches, wire, wire cutters, scissors, voltmeter, desiccants, lens cleaner, cotton swabs, distilled water, replacement screws, and replacement cable)
- 2 Batteries
- 2 Battery covers
- 2 Solar panels
- 2 Charge controllers
- Weather station equipment
- 2 Backpacks (4 if available)

Scintillometer Alignment and Power Setting Instruction / Site Maintenance Equipment:

- Scintillometer telescopes, with the same serial code as the scintillometer being visited
- Laptop (data logger cables)
- 2 Radios
- 2 GPS units
- 2 Tool kits (including the following: Flathead screwdriver, Phillips screwdriver, Allen set(metric and standard) , 2 adjustable wrenches, wire, wire cutters, scissors, voltmeter, desiccants, lens cleaner, cotton swabs, distilled water, replacement screws, and replacement cable)
- Replacement battery (2 if available)
- 2 Backpacks (4 if available)

Procedure

Before Departing for the Field

1. Gather all necessary equipment
2. Check that all equipment is working (especially GPS units and radios)
3. Double check equipment

Site Setup

- 1) Decide on location of Scintillometer transect
- 2) Scintillometer team split into two groups
 - a) **Group 1** will set up the transmitter (scintillometer transmitter, transmitter telescope, 1 sun shield, 1 cable, 1 radio, 1 GPS unit, 1 tool kit, 1 battery, 1 battery cover, 1 solar panel, 1 charge controller, and 1 backpack)
 - b) **Group 2** will set up the receiver (scintillometer receiver, receiver telescope, 1 sun shield, 1 cable, data logger and data logger box, Laptop (data logger cables), 1 radio, 1 GPS unit, 1 tool kit, 1 battery, 1 battery cover, 1 solar panel, 1 charge controller, weather station equipment, and 1 backpack)
- 3) **Group 1** will hike to the decided location for the transmitter using the GPS unit
 - a) Place the transmitter on its tripod and tighten bolts (Be careful not to over tighten the bolts, eventually someone will have to loosen these bolts)
 - b) Place the battery and solar panel close to the scintillometer
 - i) Direct solar panel to the south
 - c) Connect the battery, solar panel, and scintillometer to the charge control in the order you are instructed (charge control is numbered)
- 4) **Group 2** will hike to the decided location for the receiver using the GPS unit
 - a) Place the receiver on its tripod and tighten bolts (Be careful not to over tighten the bolts, eventually someone will have to loosen these bolts)
 - b) Place the battery and solar panel close to the scintillometer
 - i) Direct solar panel to the south

- c) Connect the battery, solar panel, and scintillometer to the charge controller in the order you are instructed (charge controller is numbered)
- 5) When both groups have their scintillometers set up then the scintillometers can be aligned, see Scintillometer Alignment Instruction
- 6) While one member of **Group 1** is aligning the other should walk from the transmitter to the receiver taking GPS points frequently (this is used to describe the topography of the transect)
- 7) While one member of **Group 2** is aligning the other should setup the data logger, data logger box, and weather station equipment

Scintillometer Alignment Instruction

- 1) Scintillometer team will split into two groups
 - a) **Group 1** will align the transmitter (transmitter telescope, 1 radio, 1 GPS unit, 1 tool kit, and 1 backpack)
 - b) **Group 2** will align the receiver (receiver telescope, Laptop (data logger cables), 1 radio, 1 GPS unit, 1 tool kit, and 1 backpack)
- 2) **Group 1** will hike to the transmitter location and **Group 2** will hike to the receiver location using their GPS units
- 3) When all parties have reached their destinations
 - a) **Group 1** will check and record the power setting on the transmitter
 - b) **Group 2** will check and report the signal strength to **Group 1**

NOTE: If the signal strength is ever greater than 90, IMMEDIATELY cover the receiver and ask **Group 1** to lower the power setting, high signal strengths can damage the scintillometer receiver's sensor and will have to be returned to the New Netherlands for repairs

- 4) Both groups remove their scintillometer's sun shield, loosen the scintillometer's base bolts, remove the scintillometer's back cover and attach their telescope (Be sure to keep all the removed parts together and in a known place)
- 5) When both groups are ready, **Group 1** can begin aligning
 - a) **Group 1** will first align the transmitter left and right:
 - i) Tell **Group 2** that you are aligning left and right over the radio (make sure to speak slowly and clearly)
 - ii) Looking through the telescope for reference, move slowly left until **Group 2** reads 0 signal strength value and stop
 - iii) Looking through the telescope for reference, move slowly right until **Group 2** reads a 0 signal strength value and stop
 - iv) Ask **Group 2** what the largest signal strength value was
 - v) Looking through the telescope for reference, move back to the center until the highest signal strength value is reached
 - b) After the largest value is reached aligning left and right, **Group 1** will align up and down
 - i) Tell **Group 2** that you are aligning up and down over the radio (make sure to speak slowly and clearly)
 - ii) Looking through the telescope for reference, move slowly up until **Group 2** reads 0 signal strength value and stop

- iii) Looking through the telescope for reference, move slowly down until **Group 2** reads a 0 signal strength value and stop
 - iv) Ask **Group 2** what the largest signal strength value was
 - v) Looking through the telescope for reference, move back to the center until the highest signal strength value is reached
- c) **Group 2** will read signal strength value to **Group 1** over the radio (make sure to speak slowly and clearly) while **Group 1** is aligning
 - i) Do not read every value
 - ii) try to tell **Group 1** the large changes (example: 0, 10, 20, 30 , 40 , 45, 50, 42, 35, 20, 10, 0)
 - iii) Keep track of the largest signal strength value reached
- 6) When **Group 1** is finished aligning, **Group 2** can start aligning
 - a) **Group 2** tell **Group 1** that you will begin aligning
 - b) First align left and right
 - i) Looking through the telescope for reference, move slowly left until a 0 signal strength value is reached and stop
 - ii) Looking through the telescope for reference, move slowly right until a 0 signal strength value is reached and stop
 - iii) Keep track of the largest signal strength value
 - iv) Looking through the telescope for reference, move back to the center until the largest signal strength value
 - c) After aligning left and right, **Group 2** will align up and down
 - i) Looking through the telescope for reference, move slowly up until a 0 signal strength value is reached and stop
 - ii) Looking through the telescope for reference, move slowly down until a 0 signal strength value is reached and stop
 - iii) Keep track of the largest signal strength value
 - iv) Looking through the telescope for reference, move back to the center until the largest signal strength value
 - d) Tell **Group 1** that you are finished align and what the final signal strength is
- 7) When both groups are finished aligning, each group will tighten down their scintillometer's base bolts (be careful not to over tighten the bolts, someone will eventually have to loosen the bolts), reattach scintillometer's back cover, and reattach the scintillometer's sun shields
 - a) If at any point the signal strength drops **Group 2** should immediately notify **Group 1** and repeat steps 5 and 6
- 8) If the signal strength at its high value is less than 50 or greater than 80, you may want to change the power setting, see Scintillometer Power Setting Instructions

Scintillometer Power Setting Instructions

1. Both groups remove their scintillometer's back cover
2. If the power setting is too low or high, **Group 1** will increase/decrease the power setting
 - a. Tell **Group 2** that you are increasing/decreasing the power setting (make sure to speak slowly and clearly)
 - b. Very slowly increase/decrease the power setting

- c. When desired a signal strength is reached, stop and ask for the final signal strength
3. **Group 2** will read the signal strength values to **Group 1** (make sure to speak slowly and clearly)
 - a. Read the values as they are increasing/decreasing
4. Both groups will replace the scintillometer's back cover and **Group 1** ask **Group 2** for the final signal strength

Site Maintenance

1. Scintillometer team will split into two groups
 - a. **Group 1** will hike to the transmitter (transmitter telescope, 1 radio, 1 GPS unit, 1 tool kit, and 1 backpack)
 - b. **Group 2** will hike to the receiver (receiver telescope, Laptop (data logger cables), 1 radio, 1 GPS unit, 1 tool kit, and 1 backpack)
2. When all parties have reached their destinations
 - a. **Group 1** will check and record the power setting on the transmitter
 - b. **Group 2** check and report the signal strength to **Group 1**
 - c. **Group 2** will download and check the data
3. If signal strength is too low the scintillometers will need to be realigned, see the Scintillometer Alignment Instructions
4. Clean the scintillometer lens and the solar panel
5. Check the battery strength with the voltmeter
 - a. Lightly kick and remove battery cover (Be careful spiders, snakes, and other animals might be here)
 - b. If the battery is lower than 11.5 you may want to replace the battery
6. Clean the area around the scintillometer, battery, and solar panel

EXPERIMENT 7: WATER SOURCE CHARACTERIZATION USING MAJOR ANIONS AND ISOTOPES

Goal

To determine water source to rivers in semi-arid regions by collecting samples of groundwater, runoff, precipitation, and stream flow and analyzing major anions and isotopes.

Materials

GeoPump
 125 ml. Plastic bottles
 10 ml. Plastic vials
 pH and EC meter
 Labeling tape
 Markers
 Cooler
 Buckets
 Screen
 Wire
 Screen scissors
 Mineral Oil
 Syringes
 Samplers
 1 lt. Plastic Bottles
 Autosamplers

Procedure

- First Day of Work (this can be done either the first or the second day of work)
 1. If not already, get in touch with the person in charge of the “El Cajon” stream gauge station to get permit to set up autosampler. (Lissette will try to do this on Friday, while in Hermosillo)
 2. Install stream flow autosampler at station .
 - This sampler will be located close to the “El cajon” stream gauge.
 - The sampler will collect every 4 hours for 4 days.
 3. Possibly set up precipitation collector in the “Torre”, where the eddy covariance station is located. More collectors will be added if some other place is seen where more could be set up.
 4. Also, set up the device for collecting precipitation samples at Summer 2006 stations 132 and 146. Further, set up sampling devise at the upper part of the basin in Cucurpe (Lissette might stop on her way to Hermosillo to set up this, and might need to come back at some point to get a sample and once she is heading back to Tucson, she will stop again), Meresichic, etc.

- Second Day of Work

1. Collect stream flow samples one or a few of the perennials reaches, which are usually around towns such as San Miguel de Horcasitas, Rayon, Opodepe, Meresichic, and Cucurpe
 - These Samples will be collected every 500m.
 - At each site 3 samples will be taken.

- Third Day of Work

1. Set up sampler for capturing runoff near rain gauges. (These will be set up once, I'll see how they work, and I'll keep collecting samples every time it rains)
2. Collect runoff captured by Samplers.
3. Collect precipitation sample (These samples will be collected every day after a rain event).

- Fourth Day of Work

These will be done the days Lissette gets free from other activities (i.e. setting up samplers, collecting rain, runoff and stream sampling)

1. If not already, get permits to access wells. (The wells to be sampled will depend on the accessibility. Lissette already talked to people about it, and also needs to talk individually to the owners. These wells are all the located in the San Miguel basin)
2. Collect 3 samples from each of the wells located at San Miguel Basin
 - For wells that are pumping at the time, just collect discharge samples
 - For wells that are not working at the time, use geopump
 - Before taking sample, pump 3 case volumes because that's the protocol established to make sure the water sampled is coming from the aquifer and hasn't been sitting in there for months, hence changing the composition.

- Fifth Day of Work

1. Take ground water samples .

- Next day of work

1. Collect rain and runoff samples .

- Next day of work

1. Collect ground water samples.

- Next day of work

1. Take rain and runoff samples

EXPERIMENT 8: SOIL SURVEYING

Goal

To further classify and characterize the soil parameters which are useful for modeling purposes at the previous soil pit locations analyzed (in Sierra Los Locos):

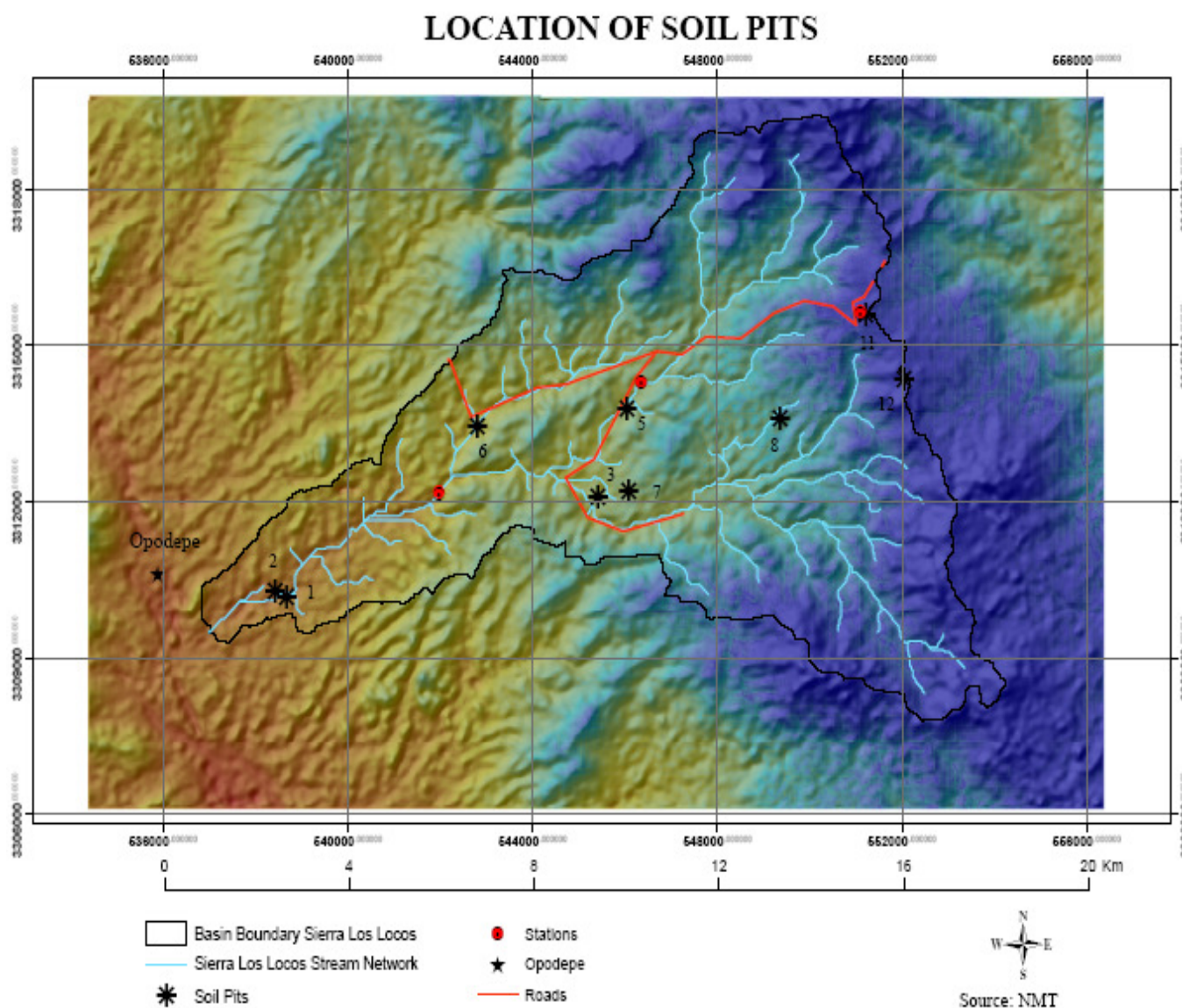


Figure 73: Location of Soil Pits

UTM 12 N Coordinates					
Soil Pit ID	X	Y	Elevation Meters, Z	Slope, Degrees	Aspect, Degrees
1	538676	3310169	669.0	7.5	148.4
2	538427	3310294	676.0	8.0	242.7
3	545410	3312106	858.0	1.4	315.0
5	546045	3313803	879.0	0.8	161.6
6	542809	3313456	779.0	2.6	150.9
7	546082	3312189	903.0	6.8	236.9
8	549357	3313609	1052.0	11.3	185.0
11	551215	3315613	1401.0	3.4	339.0
12	552045	3314362	1460.0	1.1	315.0
Tower	544807	3290184	0.0	0.0	0.0

***NOTE: Please refer to Appendix 1 for detailed characteristics of topography, vegetation, soil characteristics, photos, etc.**

Materials

- Picks
- Shovels
- Measuring tape
- Munsell color chart
- Sieves
- Soil notebook or field spreadsheets
- Digital camera
- Knife
- Bottle with HCl
- Bottle with water
- GPS device
- Compass and clinometers
- 4 mm thick soil sample storage bags (at least 13 for each pit: 8 layers max. + 5 possible horizons)
- Pedon storage containers (15 pedons for each pit: 5 possible horizons * 3 each horizon).
- Glass to scratch for parent material test
- Parafilm

Procedure

(The procedure will be provided by Dr. Bruce Harrison and Dr. Jose Luis Zarate.)

APPENDIX

APPENDIX 1: ECOSYSTEMS AND MAIN PLANT SPECIES OF THE SAN MIGUEL BASIN

The San Miguel watershed is located about 70 kilometers northeastward of Hermosillo, the capital of the Mexican state of Sonora. The San Miguel watershed is around 3,798 km² and ranges in elevation from 370 to 2440 meters above sea level. A close coupled relationship exists between elevation and plant communities, especially in this area. In the san Miguel basin we can find three main ecosystems: Subtropical scrubland, Desert scrubland, and Madrean evergreen woodland.

Subtropical Scrubland

These drought deciduous communities occupy a moisture gradient transitional between desert scrub and woodland or forest. Canopy heights tends to be from 2 to 8 m and are typically composed of spinose, microphyllous, and succulent plant life-forms. In Sonora it is usually positioned between the sonoran desertscrub and either tropical deciduous forest or madrean evergreen forest. Dominant plant species have their center of distribution and abundance here, eg. Ocotillo tree (*Fouquieria macdougalii*), see picture 1, we can also find the appearance and often heavy representation of tropical species not found in the desert scrubland like huinolo (*Acacia cochliacantha*), see picture 2, or *Acacia cymbispiana*. It is primary resident of low hills, bajadas, mesas and mountains slopes, although we can find it in low valleys where has invaded former savanna grassland. Precipitation range goes from 300-500 mm per year. Cacti are also found with two main species: pithaya (*Stenocereus thurberi*), see figure, Hecho or etcho (*Pachocereus pectin-aboriginum*), and also nopales (*Opuntia sp.*).



Picture 1: Ocotillo macho, torote verde or ocotillo tree (*Fouquieria macdougalii*). Dominant specie of subtropical scrubland. Found in hill slopes, mesas and arroyo rims. Shrub or tree 5-8 m high. Trunk usually very short, Blooms mainly in rain periods showing a bright red flower. In our experiment sites, it is usually found around the tower experiment and low hills.



Picture 2: Huinolo (*Acacia cochliacantha*). Found in mesas, valleys, and hill slopes, common between 30-900 m above sea level. It is very aggressive and quickly captures areas abandoned from cultivation; it is used as index specie for deforested zones. Normally 6-8 m of height with a short trunk.



Picture 3: Palo verde o Palo brea (*Cercidium praecox*) Found in roadsides, valleys, volcanic slopes . Common tree in lowlands, sometimes exude a sweet and odorous excretion highly attractive to insects. Flower is bright yellow.



Picture 4: Pithaya (*Stenocereus thurberi*). Found from coastal plains to barrancas in a elevation from sea to 1000 m. It is a large columnar cactus to more than 10 m in height .It is a very valuable resource in rural Sonora.



Picture 5: Tavachin (*Caesalpinia pulcherrinia*), Found in arroyos margins and roadsides. Elevation of 150-1500 above sea level. Bushy-shrub 1 to 3 meters height. It blooms during rainy season. Flowers during youth are yellow turning to red when they are mature.



Picture 6: Guayacan (*Guaiacum coulteri*). Found in canyons, arid hillslopes, roadsides, stabilized dunes. From coastline to 400 m above sea level. Small sturdy tree, closely and complexly branched. In drought season (may to june) it throws out a beautiful bright blue abundance of flowers. It responds quickly to rain.



Picture 7: Reina de la noche (*Peniocereus striatus*). Found in foothills elevation 100-250 m above sea level. A pencil stemmed cactus, sprawling in thickets of other shrubs and closely resembling their leafless, woody branches. The root system bears numerous succulent swellings, shaped like potato tubers.

Sonora Desert scrub

The sonoran desert differs markedly from the other North American desert biomes, which are dominated by low shrubs, in its arboreal elements and its truly large cacti and succulent constituents. Even in its most arid parts, the sonoran desert exhibits tree, tall shrubs and succulent life forms along drainages and in other favored habitats.

One division of the sonoran desert is known as palo verde-cacti desert. This subdivision is found from Arizona to south of Magdalena, Sonora. The lower elevation contact may be as low as 300 m to 650 m. Precipitation range goes from 200 mm to 425 mm. The most common species are saguaro (*Carnegiea gigantea*), see picture, oldman cactus (*mammillaria sp.*), see picture, barrel cactus (*ferocactus wislizenii*), palo verde (*Cercidium mycrophillum*) and ocotillo (*Fouquieria splendens*).



Picture 8: Saguaro (*Carnegiea gigantea*). Rocky , rugged slopes of volcanic slopes. Elevation from 50-500 m.



Picture 9: Ocotillo (*Fouquieria splendens*). Found from southwest USA to Sonora, Mexico. We can find ocotillo until 1500 m above sea level. Leaves are in axils of thorns; simple, in clusters, round, to 1in tall, bright green; plant is generally leafless for most of the year; in years with good rainfall leaves will persist, turning showy colors of yellow and red in the fall. 1.5 to 8 meters in height. Stems/Trunks are long slender stems rise from a common base; stems covered with 1in thorns which are gray or sometimes greenish. Flowers are bright red.



Picture 10: Biznaguita or pithayita (*Mammillaria grahamii*.) Found in rocky slides , cliff crevices, foothills and slopes. Elevation 150-600 m. One of the smallest and more abundant species of mammillaria found in Sonora. It blooms abundantly in July, with bright to pale pink flowers; fruits ripen in the fall.

Madrean evergreen woodland

In the foothills, bajadas and barrancas and mountains ranges of the Sierra Madre Occidental and its outlying ranges in Mexico, a large variety of oaks participate in both encinal and oak-pine woodlands that covers hundreds of squares miles of western Chihuahua and eastern Sonora. In both states, Chihuahuan oak (*Quercus chihuahuensis*) , see picture, is commonly the first oak encountered at the woodlands's lower edge. Other commonly found oaks found in the region are encino prieto o Encino cusi comestible (*Quercus alboncita*) and Encino cusi prieto (*Quercus durifolia*).

This biome community generally makes contact with grasslands, however, grass provide the major woodland under canopy coverage. Many of the cacti and leaf succulents of the semi desert grassland extend very well to the madrean evergreen woodland. Main species can include nopal (*Opuntia robusta*, shown in figure 12, *Opuntia spinosor*) and agaves. Precipitation goes within a range from 400-1200 mm, being 400 the mean annual precipitation.



Picture 11: Encino roble o chihuahuan oak (*Quercus chihuahuensis*). Found in rocky slopes, ridges and streams sides and altered soils. Elevation from 300 to 1900 m above sea level. Small spreading oak, with light gray, siffured bark reaching at least 10 m in height. Leaves greenish-gray, flowering May-August and producing acorns from October to December.



Picture 12: Nopal o tuna tapon (*Opuntia robusta*). Found in rocks and open places. Between 1500-1800 m above sea level. Prickly pear with massive pads, fruits barrel shaped or globose, reddish to purple. Limited to and common in high elevations, common in mountains of Sonora and Chihuahua.

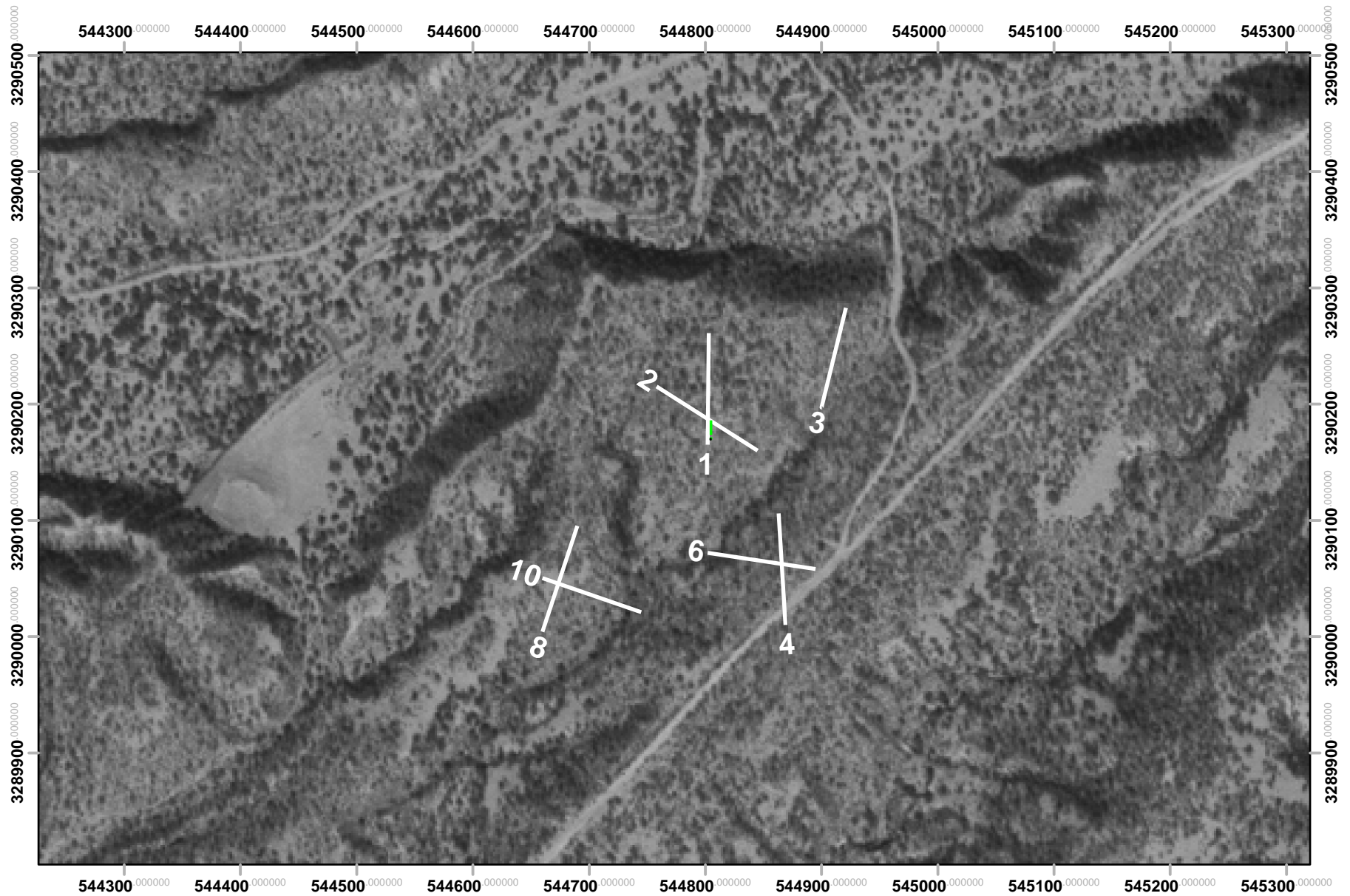


Picture 13: Leghugilla verde (*Agave bovicornuta*) . Found in rocky slopes, between 500-1900 m above sea level. It is the most common of the uplands agaves and is quickly recognized by its large size and bright green leaves. It flowers from February to May.

All photographs shown in this section were taken by 2004 field campaign participants.

APPENDIX 2: VEGETATION TRANSECTS MAP – RAYON TOWER
(DATA FROM 2007 CAMPAIGN)

VEGETATION TRANSECTS - TOWER SITE



0 100 200 400 Meters

! Eddy covariance tower

— Vegetation transects



APPENDIX 3: VEGETATION COVER BY TRANSECT (DATA FROM 2007 CAMPAIGN)

Transect ID	Coverage (%)			
	Litter	Rock	Soil	Vegetation
1	6	5	30	59
2	1	3	19	77
3	2	17	15	66
4	3	15	26	56
6	2	7	23	68
8	3	30	18	49
10	1	27	9	63

Transect 1

Especie	N	(%)
ACACIA	6	10.17%
MATORRAL	3	5.08%
MEZQUITE	24	40.68%
PALO VERDE	8	13.56%
PLANTITA	1	1.69%
SANGRENGADO	5	8.47%
SIVIRI	2	3.39%
TOROTE VERDE	10	16.95%
Total general	59	100.00%

Transect 4

Especie	N	(%)
ACACIA	14	25.00%
MATORRAL	5	8.93%
PALO BLANCO	8	14.29%
PALO VERDE	13	23.21%
SHRUB	5	8.93%
SIVIRI	1	1.79%
TOROTE	10	17.86%
Total general	56	100.00%

Transect 10

Especie	N	(%)
ACACIA	19	30.16%
MATORRAL	1	1.59%
PALO BLANCO	17	26.98%
SANGRENGADO	2	3.17%
SHRUB	12	19.05%
SIVIRI	2	3.17%
TOROTE	10	15.87%
Total general	63	100.00%

Transect 2

Especie	N	(%)
ACACIA	8	10.39%
MATORRAL	4	5.19%
MEZQUITE	31	40.26%
PALO VERDE	16	20.78%
SIVIRI	5	6.49%
TOROTE	12	15.58%
CHOYA	1	1.30%
Total general	77	100.00%

Transect 6

Especie	N	(%)
ACACIA	11	16.67%
MATORRAL	4	6.06%
MESQUITE	7	10.61%
NOPAL	1	1.52%
PALO BLANCO	18	27.27%
PALO VERDE	10	15.15%
SANGRENGADO	2	3.03%
SHRUB	7	10.61%
SIVIRI	2	3.03%
TOROTE	4	6.06%
Total	66	100.00%

Transect 3

Especie	N	(%)
ACACIA	6	9.68%
CHOYA	1	1.61%
MATORRAL	5	8.06%
MEZQUITE	20	32.26%
PLANTITA	1	1.61%
SANGRENGADO	1	1.61%
TOROTE	28	45.16%
Total general	62	100.00%

Transect 8

Especie	N	(%)
ACACIA	5	10.20%
MATORRAL	5	10.20%
PALO BLANCO	1	2.04%
SANGRENGADO	8	16.33%
SHRUB	5	10.20%
SIVIRI	2	4.08%
TOROTE	23	46.94%
Total general	49	100.00%

**APPENDIX 4: PHOTOS OF SOIL PIT LOCATION (FROM SONORA
CAMPAIGN 2007)**

Photos of Soil Pit Locations from Sonora Campaign 2007:

- **Soil pit ID: 1**
Location: 538676, 3310169 UTM 12N
Photographs are not available.

- Soil pit ID: 2
- Location: 538427, 3310294



Site description: fluvial valley located in riparian zone surrounded by crops, flat area soil composed mainly by alluvial sediment. At 120 cm depth, fine sand and gravel found.

- Soil pit ID: 3

Location: 545410, 3312106

Photos not available due to heavy rain

- Soil pit ID: 5

Location: 546045, 3313803



Site description: Alluvial valley located in subtropical scrubland near streams, flat area soil composed mainly by alluvial sediment. At 120 cm depth, fine sand and gravel found.

• Soil pit ID: 6

Location: 542809, 3313456



Located in subtropical scrubland near a rocky hill. Volcanic ash sediment, sand found at bottom of the soil pit.

- Soil pit ID: 7
- Location: 546082, 3312189



Located in subtropical scrubland, north facing slope, soil formed mainly of volcanic ash. Soil pit dug until 55 cm because bedrock was found.

- Soil pit ID: 8
- Location: 549357, 3313609



Located in subtropical scrubland at 1040 m above sea level. South facing slope, bedrock found at 50 cm. depth.

- Soil pit ID: 11
Location: 551215, 3315613



Soil located in Oak savanna, soil formed of volcanic ash, hill slope facing southwest, bedrock found at 60 cm depth.

- Soil pit ID: 12
- Location: 552045, 3314362



Soil pit located in Oak savanna, almost flat at 1450 m above sea soil formed mainly from volcanic ash.

• Soil pit ID: Tower
Location: 544807, 3290184



Soil pit is located near the eddy covariance tower in subtropical scrubland ecosystem.
Bedrock found at 70 cm.

APPENDIX 5: SOIL DATA (2007 CAMPAIGN)**Table 1: Sonora Soil Pits**

	NOTE	DEPTH	% Sand	% Silt	% Clay	LOI as % of Mass
SOIL PIT 1						
SNR 1-1		SP1 0-10cm	75.0767	24.9169	0.0064	1.17%
SNR 1-2		SP1 10-20cm	64.1543	35.8374	0.0083	1.39%
SNR 1-3		SP1 20-30cm	56.0410	43.9440	0.0150	1.26%
SNR 1-4		SP1 30-40cm				0.51%
SNR 1-5		SP1 40-60cm	88.3755	11.6222	0.0023	
SNR 1-6		SP1 60-80cm	79.1461	20.8437	0.0102	
SNR 1-7		SP1 80-110cm				
SOIL PIT 2						
SNR 2-1		SP2 0-10cm	53.7975	46.1946	0.0079	0.44%
SNR 2-2		SP2 10-20cm	74.8590	25.1311	0.0098	0.18%
SNR 2-3		SP2 20-40cm	82.4178	17.5752	0.0070	0.15%
SNR 2-4		SP2 40-60cm	70.3793	29.6133	0.0074	0.30%
SNR 2-5		SP2 60-120cm	94.0420	5.9533	0.0047	0.10%
SOIL PIT 3						
SNR 3-1 (A)	Sieved in Field	SP3 (H1) 0-10cm	65.8543	34.1373	0.0084	
SNR 3-1 (B)	Original	SP3 (H1) 0-10cm original	70.9599	29.0345	0.0056	
SNR 3-2 (A)	Sieved in Field	SP3 (H2) 10-30cm	59.4050	40.5819	0.0131	
SNR 3-2 (B)	Original	SP3 (H2) 10-30cm original	61.8182	38.1702	0.0116	
SNR 3-3		SP3 (H3) 30<cm				
SOIL PIT 4						
SNR 4-1		SP4 H1	71.1891	28.7990	0.0120	0.87%
SNR 4-2		SP4 H2	79.6102	20.3779	0.0120	
SNR 4-3		SP4 40-50cm	73.4861	26.5046	0.0093	
SNR 4-4		SP4 40-60cm	64.7354	35.2495	0.0152	0.76%
SNR 4-5		SP4 60-80cm	67.9144	32.0707	0.0150	0.65%
SNR 4-6		SP4 80-100cm				0.55%
SOIL PIT 5						
SNR 5-1		SP5 0-20cm	81.4380	18.5582	0.0038	
SNR 5-2 (A)		SP5 "0-20 or 20-45"	85.3771	14.6196	0.0034	
SNR 5-2 (B)		SP5 "0-20 or 20-45"	80.7084	19.2881	0.0036	
SNR 5-3		SP5 20-45cm	84.3641	15.6312	0.0048	
SNR 5-4		SP5 45-60cm	81.2445	18.7489	0.0066	
SNR 5-5		SP5 60-120cm	94.7755	5.2213	0.0032	
SOIL PIT 6						
SNR 6-1	Original	SP6 0-6cm				
SNR 6-2	Sieved in Field	SP6 H1				
SNR 6-3	Sieved in Field	SP6 H2				
SNR 6-4	Original	SP6 45				
SOIL PIT 7						
SNR 7-1		SP7 H1	78.9784	21.0138	0.0079	
SNR 7-3		SP7 H3	82.0737	17.9218	0.0045	

Table 1 continued: Sonora Soil Pits

	NOTE	Depth	% Sand	% Silt	% Clay	LOI as % of Mass
SOIL PIT 8						
SNR 8-1		SP8 H1	83.9799	16.013	0.0071	
SNR 8-2 (A)	Sieved in Field	SP8 H2				
SNR 8-2 (B)	Original	SP8 H2 original	72.8798	27.1081	0.0121	
SOIL PIT 9						
SNR 9-1(A)		SP9 H1	79.0561	20.934	0.01	
SNR 9-1 (B)		SP9 H1				
SNR 9-2		SP9 H??	74.0518	25.9442	0.004	
SNR 9-3		SP9 H3	85.7458	14.2512	0.003	
SOIL PIT 10						
SNR 10-1		SP10 H1	69.4116	30.582	0.0065	
SNR 10-2		SP10 H2	77.6328	22.3585	0.0088	
SOIL PIT 11						
SNR 11-1		SP11 0-10cm	62.1884	37.7967	0.0149	1.39%
SNR 11-2		SP11 10-20cm	70.569	29.416	0.0149	0.98%
SNR 11-3		SP11 20-30cm	67.365	32.6276	0.0074	0.87%
SNR 11-4		SP11 30-40cm	50.806	49.1707	0.0233	1.17%
SNR 11-5		SP11 40-60cm	60.7951	39.193	0.0119	1.05%
SOIL PIT 12						
SNR 12-1		SP12 0-10cm	71.5034	28.4859	0.0107	
SNR 12-2		SP12 10-20cm	72.7943	27.1946	0.0111	
SNR 12-3		SP12 20-30cm	69.949	30.0071	0.0439	
SNR 12-4		SP12 30-40cm	64.6427	35.3442	0.0131	
SNR 12-5		SP12 40-50cm	52.0651	47.9115	0.0234	
TOWER						
SNR 13-1		SP Tower 0-10cm	74.3025	25.6967	0.0008	NO DATA
SNR 13-2		SP Tower 10-20cm	70.6101	29.3886	0.0012	0.34%
SNR 13-3		SP Tower 20-30cm	67.2879	32.7032	0.0089	0.31%
SNR 13-4		SP Tower 30-40cm	60.6053	39.3735	0.0212	0.35%
SNR 13-5		SP Tower 40-50cm	60.375	39.6071	0.0179	0.37%

Table 2: SURFACE SOIL SAMPLES						
	Station	Site	Depth	%Sand	%Silt	%Clay
SSS-1				73.1299	26.8622	0.0079
SSS-2						
SSS-3						
SSS-4				73.3663	26.6287	0.0050
SSS-5				72.6088	27.3821	0.0091
SSS-6				77.5483	22.4485	0.0032
SSS-7				68.5590	31.4319	0.0091
SSS-8				54.9778	45.0130	0.0092
SSS-9				61.6147	38.3712	0.0141
SSS-10				63.5462	36.4438	0.0100
SSS-11				69.4659	30.5276	0.0065
SSS-12						
SSS-13				84.1603	15.8337	0.0060
SSS-14				90.0959	9.8998	0.0042
SSS-15				64.6706	35.3200	0.0094
SSS-16						
SSS-17				55.6442	44.3464	0.0094
SSS-18				62.3768	37.6087	0.0145
SSS-19				38.2254	61.7632	0.0114
SSS-20						
SSS-21						
SSS-22						
SSS-23				70.9028	29.0882	0.0090
SSS-24				65.0884	34.9025	0.0090
SSS-25						
SSS-26				73.9199	26.0750	0.0052
SSS-27						
SSS-28				59.1804	40.8090	0.0106
SSS-29				64.9110	35.0818	0.0072
SSS-30				78.4096	21.5837	0.0067
SSS-31				58.1859	41.7888	0.0253
SSS-32				64.9831	35.0085	0.0084
SSS-33				79.0625	20.9320	0.0055
SSS-34				76.7086	23.2835	0.0078
SSS-35				70.6078	29.3828	0.0094
SSS-36				79.1529	20.8409	0.0061
SSS-37				63.3633	36.6249	0.0117
SSS-38				78.3641	21.6319	0.0039
SSS-39				60.3613	39.6235	0.0152

Table 2 continued: SURFACE SOIL SAMPLES

	Station	Site	Depth	%Sand	%Silt	%Clay
SSS-40						
SSS-41				73.5809	26.4067	0.0124
SSS-42				85.7298	14.2710	-0.0008
SSS-43				72.7130	27.2826	0.0044
SSS-44				74.7671	25.2260	0.0069
SSS-45				67.2614	32.7321	0.0065
SSS-46				58.2603	41.7296	0.0101
SSS-47				62.5809	37.4082	0.0109
SSS-48				70.8127	29.1813	0.0061
SSS-49				69.6665	30.3256	0.0080
SSS-50				76.3319	23.6624	0.0057

Table 3: San Miguel and Sonora Station

	Station	Site	Depth	%Sand	%Silt	%Clay
SNR 130-1	130	1	0 - 5 cm	90.8827	9.1153	0.0020
SNR 130-2	130	1	5 - 10 cm	91.1518	8.8463	0.0020
SNR 131-1	131	2	0 - 5 cm	66.1178	33.8732	0.0090
SNR 131-2	131	2	5 - 10 cm			
SNR 132-1	132	3	0 - 5 cm	69.6193	30.3765	0.0042
SNR 132-2	132	3	5 - 10 cm	64.0592	35.9337	0.0070
SNR 133-1	133	4	0 - 5 cm	73.9010	26.0936	0.0055
SNR 133-2	133	4	5 - 10 cm	74.4764	25.5175	0.0060
SNR 134-1	134	5	0 - 5 cm	44.4079	55.5794	0.0127
SNR 134-2	134	5	5 - 10 cm	54.2254	45.7661	0.0084
SNR 135-1	135	6	0 - 5 cm	40.5232	59.4662	0.0106
SNR 135-1	135	6	5 - 10 cm	47.1409	52.8480	0.0111
SNR 136-1	136	7	0 - 5 cm	60.4572	39.5313	0.0115
SNR 136-1	136	7	5 - 10 cm	55.2352	44.7503	0.0146
SNR 137-1	137	8	0 - 5 cm	54.0181	45.9760	0.0059
SNR 137-2	137	8	5 - 10 cm	66.4414	33.5540	0.0046
SNR 139-1	139	10	0 - 5 cm	66.9374	33.0540	0.0086
SNR 139-2	139	10	5 - 10 cm	67.6187	32.3726	0.0087
SNR 140-1	140	11	0 - 5 cm	61.6391	38.3491	0.0118
SNR 140-2	140	11	5 - 10 cm	56.5961	43.3878	0.0161
SNR 143-1	143	12	0 - 5 cm	77.4351	22.5588	0.0061
SNR 143-2	143	12	5 - 10 cm	72.0166	27.9764	0.0069
SNR 144-1	144	13	0 - 5 cm	36.3389	63.6388	0.0223
SNR 144-2	144	13	5 - 10 cm	39.3877	60.5913	0.0210
SNR 147-1	147	15	0 - 5 cm	69.8236	30.1714	0.0050
SNR 147-2	147	15	5 - 10 cm	68.8333	31.1582	0.0085

APPENDIX 6: SOIL PROPERTIES RECORDING FORM

Date: ___/___/___ Time: ___:___

Location: _____ Site No. _____

Vegetation Type: _____ Elevation: _____

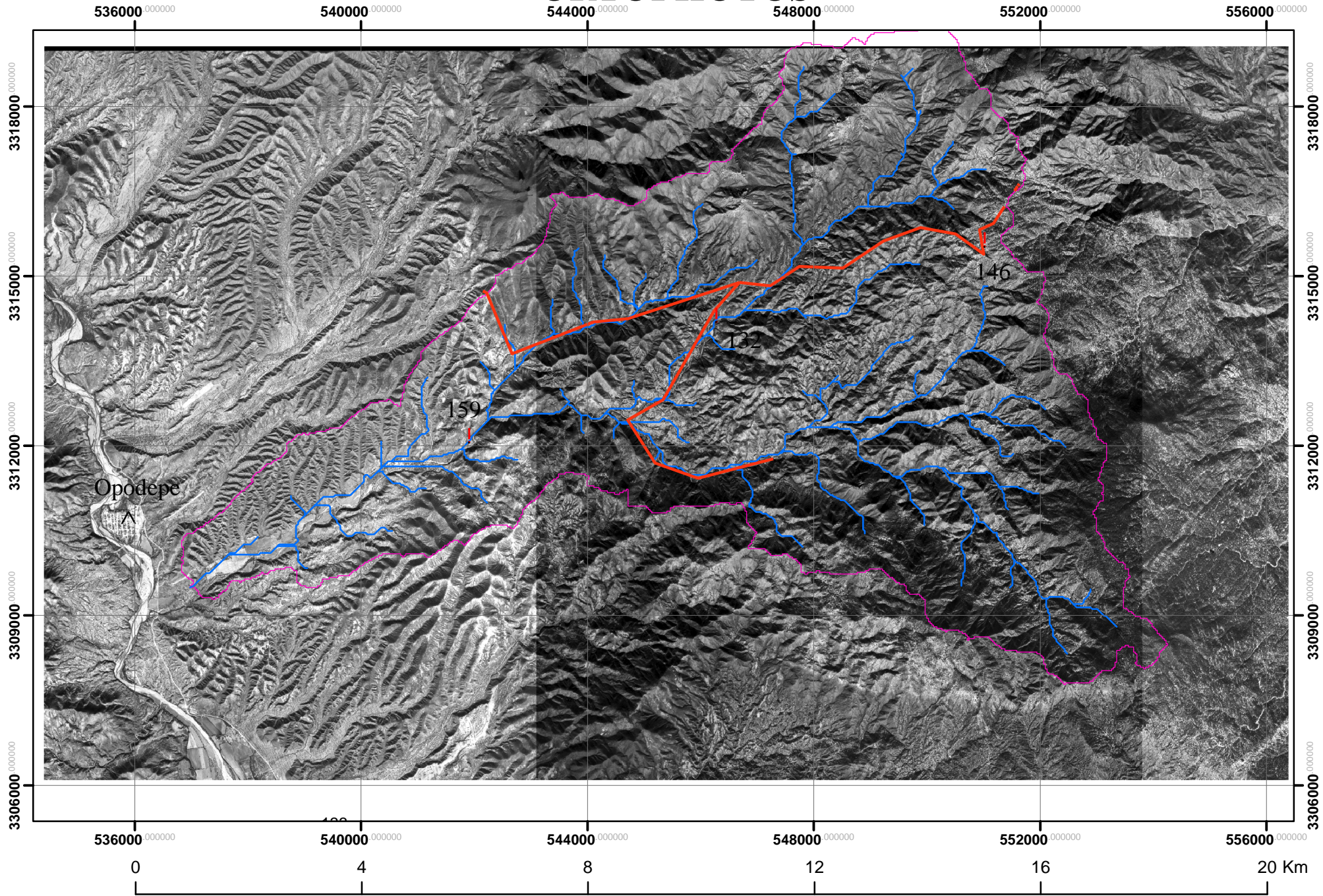
Parent Material: _____ Slope: _____



Described by: _____ Geomorphic Surface: _____ Aspect: _____




Bag Label	Depth (cm)	Horizon	Color		Structure			Grave I %	Consistence				Texture	pH	Clay films	Boundaries	Notes
			moist	dry	grade	size	structure		wet	moist	dry						
					m	vf	gr	<10	so	po	lo	lo	S SiCL		v1 f pf	a s	
					sg	f	pl	10	ss	ps	vfr	so	LS SiL		1 po	c w	
					1	m	pr	25	s	p	fr	sh	SL Si		2 d br	g I	
					2	c	cpr	50	vs	vp	fi	h	SCL SiC		3 co	d b	
					3	vc	abk	75			vfi	vh	L C		p cobr		
							sbk	>75			efi	eh	CL SC				
					m	vf	gr	<10	so	po	lo	lo	S SiCL		v1 f pf	a s	
					sg	f	pl	10	ss	ps	vfr	so	LS SiL		1 po	c w	
					1	m	pr	25	s	p	fr	sh	SL Si		2 d br	g I	
					2	c	cpr	50	vs	vp	fi	h	SCL SiC		3 co	d b	
					3	vc	abk	75			vfi	vh	L C		p cobr		
							sbk	>75			efi	eh	CL SC				
					m	vf	gr	<10	so	po	lo	lo	S SiCL		v1 f pf	a s	
					sg	f	pl	10	ss	ps	vfr	so	LS SiL		1 po	c w	
					1	m	pr	25	s	p	fr	sh	SL Si		2 d br	g I	
					2	c	cpr	50	vs	vp	fi	h	SCL SiC		3 co	d b	
					3	vc	abk	75			vfi	vh	L C		p cobr		
							sbk	>75			efi	eh	CL SC				

APPENDIX 7: MAPS OF SIERRA LOS LOCOS

ORTOPHOTOS

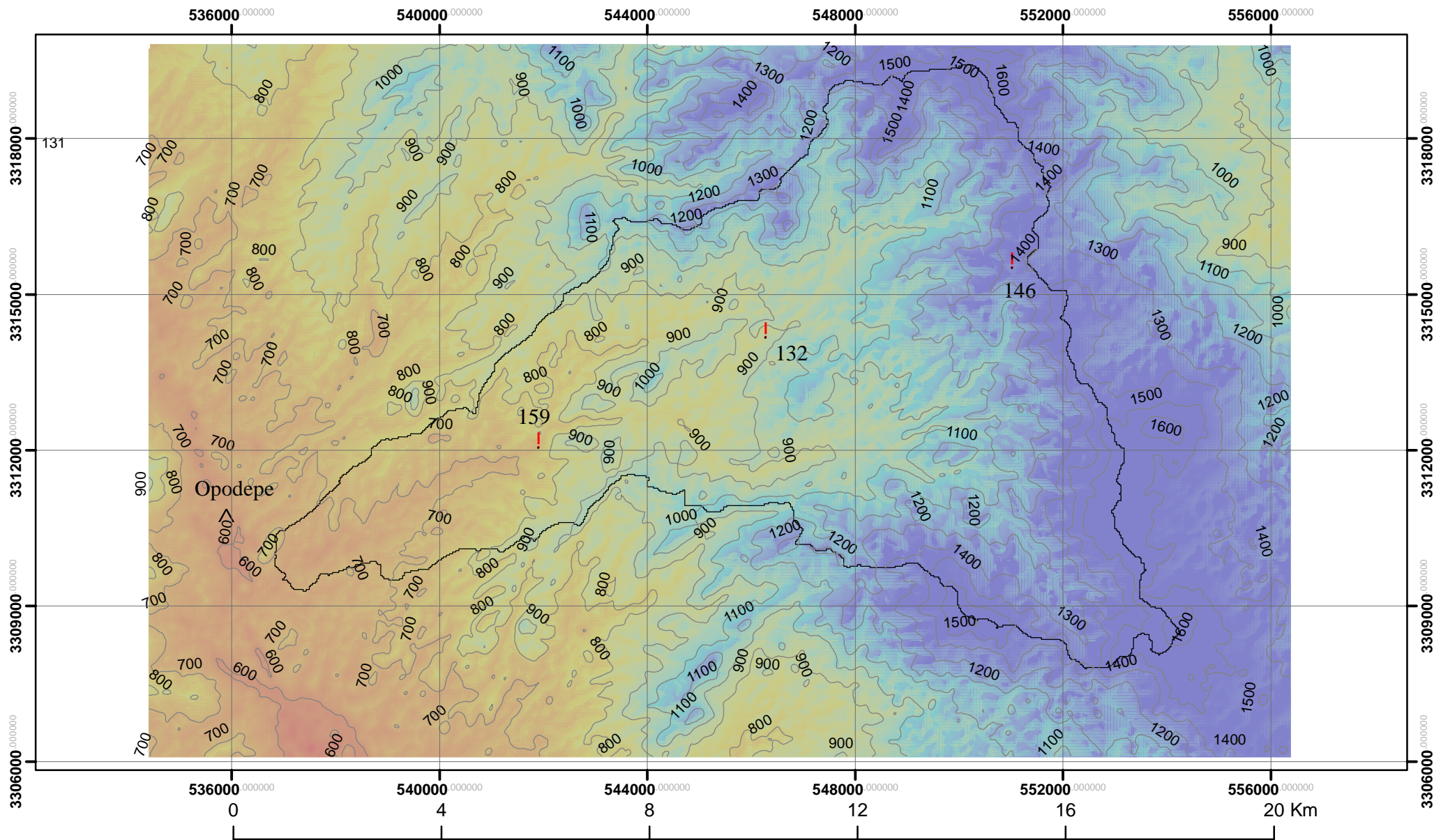


 Basin Boundary Sierra Los Locos
 Sierra Los Locos Stream Network

 Opodepe
 Stations
 Roads

Source: INEGI, 1996
Scale: 1: 75,000

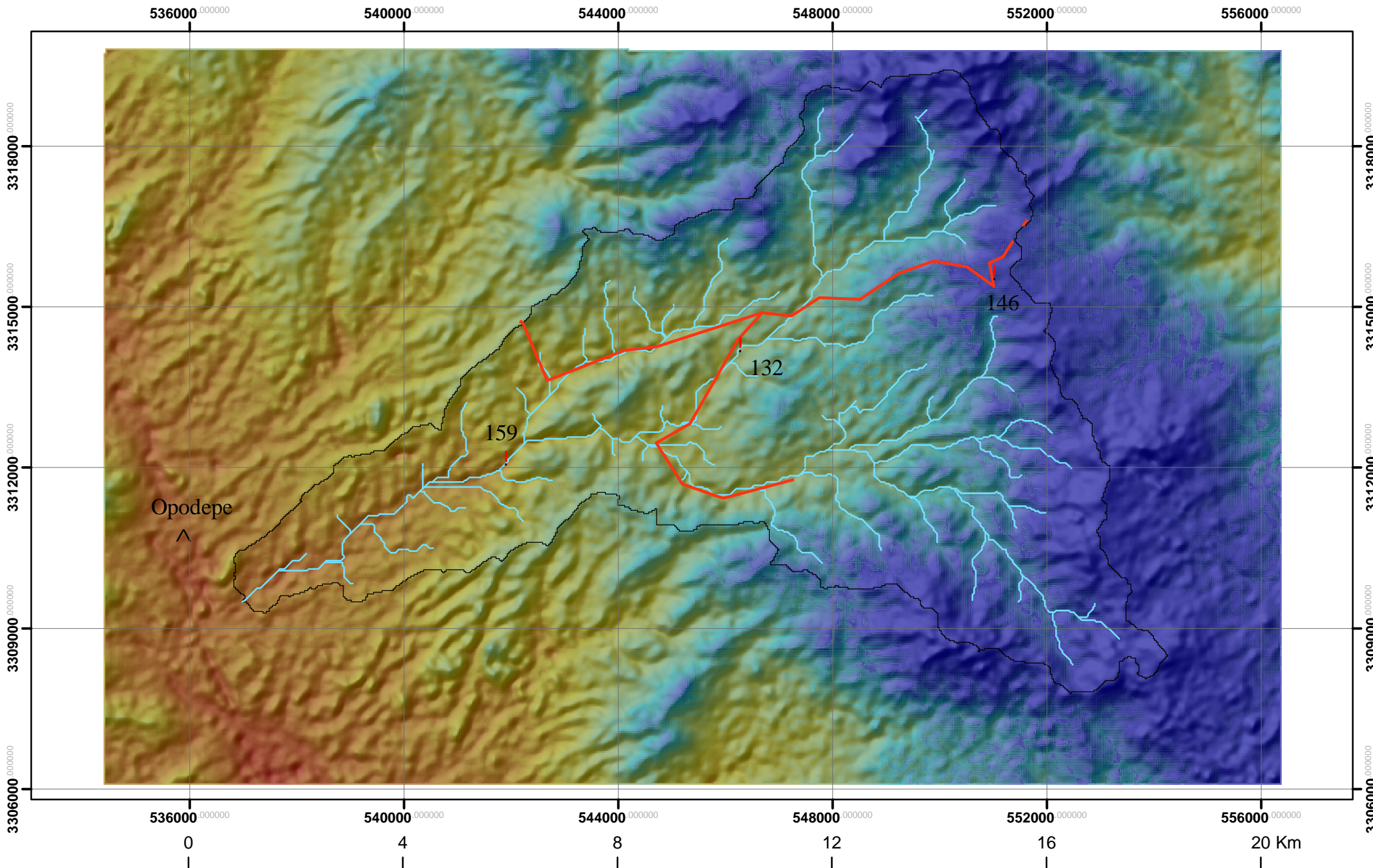
CONTOUR MAP



Basin Boundary Sierra Los Locos
Contours (30m)

! Stations
^ Opodepe

DIGITAL ELEVATION MAP

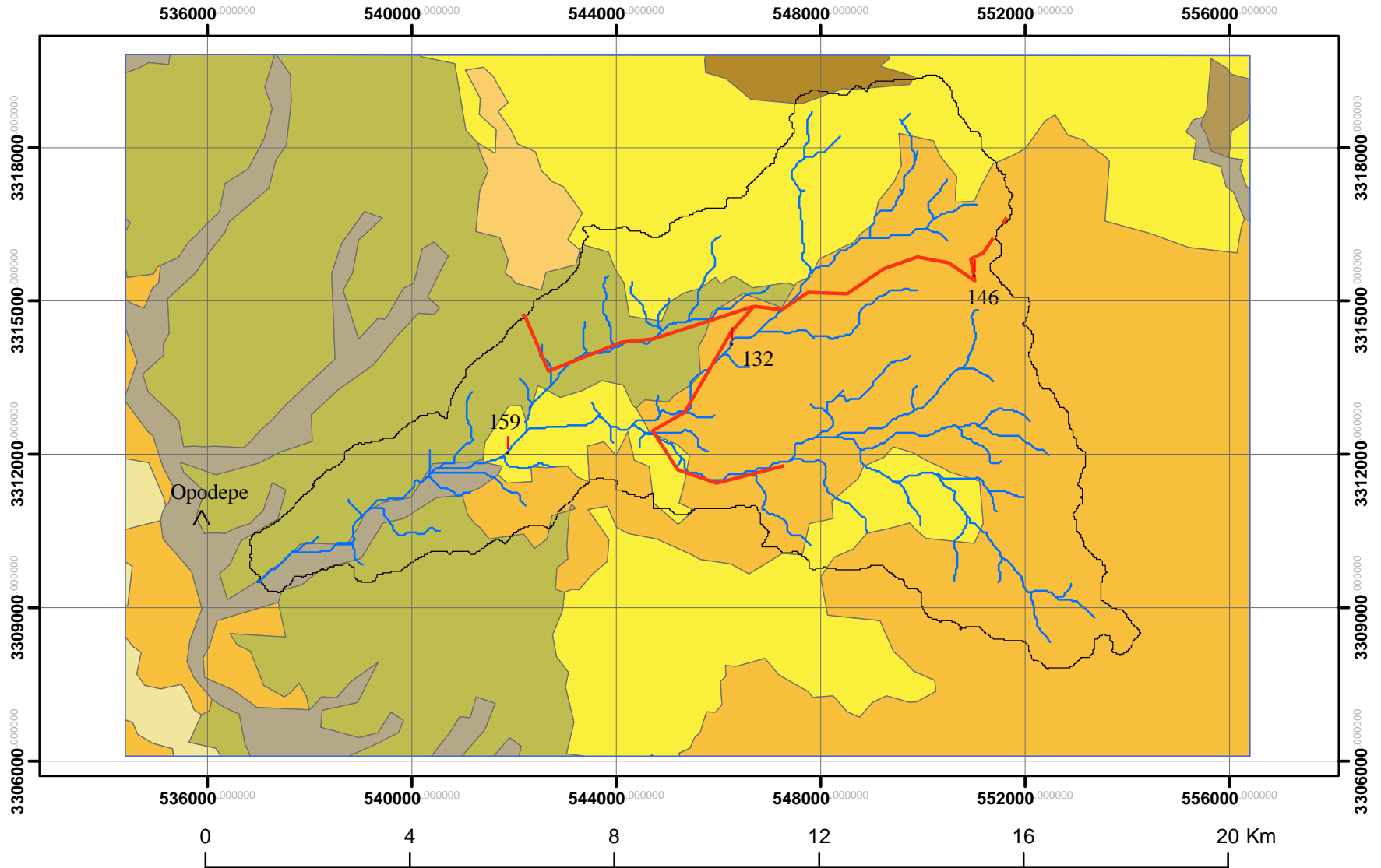


Basin Boundary Sierra Los Locos
Sierra Los Locos Stream Network




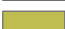




! Stations
^ Opodepe
— Roads





Source: ASTER DEM from EOS / NASA

GEOLOGIC MAP



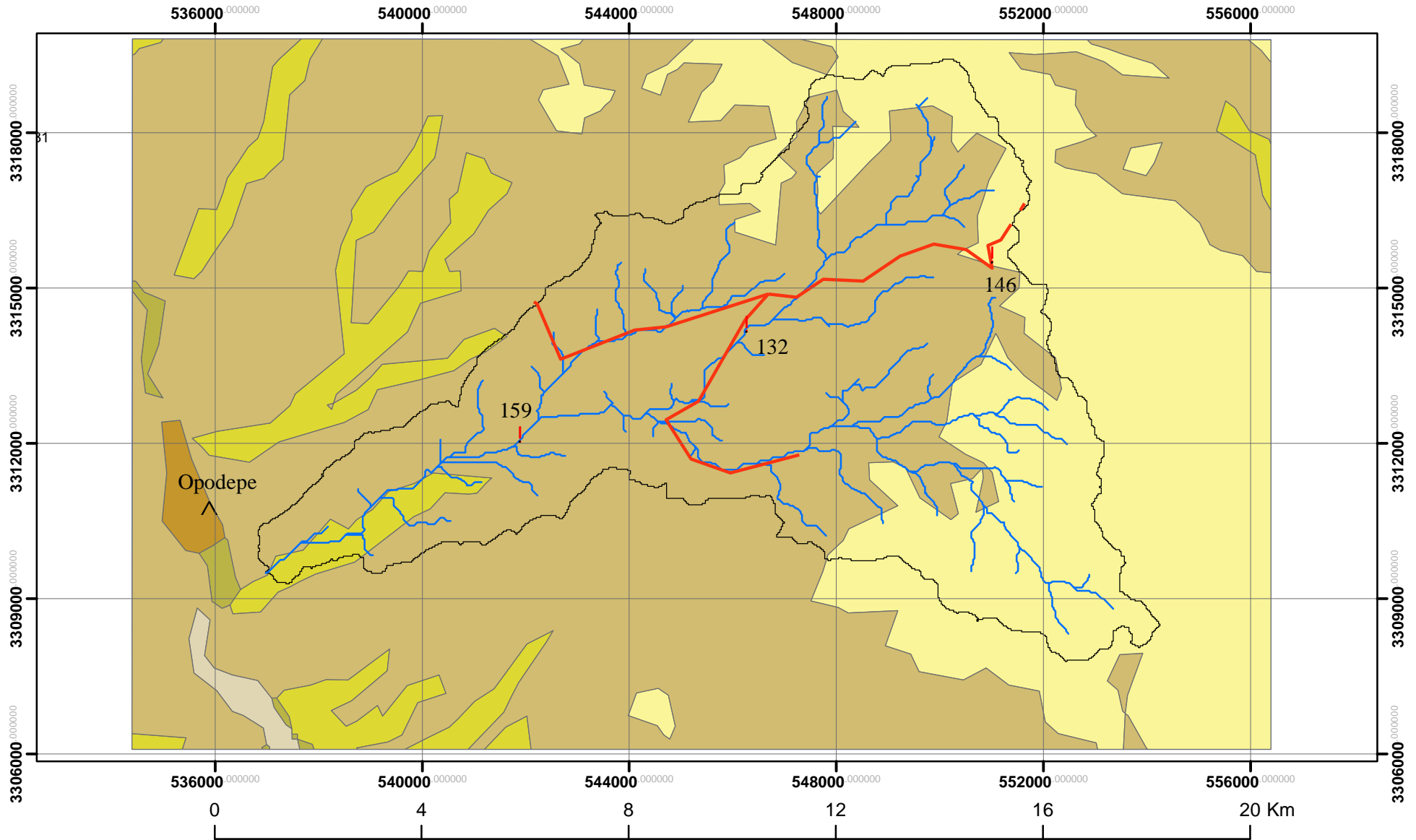
Geologic Layers

-  Aluvion del Cuaternario
-  Asociacion Riolita - Toba cida del Terciario
-  Basalto del Cenozoico
-  Conglomerado del Cenozoico
-  Gneiss del mesozoico
-  Granito del mesozoico
-  Granodiorita del mesozoico
-  Toba cida del Terciario

-  Basin Boundary Sierra Los Locos
-  Sierra Los Locos Stream Network
-  Stations
-  Roads

Source: INEGI, 2000.

VEGETATION MAP



Vegetation Types

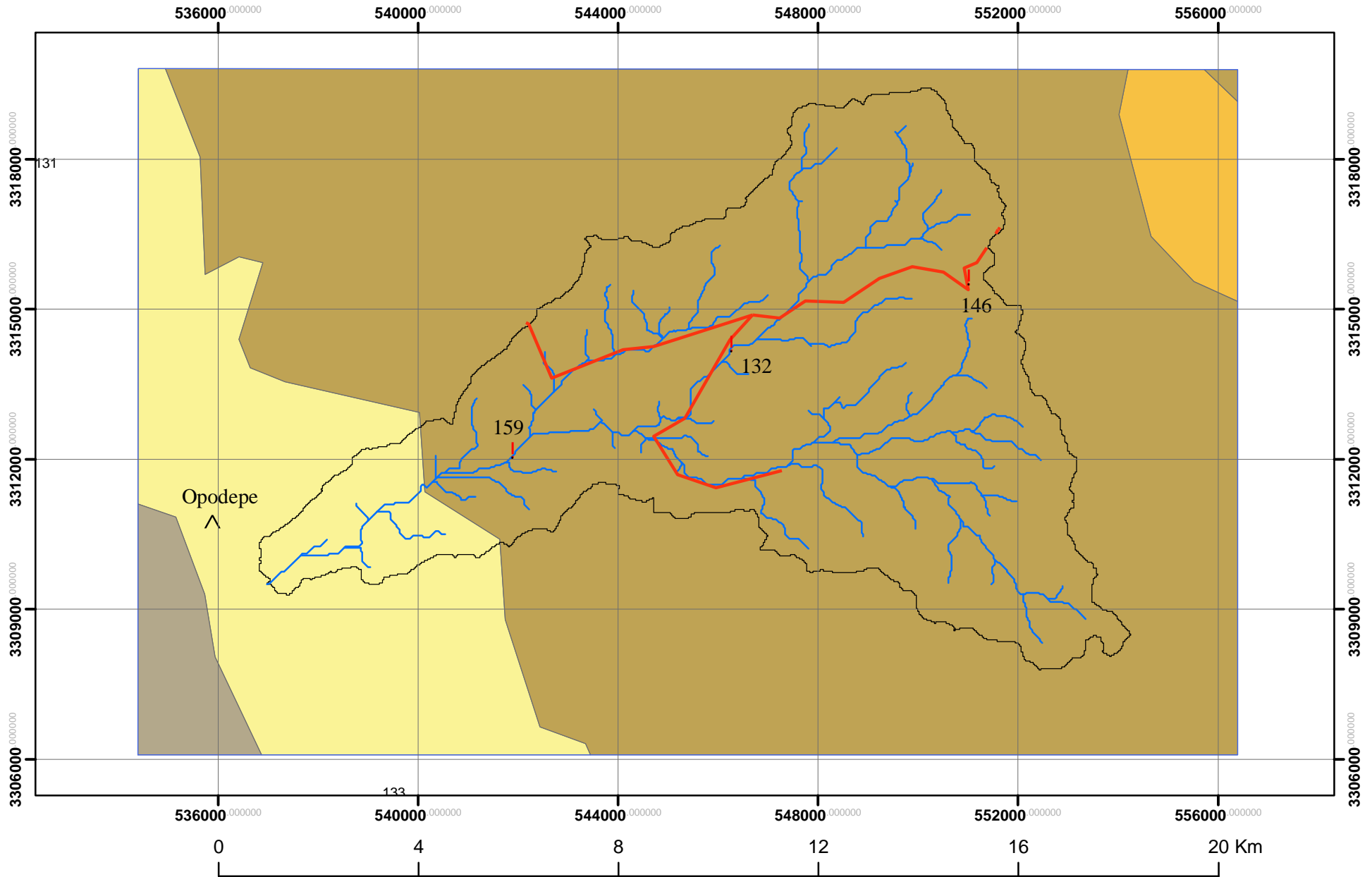
- AGRICULTURA
- BOSQUE
- MATORRALES
- MEZQUITELES
- RIEGO SUSPENDIDO
- VEGETACION DE GALERIA





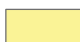



- Basin Boundary Sierra Los Locos
- Sierra Los Locos Stream Network
- Stations
- Roads



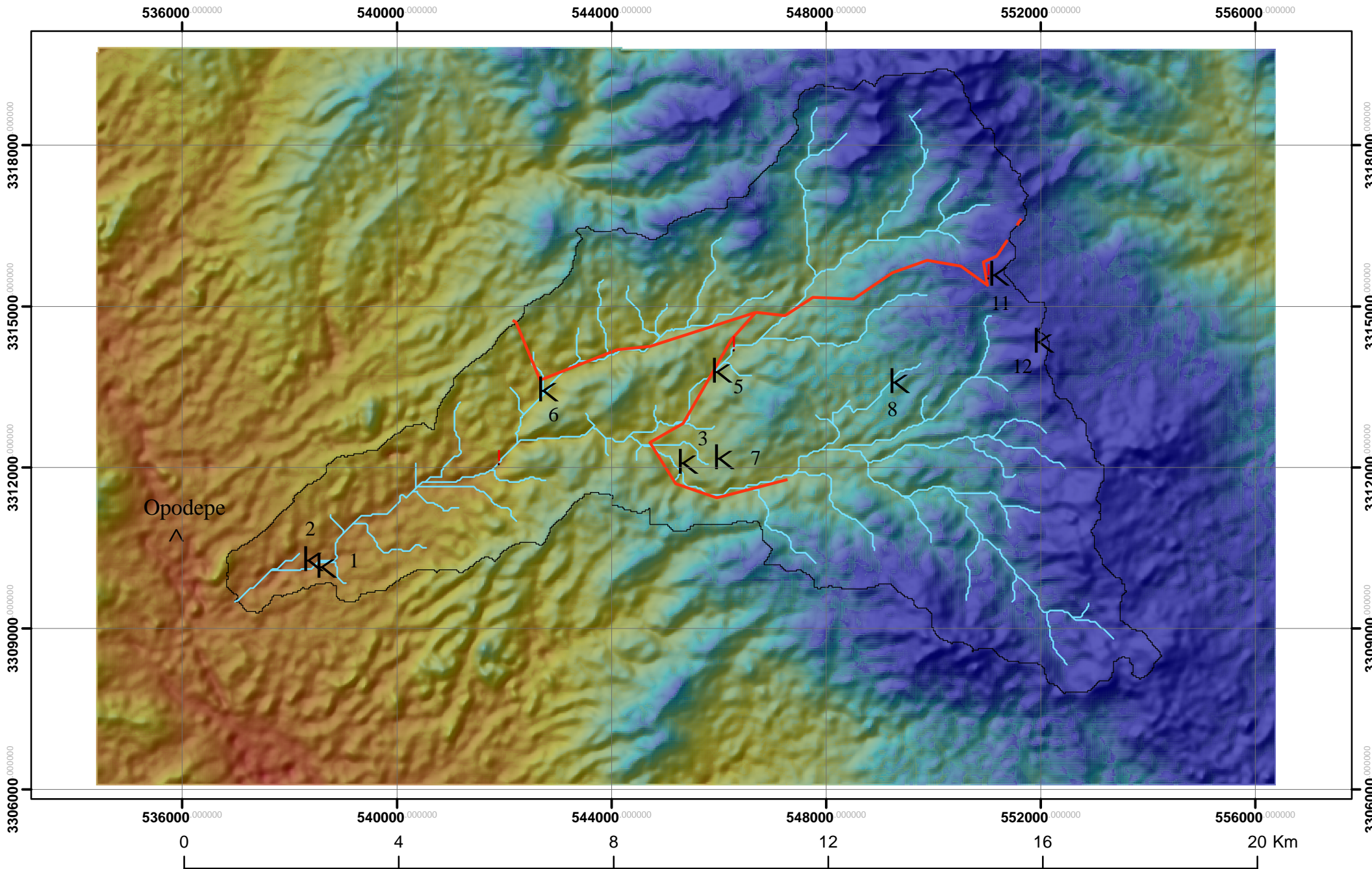
Source: INEGI, 2000.

SOIL TYPES MAP



- | | | | |
|---|---|---|---------------------------------|
|  | Suelos de textura fina, delgados, limitados por roca coherente. |  | Basin Boundary Sierra Los Locos |
|  | Suelos de textura fina, profundos, frecuentemente con piedras en la superficie. |  | Sierra Los Locos Stream Network |
|  | Suelos de textura gruesa, delgados, limitados por roca coherente. |  | Stations |
|  | Suelos de textura gruesa, profundos, localmente con gravas en la superficie. |  | Roads |

LOCATION OF SOIL PITS



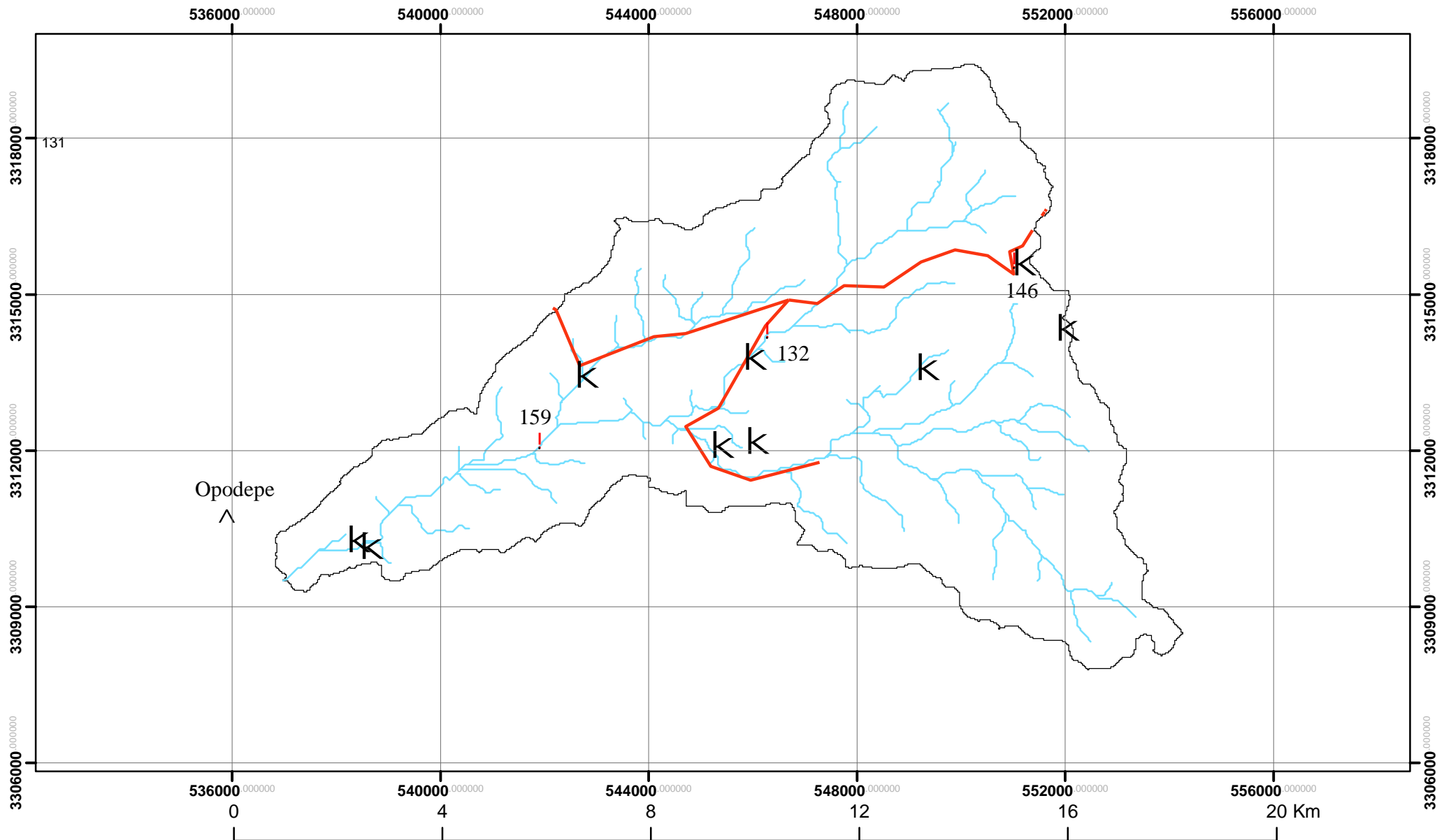
- Basin Boundary Sierra Los Locos
- Sierra Los Locos Stream Network
- Soil Pits

- Stations
- Opodepe
- Roads



Source: NMT

LOCATION OF SOIL PITS

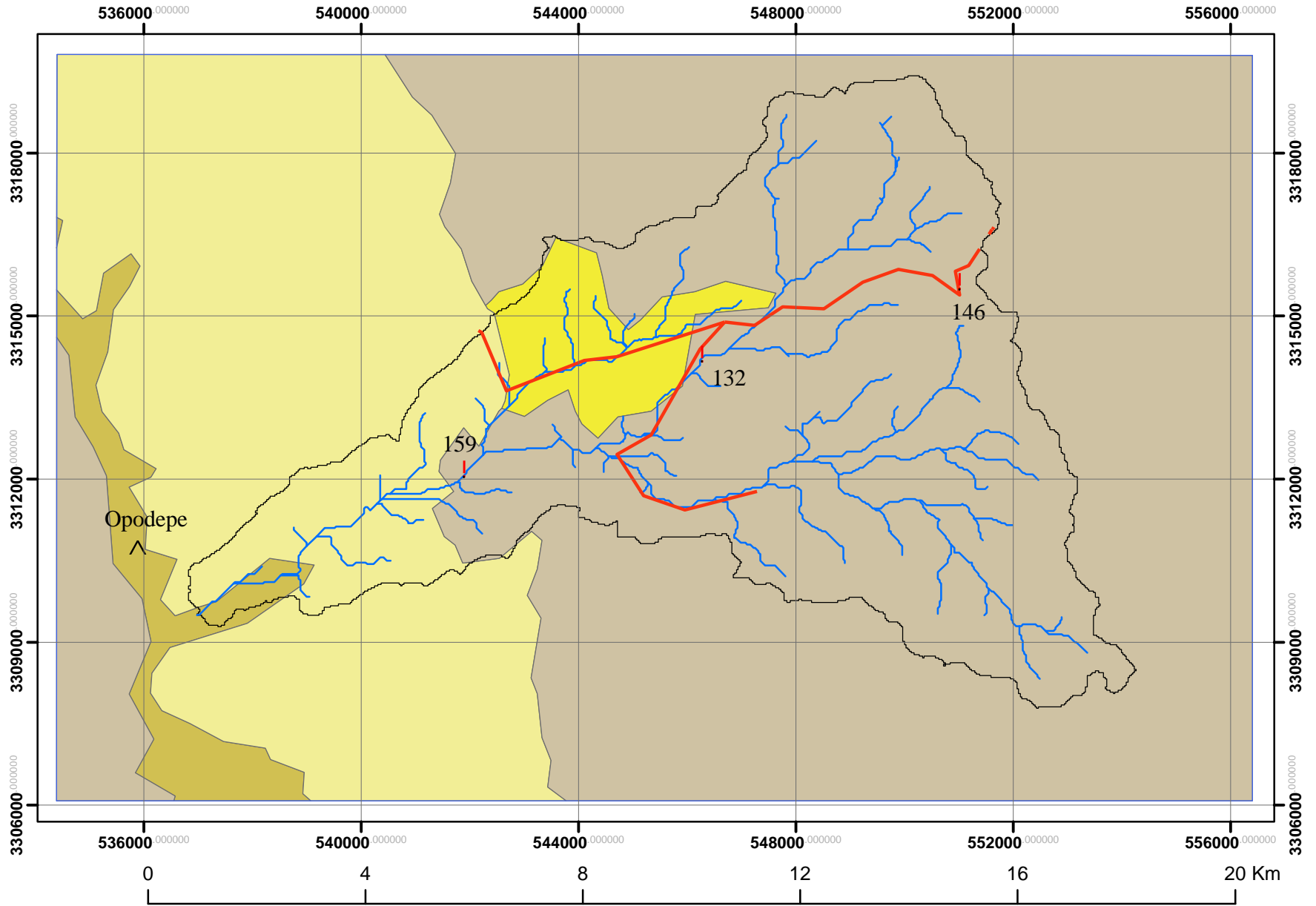


- Basin Boundary Sierra Los Locos
- Sierra Los Locos Stream Network
- Soil Pits

- Stations
- Opodepe
- Roads

Source: NMT

SOIL UNITS MAP



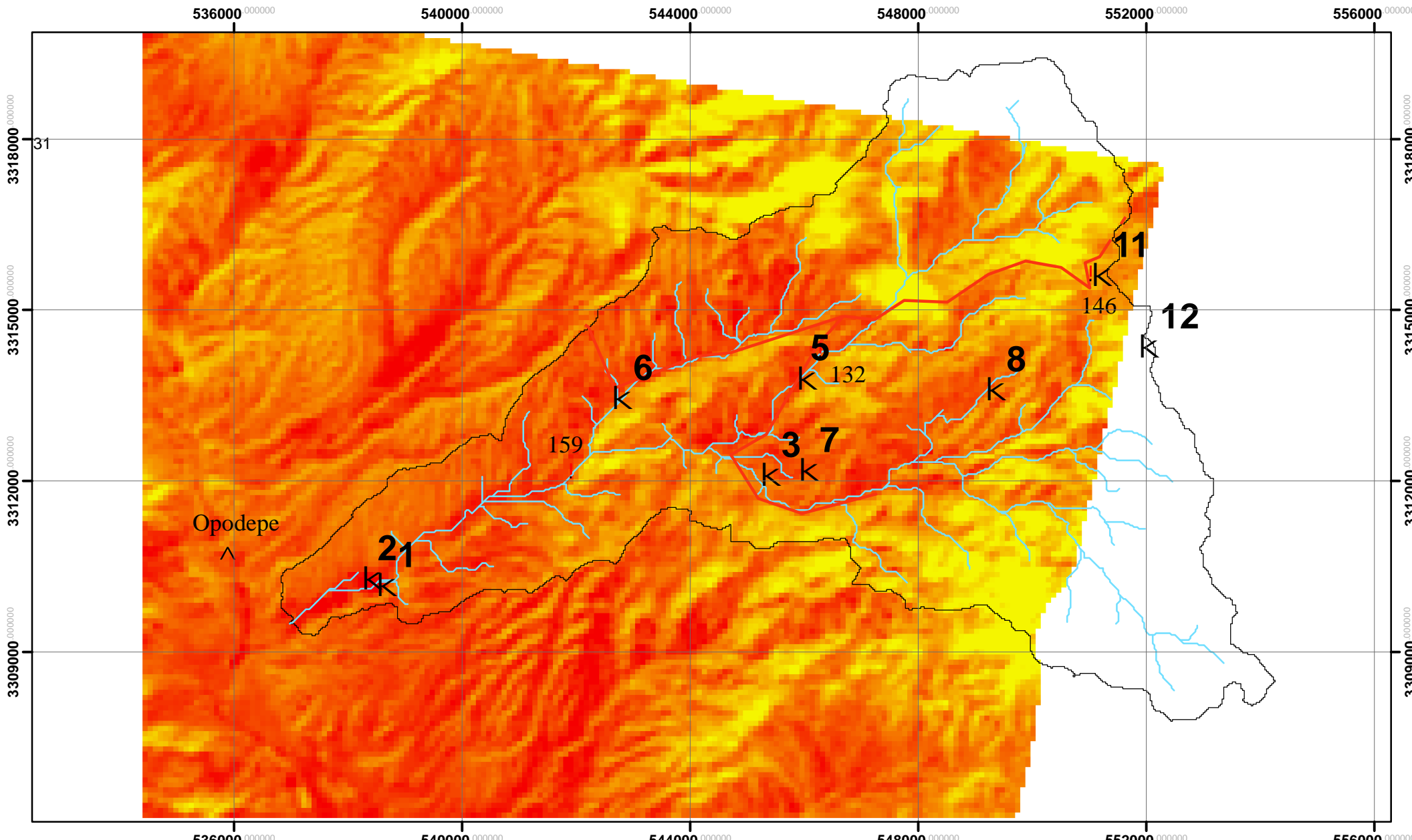
Unidades de Suelo

- Material consolidado, posibilidad baja
- Material no consolidado, posibilidad alta
- Material no consolidado, posibilidad media
- Material no consolidado, posibilidades baja

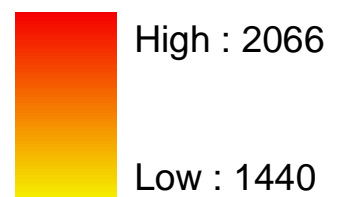
- Basin Boundary Sierra Los Locos
- Sierra Los Locos Stream Network
- Stations
- Roads

Source: INEGI, 2000.

Land Surface Temperature - September 30 2004



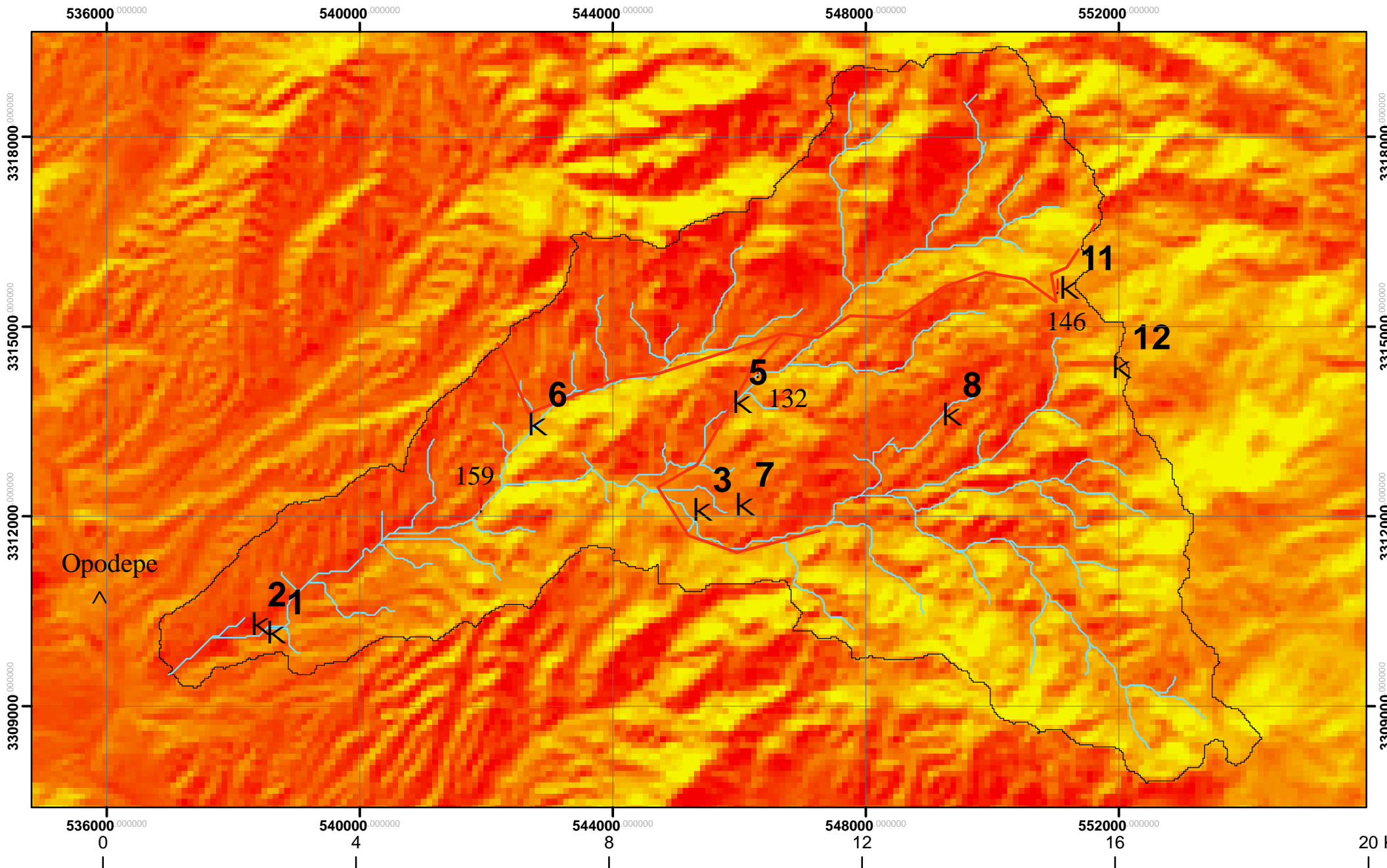
Sept 30 2004



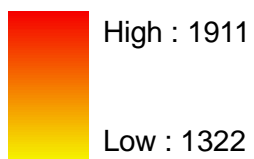
-  Soil Pits
-  Stations
-  Opodepe
-  Roads
-  Sierra Los Locos Stream Network
-  Basin Boundary Sierra Los Locos

Source: ASTER DEM from EOS / NASA

Land Surface Temperature - November 29 2005



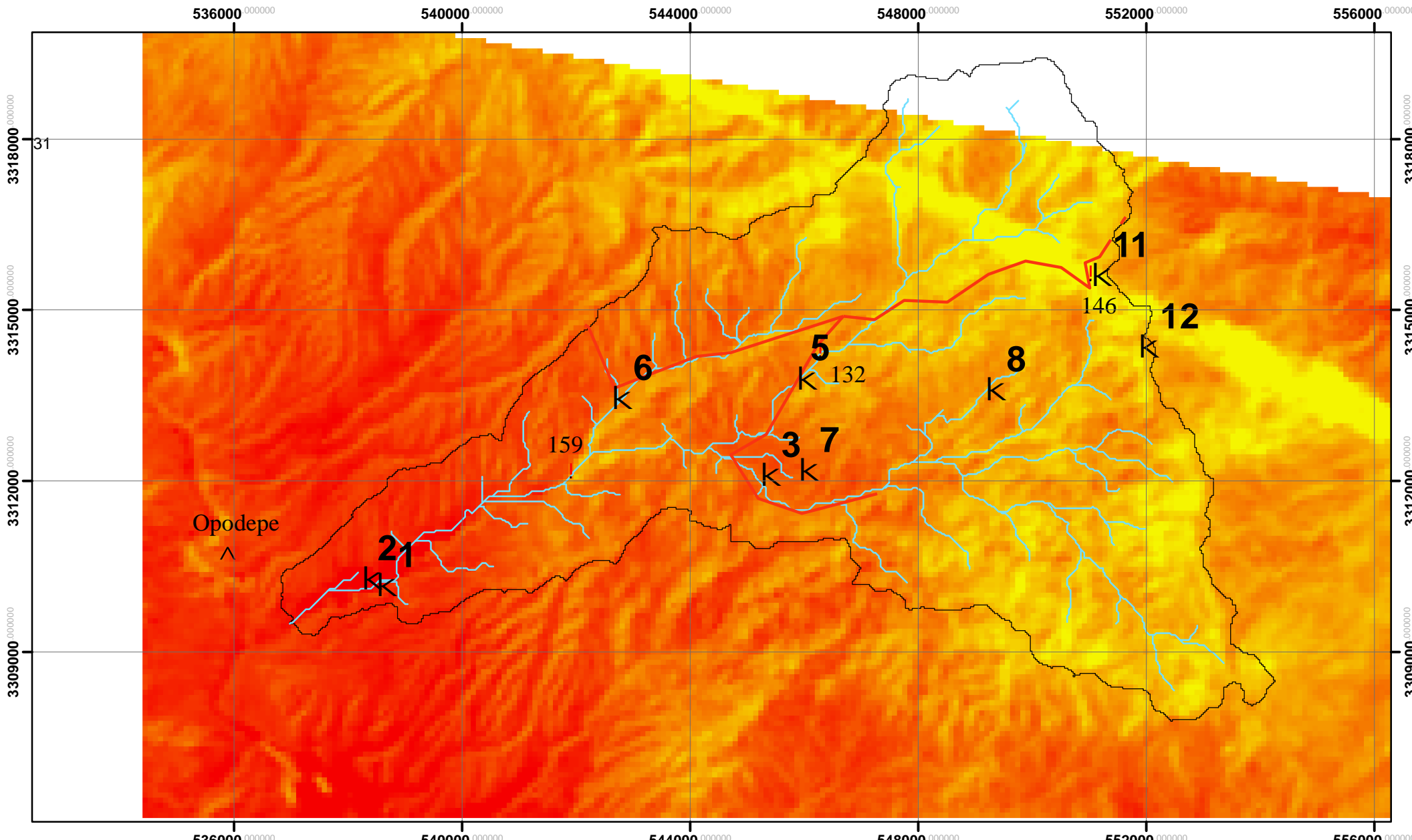
November 29 2005



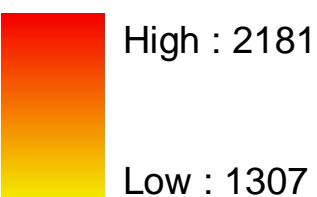
- K Soil Pits
- ! Stations
- ^ Opodepe
- Roads
- Sierra Los Locos Stream Network
- Basin Boundary Sierra Los Locos

Source: ASTER DEM from EOS / NASA

Land Surface Temperature - April 13 2006



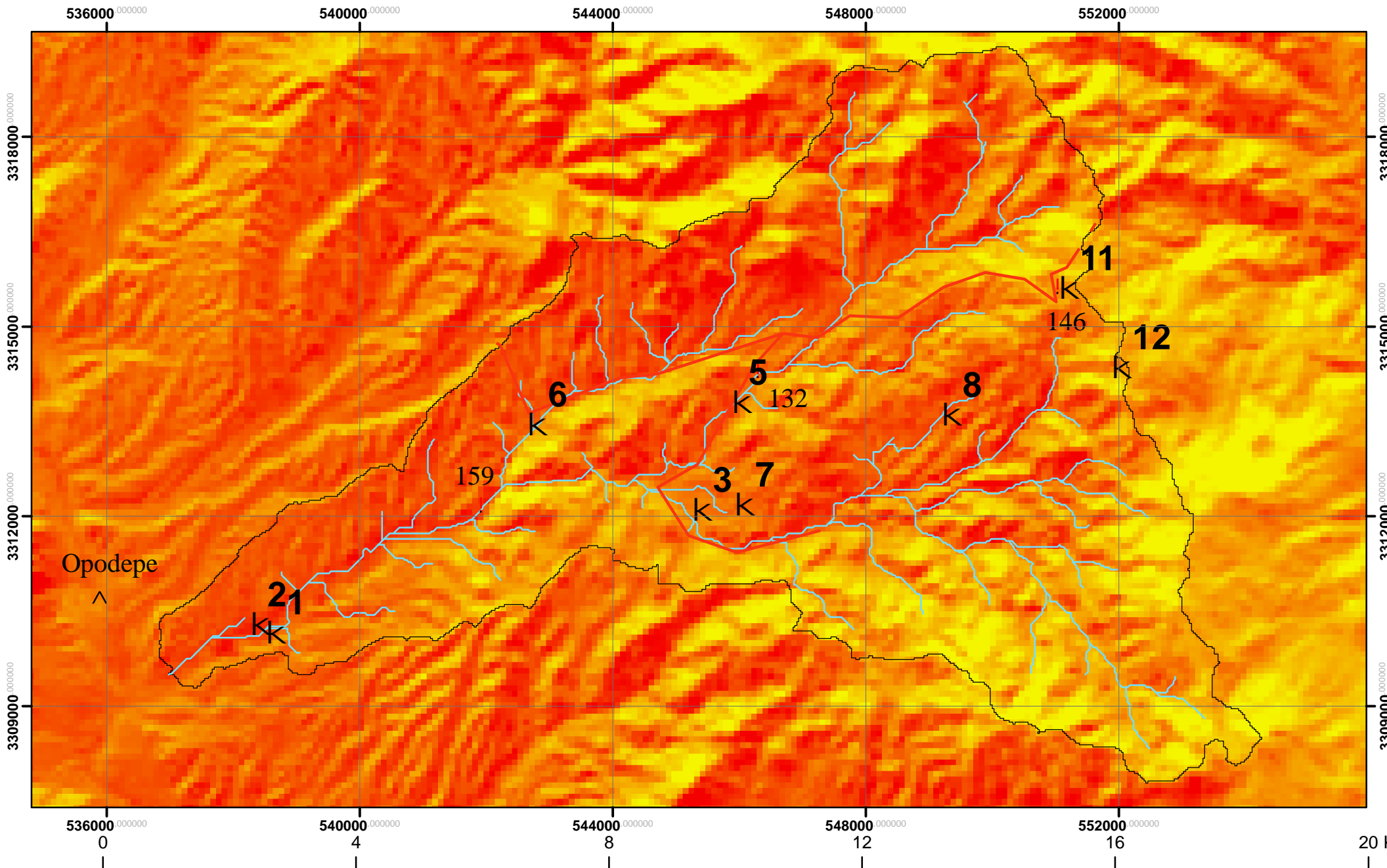
Apr 13 2006



- K Soil Pits
- ! Stations
- ^ Opodepe
- Roads
- Sierra Los Locos Stream Network
- Basin Boundary Sierra Los Locos

Source: ASTER DEM from EOS / NASA

Land Surface Temperature - December 2 2006



536000.000000 540000.000000 544000.000000 548000.000000 552000.000000

3318000.000000 3315000.000000 3312000.000000 3309000.000000

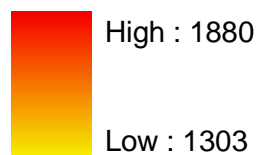
Opodepe

21 159 6 5 132 8 11 146 12 3 7

536000.000000 540000.000000 544000.000000 548000.000000 552000.000000

0 4 8 12 16 20

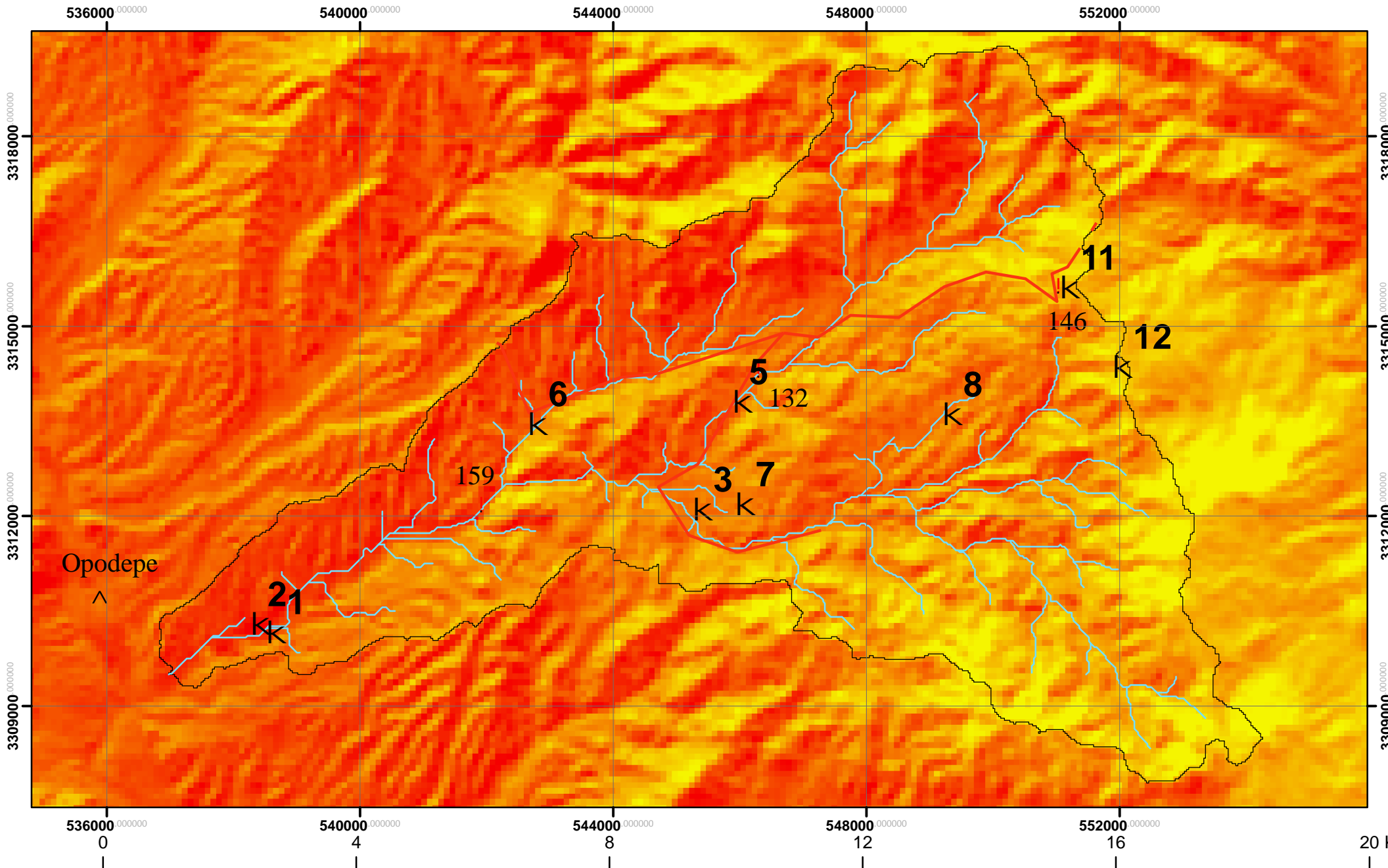
December 2 2006



-  Soil Pits
-  Stations
-  Opodepe
-  Roads
-  Sierra Los Locos Stream Network
-  Basin Boundary Sierra Los Locos

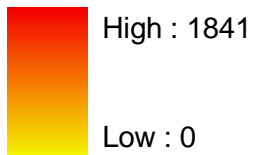
Source: ASTER DEM from EOS / NASA

Land Surface Temperature - February 4 2007



536000 000000 540000 000000 544000 000000 548000 000000 552000 000000
 3318000 000000 3315000 000000 3312000 000000 3309000 000000
 536000 000000 540000 000000 544000 000000 548000 000000 552000 000000 2000000 000000

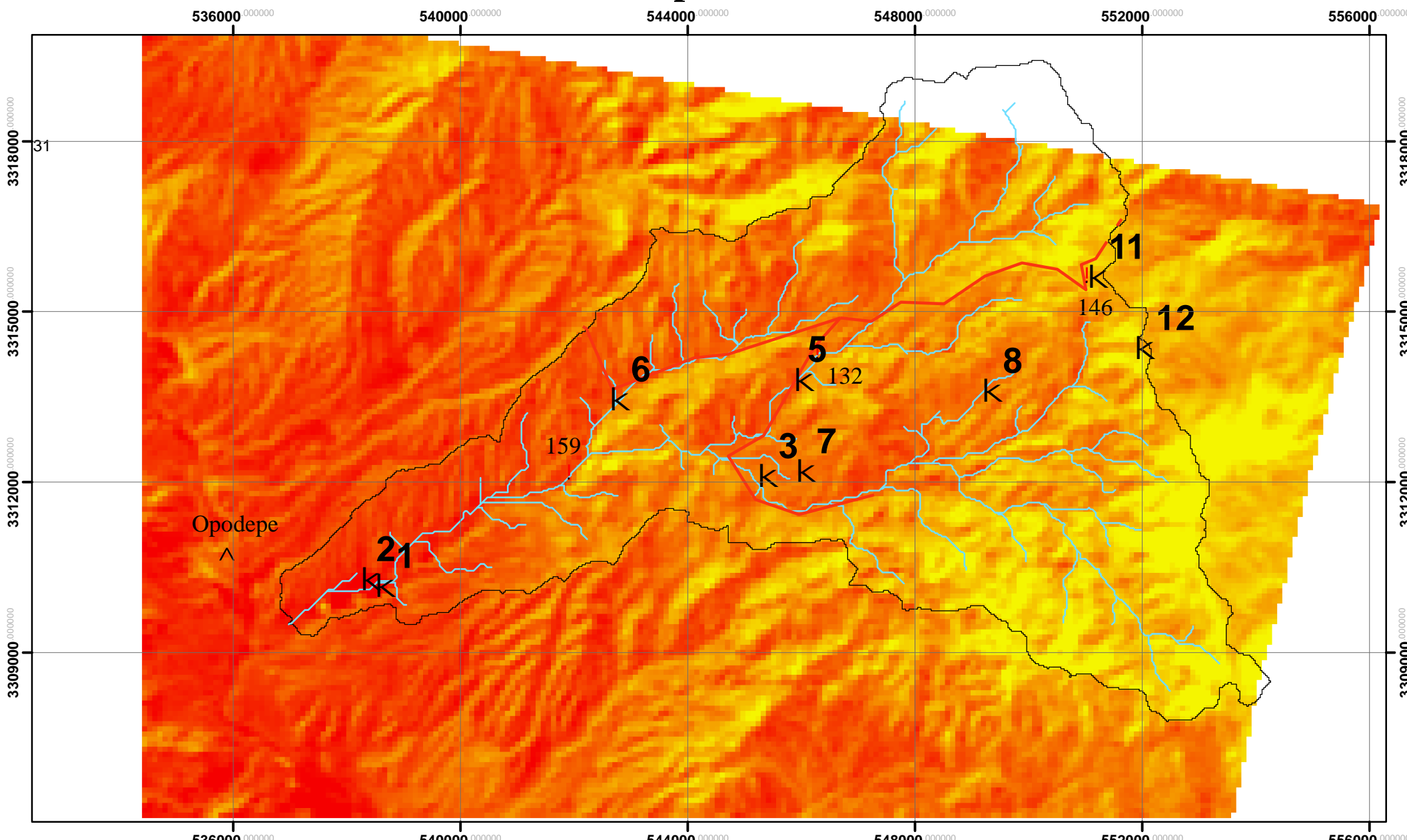
February 4 2007



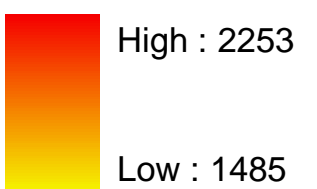
- K Soil Pits
- ! Stations
- ^ Opodepe
- Roads
- Sierra Los Locos Stream Network
- Basin Boundary Sierra Los Locos

Source: ASTER DEM from EOS / NASA

Land Surface Temperature - March 31 2007



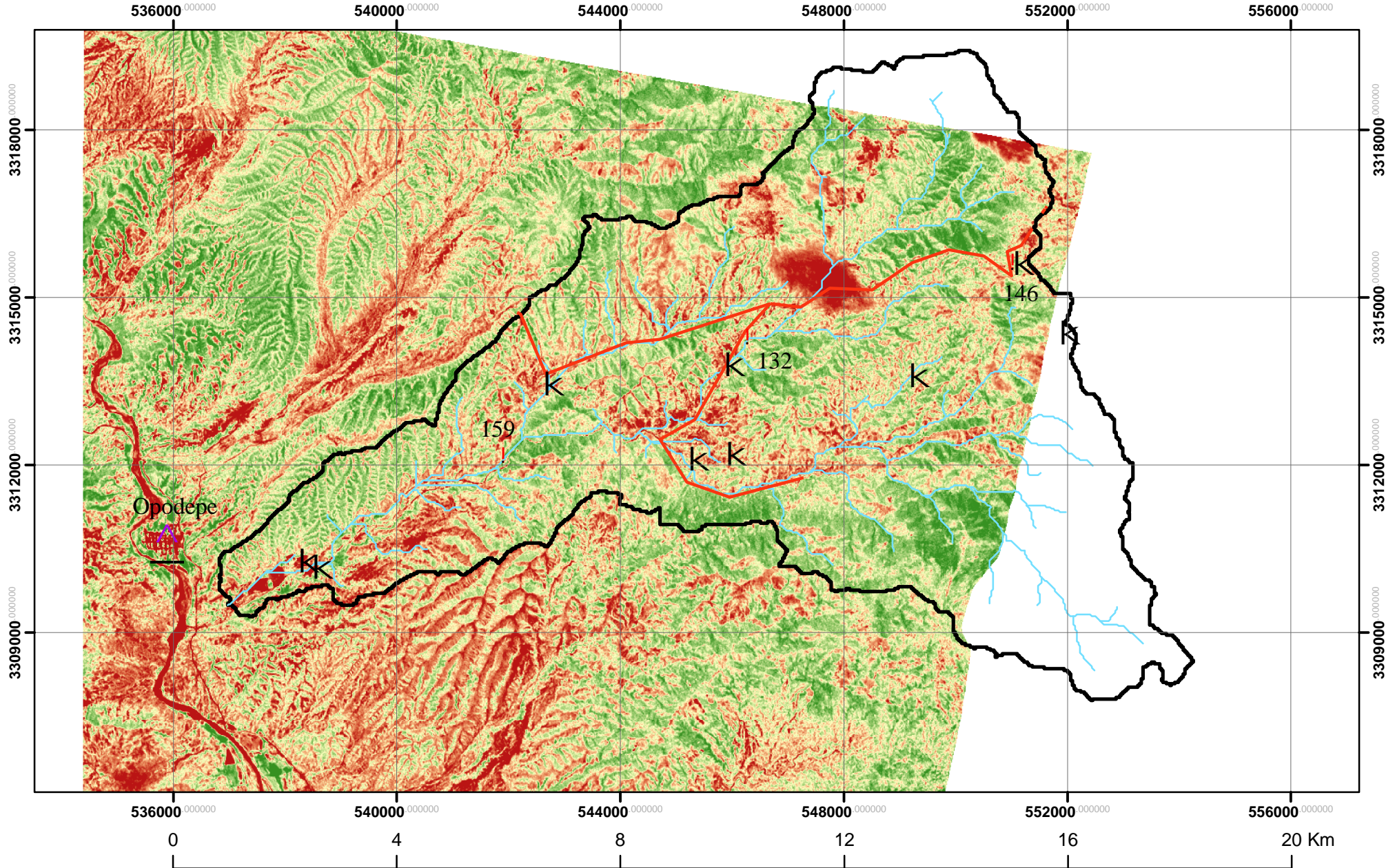
March 31 2007



- Soil Pits
- Stations
- Opodepe
- Roads
- Sierra Los Locos Stream Network
- Basin Boundary Sierra Los Locos

Source: ASTER DEM from EOS / NASA

NDVI - Septmeber 30 2004



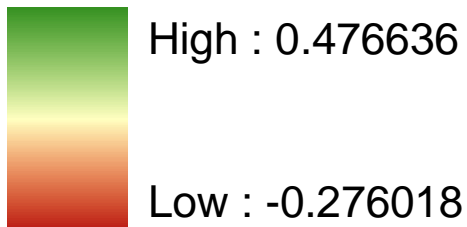
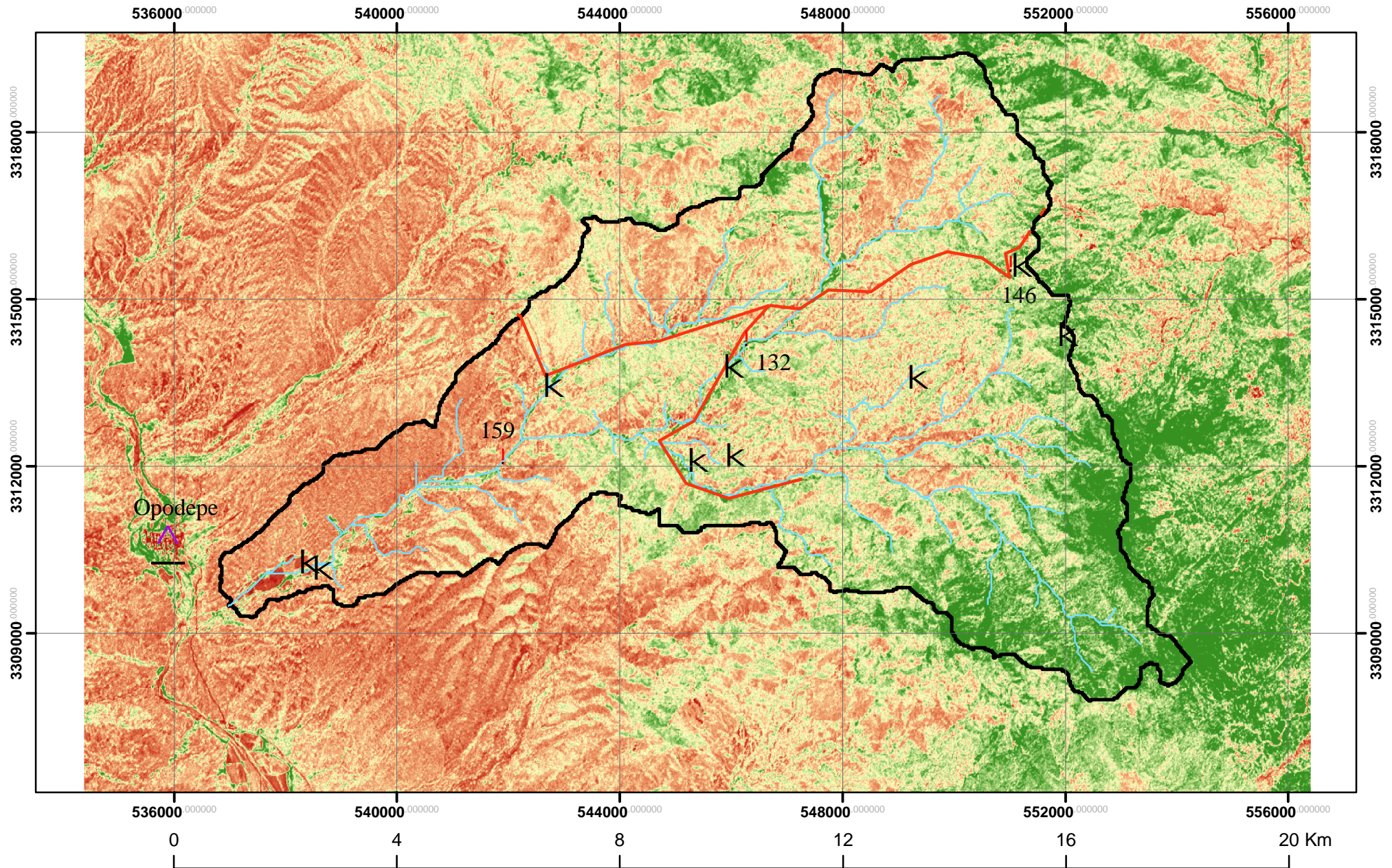
September NDVI



- K Soil Pits
- ! Stations
- ^ Opodepe
- Roads
- Sierra Los Locos Stream Network
- Basin Boundary Sierra Los Locos

Source: ASTER (EOS / NASA)

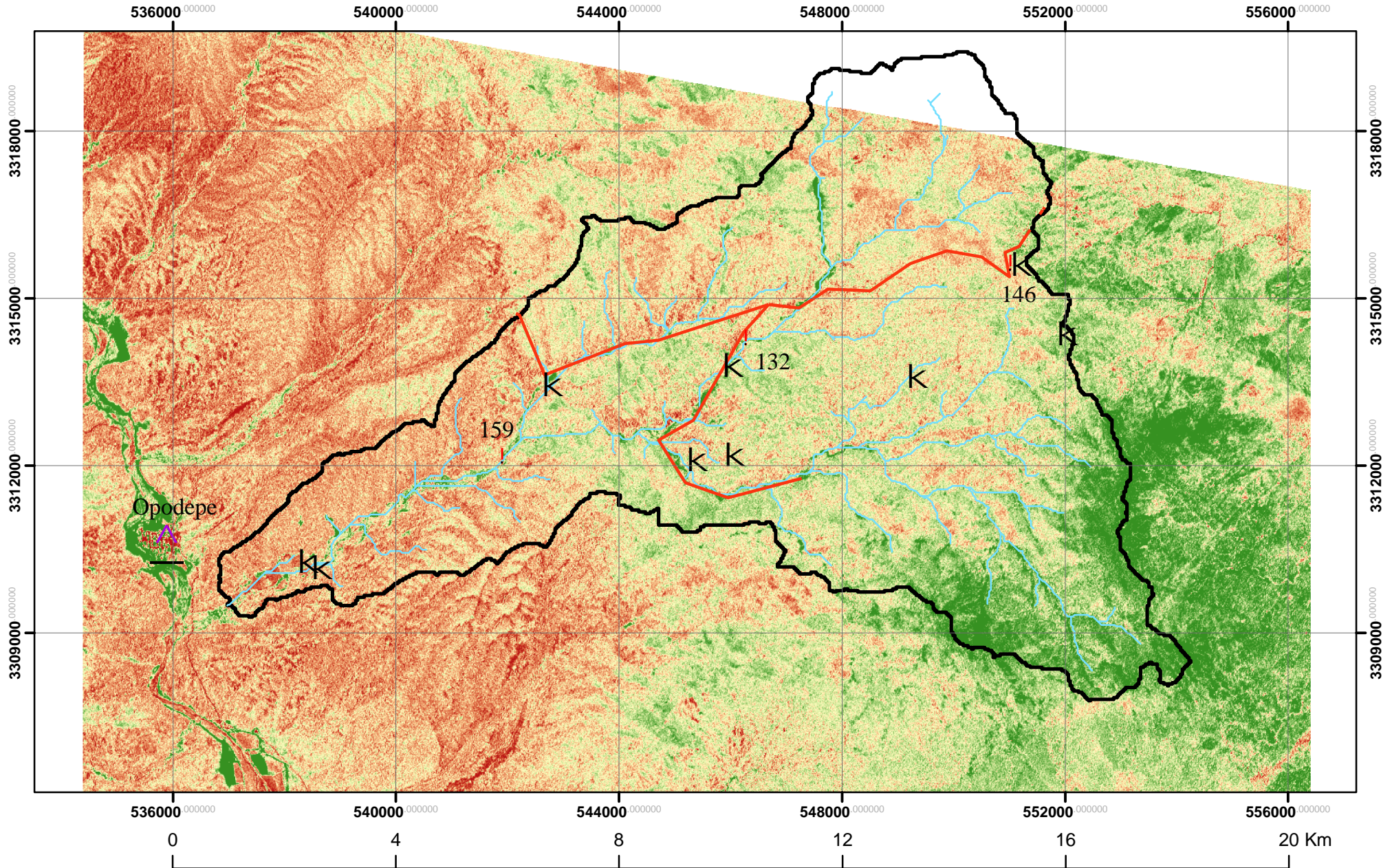
NDVI - November 29 2005



- K Soil Pits
- ! Stations
- △ Opodepe
- Roads
- Sierra Los Locos Stream Network
- Basin Boundary Sierra Los Locos

Source: ASTER (EOS / NASA)

NDVI - April 13 2006



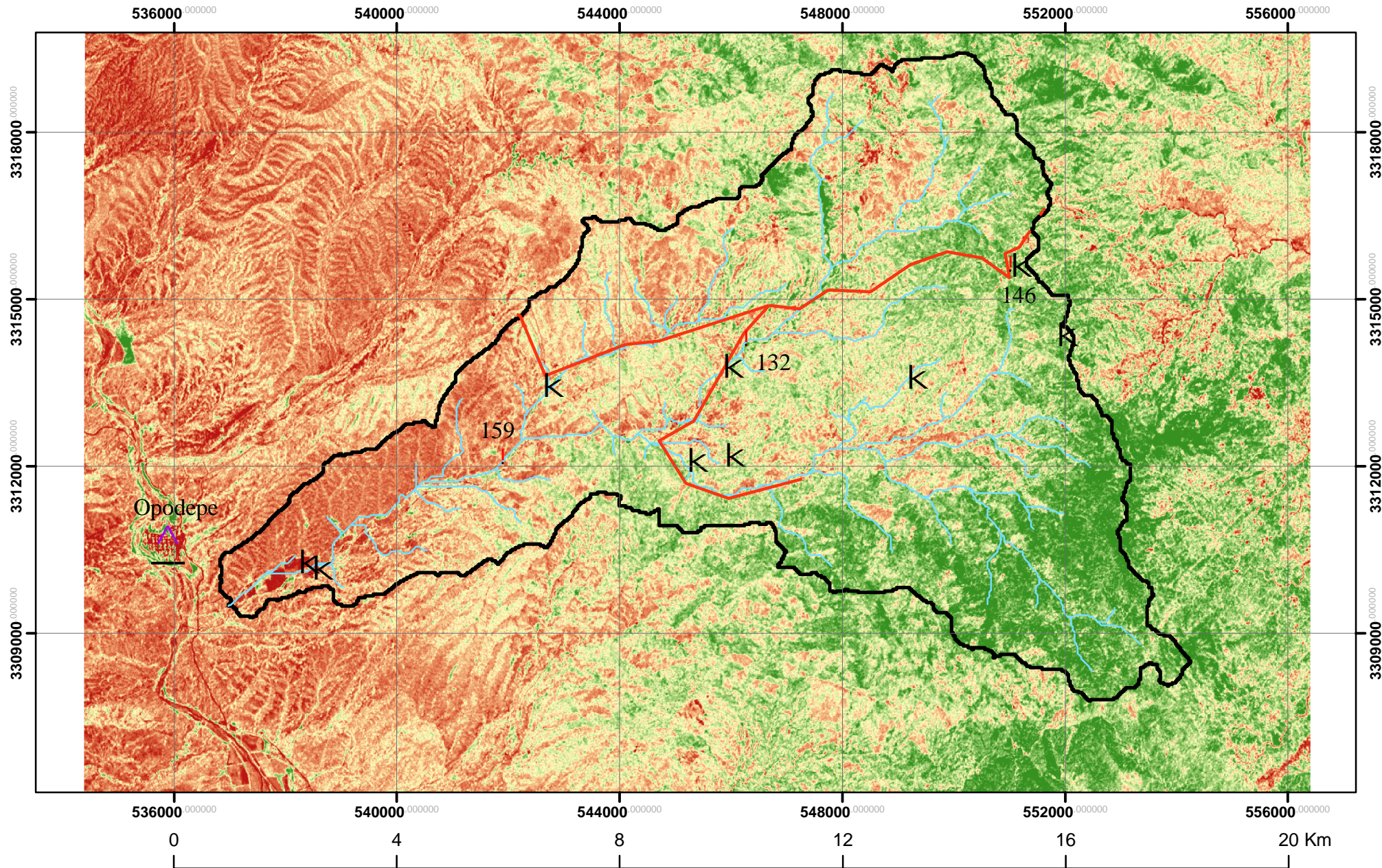
April NDVI



- K** Soil Pits
- !** Stations
- ▲** Opodepe
- Roads
- Sierra Los Locos Stream Network
- Basin Boundary Sierra Los Locos

Source: ASTER (EOS / NASA)

NDVI - December 2 2006



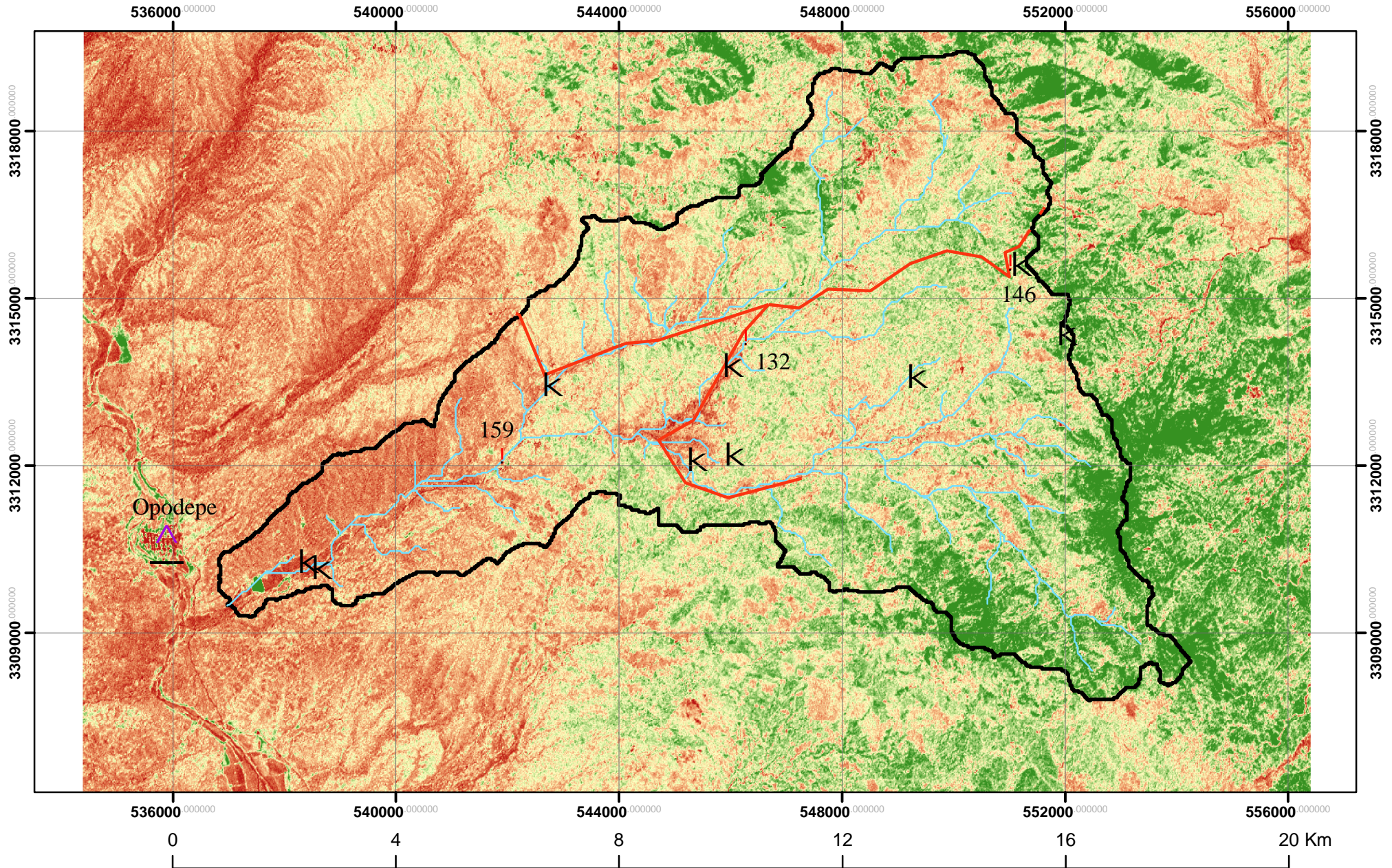
December NDVI



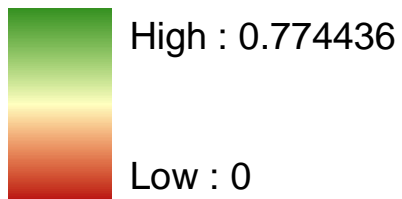
- K** Soil Pits
- !** Stations
- ▲** Opodepe
- Roads
- Sierra Los Locos Stream Network
- Basin Boundary Sierra Los Locos

Source: ASTER (EOS / NASA)

NDVI - February 4 2007



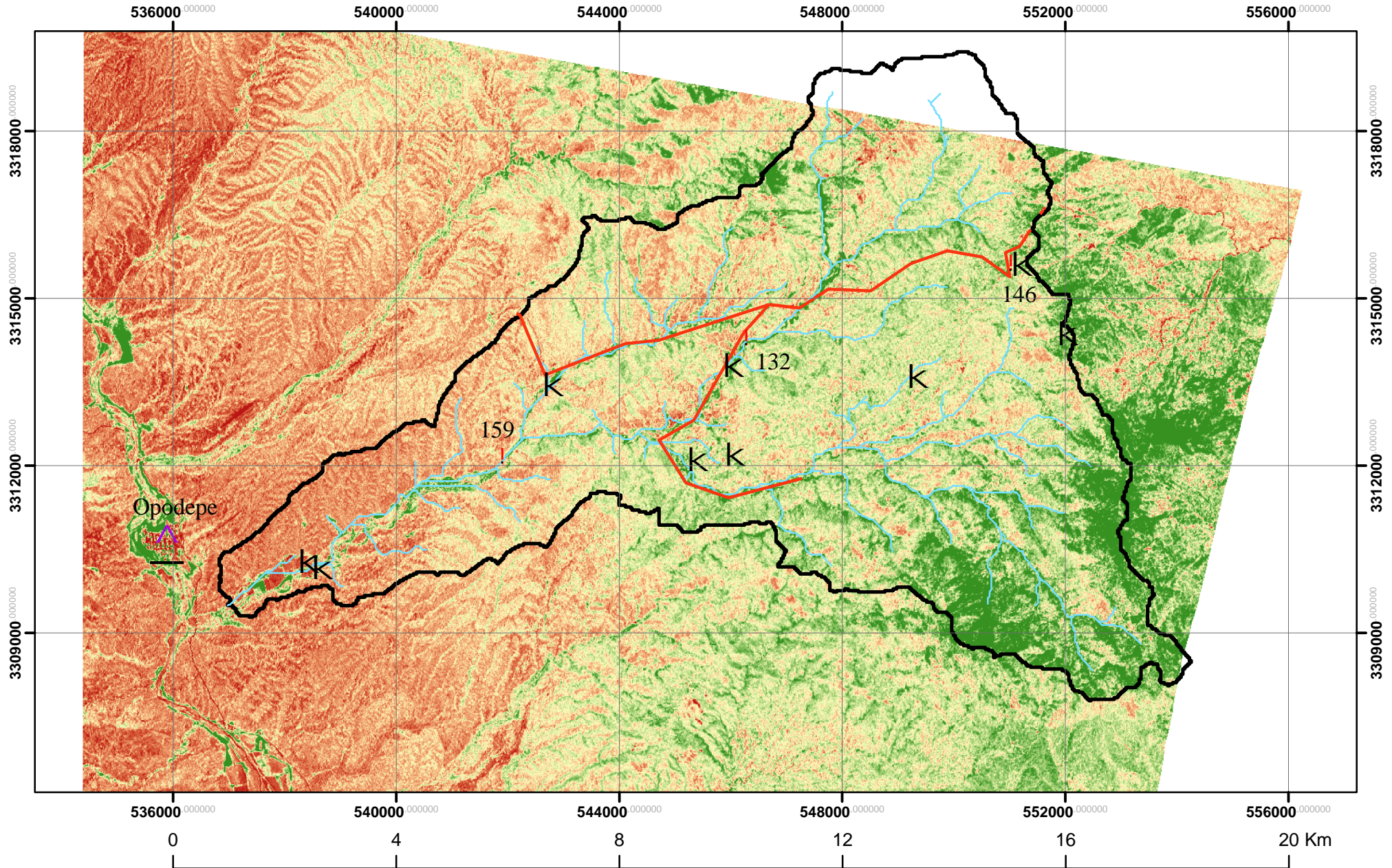
February NDVI



- K Soil Pits
- ! Stations
- △ Opodepe
- Roads
- Sierra Los Locos Stream Network
- Basin Boundary Sierra Los Locos

Source: ASTER (EOS / NASA)

NDVI - March 31 2007



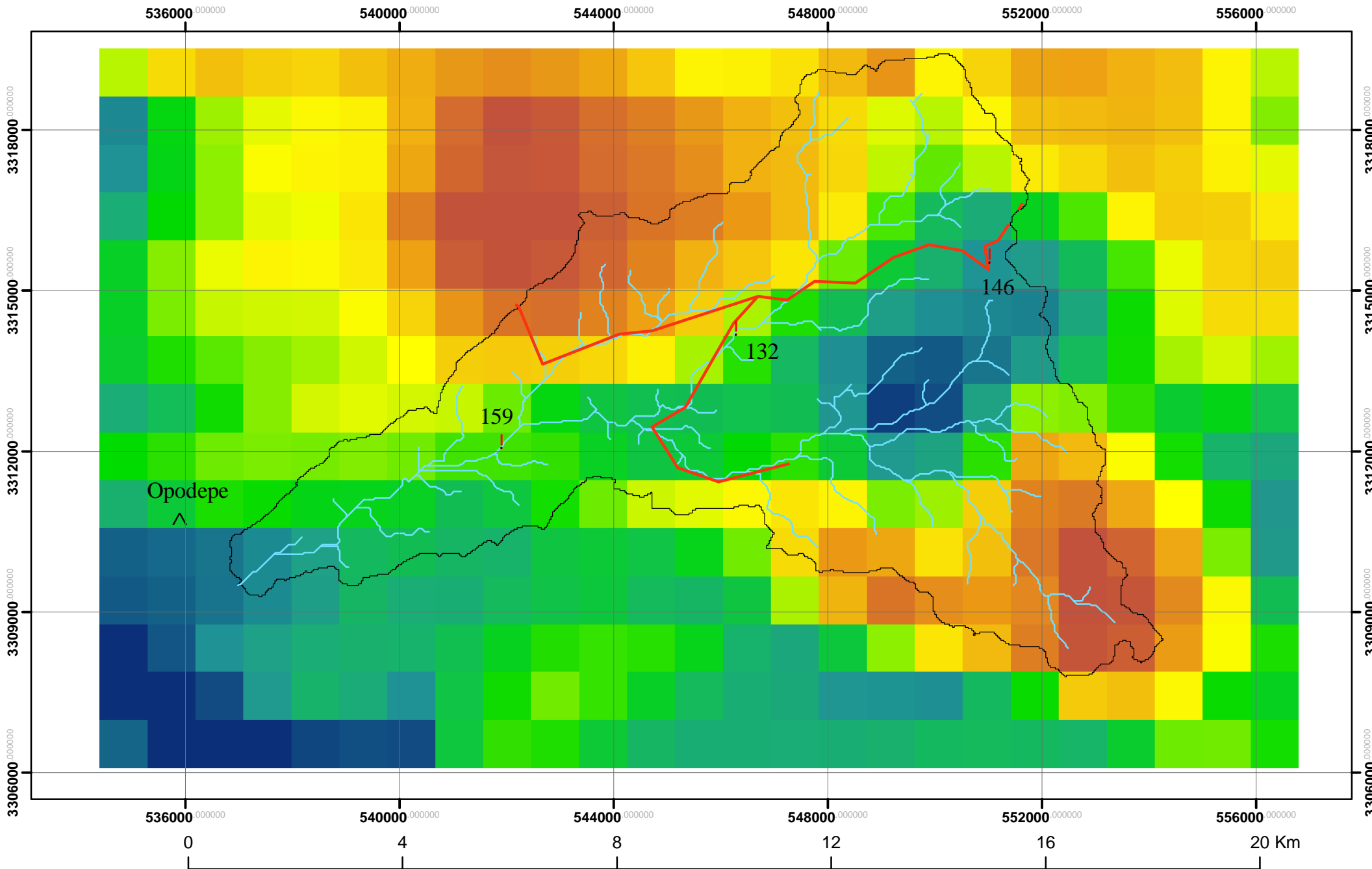
March NDVI



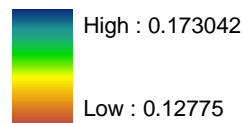
- K Soil Pits
- ! Stations
- △ Opodepe
- Roads
- Sierra Los Locos Stream Network
- Basin Boundary Sierra Los Locos

Source: ASTER (EOS / NASA)

ALBEDO MAP (MEAN DRY PERIOD)



Albedo values

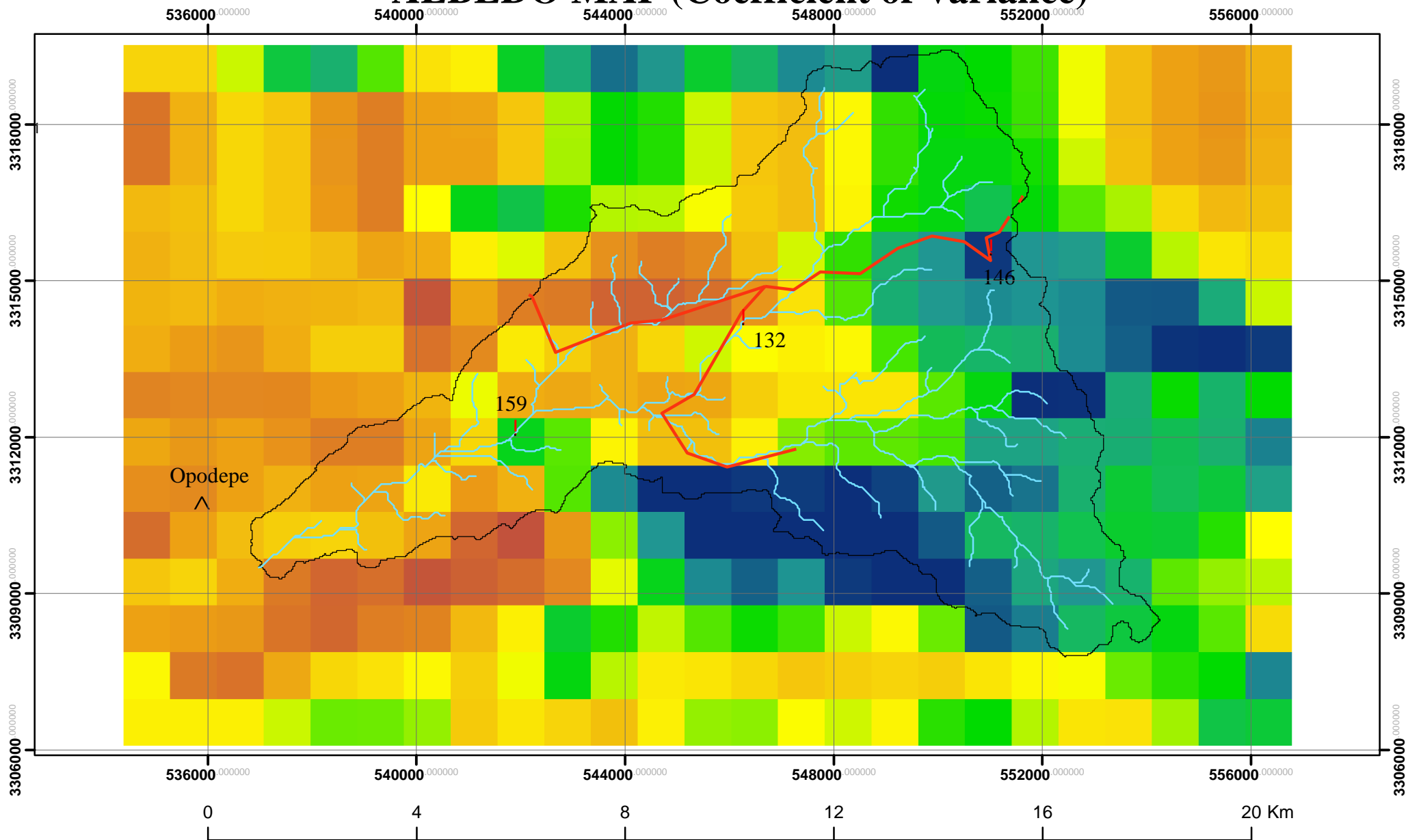


- Basin Boundary Sierra Los Locos
- Sierra Los Locos Stream Network

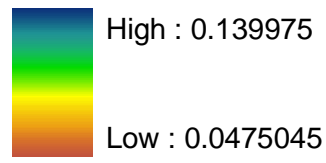
- ! Stations
- ^ Opodepe
- Roads

Source: MODIS
Description: March, Apr and May years 2004-2007

ALBEDO MAP (Coefficient of Variance)



Coefficient of Variance

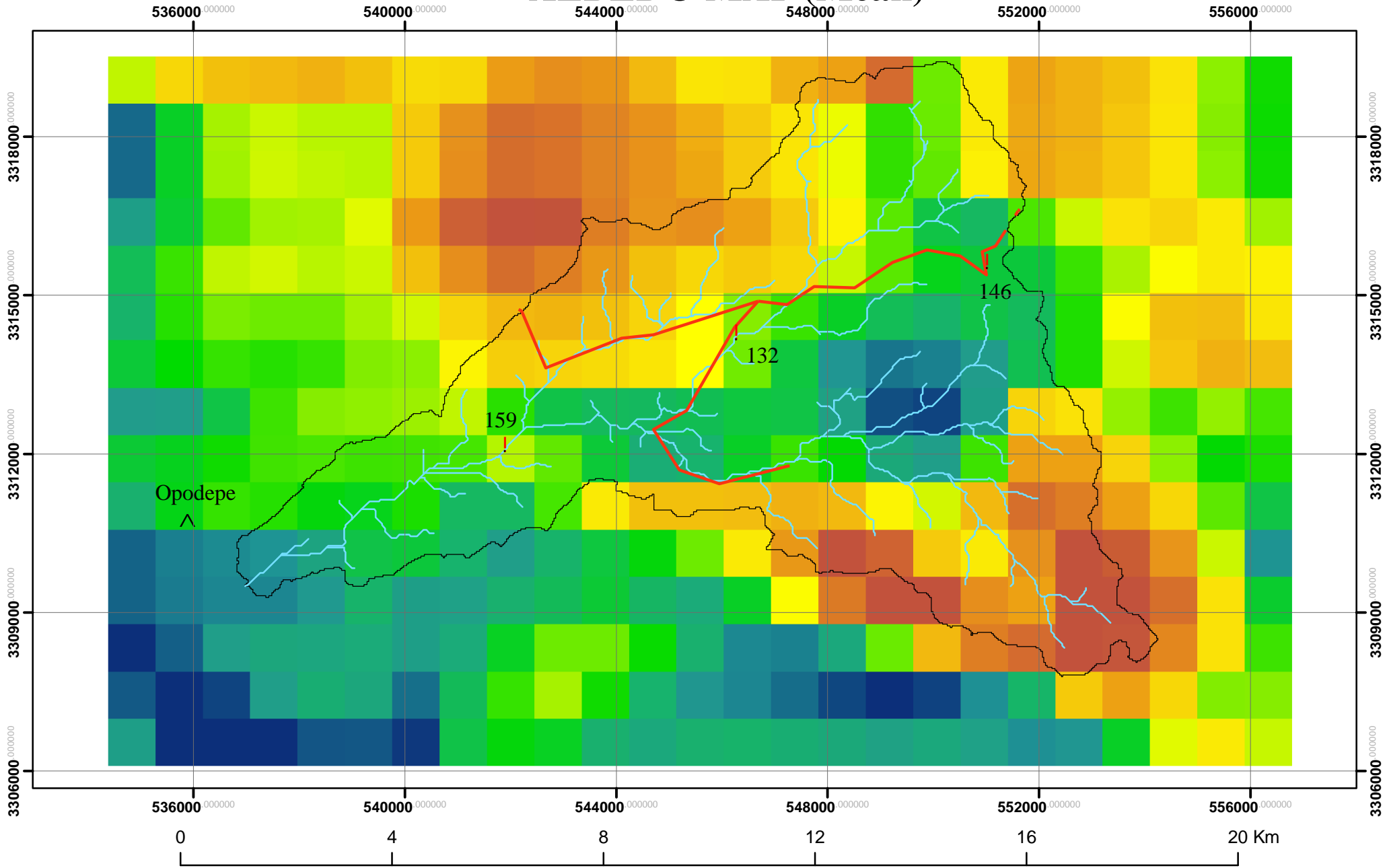


- Basin Boundary Sierra Los Locos
- Sierra Los Locos Stream Network

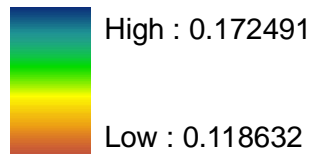
- Opodepe
- Stations
- Roads

Source: MODIS

ALBEDO MAP (Mean)



Albedo Los Locos



Basin Boundary Sierra Los Locos



Sierra Los Locos Stream Network



Opodepe



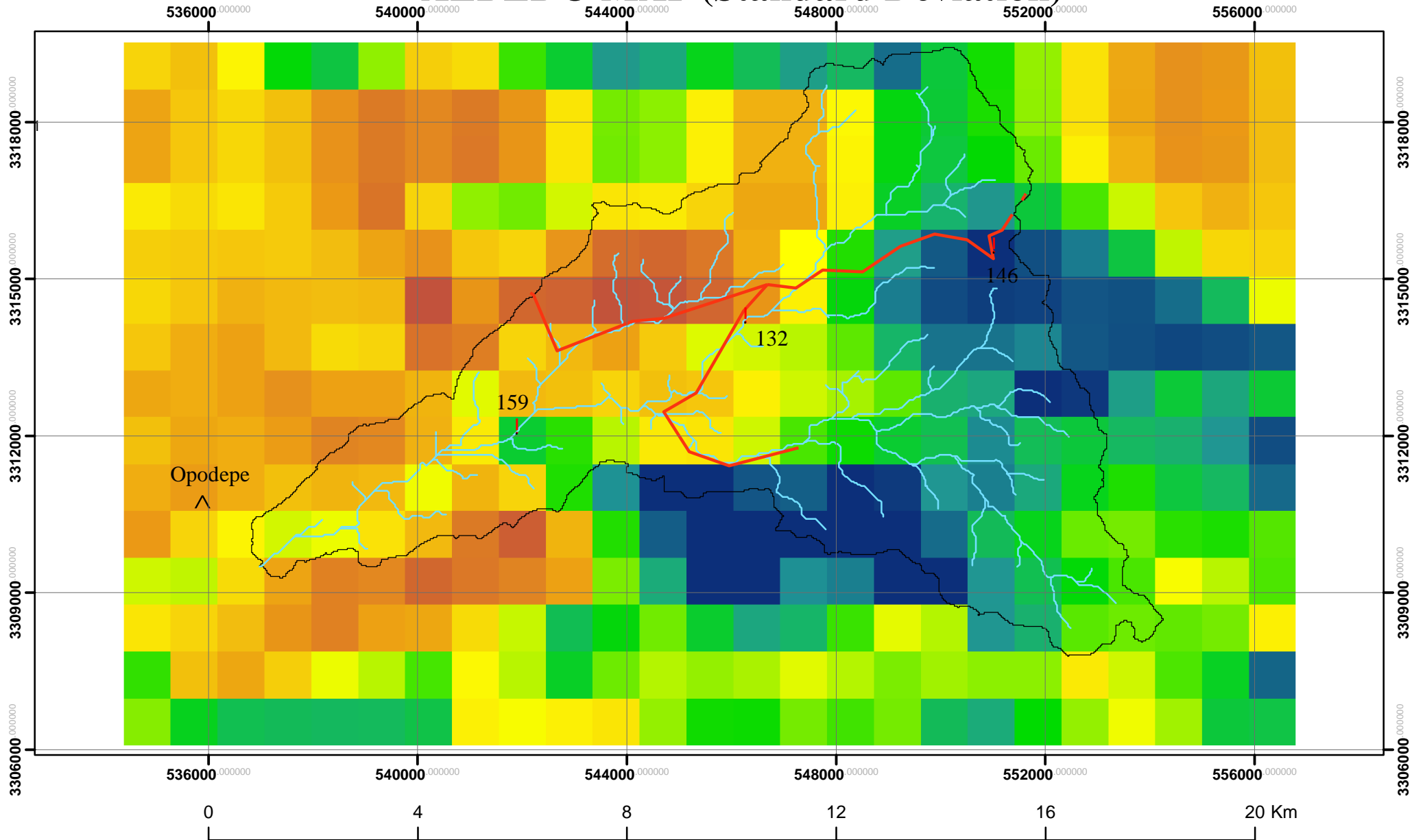
Stations



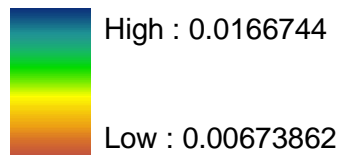
Roads

Source: MODIS

ALBEDO MAP (Standard Deviation)



Standard Deviation



Basin Boundary Sierra Los Locos

Sierra Los Locos Stream Network

^ Opodepe

! Stations

— Roads

Source: MODIS

APPENDIX 8: PUBLICATIONS

On the Spatiotemporal Organization of Soil Moisture in the North American Monsoon Region

Enrique R. Vivoni¹, Luis A. Méndez-Barroso¹, Julio C. Rodríguez², Christopher J. Watts²

1. Department of Earth and Environmental Science, New Mexico Institute of Mining and Technology, Socorro, New Mexico, USA 87801.
2. Department of Physics, University of Sonora, Hermosillo, Sonora, Mexico.

Abstract The spatiotemporal distribution of soil moisture is poorly understood in semiarid regions with complex terrain characterized by sharp transitions in land surface conditions. In the monsoon region of southwestern North America, strong seasonality in precipitation and vegetation further complicates soil moisture variability. In this study, we explore the spatiotemporal organization of soil moisture in a monsoon-dominated basin of northern Mexico through field sampling, aircraft-based retrievals and distributed hydrologic modeling. The study catchment has been under intensive investigation since the NAME-SMEX04 field experiments. We illustrate the terrain control on soil moisture distribution over a topographic transect during a dry-down period, known as a monsoon break, as determined from ground, remotely-sensed and simulated fields.

Introduction

The North American monsoon (NAM) is the primary climatologic phenomenon controlling summer precipitation in the southwestern United States and northern Mexico [e.g., Douglas *et al.*, 1993]. Monsoon convective storms (July-August-September) can account for a large percentage of the total annual precipitation, ranging from 40 – 70%. The arrival of summer storms, in turn, has a large impact on the hydroclimatology of the semiarid region, inducing seasonality in soil moisture, surface radiation and energy fluxes, vegetation phenology, streamflow and aquifer recharge [e.g., Scott *et al.*, 2000; Salinas-Zavala *et al.*, 2002; Kurc and Small, 2004; Gochis *et al.*, 2006; Watts *et al.*, 2007; Vivoni *et al.*, 2007]. Despite the impact of the NAM on hydrologic processes, relatively little is known on the spatiotemporal organization of land surface properties, including soil moisture, vegetation and surface turbulent fluxes, and their potential roles in influencing basin response and land-atmosphere interactions [e.g., Vera *et al.*, 2006].

The spatiotemporal soil moisture organization is further complicated by the complex terrain of the NAM region. Topographic patterns play an important role in the distribution of precipitation forcing [e.g., Negri *et al.*, 1993; Gochis *et al.*, 2004], ecosystem types and function [e.g., Coblenz and Riitters, 2004; Vivoni *et al.*, 2007] and soil characteristics [e.g., Wierenga *et al.*, 1987; Descroix *et al.*, 2002]. Topographic control on land surface conditions suggests that soil moisture may exhibit characteristic properties of the terrain distribution. While this has been

observed in humid regions with low relief [Grayson *et al.*, 1997; Kim and Barros, 2002], we do not have evidence of large-scale coupling of soil moisture and topography in semiarid regions. For the most part, the effects of topography are ignored in semiarid areas based on the assumption that high evapotranspiration effectively leads to one-dimensional land surface processes. Ignoring lateral redistribution of soil moisture, however, cannot explain vegetation patterns in semiarid regions, including the zoning along elevation bands, organization along drainage lines or stripping patterns following contour lines [*e.g.*, Wilcox *et al.*, 2003; Caylor *et al.*, 2005; Vivoni *et al.*, 2007].

In this study, we present the spatiotemporal soil moisture distribution in a semiarid mountain basin in the NAM region based on field observations, passive microwave retrievals and hydrologic simulations that incorporate observed catchment characteristics. We focus on soil moisture along a two-dimensional topographic transect to simplify inferences on soil moisture-topographic coupling.

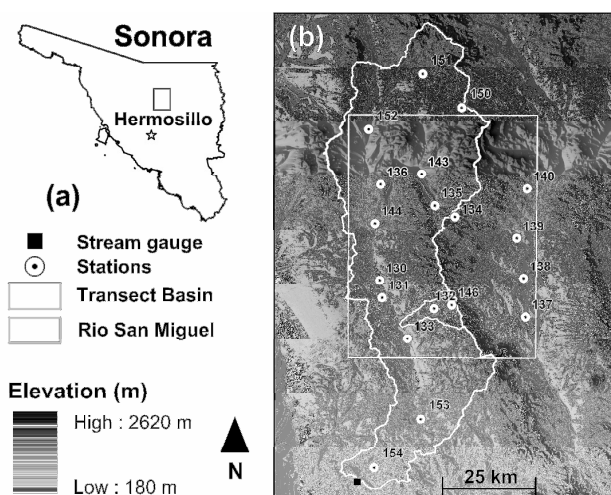


Figure 1. (a) Study site in northern Sonora, Mexico. (b) Location of 20 regional precipitation and soil moisture stations and small study catchment (~ 100 km²) in Río San Miguel basin (~ 3796 km²). Digital elevation model (DEM) at 90-m resolution depicts the north-to-south trending mountains and major river valleys which are a northern extension of the Sierra Madre Occidental (SMO) in the NAM region.

Study Region, Ground and Remote Sensing Observations

The study site is located in northern Sonora, Mexico in a region characterized by complex terrain, ephemeral rivers and seasonally-green vegetation [Vivoni *et al.*, 2007]. The mean annual rainfall in the region ranges from 400 to 500 mm, with 50–70% during the NAM. Figure 1 depicts the study location including the topographic distribution characterized by a high mean elevation and a large range due to channel incision. Two major ephemeral rivers flow north to south in the region. Here, we focus on the Río San Miguel upstream of a discharge observation point (~ 3796 km²) and a sub-catchment known as the Sierra Los Locos (SLL, ~ 100 km²). The SLL basin is characterized by the elevation control on ecosystem type and surface soil distribution [Vivoni *et al.*, 2007], as observed along a rural road that traverses the basin, climbing nearly 700-m over a distance of ~ 22 -km (Figure 2). A field experiment along the topographic transect was carried out during in August 2004 as part of NAME-SMEX04 [Higgins and Gochis, 2007]. Sampling at thirty sites arranged along the topographic transect was performed daily for soil and atmospheric variables in ~ 1 m² plots to coincide with aircraft data acquisition. Surface soil moisture (0-5 cm depth) was sampled using an impedance probe [Cosh *et al.*, 2005] at five locations in each plot. Soil moisture estimates from the Polarimetric Scanning Radiometer (PSR/CX), a passive microwave imaging radiometer [Jackson *et al.*, 2005], were available on 8

days during the field campaign. The PSR/CX data was processed to obtain a 7.32H GHz brightness temperature and then converted via a retrieval algorithm to an 800-m soil moisture field [Bindlish *et al.*, 2008]. Vivoni *et al.* [2008] compared the ground and aircraft-based soil moisture estimates using a variety of statistical measures.

Distributed Hydrologic Simulations for Monsoon Period

Spatially-distributed soil moisture simulations are conducted using the TIN-based Real-time Integrated Basin Simulator (tRIBS) [Ivanov *et al.*, 2004] applied to the SLL basin. The distributed model simulates the coupled surface-subsurface response to rainfall by tracking infiltration fronts, water table fluctuations and lateral moisture exchanges. Runoff is generated via four mechanisms and routed via overland, channel and subsurface pathways. Figure 2 shows the spatial domain based on a triangulated irregular network (TIN) developed using a 29-m DEM [Vivoni *et al.*, 2004]. Also shown are the vegetation cover derived from a field-verified classification of Landsat TM scenes [Hunt *et al.*, 2008] and the soil textural classification developed from FAO maps and terrain slope features. The spatial variability in surface terrain, soils and vegetation in the hydrological model can induce spatiotemporal organization in basin hydrologic states and fluxes when forced with appropriate precipitation forcing. We use Thiessen interpolation of three hourly rain gauges in the vicinity of the SLL basin (stations 132, 133, 146 along the topographic transect) as model forcing, along with meteorological data from a nearby (<10 km) flux tower (station 147). We conduct simulations from June 14 to September 30, 2004 to capture the entire monsoon season. Our particular focus here is on the overlapping period with the ground and aircraft-based measurements.

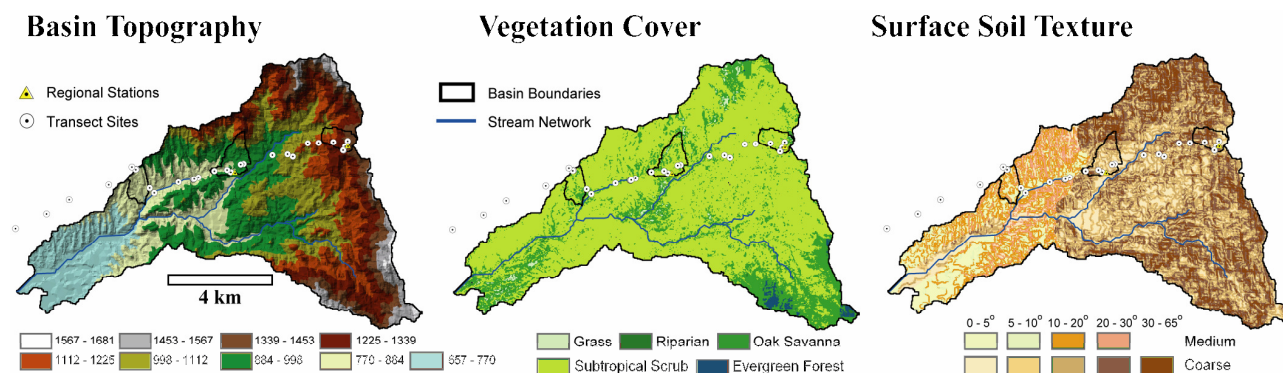


Figure 2. tRIBS hydrologic model setup for the Sierra Los Locos ($\sim 100 \text{ km}^2$) in the study area. (left) TIN topographic distribution derived from the 29-m DEM and including the thirty transect sites and two regional stations. (middle) Land cover from Landsat TM reclassification. (right) Soil texture from FAO classification and terrain slope classes.

Results and Discussion

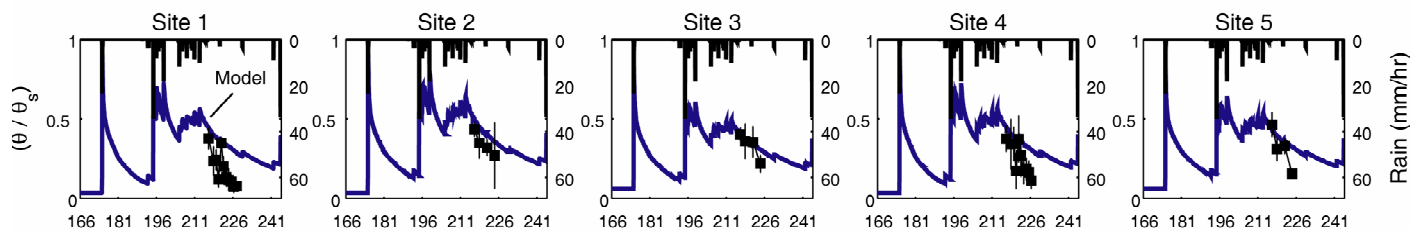
Due to space limitations, the comparison of the ground observations, remotely-sensed fields and distributed simulations is constrained to surface soil moisture (0 to 5 cm soil depth, expressed as relative saturation, $S = \theta/\theta_s$) in the upper basin (see basin boundary in Fig. 2). Figure 3 (top row) compares the daily transect observations at five sites in the upper basin. Daily measurements consist of the plot mean S calculated from the interior samples and the standard deviation (as vertical bars). Vivoni *et al.* [2007] compared the plot- and transect-scale variability along the topographic transect. Model simulations show the spatiotemporal soil moisture in the

upper sites composed of coarse soil texture and an oak savanna ecosystem. Note the correspondence between the hourly rainfall forcing (at station 146) and the simulated soil moisture time series. Most precipitation occurred in July, while August (julian days 214 to 244) was fairly dry, inducing a regional scale dry-down in the land surface [Vivoni *et al.*, 2007, 2008]. Soil moisture response during the monsoon break varied among sites, but was generally consistent between ground samples and model simulations. Note the sharp soil moisture recession in site 1 which is not properly captured in the model, potentially due to local scale surface slopes not represented at the element scale. Soil moisture response at sites 2, 3 and 5, on the other hand, are captured well in the simulations, suggesting adequate model performance.

Figure 3 also presents the simulated surface soil moisture fields at two instances during the regional dry-down. Note the complex spatial pattern reflecting the precipitation forcing, soil texture, vegetation cover and topographic distribution. Model simulations are consistent with the decrease in soil moisture observed at most transect sites and with the remotely-sensed dry-down [Vivoni *et al.*, 2007, 2008; Bindlish *et al.*, 2008]. Note that the subtropical scrubland, capable of sustaining high transpiration, experiences large soil moisture decreases in a broad swath of intermediate elevations. A similar qualitative behavior was also reported by Vivoni *et al.* [2008] in the PSR/CX fields (not shown). A quantitative comparison between the simulated and remotely-sensed spatial patterns is currently underway. Despite the promising results, improvements are required to: 1) reduce the soil moisture in high-slope, exposed outcrops, 2) capture the ecosystem variability in evapotranspiration flux and its impact on soil moisture, and 3) constrain lateral water redistribution to valley bottoms. This exercise had indicated the need for improved spatial distributions of precipitation and soil properties in the basin, activities to be carried out during a field experiment in summer 2007.

Conclusions

In this study, we present the spatiotemporal soil moisture distribution in a semiarid mountain basin in the NAM region based on field observations, passive microwave retrievals and hydrologic simulations that incorporate observed catchment characteristics. Our preliminary simulations show promise in capturing observed soil moisture variations in space and time within the complex basin.



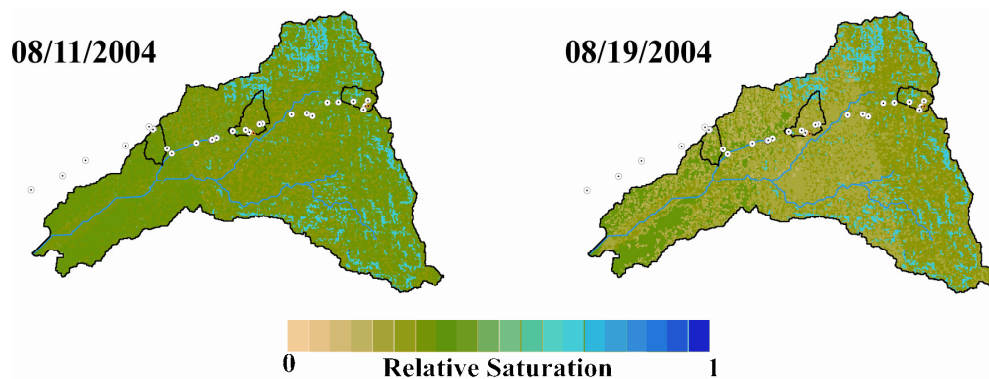


Figure 3. (top row) Comparison of transect soil moisture observations (sites 1 through 5 in upper basin) with the tRIBS simulations for the surface layer (0-5 cm depth) over the period June 14 to August 31, 2004. (bottom panels). Simulated soil moisture spatial patterns during the dry-down period (coincident with PSR/CX retrievals, not shown). For each case, the relative soil moisture ($S = \theta / \theta_s$) is shown which accounts from the spatial variations in soil textural properties.

References

- Bindlish, R., Jackson, T. J., Gasiewski, A. J., Stankov, B., Cosh, M. H., Mladenova, I., Vivoni, E. R., Lakshmi, V., Watts, C. J., and Keefer, T., 2008: PSR based soil moisture estimates in high vegetation and topographic domain, *Remote Sens. Env.*, In Press.
- Caylor, K. K., S. Manfreda and I. Rodríguez-Iturbe, 2005: On the coupled geomorphological and ecohydrological organization of river basins, *Advances in Water Resources*, **28**(1), 69-86.
- Coblentz, D. D. and K. H. Riitters, 2004: Topographic controls on the regional-scale biodiversity of the south-western USA, *Journal of Biogeography*, **31**(7), 1125-1138.
- Cosh, M. H., Jackson, T. J., Bindlish, R., Famiglietti, J. S., and D. Ryu, 2005: Calibration of an impedance probe for estimation of surface soil water content over large regions. *J. Hydrol.*, **311**, 49-58.
- Descroix, L., J. L. Gonzalez Barrios, J. P. Vandervaere, D. Viramontes and A. Bollery, 2002: An experimental analysis of hydrodynamic behavior on soils and hillslopes in a subtropical mountainous environment (Western Sierra Madre, Mexico), *Journal of Hydrology*, **266**, 1-14.
- Douglas, M. W., R. A. Maddox, K. Howard and S. Reyes, 1993: The Mexican Monsoon, *J. Climate*, **6**, 1665-1677.
- Gochis, D. J., A. Jiménez, C. J. Watts, J. Garatuza-Payán, and W. J. Shuttleworth, 2004: Analysis of 2002 and 2003 warm-season precipitation from the North American monsoon experiment event rain gauge network, *Monthly Weather Review*, **132**(12), 2938-2953.
- Gochis, D. J., L. Brito-Castillo and W. J. Shuttleworth, 2006: Hydroclimatology of the North American Monsoon region in northwest Mexico, *Journal of Hydrology*, **316**(1-4), 53-70.
- Higgins, R. W. and D. J. Gochis, 2007: Synthesis of results from the North American Monsoon Experiment study, *J. Climate*, **20**(9), 1601-1607.
- Ivanov, V. Y., E. R. Vivoni, R. L. Bras and D. Entekhabi, 2004: Catchment hydrologic response with a fully-distributed triangulated irregular network model, *Water Resources Research*, **40**, 10.1029/2004WR003218.
- Kim, G., and A. Barros, 2002: Space-time characterization of soil moisture from passive microwave remotely sensed imagery and ancillary data. *Remote Sensing of Environment*, **81**, 393-403.
- Kurc, S. A. and E. E. Small, 2004: Dynamics of evapotranspiration in semiarid grassland and shrubland ecosystems during the summer monsoon season, central New Mexico, *Water Resources Research*, **40**(9), W09305, doi:10.1029/2004WR003068.
- Negri, A. J., R. F. Adler, R. A. Maddox, K. W. Howard and P. R. Keehn, 1993: A regional rainfall climatology over Mexico and the southwestern United States derived from passive microwave and geosynchronous infrared data, *Journal of Climate*, **6**(11), 2144-2161.
- Salinas-Zavala, C., A. V. Douglas and H. F. Díaz, 2002: Interannual variability of NDVI in northwest Mexico. Associated climatic mechanisms and ecological implications, *Remote Sens. Env.*, **82**(2-3), 417-430.
- Scott, R. L., W. J. Shuttleworth, T. O. Keefer and A. W. Warrick, 2000: Modeling multi-year observations of soil moisture recharge in the American Southwest, *Water Resources Research*, **36**(8), 2233-2247.
- Vera, C., W. Higgins, J. Amador, T. Ambrizzi, R. Garreaud, D. Gochis, D. Gutzler, D. Lettenmaier, J. Marengo, C. R. Mechoso, J. Noguez-Paele, P. L. Silva Dias and C. Zhang, 2006: Toward a unified view of the American Monsoon Systems, *Journal of Climate*, **19**(20), 4977-5000.
- Vivoni, E. R., V. Y. Ivanov, R. L. Bras and D. Entekhabi, 2004: Generation of triangulated irregular networks based on hydrological similarity, *Journal of Hydrologic Engineering*, **9**(4), 288-302.
- Vivoni, E. R., H. A. Gutiérrez-Jurado, C. A. Aragón, L. A. Méndez-Barroso, A. J. Rinehart, R. L. Wyckoff, J. C. Rodríguez, C. J. Watts, J. D. Bolten, V. Lakshmi and T. J. Jackson, 2007: Variation of hydrometeorological conditions along a topographic transect in northwestern Mexico during the North American Monsoon, *Journal of Climate*, **20**(9), 1792-1809.
- Vivoni, E. R., M. Gebremichael, C. J. Watts, R. Bindlish and T. J. Jackson, 2008: Comparison of ground-based and remotely-sensed surface soil moisture estimates over complex terrain during SMEX04, *Remote Sensing of Environment*, In Press.
- Watts, C. J., R. L. Scott, J. Garatuza-Payan, J. C. Rodríguez, J. H. Prueger, W. Kustas and M. Douglas, 2007: Changes in vegetation condition and surface fluxes during NAME 2004, *J. Climate*, **20**(9), 1810-1820.
- Wierenga, P. J., J. M. H. Hendrickx, M. H. Nash, J. Ludwig and L. A. Daugherty, 1987: Variation of soil and vegetation with distance along a transect in the Chihuahuan Desert, *J. of Arid Env.*, **13**(1), 53-63.

Wilcox, B.P., D. D. Breshears and C. D. Allen, 2003: Ecohydrology of a resource-conserving semiarid woodland: effects of scale and disturbance, *Ecological Monographs*, **73**(2), 223-239.

Relation between Surface Flux Measurements and Hydrologic Conditions in a Subtropical Scrubland during the North American Monsoon

Enrique R. Vivoni^{1,*}, Christopher J. Watts², Julio C. Rodríguez², Jaime Garatuza-Payan³, Luis A. Méndez-Barroso¹, Enrico A. Yepez⁴, Juan Saiz-Hernández², and David J. Gochis⁵

1. Department of Earth and Environmental Science
New Mexico Institute of Mining and Technology
Socorro, NM 87801

2. Departamento de Física
Universidad de Sonora
Hermosillo, Sonora, México

3. Departamento de Ciencias del Agua y del Medioambiente
Instituto Tecnológico de Sonora
Ciudad Obregón, Sonora, México

4. Department of Biology
University of New Mexico
Albuquerque, NM 87131

5. National Center for Atmospheric Research
Boulder, CO 80305

To be submitted to *CLIVAR Exchanges*
February 4, 2008

Special Issue on North American Monsoon Experiment (NAME)

* *Corresponding author address:* Enrique R. Vivoni, Department of Earth and Environmental Science, New Mexico Institute of Mining and Technology, 801 Leroy Place, MSEC 244, Socorro, NM 87801, tel (575) 835-5611, fax (575) 835-5634, email vivoni@nmt.edu.

Introduction

The North American monsoon (NAM) is the primary climatological phenomenon in the southwestern United States and northwestern Mexico, leading to large changes in precipitation, lower atmospheric conditions and land surface properties in the region (e.g., Douglas et al., 1993). Previous studies carried out under the auspices of the North American Monsoon Experiment (NAME) have focused on the relationship and potential feedbacks between the NAM system and the conditions of the land surface over southwestern North America, including changes in vegetation, soil moisture and streamflow (Zhu et al., 2005; Gochis et al., 2006; Watts et al., 2007; Vivoni et al., 2007). Evidence from these studies suggest that dramatic transitions, such as the seasonal march of the runoff ratio (Gochis et al., 2006), occur in the hydrological conditions of the semiarid basins in the region. In addition, Watts et al. (2007) illustrated the sharp changes occurring in the surface turbulent fluxes across several sites in the region during the NAME 2004 field experiment. Here, we present multiple-year evidence for the relation between surface flux measurements and hydrologic conditions in a subtropical scrubland, one of the major ecosystems in northwestern Mexico, which experiences significant greening during the NAM period (Salinas-Zavala et al., 2002; Watts et al., 2007). The analysis is based on measurements at and around an eddy covariance (EC) tower located in northern Sonora, Mexico within the Río San Miguel river basin.

Surface Flux Measurements

Recent land-atmosphere interaction studies in the NAM region have focused on understanding the impact of vegetation greening on the measurement of surface soil moisture and radiation and energy balance components, including evapotranspiration. While these efforts began during the NAME 2004 field campaign, subsequent studies have been sponsored by the National Science Foundation (NSF), the Consejo Nacional de Ciencias y Tecnología (CONACYT) and the NOAA Climate Program Office. Our focus here is on surface flux and land surface condition measurements at the Rayón Eddy Covariance site (denoted as STS in Watts et al., 2007). The measurement site is located at ~630 m above sea level in the Río San Miguel, a large ephemeral river basin (~3500 km²) flowing north to south in the northern Sierra Madre Occidental. Vegetation at the site is classified as subtropical scrubland (known as Sinaloan thornscrub) and is a mixture of trees, shrubs and desert cactus that respond to the precipitation

pulses during the NAM season. Soil profiles in the region are shallow (~70 cm in depth above an impermeable clay lens) and primarily composed of loamy sand and sandy loam with intermixed clasts.

Figure 1 illustrates the experimental design for surface turbulent and radiation fluxes and footprint measurements of soil moisture and soil temperature. The footprint of the EC tower is defined here as a 250-m by 250-m region around the site, selected based on the pixel dimensions of the reflectance measurements obtained from the MODIS sensor. Thirty sampling plots were established in the EC tower footprint (see descriptions below) to relate these land surface conditions to the surface flux measurements. The 10-m tower contains a 3D sonic anemometer, as well as high frequency measurements of air temperature and relative humidity to estimate the covariance terms necessary to obtain the latent and sensible heat fluxes (Watts et al., 2007). Hydrometeorological observations at the site also include precipitation, soil moisture and temperature (at 3 depths), and radiation components used to estimate albedo and net radiation. Operation of the Rayón Eddy Covariance site has concentrated on summer campaign periods in 2004, 2006 and 2007, in particular to capture conditions during the NAM onset, peak and demise (see Figure 1b, c for impact of vegetation greening at tower site).

In Figure 2, we present a comparison of remotely-sensed and field observations during three monsoon periods (2004, 2006, 2007) at the EC tower site. Several interesting transitions are observed in vegetation cover, surface albedo and surface fluxes during the NAM period, as well as important differences between the various monsoon seasons. Note that the vegetation dynamics are captured here by the Normalized Difference Vegetation Index (*NDVI*) estimated at the tower pixel (250-m by 250-m) from 16-day MODIS composites. The vegetation dynamics are clearly tied to the daily precipitation observed at the tower rain gauge, with early or late monsoon greening related to the onset of precipitation. Similarly, the decrease in *NDVI* during the monsoon demise is tied to the precipitation variability in the late summer period. It is interesting to compare, for example, monsoon 2006 (Fig. 2b) with a high peak *NDVI* and early onset, with the monsoon 2007 (Fig. 2c) with a reduced *NDVI* peak, late onset but more longer duration.

Vegetation greening is closely tied to the changes in albedo observed at the site from two sources: MODIS 16-day broadband albedo composites (1-km resolution) and EC tower albedo estimates obtained from measurements of incoming and outgoing shortwave radiation.

Comparison between the two albedo estimates is remarkably good given the differences in spatial resolution (1-km² versus ~4 m² field of view), suggesting a spatially coherent change in vegetation cover in the vicinity of the tower. The clearest transition in albedo is observed for monsoon 2007 (Fig. 2c) which spans the largest time period. Note that the vegetation greening indicated by the increase in *NDVI* is coincident with the observed decrease in albedo from both estimation methods. As expected, the greening of the land surface decreases the surface albedo, although the change is not very large, from ~0.18 to ~0.15. Given the high amounts of incoming solar radiation at the site, even small changes in albedo can significantly affect the radiation balance at the site. Note that as vegetation cover is reduced in the late monsoon 2004 (Fig. 2a), the albedo of the land surface begins to increase once again to reflect the drier, desert conditions.

Along with changes in albedo, vegetation greening leads to significant variations in the partitioning of surface turbulent fluxes, as captured by the evaporative fraction, $EF = \lambda E / (\lambda E + H)$, where H and λE are the daily-averaged sensible and latent heat fluxes measured by the eddy covariance method. This is most clearly observed in monsoon 2007 (Fig. 2c) where the measurements span the monsoon onset and vegetation response. Note the low values of EF (near zero), implying higher sensible heat fluxes, prior to the *NDVI* increase, and the dramatic increase in EF (~0.7 to 0.9) as the available soil moisture from precipitation pulses is transferred back to the atmosphere via evapotranspiration. During each summer, individual precipitation events lead to increases in EF (e.g., higher latent heat flux) that are sustained over periods of several days. Interestingly, for periods with consecutive storms (low interstorm duration), sustained EF at high values may last for several weeks, for example in monsoon 2006 (Fig. 2c). During the monsoon demise, vegetation becomes senescent and the EF decreases toward low values (see latter part of monsoon 2004, Fig. 2a), implying a return to high sensible heat fluxes at the land surface.

Footprint-Averaged Hydrologic Conditions

In an effort to understand land-atmosphere interactions at the Rayón EC site, we conducted a set of intensive surface measurements in the footprint of the tower (Fig. 1a). For simplicity, we defined the footprint as 250-m by 250-m box around the tower, while recognizing that the actual measurement footprint will vary with wind conditions. For our purposes, this definition allows comparison of the estimated surface conditions (soil moisture and soil temperature) to remotely-sensed vegetation observations from MODIS. As shown in Fig. 1a, the topographic conditions around the tower are fairly uniform, as determined from a satellite-derived digital elevation model (30-m DEM from ASTER). Nevertheless, the terrain variability at the site does lead to two first-order stream channels, which have more abundant riparian vegetation as compared to more exposed hillslopes at the site. As a result, we expected to capture spatiotemporal variations in soil temperature and soil moisture through daily sampling at the thirty (30) sampling plots in the tower footprint. Each sampling plot (~1-m by 1-m) was sampled at similar times each day during two week intervals in July and August 2006 and 2007. Measurements were performed using portable sensors, as described more fully in Vivoni et al. (2007).

Figure 3 presents a comparison between the footprint-averaged, daily soil moisture (blue circles) and soil temperature (red triangles) conditions and the estimated daily Bowen Ratio ($B = H/\lambda E$, black circles) at the EC tower (located in the center of the 250-m by 250-m area). Surface fluxes and footprint hydrologic conditions are presented for monsoon 2006 (July 5 to 20, Fig. 3a) and monsoon 2007 (July 19 to August 4, Fig. 3b) for the days during which field sampling was conducted. The soil moisture and temperature symbols represent the average of the thirty sampling plots, while the bars capture the spatial variability as ± 1 std. The daily precipitation (bars) measured at the tower is included for reference. Note the good correspondence between the soil moisture and soil temperature and their relation to storm and interstorm periods. As expected, precipitation pulses promote a decrease in soil temperature and an increase in soil moisture, with consecutive storms leading to sustained wet and cool surface conditions. Interestingly, the spatial variability in the footprint is different in the two years, with monsoon 2007 exhibiting smaller spatial variations in soil moisture and temperature, due to the effects of sustained cloud cover on limiting incoming solar radiation.

Of particular relevance is the relation between land surface conditions and the Bowen Ratio ($B = H/\lambda E$) measured at the tower during monsoons 2006 and 2007. Note the excellent correspondence between footprint-averaged soil moisture and B , where periods of high B (large H) occur during interstorm periods, with rapid decreases in B (high λE) after precipitation pulses wet the land surface. Further analysis of the relation between B and footprint-averaged soil moisture (not shown) indicates that a power law behavior is observed for both monsoon seasons: $B = 4.95 \langle \theta \rangle^{-0.95}$ ($R^2 = 0.6$), where $\langle \theta \rangle$ is the footprint-averaged, daily volumetric soil moisture (in %). Furthermore, this relation is significantly weakened when using the soil moisture conditions at the sampling plot near the tower. This suggests that the surface flux measurements are directly linked to the averaged soil moisture conditions in the EC tower footprint. Analysis comparing the tower and footprint-averaged conditions also revealed that the region around the tower is wetter and cooler than the tower plot, on average, for the two sampling periods.

Soil Moisture Controls on Evapotranspiration

The relation between surface flux measurements and soil moisture conditions is particularly important as it forms an important parameterization in many land surface and watershed models (e.g. Vivoni et al., 2005). Typically, actual evapotranspiration (ET) is regulated by amount of soil moisture present in the root zone or surface layer, following a functional form that recognizes soil moisture limitations on ET below a threshold value (Rodríguez-Iturbe and Porporato, 2004). The functional form varies across different land surface models, but is generally assumed to be constant in time, with appropriate parameters selected for the ecosystem of interest. Unfortunately, few studies have attempted to establish the appropriate relationships between ET and soil moisture in ecosystems experiencing monsoonal greening. As a result, most hydrological and climate models operating in the NAM region do not adequately capture vegetation dynamics in the parameterization of surface fluxes.

Figure 4 provides initial evidence for the temporal (and vegetation-dependent) variation of the relation between evapotranspiration and soil moisture in the subtropical scrubland at the EC tower site. Daily estimates of latent heat flux (λE), consisting of both soil evaporation and plant transpiration, are plotted as a function of the daily-averaged surface soil moisture from the tower sensor (at 5-cm depth, θ in vol. %) in Fig. 4a. We use the tower site soil moisture data due to the longer period of coincident λE and θ measurements. Note the differences in the relation

between λE and θ for each monsoon, suggesting that the functional form may have interannual variations that depend on the vegetation state of the ecosystem. For example, monsoon 2004 exhibits a maximum λE that asymptotes for high soil moisture values (~ 12 to 15%) at ~ 4 MJ/day, while monsoon 2006 shows a maximum λE of nearly 12 MJ/day for soil moisture values of 10 to 12%.

Inspection of the *NDVI* time series for each monsoon season (Fig. 4b), indicates that the sequence of $\lambda E(\theta)$ relations follows a similar order to that observed in the maximum *NDVI*. Monsoon 2006, which exhibited the higher values of λE for a given θ , also shows the highest vegetation greenness. This suggests that the subtropical scrubland at the Rayón EC tower site has a greater transpiration capacity for years with increased greenness and biomass resulting from above average precipitation. As a result, the soil moisture control on *ET* varies temporally according to the ecosystem state.

Discussion and Conclusions

The evidence presented here on the interactions of surface fluxes and hydrological conditions in the North American monsoon region is based upon integrated, multiple-year studies at an eddy covariance tower site in the subtropical scrubland of northern Sonora, Mexico. The use of remote sensing data, EC tower observations and measurements of surface conditions in the tower footprint have revealed that: (1) the onset of the NAM leads to dramatic changes in surface properties and the partitioning of energy fluxes; (2) footprint-averaged soil moisture and soil temperature conditions are closely related to the flux tower observations; and (3) considerable variations exist between monsoon seasons, leading to vegetation-dependence on the relation between soil moisture and *ET*. On-going and future efforts in the study region have included a detailed *ET* partitioning experiment based on the isotopic signature of water vapor, vegetation and soil samples (summer 2007), expansion of current studies to an existing tower site in Tesopaco, Sonora and a new EC tower site to be deployed in the Río San Miguel (summer 2008) and land surface modeling using one-dimensional and distributed approaches to assess implications of our findings toward improved simulations and forecasts in the NAM region.

References

- Douglas, M. W., Maddox, R. A., Howard, K., and S. Reyes, 1993: The Mexican Monsoon. *J. Climate*, **6**, 1665-1677.
- Gochis, D. J., Brito-Castillo, L., and W. J. Shuttleworth, 2006: Hydroclimatology of the North American monsoon region in northwest Mexico. *J. Hydrol.*, **316**, 1-4, 53-70.
- Rodríguez-Iturbe, I., and A. Porporato, 2004: *Ecohydrology of water-controlled ecosystems: Soil moisture and plant dynamics*. Cambridge University Press, 442 pp.
- Salinas-Zavala, C. A., Douglas, A. V., and H. F. Díaz, 2002: Interannual variability of NDVI in northwest Mexico. Associated climatic mechanisms and ecological implications. *Remote Sens. Env.*, **82**, 2-3, 417-430.
- Vivoni, E. R., Ivanov, V. Y., Bras, R. L., and D. Entekhabi, 2005: On the effects of triangulated terrain resolution on distributed hydrologic model response. *Hydrol. Process.*, **19**(11): 2101-2122.
- Vivoni, E. R., Gutiérrez-Jurado, H. A., Aragón, C.A., Méndez-Barroso, L. A., Rinehart, A. J., Wyckoff, R. L., Rodríguez, J. C., Watts, C. J., Bolten, J. D., Lakshmi, V. and Jackson, T. J. 2007: Variation of hydrometeorological conditions along a topographic transect in northwestern Mexico during the North American monsoon. *J. Climate*, **20**(9), 1792-1809.
- Watts, C. J., Scott, R. L., Garatuza-Payan, J., Rodríguez, J. C., Prueger, J. H., Kustas, W. P. and Douglas, M. 2007: Changes in vegetation condition and surface fluxes during NAME 2004. *J. Climate*, **20**(9), 1810-1820.
- Zhu, C., Lettenmaier, D. P., and T. Cavazos, 2005: Role of antecedent land surface conditions on North American monsoon rainfall variability. *J. Climate*, **18**, 3104-3121.

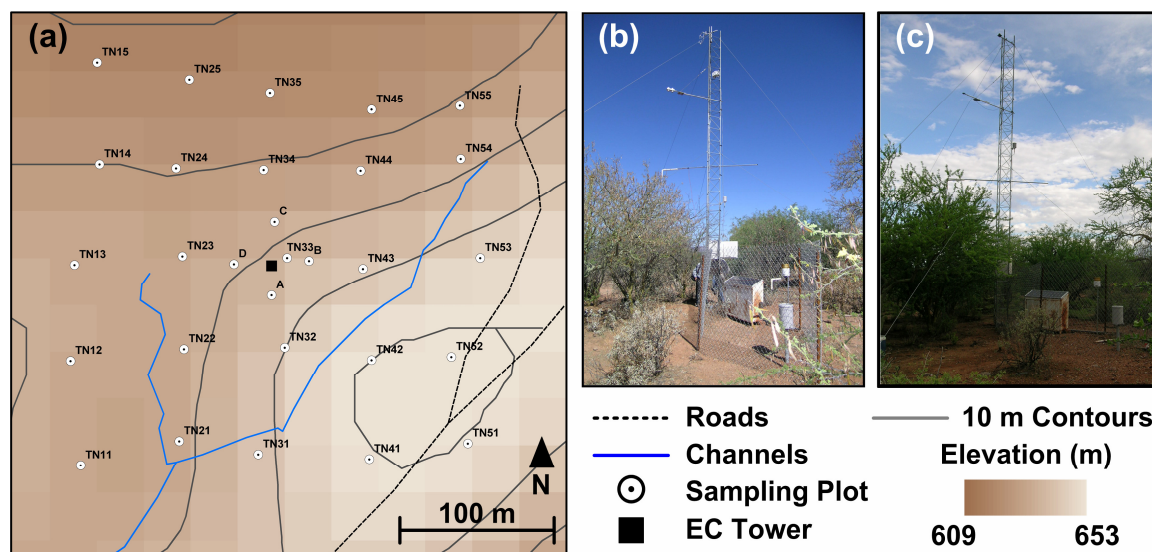
Figure Captions

Figure 1. Eddy covariance (EC) tower location and footprint sampling plots in Rayón, Sonora, Mexico (latitude 30.04 °N, longitude 110.67 °W). (a) Thirty (30) sampling plots (white circles) in a 250-m box surrounding tower site (black square) overlain on a 30-m digital Elevation Model (DEM) derived from ASTER (Advanced Spaceborne Thermal Emission and Reflection Radiometer). The roads and channels were traced in the field using a GPS. The 10-m contours from the DEM are shown for visualization purposes. (b) and (c) are photographs of the EC tower taken during a June period prior to the monsoon onset and a July period after monsoon greening, respectively. Note the differences in soil color, vegetation biomass and sky cover.

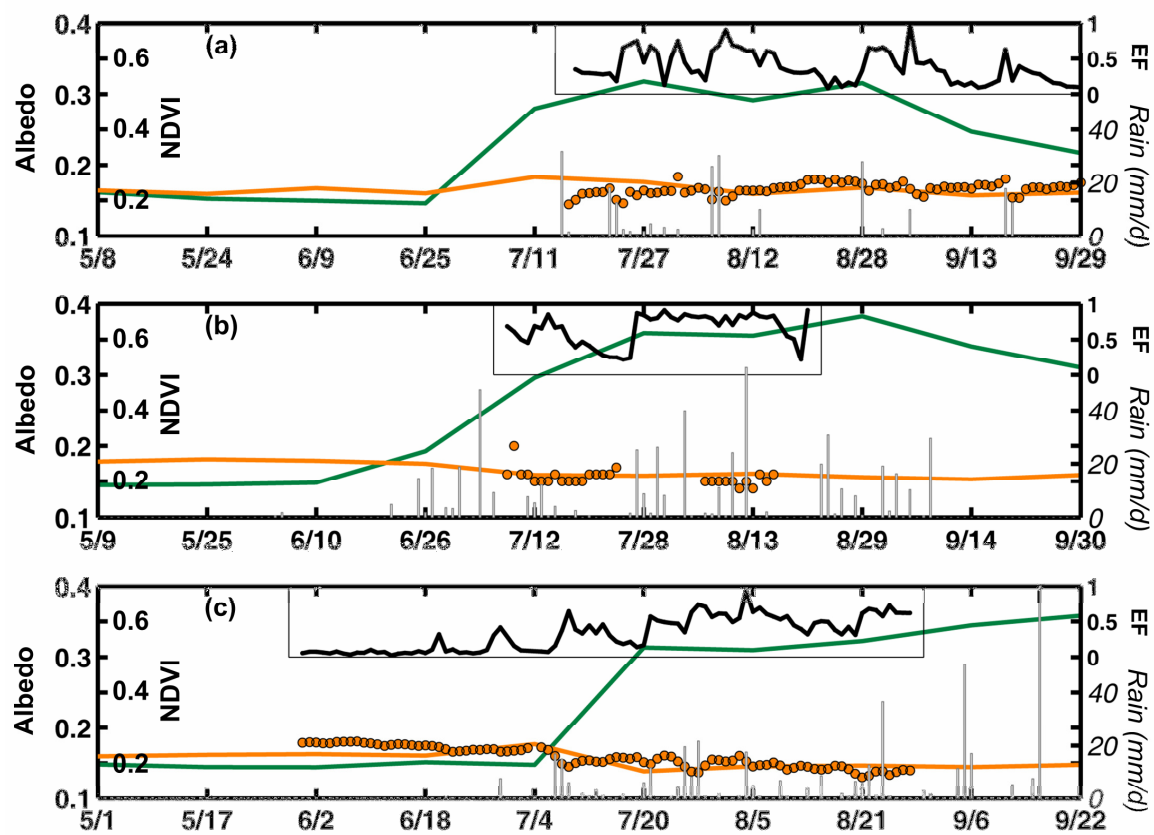
Figure 2. Seasonal evolution and interannual variability of rainfall, surface turbulent fluxes and land surface conditions at the EC tower for three summer monsoons: (a) 2004, (b) 2006, and (c) 2007. Rainfall (mm/day) is obtained from a tipping bucket rain gauge at the tower site (gray bars). The MODIS sensor used to derive the Normalized Difference Vegetation Index (NDVI, 250-m resolution, 16-day composites, green solid line) and Albedo (1-km resolution, 16-day composites, orange solid line) at the EC tower. MODIS Albedo is compared to daily estimates at the EC tower obtained as the ratio of outgoing shortwave radiation to incoming shortwave radiation ($a = R_{sout}/R_{sin}$, orange circles). Daily estimates of the surface turbulent fluxes (sensible heat, H and latent heat, λE) are used to compute the evaporative fraction, $EF = \lambda E / (\lambda E + H)$, black solid line.

Figure 3. Footprint-averaged daily volumetric soil moisture (%), blue circles), surface soil temperature (C , red triangles) and Bowen ratio ($B = H / \lambda E$, black circles) estimated from the EC tower during field campaigns in (a) 2006 and (b) 2007. Footprint-averaging considers all thirty sampling plots in 250-m by 250-m pixel around tower site (symbol is the spatial average and bars represent ± 1 standard deviation or spatial variability). Daily rainfall (mm/day) from the tower site (bars) shown as reference.

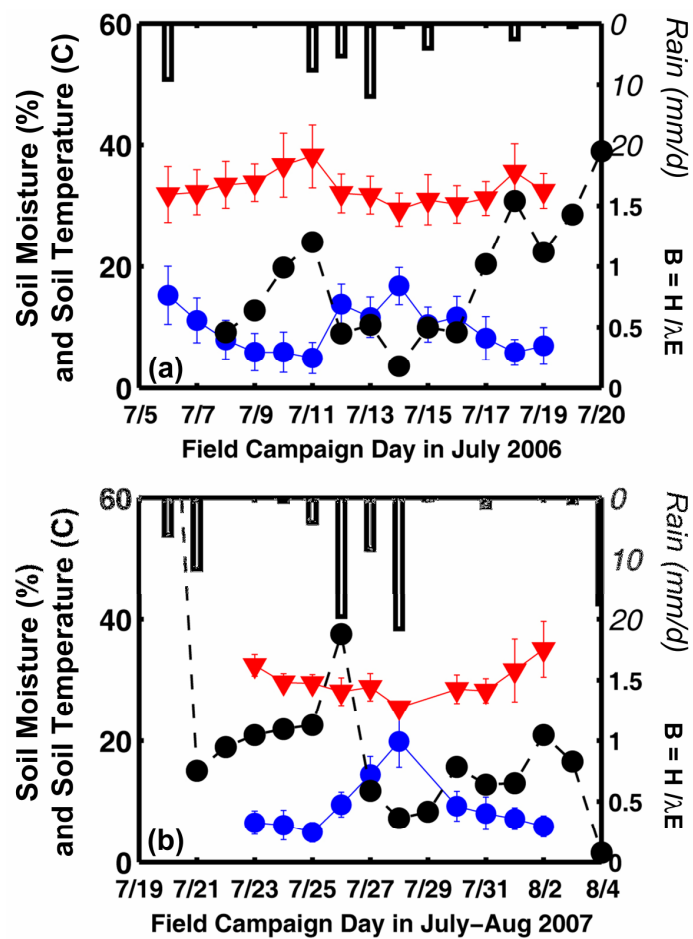
Figure 4. (a) Relation between daily latent heat flux (λE in MJ/day) and daily-average volumetric soil moisture (θ_v in %) obtained from the 5-cm depth sensor at the EC tower site for 2004 (JD 205 to 275), 2006 (JD 189 to 228), and 2007 (JD 186 to 240). (b) Temporal evolution of NDVI at the EC tower from MODIS 16-day composites (250-m resolution) for 2004, 2006 and 2007, including spatial average of nine surrounding pixels (symbols) and ± 1 standard deviation or spatial variability (bars).



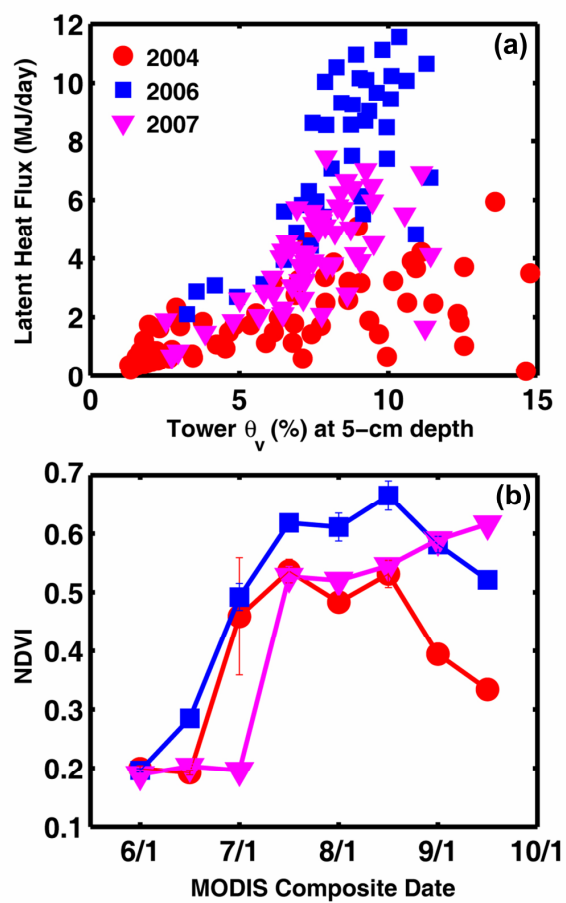
(Vivoni et al., Figure 1)



(Vivoni et al., Figure 2)



(Vivoni et al., Figure 3)



(Vivoni et al., Figure 4)

Seasonal and Interannual Relations between Precipitation, Soil Moisture and Vegetation Dynamics in the North American Monsoon Region

Luis A. Méndez-Barroso¹, Enrique R. Vivoni^{*1},
Christopher J. Watts² and Julio C. Rodríguez³

1. Department of Earth and Environmental Science,
New Mexico Institute of Mining and Technology, Socorro, NM, 87801.

2. Departamento de Física, Universidad de Sonora,
Hermosillo, Sonora, México.

3. Departamento de Agricultura y Ganadería,
Universidad de Sonora, Hermosillo, Sonora, México.

Submitted to *Journal of Hydrology*
Date: June 13, 2008

* Corresponding author: Enrique R. Vivoni, Associate Professor of Hydrology, Department of Earth and Environmental Science, 801 Leroy Place, MSEC 244, Socorro, NM. tel. (575) 835-5611. fax (575) 835-6436. vivoni@nmt.edu

Abstract

The North American monsoon (NAM) region in northwestern Mexico is characterized by seasonal precipitation pulses which lead to a major shift in vegetation greening and ecosystem processes. Seasonal greening in the desert region is particularly important due to its impact on land surface conditions and its potential feedback to atmospheric and hydrologic processes. Vegetation dynamics were analyzed using remotely-sensed Normalized Difference Vegetation Index (NDVI) images over the period 2004 to 2006 for the Río San Miguel and Río Sonora basins, which contain a regional network of precipitation and soil moisture observations. Results indicate that seasonal changes in vegetation greenness are dramatic for all regional ecosystems and are related to interannual differences in hydrologic conditions. Vegetation responses depend strongly on the plant communities in each ecosystem, with the highest greening occurring in the mid elevation Sinaloan thornscrub. Spatial and temporal persistence of remotely-sensed NDVI fields are then used to distinguish the arrangement of regional ecosystems and their organization along selected mountain fronts. Our study indicates that accumulated seasonal precipitation is a strong indicator of biomass production across the regional ecosystems, with higher rainfall use efficiency for the Sinaloan thornscrub. Further, precipitation was found to have higher lagged correlations to the vegetation dynamics, while soil moisture was the primarily factor influencing vegetation during concurrent periods. This suggests that soil moisture is an intermediary between NAM precipitation and the vegetation greening. Comparisons across ecosystems indicate that different plant water use strategies exist in response to interannual hydrologic variations and are strongly controlled by elevation along semiarid mountain fronts.

Keywords: North American monsoon, semiarid ecosystems, ecohydrology, remote sensing, spatiotemporal variability, watershed.

1. Introduction

Remote sensing from satellite platforms has become an indispensable tool for monitoring the phenological status of vegetation and its potential role in controlling the land surface energy and water balance in terrestrial ecosystems (e.g., Xinmei et al., 1993; Guillevic et al., 2002; Bounoua et al., 2000; Wang et al., 2006; Watts et al., 2007; Méndez-Barroso et al., 2008). The spatiotemporal characteristics of remote sensing data provide an advantage as compared to ground observations by allowing quantification of vegetation phenological changes over large areas and extended periods. For example, the Normalized Difference Vegetation Index (NDVI) is a useful ratio widely used to estimate seasonal changes in plant greenness (Sellers, 1985; Tucker et al., 1985; Goward, 1989; Anyamba and Estman, 1996; Zhang et al., 2003). NDVI is based on the reflection properties of green vegetation and is determined by the ratio of the amount of absorption by chlorophyll in the red wavelength (600-700 nm) to the reflectance of the near infrared (720-1300 nm) radiation by plant canopies. Through the use of spatiotemporal NDVI fields, the seasonal and interannual changes in vegetation greenness can be analyzed and related to biotic and abiotic factors, including rainfall, fire and land cover disturbances (Zhang et al., 2004; Franklin et al., 2006; Wittenberg et al., 2007).

Currently, one of the most reliable sources of remotely-sensed NDVI data at moderate resolutions is the MODIS (Moderate Resolution Imaging Spectroradiometer) sensor on board the EOS Terra and Aqua satellites (Huete et al., 1997, 2002). This sensor offers excellent radiometric and geometric properties, as well as improved atmospheric and cloud corrections (see Huete and Liu, 1994 for design details). For studies of vegetation phenology, MODIS products can be used to indicate the spatial and temporal variations in: (1) the onset of photosynthesis, (2) the peak photosynthetic activity, and (3) the senescence, mortality or removal

of vegetation (e.g., Reed et al., 1994; Zhang et al., 2003). In this study, we use MODIS-derived NDVI fields to examine a set of semiarid, mountainous ecosystems in northwestern Mexico, which respond vigorously to summer precipitation during the North American monsoon (NAM) (Salinas-Zavala et al., 2002; Watts et al., 2007; Vivoni et al., 2007). The NAM is the main climate phenomenon controlling summer rainfall in northwestern Mexico and the southwestern U.S. (Douglas et al., 1993; Adams and Comrie, 1997; Sheppard et al., 2002) and accounts for ~40 to 70% of the annual precipitation in the region. Understanding vegetation dynamics and its relation to hydrologic conditions during the NAM is important as this period coincides with the plant greening and growing season in the region (Watts et al., 2007). Fig. 1 is an example of the vegetation greening observed in the mountainous study area of northwestern Mexico.

The ecohydrology of northwestern Mexico is particularly interesting as the seasonal precipitation pulses from the NAM lead to a major shift in vegetation greening and ecosystem processes. Plant responses during the monsoon include the production of leaf biomass required for photosynthesis, flowering and seed dispersal (e.g., Reynolds et al., 2004; Weiss et al., 2004; Caso et al., 2007). The vegetation transition occurs relatively rapidly and is closely tied to the monsoon onset and its variability. While this has been recognized previously (e.g., Brown, 1994; Salinas-Zavala et al., 2002; Higgins et al., 2003), the linkage between hydrologic conditions and ecosystem responses has not been quantified, primarily due to a lack of observations in the mountainous region. Fortunately, the scarcity of field observations has been recently addressed through the North American Monsoon Experiment (NAME) and Soil Moisture Experiment 2004 (SMEX04) (Higgins and Gochis, 2007; Watts et al., 2007; Vivoni et al., 2007, 2008; Bindlish et al., 2008). As a result, an opportunity exists to quantify vegetation dynamics from remote sensing data and relate these directly to ground-based observations. For example, Vivoni et al.

(2008) analyzed soil moisture for different ecosystems arranged across an elevation gradient through field and remote sensing observations.

Seasonal characteristics of vegetation dynamics, such leaf emergence or senescence, are strongly linked with atmospheric conditions and surface processes such as rainfall, soil moisture and temperature. As a result, the detection of phenological changes in entire ecosystems from remote sensing may allow us to monitor seasonal variability as well as distinguish spatial patterns in hydrologic processes. In prior studies, remote sensing of vegetation has yielded metrics that are useful for monitoring ecosystem changes (e.g., Lloyd et al., 1990; Reed et al., 1994; Zhang et al., 2003). An important contribution has been the time integrated NDVI (iNDVI) over a seasonal period, which is related to the net primary productivity (NPP) in an ecosystem (Reed et al., 1994). iNDVI measures the magnitude of greenness integrated over time and reflects the capacity of an ecosystem to support photosynthesis and biomass production. As a result, the relation between rainfall and iNDVI has been utilized as an indicator of ecosystem productivity. For example, Prasad et al. (2005) and Li et al. (2004) used iNDVI to study the relation between precipitation and vegetation in several ecosystems in India and Senegal, respectively. In both studies, iNDVI showed a strong relationship with rainfall, suggesting this method may be useful for inferring hydrologic controls on vegetation dynamics in other regions.

Relations between vegetation and precipitation have been studied widely in water-limited ecosystems. In previous studies, the maximum photosynthetic activity in the plant growing season has been linked with precipitation in the current and preceding months (Davenport and Nicholson, 1993; Wang et al., 2003; Al-Bakri and Suleiman, 2004; Chamaille-Jammes et al., 2006; Prasad et al., 2007). For water-limited ecosystems, the greenness-precipitation ratio (GPR) has been used to infer the productivity of different plant associations (Davenport and Nicholson,

1993; Prasad et al., 2005). GPR is analogous to rainfall use efficiency (RUE) and is defined as the net primary productivity per unit of rainfall (Le Houerou, 1984). Although vegetation growth is correlated to rainfall, the incoming precipitation is also modified by the soil water balance, such that soil moisture is a key intermediary between storm pulses and plant available water (Breshears and Barnes, 1999; Loik et al., 2004). Soil moisture is also closely tied to vegetation form and function (Eagleson, 2002; Rodríguez-Iturbe and Porporato, 2004), exerting both a control on vegetation and being influenced by plant processes. For example, Farrar et al. (1994) found that the correlation between NDVI and soil moisture is a concurrent effect, suggesting a direct linkage between vegetation dynamics and soil wetness. In addition, the authors found that the accumulated precipitation over several previous months was related to the vegetation response. Grist et al. (1997) also found discrepancies in NDVI-rainfall relationships and attributed these to the role played by soil moisture.

The objectives of our study are to use remote sensing data to quantify the seasonal and interannual vegetation dynamics in the North American monsoon region and relate these to ground-based measurements of precipitation and soil moisture. The study is organized as follows. Section 2 presents a description of the study region and its ecosystem characteristics as well as the regional network of precipitation and soil moisture observations. In section 3, we present the study results, focusing on the spatial and temporal variability of vegetation dynamics at the regional scale. This section also explores the use of vegetation metrics, time stability analysis and topographic gradients for quantifying vegetation dynamics. We then synthesize the study results using a set of vegetation and hydrologic metrics. Finally, section 4 summarizes our study conclusions and addresses the implications of our work toward ecohydrological processes in the semiarid NAM region.

2. Methods

In the following, we describe the study region in northwestern Mexico, the continuous precipitation and soil moisture observations, and the remotely-sensed NDVI datasets processed from the MODIS sensor. We selected a three year period (2004 to 2006, with portions of 2007) to capture vegetation dynamics during three separate monsoon seasons that exhibited different rainfall amounts and coincided with the operation of the regional network. We also describe a set of spatiotemporal analyses used to investigate the relationships between precipitation, soil moisture and vegetation dynamics for different ecosystems in the mountainous region.

2.1. Study Region and Ecosystem Distributions

Our study region is a large domain that encompasses the Río San Miguel and Río Sonora basins in northwestern Mexico in the state of Sonora (Fig. 2). The total area for both watersheds is ~15,842 km² (3798 km² for the Río San Miguel and 11,684 km² for the Río Sonora). Our analysis extends beyond the basin boundaries to cover an area of 53,269 km² including portions of the Río Yaqui and San Pedro River basins. The study region is characterized by complex terrain in the Sierra Madre Occidental with north-south trending mountain ranges. The two major ephemeral rivers are Río San Miguel and Río Sonora, which run from north to south. Basin areas were delineated from a 29-m digital elevation model (DEM) using two stream gauging sites as outlet points (Fig. 2). For the Río San Miguel, the outlet is a gauging site managed by the Comisión Nacional del Agua (CNA) known as El Cajón (110.73° W; 29.47° N), while the Río Sonora was delineated with respect to the El Oregano CNA gauge (110.70° W; 29.22° N). Elevation above sea level in the region fluctuates between 130 and 3000 m, with a mean elevation of 983 m and a standard deviation of 391 m. The mean annual precipitation in the

region varies approximately from 300 to 500 mm and it is controlled by latitudinal position and elevation (Chen et al., 2002; Gochis et al., 2007).

A wide variety of ecosystems are found in the study region due to the strong variations in elevation and climate in short distances (e.g., Brown, 1994; Salinas-Zavala et al., 2002; Coblenz and Riitters, 2004). Ecosystems are arranged along elevation gradients in the following fashion (from low to high elevation): Sonoran desert scrub, Sinaloan thornscrub, Sonoran riparian deciduous woodland, Sonoran savanna grassland, Madrean evergreen woodland and Madrean montane conifer forest. Brown (1994) presented the following ecosystem descriptions.

Sonoran desert scrub: The desert region spans from 23° to 35° N and includes two subdivisions: Arizona uplands and Plains of Sonora. The Sonoran desert differs from other North American deserts due to its trees, large cacti and succulents. Arizona uplands are encountered on slopes, rocky surfaces and sloping plains, with an elevation range of 300 to 1000 m. The Plains of Sonora is characterized by open stands of low branching trees and shrubs, interspaced with short lived herbaceous plants and bare ground, with an increment in tropical species. This subdivision is primarily found in alluvial valleys and hills closer to the coastal plain.

Sinaloan thornscrub: The Sinaloan thornscrub covers southern and southeastern Sonora south of 28° N from sea level to over 900 m. An abundance of shrubbery, short microphyllus trees and subtropical species is observed along with the absence of common Sonoran desert species. The basic structure and composition is of drought-deciduous, often thorny, pinnate-leaved, multi-trunked trees and shrubs, typically found on hillslopes and alluvial fans.

Sonoran riparian deciduous woodland: In this ecosystem, we find associations of tropical and subtropical trees such as willows, cottonwood and mesquite, which are restricted to near stream areas below 1100 m. Mesquite woodlands attain their maximum development on

alluvial material on old dissected floodplains. Riparian woodlands along streams are also interspersed with herbaceous and shrub species in understory and intercanopy patches.

Sonoran savanna grassland: These subtropical grasslands are encountered at elevations between 900 and 1000 m on flat plains and along large river valleys on deep, fine textured soils. This ecosystem is commonly found in central and eastern Sonora. Tree and scrub components vary in composition, with mesquite as the dominant tree and the presence of large cacti.

Madrean evergreen woodland: This ecosystem is found in the foothills and mountains of the Sierra Madre Occidental. A large variety of oak species are present, including Chihuahuan oak and Mexican blue oak. In northern Sonora, oak woodlands descend to about 1200 to 1350 m in proximity to savanna grasslands, while in central and southern Sonora, this ecosystem occurs as low as 880 to 950 m and borders Sinaloan thornscrub. Some cacti and leaf succulents of the savanna grassland also extend into this ecosystem.

Madrean montane conifer forest: These forests are encountered in higher plateaus and mountains of Sonora with an elevation range from 2000 m to 3050 m, but more commonly from 2200-2500 m. The most common tree species include white Mexican pine and Chihuahuan pine. The lower limits of the conifer forest are in contact with Madrean evergreen woodland.

2.2. Field and Remote Sensing Datasets

Ground-based precipitation and soil moisture observations were obtained from a network of fifteen instrumentation sites installed during 2004 as part of SMEX04 (Vivoni et al., 2007). Fig. 2 presents the locations of the continuous stations, with five sites in the Río Sonora and ten sites in the Río San Miguel. Table 1 presents the station locations, ecosystem classifications and elevations. Precipitation data (mm/hr) were acquired with an 8-inch funnel tipping bucket rain gauge (Texas Electronics, T525I), while volumetric soil moisture (% in hourly intervals) was

obtained at a 5-cm depth with a 50-MHz soil dielectric sensor (Stevens Water Monitoring, Hydra Probe). The Hydra Probe determines soil moisture by making high frequency measurements of the complex dielectric constant in a 22 cm³ soil sampling volume. We used a factory calibration for sandy soils to transform the dielectric measurement to volumetric soil moisture (%) (Seyfried and Murdock, 2004). Table 2 presents the limited amounts of missing data during the study period due to equipment malfunction or data loss related to site inaccessibility during floods.

MODIS NDVI datasets were acquired from the EOS Data Gateway. Sixteen day composites of the 250-m NDVI products from MODIS-Terra were obtained from January 2004 to June 2007 for a total of 83 images. MODIS-Terra overpasses the region around 11:00 A.M. local time (18:00 UTC). For each overpass, the NDVI is calculated from reflectance as:

$$NDVI = \frac{\rho_{NIR} - \rho_{red}}{\rho_{NIR} + \rho_{red}}, \quad (1)$$

where ρ_{NIR} and ρ_{red} are the surface bidirectional reflectance factors for MODIS bands 2 (841-876 nm) and 1 (620-670 nm), respectively. The main purpose of compositing over the 16-day periods is to select the best observation, on a per pixel basis, from all the retained data. The MODIS vegetation index compositing algorithm utilizes two main components: (1) Maximum Value Composite (MVC) and (2) Constrained-View angle Maximum Value Composite (CV-MVC). The MVC selects the pixel observation with the highest NDVI to represent the compositing period (Holben, 1986). A disadvantage of the MVC approach is that it selects pixels with NDVI values greater than the nadir value. As a result, the CV-MVC technique is then used to constrain the angular variations in the MVC method by comparing the two highest NDVI values and selecting the observation closest to nadir to represent the 16-day composite (Huete et al., 2002).

Each of the MODIS images was mosaicked, clipped and reprojected using the HDF-EOS to GIS Format Conversion Tool (HEG tools version 2.8). This tool allows reprojection from the

native MODIS Integerized Sinusoidal (ISIN) grid to the Universal Transverse Mercator (UTM) Zone 12N projection used in our analysis. To minimize the effect of human-impacted regions, we created a mask excluding zones with minimal NDVI changes over time (e.g., mines, urban areas and water bodies), thus focusing our analysis to areas of natural vegetation.

2.3. Metrics of the Spatial and Temporal Vegetation Dynamics

In the following, we describe analyses conducted to quantify the seasonal and interannual vegetation dynamics. Remotely-sensed NDVI data were characterized through: (1) analysis of temporal variations at each continuous station; (2) derivation of vegetation metrics; (3) analysis of time stability of the spatiotemporal fields; and (4) identification of elevation controls on the vegetation statistics along two transects. Temporal variations at specific sites were obtained by determining the mean and standard deviation of NDVI for each MODIS composite image from the 3×3 pixel domain around a station. The arithmetic mean provides the averaged conditions at a site and accounts for uncertainties in the georeferencing of the station and MODIS image. The standard deviation captures the spatial variability around an instrument site.

Temporal variations of NDVI were then used to estimate a set of vegetation metrics using the methods of Lloyd (1990) and Reed et al. (1994). In order to extract the vegetation metrics, we applied a smoothing method to the raw NDVI time series using a LOESS regression. This algorithm reduces the effects of outliers and preserves the essential features of the NDVI variations. With the smoothed NDVI, we generated two different moving averages following Reed et al. (1994): (1) a backward moving average (BMA) applied in reverse chronological order; and (2) a forward moving average (FMA). The two moving average were subsequently lagged by 5 time periods, each 16 days in length, to detect the crossing properties of the NDVI

time series (e.g., timing of vegetation greening and senescence). We tested the sensitivity of the method to different lag lengths to best match the annual NDVI cycle in the study region.

Based on the above, we found the beginning of the vegetation greening as the crossing between the smoothed NDVI and the FMA. Similarly, the end of the greening season was found as the crossing between the smoothed series and the BMA. Fig. 3a is an example of the original NDVI data, the smoothed series and moving averages. Once the start and end of the greening are found, several vegetation metrics can be estimated (Reed et al., 1994): (1) Duration of Greenness (days), defined as the period between the onset and end of the greenness; (2) Growing season integrated NDVI (iNDVI, dimensionless), measured as the area under the smoothed NDVI series; (3) Seasonal range of NDVI (ΔNDVI , dimensionless) determined from the maximum (NDVI_{max}) and minimum (NDVI_{min}) NDVI values; and the (4) Rate of Greenup and the (5) Rate of Senescence, defined as the change in NDVI per time (day^{-1}) for the beginning and end of the greening season, respectively. Fig. 3b presents an example of the determination of the vegetation metrics for a Sinaloan thornscrub site during the 2004 growing season.

To analyze the temporal and spatial variability of NDVI, we applied the concepts of spatial and temporal persistence (e.g., Vachaud et al., 1985; Mohanty and Skaggs, 2001; Grant et al., 2004; Jacobs et al., 2004; Vivoni et al., 2008). We quantified the spatial and temporal root mean square error (RMSE) of the mean relative difference (δ) for each NDVI pixel during the study period. The main difference between the spatial and temporal RMSE δ is the mean value used to compute the relative difference. In the case of the spatial RMSE δ_s , we used the spatial mean NDVI of each image and calculated the difference between every pixel and the spatial mean. Conversely, for the temporal RMSE δ_t , we used the temporal NDVI mean for each pixel over all images and then calculated the difference between each pixel and its temporal mean.

To compute the spatial RMSE δ_s , we first calculated the spatial mean of NDVI in the region for each MODIS composite as:

$$\overline{NDVI}_{sp,t} = \frac{1}{n} \sum_{s=1}^n NDVI_{s,t} \quad , \quad (2)$$

where $\overline{NDVI}_{sp,t}$ is the spatial mean NDVI for each date (t) over all pixels (s) and n is the total number of pixels (i.e., 992,450 pixels, 863×1150). Using this method, we obtained 83 spatially-averaged NDVI values. Conversely, the temporal mean of NDVI in each pixel is computed as:

$$\overline{NDVI}_{tm,s} = \frac{1}{N_t} \sum_{t=1}^{N_t} NDVI_{s,t} \quad , \quad (3)$$

where $\overline{NDVI}_{tm,s}$ is the temporal mean NDVI and N_t is the total number of processed MODIS images (83 in total). In (2) and (3), $NDVI_{s,t}$ is the NDVI value for pixel (s) at time (t). The mean relative difference captures the difference between a pixel and the mean (spatial or temporal) for all NDVI images. In the spatial case, the mean relative difference $\overline{\delta}_s$ is computed as:

$$\overline{\delta}_s = \frac{1}{N_t} \sum_{t=1}^{N_t} \frac{NDVI_{s,t} - \overline{NDVI}_{sp,t}}{\overline{NDVI}_{sp,t}} \quad . \quad (4)$$

In addition, the temporal mean relative difference $\overline{\delta}_t$ is computed as:

$$\overline{\delta}_t = \frac{1}{N_t} \sum_{t=1}^{N_t} \frac{NDVI_{s,t} - \overline{NDVI}_{tm,s}}{\overline{NDVI}_{tm,s}} \quad . \quad (5)$$

The variances of the relative difference ($\sigma(\delta_t)^2$ for temporal and $\sigma(\delta_s)^2$ for spatial cases) are:

$$\sigma(\delta_s)^2 = \frac{1}{N_t - 1} \sum_{t=1}^{N_t} \left(\frac{NDVI_{s,t} - \overline{NDVI}_{sp,t}}{\overline{NDVI}_{sp,t}} - \overline{\delta}_s \right)^2 \quad , \quad \text{and} \quad (6)$$

$$\sigma(\delta_t)^2 = \frac{1}{N_t - 1} \sum_{t=1}^{N_t} \left(\frac{NDVI_{s,t} - \overline{NDVI}_{tm,s}}{\overline{NDVI}_{tm,s}} - \overline{\delta}_t \right)^2 \quad . \quad (7)$$

Finally, the root mean square error of the mean relative difference ($RMSE \delta$) is a single metric which captures both the bias and the spread around the bias (Jacobs et al., 2004). It is computed here for the temporal and spatial cases as:

$$RMSE \delta_s = \left(\bar{\delta}_s^2 + \sigma(\delta_s)^2 \right)^{1/2}, \text{ and} \quad (8)$$

$$RMSE \delta_t = \left(\bar{\delta}_t^2 + \sigma(\delta_t)^2 \right)^{1/2}. \quad (9)$$

Low $RMSE \delta_s$ sites are stable pixels that closely track the spatially-averaged conditions in the region over time. This metric can identify ecosystems that capture the temporal NDVI dynamics for an entire region. We would expect ecosystems that dominate the regional greening, such as the Sinaloan thornscrub, would exhibit low $RMSE \delta_s$. On the other hand, low $RMSE \delta_t$ indicates pixels with values close to the temporal mean at the site. This metric indicates ecosystems that have more limited seasonal changes. We expect that ecosystems, such as the Madrean evergreen woodland with lower seasonality, would exhibit low $RMSE \delta_t$.

We also established two topographic transects to assess the variability of NDVI and its statistical properties with elevation, along different locations in the Río San Miguel and Río Sonora (Fig. 2). Each transect is ~23 km in length, samples elevations from nearly 600 m to 1600 m above sea level, and traverses different ecosystems along the elevation gradient.

2.4. Relationships between NDVI, Precipitation and Soil Moisture

Several approaches were pursued to explore the relations between NDVI, precipitation and soil moisture. A linear regression between vegetation greening and precipitation was carried out using iNDVI and accumulated seasonal rainfall. Due to sampling gaps, this analysis was focused on the 2005 monsoon. For this season, we also computed the greenness-precipitation ratio (GPR) to assess the efficiency of converting incoming rainfall into vegetation biomass. This

ratio was calculated by dividing iNDVI by the seasonal precipitation. In addition, we calculated correlation coefficients between NDVI and accumulated rainfall and time-averaged soil moisture in the current and previous months using a combination of different monthly lags for 2005.

3. Results and Discussion

In the following, we present the set of spatial and temporal analyses used to quantify the vegetation dynamics in the study region and relate these to metrics that quantify the precipitation and soil moisture observations from the regional network. Our focus is primarily on the regional characterization of vegetation dynamics afforded by the remote sensing data, with more detailed study at representative stations of particular ecosystems arranged along topographic transects.

3.1. Spatial and Temporal Vegetation Dynamics in Regional Ecosystems

Vegetation conditions in the regional ecosystems are assessed to determine the seasonal and interannual variations induced by differing amounts of NAM precipitation and soil moisture. Fig. 4 presents spatial maps of the seasonal change in NDVI ($D_{\text{NDVI}} = (\text{NDVI}_{\text{max}} - \text{NDVI}_{\text{min}}) / \text{NDVI}_{\text{min}}$, expressed as a percentage) for the three monsoons (2004 to 2006). There is an evident variation in the spatial pattern of D_{NDVI} related to ecosystem distributions, terrain characteristics and rainfall amounts. The spatial distribution of D_{NDVI} and its range varies for each year, following the total rainfall averaged over all regional stations ($\overline{R_s}$) from July to September. In the year 2004 ($\overline{R_s} = 251$ mm), the largest degree of vegetation greening occurs in the southeastern part of the domain, outside the regional network. Nevertheless, the region between stations 146 and 147 in the Río San Miguel exhibited high greening, in agreement with the elevated soil moisture observed from aircraft-based retrievals (Vivoni et al., 2008). In contrast, the year 2005 was the driest in the record ($\overline{R_s} = 222$ mm) and as a result experienced the

smallest D_{NDVI} , with a range from 50 to 150%. Note, however, that isolated patches experience high degrees of greening, suggesting localized storms during this monsoon. Conversely, the year 2006 exhibited the largest change in NDVI due to the elevated precipitation ($\overline{R}_y = 350$ mm). The spatial distribution of D_{NDVI} is also more uniform in the region, ranging from 200 to 300%, indicating that the overall ecosystem response was vigorous and spatially extensive. Interestingly, small changes in seasonal NDVI are always observed in forested riparian corridors (Sonoran riparian deciduous woodland) and high altitude mountains (Madrean montane conifer forests) as these remain green throughout the year. Overall, the spatial NDVI fields indicate seasonal and interannual changes linked to rainfall, ecosystem pattern and topography.

Fig. 5 presents the temporal variations of NDVI, precipitation and soil moisture over the period January 2004 to June 2007 (at 16-day intervals) at four regional stations: (a) station 146 (Madrean evergreen woodland), (b) station 132 (Sinaloan thornscrub), (c) station 139 (Sonoran savanna grassland), and (d) station 144 (Sonora desert scrub). The four stations were selected to represent different ecosystems as well as the changes in hydrologic conditions along elevation gradients (see Table 1 for station descriptions). For each site, hourly precipitation and soil moisture observations were accumulated or averaged, respectively, over the 16-day intervals to match the MODIS compositing period. Remotely-sensed NDVI time series are depicted as the station mean (symbols) and ± 1 standard deviation (error bars) over a 3×3 window (250-m pixels) around the station. Any data gaps in the ground or remotely-sensed observations resulted in the removal of the composites and are shown as broken lines (see Table 2 for missing data).

The temporal variations in vegetation greenness, as captured by the station NDVI, are dramatic in each ecosystem and closely related to the hydrologic conditions at each site. The Madrean evergreen woodland (Fig. 5a) exhibited the highest precipitation of the ecosystems in

the region, with an exceptional rainfall in 2006 (up to 300 mm in July). In response, soil moisture was elevated in the 2006 summer, reaching >20% in the surface soil layer. This plant-available water led to a vigorous summer greening reflected in a peak NDVI of nearly 0.8. Similar summer processes are observed in station 146 for 2004 and 2005, albeit with lower precipitation, soil moisture and peak NDVI. In contrast, the Sinaloan thornscrub (Fig. 5b) showed less rainfall than higher sites, but more consistent greening in the different summers. The NDVI range (~0.25 to ~0.8) varied slightly across the different monsoons, suggesting this ecosystem is fairly resilient to hydrologic changes. Sonoran savanna grasslands (Fig. 5c) have a more muted vegetation response (smaller NDVI range) as compared to the other ecosystems. Nevertheless, the station NDVI exhibits high temporal variations in response to wet and dry periods, including a spring peak in 2005 after a wet winter. Finally, the Sonoran desert scrub (Fig. 5d) also experiences summer greening, with relatively small year-to-year variations in response to variations in rainfall and soil moisture. Interestingly, summer 2005 had more favorable hydrologic conditions than 2006 at this station and thus the highest peak NDVI in the three-year record.

Fig. 5 also allows inspection of vegetation response in the three winter seasons, receiving smaller and more variable rainfall amounts (e.g., Sheppard et al., 2002; Nagler et al., 2007). While this is not the primary focus of this study, it is important to highlight these variations. A relatively wet winter in 2005 impacted vegetation dynamics in two ways: (1) maintaining green conditions for a longer period of time, or (2) leading to spring season plant growth. In contrast, a relatively dry winter in 2006 caused a significant decrease in NDVI in spring and early summer for all ecosystems. The linkages between winter and summer precipitation, soil moisture and vegetation greening is of considerable importance and has not been addressed in the region.

3.2. Quantifying Ecosystem Dynamics through Vegetation Metrics

Vegetation metrics can aid in the quantification of ecosystem responses to the precipitation and soil moisture during the North American monsoon. Table 3 presents the phenological metrics obtained for each regional station during the monsoon seasons in 2004 to 2006. Overall, the various metrics, in particular the $iNDVI$ and $\Delta NDVI$, confirm that summer 2006 had the most dramatic vegetation greening in most of the regional stations. In contrast, stations during summer 2004 exhibited the shortest Duration of Greenness and Days to $NDVI_{max}$ as well as the smallest $iNDVI$ and $\Delta NDVI$. The metrics also reveal differences and similarities in vegetation productivity among the regional stations. As observed in Fig. 5, the ecosystem composition at each site has a strong control on the vegetation metrics for the different years. Stations with common plant communities share similar response to summer rainfall. For example, lower productivity stations are all in Sonoran savanna grasslands (stations 137, 138, 139) with low $iNDVI$, $\Delta NDVI$ and Duration of Greenness. Similarities are also observed in vegetation metrics for stations in the Sonoran riparian deciduous woodland (stations 135, 143). For the wet 2006 summer, however, precipitation amount and soil water availability lead to certain degrees of homogenization in the vegetation response across different ecosystems. For instance, Madrean evergreen woodlands (station 146) and Sinaloan thornscrub (station 132) share similar responses to the 2006 NAM precipitation (e.g., $iNDVI = 8.69$ and 8.68 for 2006, respectively), despite having different plants and ecophysiological processes. Differences in vegetation metrics among regional stations are stronger during drier monsoons.

To explore this further, Table 4 presents temporal coefficients of variation (CVs) for each vegetation metric computed for the average conditions in each ecosystem across all years. As a result, the CV primarily captures the interannual variations in vegetation metrics in a particular

ecosystem. Ecosystems with high CVs imply large interannual changes in the 2004 to 2006 summer monsoons. Note that Sonoran savanna grassland and Sonoran riparian deciduous woodlands exhibit higher CVs for iNDVI, Δ NDVI and Duration of Greenness, indicating strong variations between years. Small CV in iNDVI and high CV in Δ NDVI is observed in the Sonoran desert scrub, suggesting this ecosystem varies primarily in the NDVI range from year-to-year. The Madrean evergreen woodland and Sinaloan thornscrub have intermediate CVs for the vegetation metrics that appear to offset each other. For example, in the Madrean evergreen woodland, CV in iNDVI is lower than the Sinaloan thornscrub, while CV in Δ NDVI is higher. This suggests that different ecosystems in the region respond in variable ways to interannual hydrologic changes. Evergreen woodlands appear to vary their maximum greening (Δ NDVI) in response to increased rainfall amounts, while deciduous trees and shrubs vary the total productivity (iNDVI) during the growing season. These two plant greenup strategies may explain how these ecosystems exist at different elevation in the region. Finally, the vegetation metric with the highest year-to-year variation is Days to NDVI_{max}, indicating that the rate of ecosystem greening is highly influenced by rainfall amounts during the monsoon onset.

3.3. Spatial and Temporal Stability Analyses of Vegetation Dynamics

The ecosystem response to precipitation and soil moisture conditions, as captured by the NDVI fields, during the study period can be discerned through spatial and temporal persistence. Fig. 6 presents spatial maps of: (a) the spatial RMSE δ_s , and (b) the temporal RMSE δ_t , calculated using the eighty-three (83) MODIS NDVI images in the domain. Regions with low spatial RMSE δ_s (Fig. 6a, red colors) correspond to zones that closely track the spatially-averaged conditions in the two basins. These areas coincide well with the location of Sinaloan thornscrub and Sonoran desert scrub (Brown, 1994) that exhibit strong seasonal variations in

NDVI and occupy large regional extents. Note these areas are located over a range of elevations, but are not observed in the highest peaks or riparian corridors (Vivoni et al., 2007). In these locations, high spatial RMSE δ_s (Fig. 6a, blue colors) indicate zones behaving differently from the spatial mean and correspond to Madrean evergreen woodland and montane conifer forests at high elevations and Sonoran riparian deciduous woodland along the main stems of the Río San Miguel and Río Sonora. Clearly, the distribution of RMSE δ_s is a useful tool to classify ecosystem patterns, in particular to sharply distinguish between evergreen woodlands at high elevations and deciduous scrublands at mid elevations.

The temporal RMSE δ_t (Fig. 6b) supports the above analysis by distinguishing locations in the domain that closely track the temporal mean in each pixel. Regions with low RMSE δ_t (blue colors) have relatively smaller changes in time and correspond to Madrean evergreen woodland and montane conifer forests at high elevations and Sonoran riparian deciduous woodlands along rivers. Despite having deciduous trees, the riparian woodlands are able to directly access groundwater and thus remain green during longer periods of time, as compared to ecosystems that rely solely on summer rainfall. Lower temporal persistence is observed for regions with high RMSE δ_t (red colors) which depict zones with large temporal changes. Clearly, these match the areas with low RMSE δ_s , in particular the Sinaloan thornscrub and Sonoran desert scrub. Interestingly, the temporal RMSE δ_t is able to more clearly separate the locations of these ecosystems, with Sinaloan thornscrub further south in the domain and replaced by Sonoran desert scrub at similar elevations in the north (Brown, 1994). In conjunction, the spatial and temporal persistence maps reveal ecosystem patterns that are not observed through simpler metrics such as seasonal NDVI changes (Fig. 4). Further, this analysis extends applications of RMSE δ beyond traditional soil moisture studies (e.g., Jacobs et al., 2004; Vivoni et al., 2008).

Given the observed effects of topography on spatial and temporal persistence, it is important to understand how ecosystem responses vary along elevation gradients in the study region. Figs. 7 and 8 present the variation of NDVI, spatial RMSE δ_s and temporal RMSE δ_t for two topographic transects depicted in Fig. 2 (A–A' in the Río San Miguel and B–B' in the Río Sonora). The transects were selected to capture a range of elevations (550 to 1900 m in A–A', and 680 to 1600 m in B–B'), span several ecosystems and be in proximity to a subset of the regional stations. Note that Figs. 7 and 8 indicate the topographic variations (solid lines) with distance along the transects, which have a total planform length of ~23 km. In both topographic transects, the temporal mean NDVI (symbols) increases with elevation, while the temporal standard deviation (vertical bars depict ± 1 std) typically decreases with altitude. These variations indicate that the mid elevation Sinaloan thornscrub and Sonoran desert scrub are characterized by lower time-averaged greenness, which is more variable in time, as compared to the high elevation Madrean evergreen woodland. Notably, the Río San Miguel transect exhibits higher NDVI (> 0.70) in the mountain peak (up to 1900 m) than the Río Sonora peak (NDVI > 0.55). Interestingly, the relation between NDVI and elevation at lower and mid elevations (e.g., ~600 to 1000 m for Río San Miguel) is linear, with similar rates of increase along the transect. At high elevations, however, a lag is observed in the increase in NDVI as compared to elevation as well as a displacement of the NDVI maximum value away from the peak elevation.

The relation between elevation and ecosystem response is further analyzed using the spatial and temporal persistence in Fig. 7b and 8b. In both transects, the mid elevation ecosystems exhibit low spatial RMSE δ_s and high temporal RMSE δ_t , which indicate areas closely tracking the mean conditions in the region. These elevations correspond to Sinaloan thornscrub and Sonoran desert scrub which are highly responsive to NAM precipitation and

occupy large regional extents. At high elevations along each transect, the Madrean evergreen woodland has a larger spatial RMSE δ_s and a smaller temporal RMSE δ_t . This suggests that the evergreen species have time-stable conditions that do not track the spatially-averaged response. In addition, the maximum spatial RMSE δ_s is displaced slightly from the mountain peak, as observed for the mean NDVI. In both transects, a range of elevations (e.g., ~600 to 900 m in the Río San Miguel) simultaneously have small spatial and temporal RMSE δ . We interpret this as an elevation band of significant monsoonal response which dominates the regional greening, as suggested by Vivoni et al. (2007). Clearly, spatial and temporal persistence reveal variations in vegetation dynamics along topographic transects and can aid in the interpretation of vegetation-elevation relations in semiarid mountain fronts.

3.4. Relations between Vegetation and Hydrologic Indices

To further explore the relation between ecosystem dynamics and the precipitation and soil moisture conditions, we compared iNDVI, the greenness-precipitation ratio ($GPR = iNDVI/R_s$) and the total precipitation (R_s) at each station for the 2005 monsoon (Table 5). This particular summer was selected due to its limited amounts of missing data in the regional stations. Fig. 9 presents a linear relation between iNDVI and precipitation (R_s) at the 12 stations with complete data. The linear regression between iNDVI and R_s results in ($r^2 = 0.64$):

$$iNDVI = 0.017R_s + 1.369 \quad . \quad (2)$$

Clearly, as rainfall amounts increase across the regional stations, ecosystem productivity during the summer monsoon also increases. While ecophysiological differences are present in the regional ecosystems, seasonal rainfall is good predictor of biomass production. Station 132 (Sinaloan thornscrub) is an outlier in the general trend, exhibiting a higher than expected iNDVI for the given precipitation, possibly due to rainfall underestimation in the MODIS pixel around

the site. Results are consistent with studies in other regions where higher iNDVI and biomass production are observed with increasing rainfall (e.g., Li et al., 2004; Prasad et al., 2005). Further testing of the proposed relation during other summers and for a larger number of stations may provide an indication of its robustness.

The greenness-precipitation ratio for summer 2005 is presented in Fig. 10 as a spatial map overlaid on the distribution of regional ecosystems. The GPR is a measure of the efficiency of an ecosystem to convert available water into biomass. As shown in Table 5, the range in GPR among the regional stations is from 1.86 (station 144, Sonoran desert scrub) to 2.87 (station 133, Sinaloan thornscrub). The spatial variability in GPR indicates that ecosystems in the southern region of the Río San Miguel were able to more efficiently use precipitation for biomass production. Interestingly, each of these ecosystems corresponds to the Sinaloan thornscrub (stations 130, 131, 132, 133, 147), suggesting that this plant community is well-tuned to utilizing summer rainfall to produce vegetation greening. The response in the Sinaloan thornscrub is consistent with seasonal changes in NDVI for 2005 (Fig. 4b) and a high temporal RMSE δ_t (Fig. 6b). Other regional ecosystems, such as Sonoran savanna grassland (stations 137, 138, 139) and Sonoran riparian deciduous woodland (stations 135, 143), show smaller GPR, suggesting lower rainfall use efficiency in grasslands and riparian trees. GPR estimates in the regional ecosystems for different monsoons would indicate if a convergence to a common rainfall use efficiency occurs during dry periods, as noted by Huxman et al. (2004).

The relationships between vegetation dynamics as quantified by NDVI and the hydrologic conditions in each regional station are explored using lagged Pearson correlation coefficients. The analysis consists of correlating the monthly-averaged NDVI (consisting of two compositing periods) with the current (lag 0) or preceding (monthly lags from 1 to 3)

accumulated precipitation (Table 6) or time-averaged surface soil moisture in the top 5 cm (Table 7). To obtain significant relations, the correlation coefficients (CCs) are averaged for all months during the 2005 year, selected due to its limited amounts of missing data. For each table, maximum CCs at each regional station are italicized. Table 6 reveals that most stations have strong correlations between NDVI and accumulated rainfall in the current plus the two previous months (lag 0+1+2), while none of the stations have high CCs in the current month (lag 0). This suggests that regional ecosystem responses depend on the accumulated seasonal rainfall during the current and previous two months, with limited controls of the current conditions.

Conversely, the correlation coefficients between monthly NDVI and time-averaged soil moisture in Table 7 exhibit larger values for the current (lag 0), previous (lag 1) or current and previous (lag 0+1) months. The shorter monthly lags observed for the maximum CCs between NDVI and soil moisture are evidence of a more immediate control of plant available water on vegetation dynamics, as compared to current precipitation. Nevertheless, overall CCs between NDVI and precipitation are higher than those for soil moisture at longer monthly lags across most of the regional stations. Fig. 11 summarizes the differences between the precipitation and soil moisture correlations with NDVI for a range of lags arranged from the current month (lag 0) toward longer prior periods (lag 0+1+2). Results are shown as average values (symbols) over all stations and their variability depicted as the ± 1 standard deviation (vertical bars). Clearly, the concurrent correlation (lag 0) is higher between soil moisture and NDVI, as compared with the current precipitation amount. For longer lags (e.g., lag 0+1, 0+1+2), however, the accumulated precipitation has a stronger relation with the vegetation dynamics, indicating that the delayed response between NAM rainfall and seasonal greening in the region.

4. Summary and Conclusions

Vegetation dynamics in the North American monsoon region are closely linked to seasonal changes in precipitation (e.g., Salinas-Zavala et al., 2002; Matsui et al., 2005; Watts et al., 2007; Vivoni et al., 2007). To the authors' knowledge, however, the controls exerted by soil moisture on seasonal vegetation greening have not been studied for the broader NAM region in northwestern Mexico. Furthermore, the seasonal, interannual and spatial variations in vegetation response during the NAM are not well understood. Quantifying these spatiotemporal variations in a range of ecosystems is fundamental for assessing the degree of coupling between ecologic, hydrologic and atmospheric processes during the summer season. For example, Dominguez et al. (2008) found that the dynamics of evapotranspiration in the NAM ecosystems leads to a positive feedback on rainfall generation and to local precipitation recycling. Since the spatiotemporal variations of vegetation greening are directly linked to photosynthesis and evapotranspiration, quantifying vegetation dynamics using remote sensing observations represents an important step towards investigating ecohydrological processes in the NAM region. While vegetation greening should clearly be related to precipitation and soil moisture in the water-limited ecosystems, no prior attempts have been made to quantify the hydrologic controls on the vegetation dynamics.

In this study, we quantify the seasonal and interannual changes in vegetation greenness through the use of remotely-sensed NDVI fields from the MODIS sensor over the period 2004 to 2006. Our regional analysis focuses on a large area in northern Sonora comprised by two major basins (Río San Miguel and Río Sonora) and parts of the Río Yaqui and San Pedro River basins in the Sierra Madre Occidental. The regional extent and the study duration were selected to take advantage of the regional instrument network with precipitation and soil moisture observations. By relating and interpreting the remotely-sensed and ground-based measurements, we identify

the following characteristics of the regional vegetation dynamics in the Sierra Madre Occidental of northern Sonora and their relation to precipitation and soil moisture:

(1) Seasonal changes in vegetation greenness are dramatic in all the regional ecosystems and are related to hydrologic conditions and their spatial distribution during a particular monsoon season. As a result, interannual variability is observed in the seasonal vegetation greening and the metrics used to quantify biomass production. The vegetation response was most intense and extensive during the wet 2006 monsoon, reaching up to a 300% seasonal increase in NDVI.

(2) Vegetation responses to NAM precipitation and soil moisture depend strongly on the plant communities in each ecosystem. The ecosystem with consistently high monsoon greening is the mid elevation Sinaloan thornscrub, as suggested by Watts et al. (2007) and Vivoni et al. (2007). Other ecosystems in the region either exhibited lower seasonal changes in NDVI or less consistent year-to-year variations. Comparisons across ecosystems indicate that different plant greenup strategies are utilized in response to interannual hydrologic variations.

(3) Spatial and temporal persistence of remotely-sensed NDVI fields reveal ecosystem patterns that are not observed using simple metrics. In particular, RMSE δ_s distinguishes between evergreen woodlands at high elevations and deciduous scrublands at mid elevations, while the temporal RMSE δ_t can more clearly separate different ecosystems at similar elevations. Analysis along two topographic transects indicate that elevation controls vegetation dynamics and serves to organize ecosystems into elevation bands, with high monsoonal response at mid elevations.

(4) Accumulated seasonal precipitation is a strong indicator of biomass production across the regional ecosystems, with Sinaloan thornscrub exhibiting the highest rainfall use efficiency. During the study period, differences between ecosystem responses were minimized during the wet 2006 monsoon and maximized during drier monsoons, in contrast to the common rainfall use

efficiency found by Huxman et al. (2004) during drought years. Additional studies are required to quantify rainfall use efficiency in wet and dry periods in the regional ecosystems.

(5) Lagged correlation analysis indicates a strong degree of coupling between vegetation greening and the precipitation and soil moisture conditions at each regional station. Interestingly, concurrent correlations for monthly NDVI are higher with surface soil moisture, while lagged correlations are more significant for accumulated precipitation. This suggests that soil moisture plays an important intermediary role between NAM precipitation and vegetation response.

The observational analysis and interpretations conducted here show the importance of combining satellite remote sensing and ground networks for monitoring ecosystem dynamics and their link to hydrologic conditions. The use of multiple observation scales allows understanding the regional context in which detailed precipitation, soil moisture or surface flux measurements have been made (Gebremichael et al., 2007; Vivoni et al., 2007; Watts et al., 2007). In particular, it is clear that substantial interannual variations are present in monsoon vegetation greening. As a result, evapotranspiration estimates by Watts et al. (2007) for a single season should be revisited for additional summer periods. Further, the soil moisture conditions documented by Vivoni et al. (2007, 2008) along a semiarid mountain should be repeated for longer periods to understand the seasonal and interannual variations in the soil moisture-vegetation-topography relations. Clearly, the duration of our study is a limitation in our interannual analysis, primarily due to the recent establishment of the regional network. Additional analysis is desirable either by extending the work as new data sets become available or performing retrospective analysis with satellite data (though ground data would be limited) over the current basins or the broader NAM region.

Several additional questions have arisen through the analysis conducted in this study. While our focus has been on the summer season, the response to lower and more variable winter

precipitation appears to be significant, in particular for Sonoran savanna grasslands during wet winters. The other regional ecosystems also appear to maintain greener conditions for longer periods when winter rainfall is available. Spring season growth is more common in higher latitude desert grasses (e.g., Pennington and Collins, 2007). As a result, the influence of winter precipitation on the annual hydrologic cycle and vegetation dynamics warrants further study.

The linkages between winter and summer ecohydrological processes are of considerable interest to understand the interannual variations in both the land surface conditions and the North American monsoon system. The interannual variability of NAM precipitation has been related to several factors, including sea surface temperature (e.g., Vera et al., 2006; Castro et al., 2007) and continental snow and soil moisture anomalies (e.g., Gutzler, 2000; Zhu et al., 2007). While the potential role of vegetation greening on the NAM has been proposed (Higgins et al., 2003), there is a lack of consensus regarding if vegetation dynamics impact the monsoon (Salinas-Zavala et al., 2002; Matsui et al., 2005; Dominguez et al., 2008). If a vegetation-atmosphere feedback exists in the NAM region, then understanding the spatiotemporal vegetation dynamics from remote sensing would be a critical link toward enhancing rainfall and streamflow predictability.

Acknowledgements

We would like to acknowledge funding from the National Science Foundation IRES program (Grant OISE_0809946), the NOAA Climate Program Office (Grant CPPA GC07-019), and the Consejo Nacional de Ciencias y Tecnología (CONACYT) fellowship to the first author.

References

- Adams, D.K., Comrie, A.C. 1997. The North American Monsoon. *Bulletin of the American Meteorological Society*, **78**(10): 2197-2213.
- Al-Bakri, J.T., Suleiman, A.S. 2004. NDVI response to rainfall in different ecological zones in Jordan. *International Journal of Remote Sensing*, **25**(19): 3897-3912.
- Anyamba, A., Estman, J.R. 1996. Interannual variability of NDVI over Africa and its relation to El Niño/Southern Oscillation. *International Journal of Remote Sensing*, **17**: 2533-2548.
- Bindlish, R., Jackson, T.J., Gasiewski, A.J., Stankov, B., Cosh, M.H., Mladenova, I., Vivoni, E.R., Lakshmi, V., Watts, C.J., and Keefer, T. 2008. Aircraft-based soil moisture retrievals in mixed vegetation and topographic conditions. *Remote Sensing of Environment*, **112**(2): 375-390.
- Bounoua, L., Collatz, C.J., Los, S.O., Sellers, P.J., Dazlich, D.A., Tucker, C.J., Randall, D.A. 2000. Sensitivity of climate to NDVI changes. *Journal of Climate*, **13**: 2277-2292.
- Breshears, D.D., Barnes, F.J. 1999. Interrelationships between plant functional types and soil moisture heterogeneity for semiarid landscapes within the grassland/forest continuum: a unified conceptual model. *Landscape Ecology*, **14**(5): 465-478.
- Brown, E.D. 1994. *Biotic communities: Southwestern United States and Northwestern Mexico*. University of Utah Press. 342 pp.
- Caso, M., Gonzalez-Abraham, C., Ezcurra, E. 2007. Divergent ecological effects of oceanographic anomalies on terrestrial ecosystems of the Mexican Pacific coast. *Proceedings of the National Academy of Sciences*, **104**(25): 10530-10535.
- Castro, C.L., Pielke, R.A., Adegoke, J.O., Schubert, S.D., Pegion, P.J. 2007. Investigation of the summer climate of the contiguous United States and Mexico using the regional atmospheric

- modeling system (RAMS). Part II: Model climate variability. *Journal of Climate*, **20**(15): 3866-3887.
- Chamaille-Jammes, S., Fritz, H., Murindagomo, F. 2006. Spatial patterns of the NDVI-rainfall relationship at the seasonal and inter-annual time scales in an African savanna. *International Journal of Remote Sensing*, **27**(23): 5185-5200.
- Chen, M., P. Xie, J. E. Janowiak, and P. A. Arkin. 2002. Global land precipitation: A 50-yr monthly analysis based on gauge observations. *Journal of Hydrometeorology*, **3**: 249-266.
- Coblentz, D.D., Riitters, K.H. 2004. Topographic controls on the regional-scale biodiversity of the south-western USA. *Journal of Biogeography*, **31**(7): 1125-1138.
- Davenport, M.L., Nicholson, S.E. 1993. On the relationship between rainfall and the Normalized Difference Vegetation Index for diverse vegetation types in East Africa. *International Journal of Remote Sensing*, **14**(12): 2369-2389.
- Dominguez, F., Kumar, P., Vivoni, E.R. 2008. Precipitation recycling variability and ecoclimatological stability-A study using NARR data. Part II: North American monsoon region. *Journal of Climate* (In Press).
- Douglas, M.W., Maddox, R.A., Howard, K., Reyes, S. 1993. The Mexican Monsoon. *Journal of Climate*, **6**(8): 1665-1677.
- Eagleson, P.S. 2002. *Ecohydrology: Darwinian expression of vegetation form and function*. Cambridge Press. Cambridge, UK, 443 pp.
- Farrar, T.J., Nicholson, S.E., Lare, A.R. 1994. The influence of soil type on the relationships between NDVI, rainfall and soil moisture in semiarid Botswana. II. NDVI response to soil moisture. *Remote Sensing of Environment*, **50**(2): 121-133.

- Franklin, K.A., Lyons, K., Nagler, P.L., Lampkin, D., Glenn, E.P., Molina-Freaner, F., Markow, T., Huete, A.R. 2006. Buffel grass (*Pennisetum ciliare*) land conversion and productivity in the plains of Sonora, Mexico. *Biological Conservation*, **127**(1): 62-71.
- Gebremichael, M., Vivoni, E.R., Watts, C.J., Rodríguez, J.C. 2007. Submesoscale spatiotemporal variability of North American monsoon rainfall over complex terrain. *Journal of Climate*, **20**(9): 1751-1773.
- Gochis, D.J., Watts, C.J., Garatuza-Payan, J., Rodríguez, J.C. 2007. Spatial and temporal patterns of precipitation intensity as observed by the NAME Event Rain gauge Network from 2002 to 2004. *Journal of Climate*, **20**(9): 1734-1750.
- Goward, N.S. 1989. Satellite Bioclimatology. *Journal of Climate*, **2**(7): 710-720.
- Grant, L., M. Seyfried, and J. McNamara. 2004. Spatial variation and temporal stability of soil water in a snow-dominated mountain catchment. *Hydrological Processes*. **18**(18): 3493–3511.
- Grist, J., Nicholson, Nicholson, S.E., Mpolokang, A. 1997. On the use of NDVI for estimating rainfall fields in the Kalahari of Botswana. *Journal of Arid Environments*, **35**(2): 195-214.
- Guillevic, P., Koster, R.D., Suarez, M.J., Bounoua, L., Collatz, G.J., Los, S.O., Mahanama, S.P.P. 2002. Influence of the interannual variability of vegetation on the surface energy balance: A global sensitivity study. *Journal of Hydrometeorology*. **3**(6): 617-629.
- Gutzler, D.S. 2000. Covariability of spring snowpack and summer rainfall across the southwest United States. *Journal of Climate*. **13**(22): 4018-4027.
- Higgins, R.W., Douglas, A., Hahmann, A., Berbery, E.H., Gutzler, D., Shuttleworth, J., Stensrud, D., Amador, J., Carbone, R., Cortez, M., Douglas, M., Lobato, R., Meitin, J.,

- Ropelewski, C., Schemm, J., Schubert, S., Zhang, C. 2003. Progress in Pan American CLIVAR Research: North American Monsoon System. *Atmósfera*, 16: 29-65.
- Higgins, R.W., Gochis, D.J. 2007. Synthesis of results from the North American Monsoon Experiment (NAME) process study. *Journal of Climate*, **20**(9): 1601-1607.
- Holben, B.N. 1986. Characterization of maximum value composites from temporal AVHRR data. *International Journal of Remote Sensing*, **7**(11):1417-1434.
- Huete, A.R., Liu, H.Q. 1994. An error and sensitivity analysis of the atmospheric-correcting and soil-correcting variants of the NDVI for the MODIS-EOS. *IEEE Transactions on Geoscience and Remote Sensing*, **32**(4): 897-905.
- Huete, A.R., Liu, H.Q., Batchily, K., vanLeeuwen, W. 1997. A comparison of vegetation indices global set of TM images for EOS-MODIS. *Remote Sensing of Environment*, **59**(3): 440-451.
- Huete, A.R., Didan, K., Miura, T., Rodriguez, E.P., Gao, X., Ferreira, L.G. 2002. Overview of the radiometric and biophysical performance of the MODIS vegetation indices. *Remote Sensing of Environment*, **83**(1-2): 195-213.
- Huxman, T.E., Smith, M.D., Fay, P.A., Knapp, A.K., Shaw, M.R., Loik, M.E., Smith, S.D., Tissue, D.T., Zak, J.C., Weltzin, J.F., Pockman, W.T., Sala, O.E., Haddad, B.M., Harte, J., Koch, G.W., Schwinning, S., Small, E.E., Williams, D.G. 2004. Convergence across biomes to a common rain-use efficiency. *Nature*, **429**: 651-654.
- Jacobs, M.J., Mohanty, P.B., Hsu, C.E., Miller, D. 2004. SMEX02: Field scale variability, time stability and similarity of soil moisture. *Remote Sensing of Environment*, **92**(4): 436-446.
- Le Houerou, H.N. 1984. Rain use efficiency: a unifying concept in arid-land ecology. *Journal of Arid Environments*, **7**: 213-247.

- Li, D. Lewis, J., Rowland, J. Tappan, G. Tieszen, L.L. 2004. Evaluation of land performance in Senegal using multi-temporal NDVI and rainfall series. *Journal of Arid Environments*, **59**(3): 463-480.
- Lloyd, D. 1990. A phenological classification of terrestrial vegetation cover using shortwave vegetation index imagery. *International Journal of Remote Sensing*, **11**: 2269-2279.
- Loik, M.E., Breshears, D.D., Lauenroth, W.K., Belnap, J. 2004. A multi-scale perspective of water pulses in dryland ecosystems: climatology and ecohydrology of the western USA. *Oecologia*, **141**(2): 269-281.
- Matsui, T., Venkataraman, L., Small, E.E. 2005. The effects of satellite-derived vegetation cover variability on simulated land-atmosphere interactions in the NAMS. *Journal of Climate*, **18**: 21-40.
- Méndez-Barroso, L.A., Garatuza-Payán J., [Vivoni E.R.](#) 2008. Quantifying water stress on wheat using remote sensing in the Yaqui Valley, Sonora, Mexico. *Agricultural Water Management*, **95**(6): 725-736.
- Mohanty, B.P., and T.H. Skaggs. 2001. Spatio-temporal evaluation and time-stable characteristics of soil moisture within remote sensing footprints with varying soil, slope, and vegetation. *Advances in Water Resources*, **24**(9-10):1051–1067
- Nagler, P.L., Glenn, E.P., Kim, H., Emmerich, W., Scott, R.L., Huxman, T.E., Huete, A.R. 2007. Relationship between evapotranspiration and precipitation pulses in a semiarid rangeland estimated by moisture flux towers and MODIS vegetation indices. *Journal of Arid Environments*, **70**(3): 443-462.
- Pennington, D.D., Collins, S.L. 2007. Response of an aridland ecosystem to interannual climate variability and prolonged drought. *Landscape Ecology*, **22**(6): 897-910.

- Prasad, V.K., Anuradha, E., Badarinath, K.V.S. 2005. Climatic controls of vegetation vigor in four contrasting forest types of India. Evaluation from National Oceanic and Atmospheric Administration's Advanced Very High Resolution Radiometer datasets (1990-2000). *International Journal of Biometeorology*, **50**(1): 6-16.
- Prasad, V.K., Badarinath, K.V.S., Eaturu, A. 2007. Spatial patterns of vegetation phenology metrics and related climatic controls of eight contrasting forest types in India. Analysis from remote sensing datasets. *Theoretical and Applied Climatology*, **89**(1-2): 95-107.
- Reed, B.C., Brown, J.F., VanderZee, D., Loveland, T.R., Merchant, J.W., Ohlen, D.O. 1994. Measuring phenological variability from satellite imagery. *Journal of Vegetation Science*, **5**(5): 703-714.
- Reynolds, J.F., Kemp, P.R., Ogle, K., Fernandez, R.J. 2004. Modifying the 'pulse-reserve' paradigm for deserts of North America: precipitation pulses, soil water, and plant responses. *Oecologia*, **141**(2): 194-210.
- Rodríguez-Iturbe, I., Porporato, A. 2004. *Ecohydrology of water-controlled ecosystems: Soil moisture and plant dynamics*. Cambridge Press. Cambridge, UK, 422 pp.
- Salinas-Zavala, C.A., Douglas, A.V., Diaz, H.F. 2002. Interannual variability of NDVI in northwest Mexico: Associated climatic mechanisms and ecological implications. *Remote Sensing of Environment*, **82**(2-3): 417-430.
- Sellers, P.J. 1985. Canopy reflectance, photosynthesis and transpiration. *International Journal of Remote Sensing*, **6**: 1335-1372.
- Seyfried, M.S, Murdock, M. 2004. Measurement of soil water content with a 50 MHz soil dielectric sensor. *Soil Science Society of America Journal*, **68**(2): 394-403.

- Sheppard, P.R., Comrie, A.C., Packin, G.D., Angersbach, K., Hughes, M.K. 2002. The climate of the US Southwest. *Climate Research*, **21**(3): 219-238.
- Tucker, C.J., Townsend, J.R.G., Goff, T.E. 1985. African land cover classification using satellite data. *Science*, **227**: 369-375.
- Vachaud, G., Passerat De Silans, A., Balanis, P., Vauclin, M. 1985. Temporal stability of spatially measured soil water probability density function. *Journal of the Soil Society of America*, **49**: 822-828.
- Vivoni, E.R., Gutiérrez-Jurado, H.A., Aragón, C.A., Méndez-Barroso, L.A., Rinehart, A.J., Wyckoff, R.L., Rodríguez, J.C., Watts, C.J., Bolten, J.D., Lakshmi, V. and Jackson, T.J. 2007. Variation of hydrometeorological conditions along a topographic transect in northwestern Mexico during the North American monsoon. *Journal of Climate*, **20**(9): 1792-1809.
- Vivoni, R.E., Gebremichael, M., Watts, J.C., Bindlish, R., Jackson, J.T. 2008. Comparison of ground-based and remotely-sensed surface soil moisture estimates over complex terrain during SMEX04. *Remote Sensing of Environment*, **112**(2): 314-325.
- Wang, J., Rich, P.M., Price, K.P. 2003. Temporal responses of NDVI to precipitation and temperature in the central Great Plains, USA. *International Journal of Remote Sensing*, **24**(11): 2345-2364.
- Wang, W., Anderson, T.B., Phillips, N., Kaufman, K.R., Potter, C., Myneni, B.R. 2006. Feedbacks of Vegetation on Summertime Climate Variability over the North American Grasslands. Part I: Statistical Analysis. *Earth Interactions*. **10**(17):1-27.

- Watts, C.J., Scott, R.L., Garatuza-Payan, J., Rodriguez, J.C., Prueger, J.H., Kustas, W.P., Douglas, M. 2007. Changes in vegetation condition and surface fluxes during NAME 2004. *Journal of Climate*, **20**(9): 1810-1820.
- Weiss, J.L., Gutzler, D.S., Coonrod, J.E.A., Dahm, C.N. 2004. Seasonal and inter-annual relations between vegetation and climate in central New Mexico, USA. *Journal of Arid Environments*, **57**(4): 507-534.
- Wittenberg, L., Malkinson, D., Beeri, O., Halutz, A., Tesler, N. 2007. Spatial and temporal patterns of vegetation recovery following sequences of forest fires in a Mediterranean landscape, Mt. Carmel Israel. *Catena*, **71**(1): 76-83.
- Xinmei, H., Lyons, T.J, Smith, R.C.G., Hacker, J.M., Schwerdtfeger, P. 1993. Estimation of surface energy balance from radiance surface temperature and NOAA-AVHRR sensor reflectances over agricultural and native vegetation. *Journal of Applied Meteorology*, **32**(8): 1441-1449.
- Zhang, P., Anderson, B., Barlow, M. 2004. Climate-related vegetation characteristics derived from Moderate Resolution Imaging Spectroradiometer (MODIS) leaf area index and normalized difference vegetation index. *Journal of Geophysical Research*, **109**(D20): D20105.
- Zhang, X., Friedl, M.A., Schaaf, C.B., Strahler, A.H., Hodges, J.C.F., Gao, F., Reed, B.C., Huete, A. 2003. Monitoring vegetation phenology using MODIS. *Remote Sensing of Environment*, **84**(3): 471-475.
- Zhu, C.M., Cavazos, T., Lettenmaier, D.P. 2007. Role of antecedent land surface conditions in warm season precipitation over northwestern Mexico. *Journal of Climate*, **20**(9): 1774-1791.

Figure Captions

Figure 1. Vegetation greening in the study region during (a) June 30, 2007 and (b) August 12, 2008. Note the mountainous terrain (~820 m) and the Sinaloan thornscrub ecosystem.

Figure 2. (a) Regional map showing the location of the Río San Miguel (3798 km²) and Río Sonora (11684 km²) basins in Sonora, Mexico. (b) Location of the 15 regional stations with precipitation and soil moisture observations. Note the elevation differences from 180 to 2618 m.

Figure 3. Determination of vegetation metrics. (a) Identification of the beginning and end of the vegetation greening using the smoothed NDVI series and the backward (BMA) and forward (FMA) moving averages for station 130 (Sinaloan thornscrub). The original NDVI data is represented by the open circles. (b) Example of the vegetation metrics (iNDVI, Δ NDVI, Rate of Greenup, Rate of Senescence and Duration of Greenness) for station 130 during the 2004 season.

Figure 4. Comparison of seasonal NDVI change (%). The percentage of NDVI change is calculated using the lowest and highest NDVI for a particular summer season (2004 to 2006). \overline{R}_s is the total summer rainfall (July to September) averaged over all regional stations.

Figure 5. Temporal variation of NDVI among different regional ecosystems: (a) Madrean evergreen woodland (station 146), (b) Sinaloan thornscrub (station 132), (c) Sonoran savanna grassland (station 139), and (d) Sonoran desert scrub (station 144). NDVI symbols correspond to the average value calculated in the 3 × 3 pixel region around each station for each composite. The vertical bars depict the ±1 standard deviation of the 3 × 3 pixel region. Precipitation (mm) is accumulated during 16-day intervals and shown as gray bars, while the averaged surface volumetric soil moisture (%) during the 16-day periods is shown as open circles.

Figure 6. Temporal and spatial RMSE (root mean square error) of the mean relative difference (δ) in the Río San Miguel and Río Sonora basins calculated during the study period.

Figure 7. Topographic control on vegetation metrics in the Río San Miguel transect. (a) Relation between elevation and temporal mean NDVI (closed circles) and the temporal standard deviation (± 1 std as vertical bars). (b) Relation between elevation and spatial and temporal RMSE δ .

Figure 8. Topographic control on vegetation metrics in the Río Sonora transect. (a) Relation between elevation and temporal mean NDVI (closed circles) and the temporal standard deviation (± 1 std as vertical bars). (b) Relation between elevation and spatial and temporal RMSE δ .

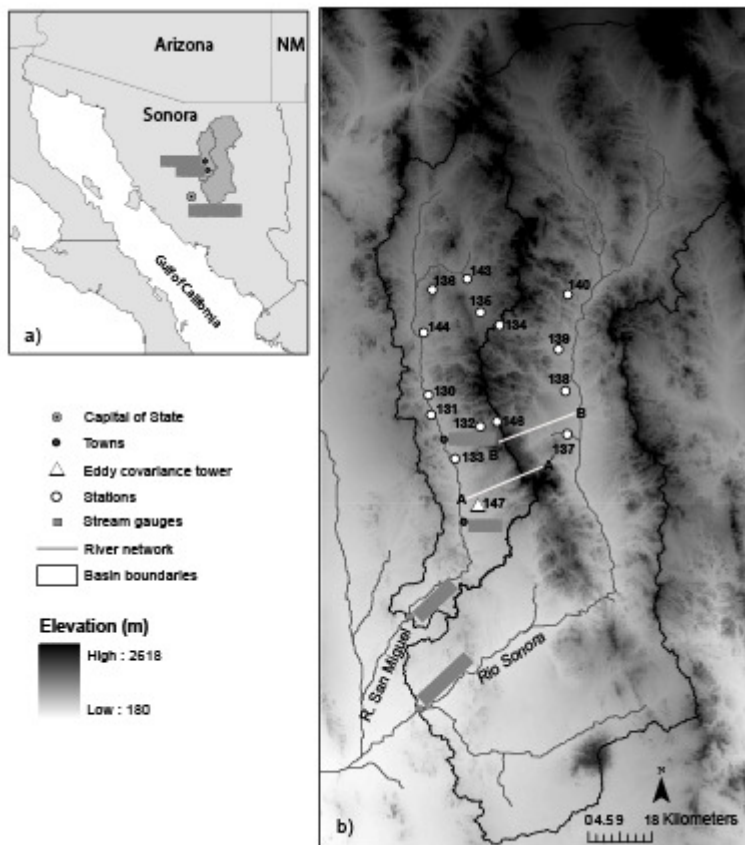
Figure 9. Relation between the seasonal precipitation accumulation and iNDVI for the monsoon season in 2005. Each point is a station located in a different ecosystem.

Figure 10. Distribution of greenness-precipitation ratio (GPR) at the stations in the Río San Miguel and Río Sonora basins. For reference, the spatial distribution of ecosystems as mapped by INEGI (Instituto Nacional de Estadística, Geografía e Informática) is shown.

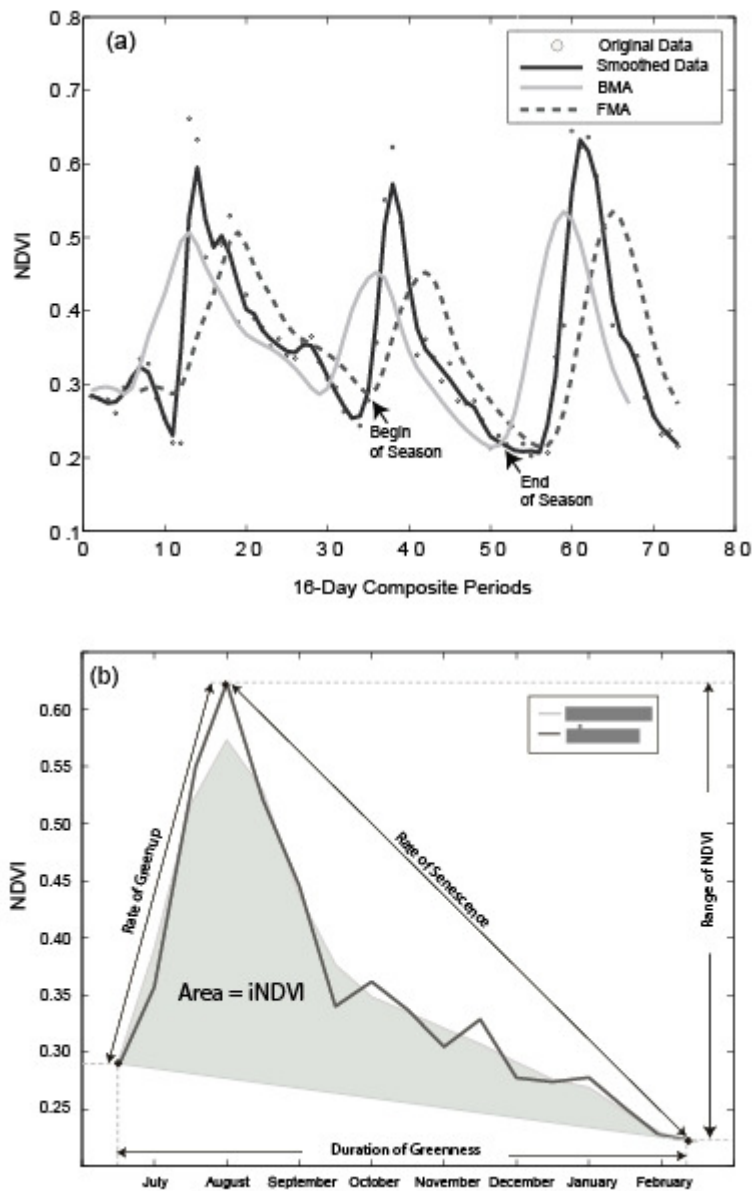
Figure 11. Linear correlation coefficients (CCs) between monthly NDVI and accumulated precipitation and averaged soil moisture over a range of different monthly lags, arranged from current (lag 0) toward longer prior periods (lag 0+1+2). CCs are shown as averages (symbols) and standard deviations (± 1 std as vertical bars) over all stations in 2005 (see Tables 6 and 7).



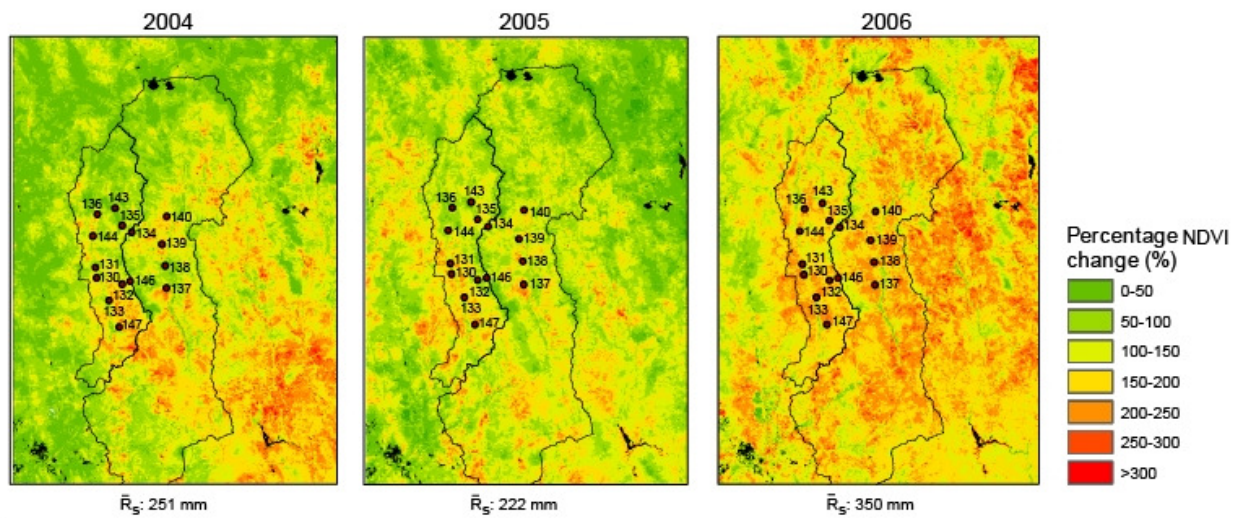
(Méndez-Barroso et al., Figure 1)



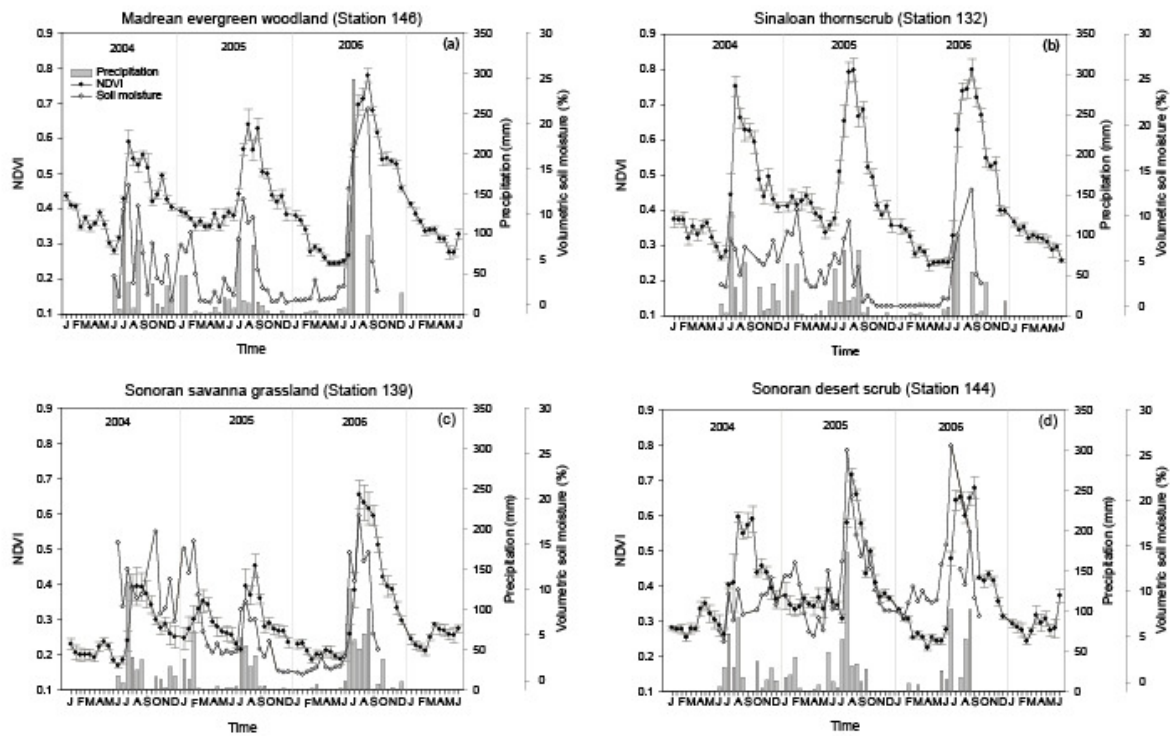
(Méndez-Barroso et al., Figure 2)



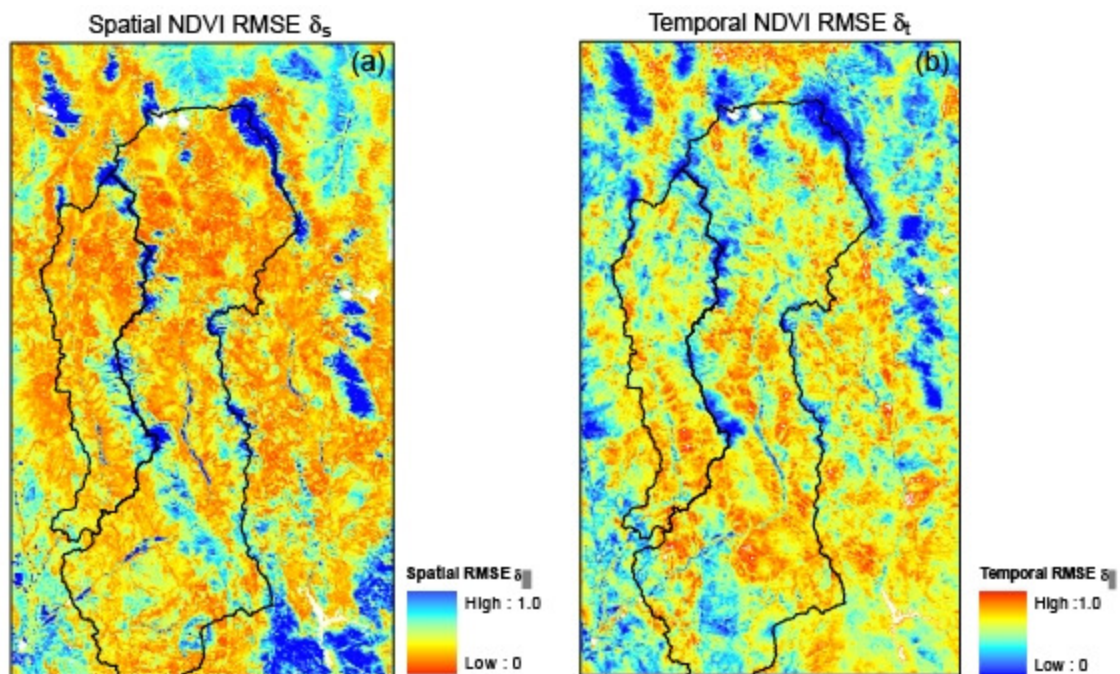
(Méndez-Barroso et al., Figure 3)



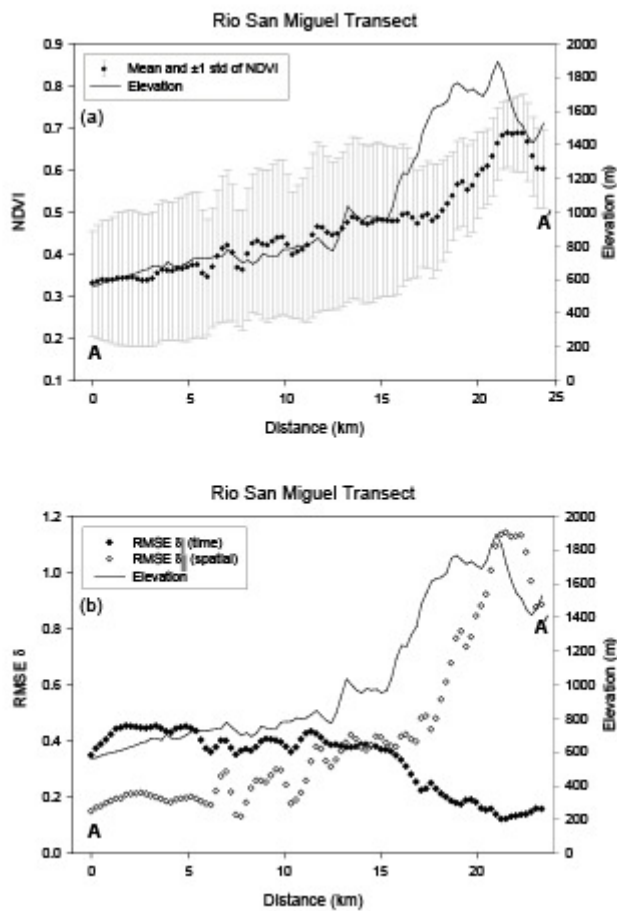
(Méndez-Barroso et al., Figure 4)



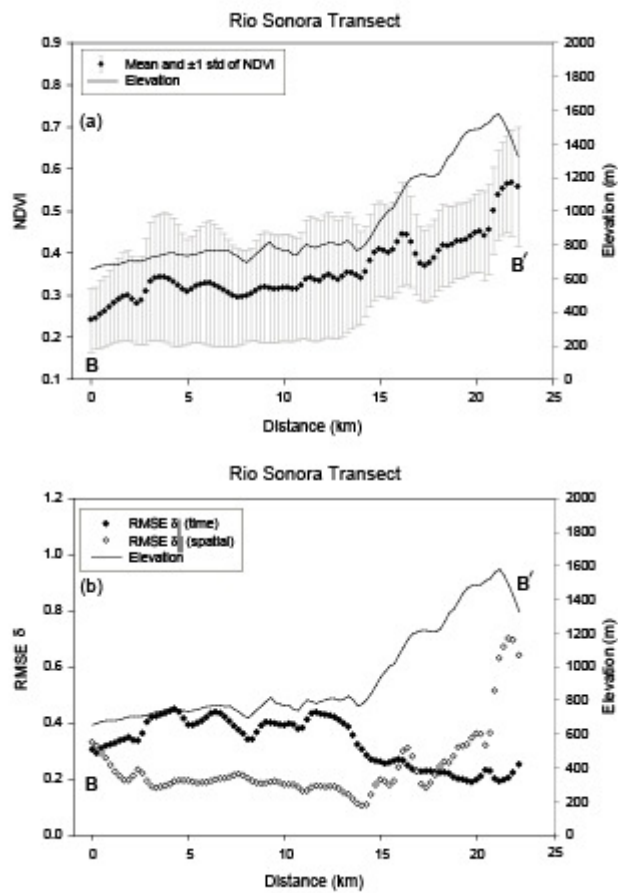
(Méndez-Barroso et al., Figure 5)



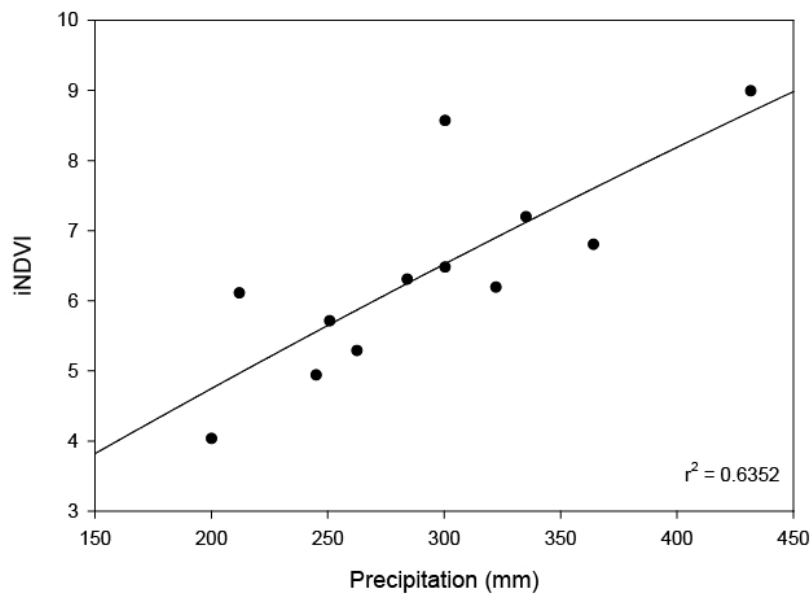
(Méndez-Barroso et al., Figure 6)



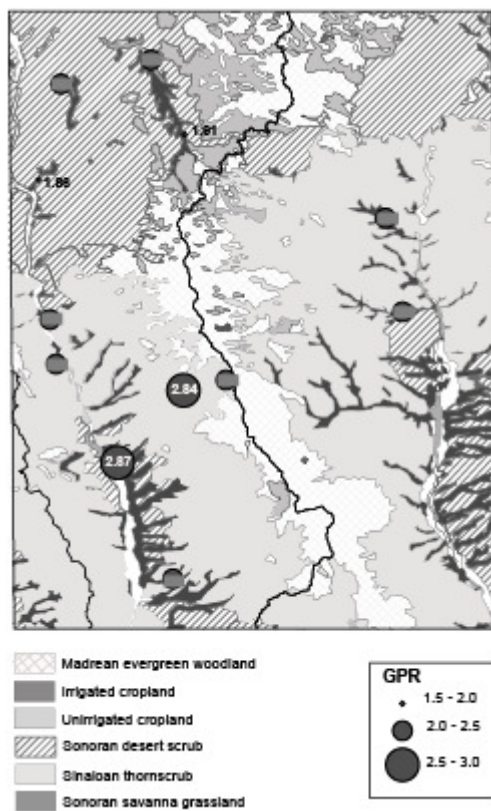
(Méndez-Barroso et al., Figure 7)



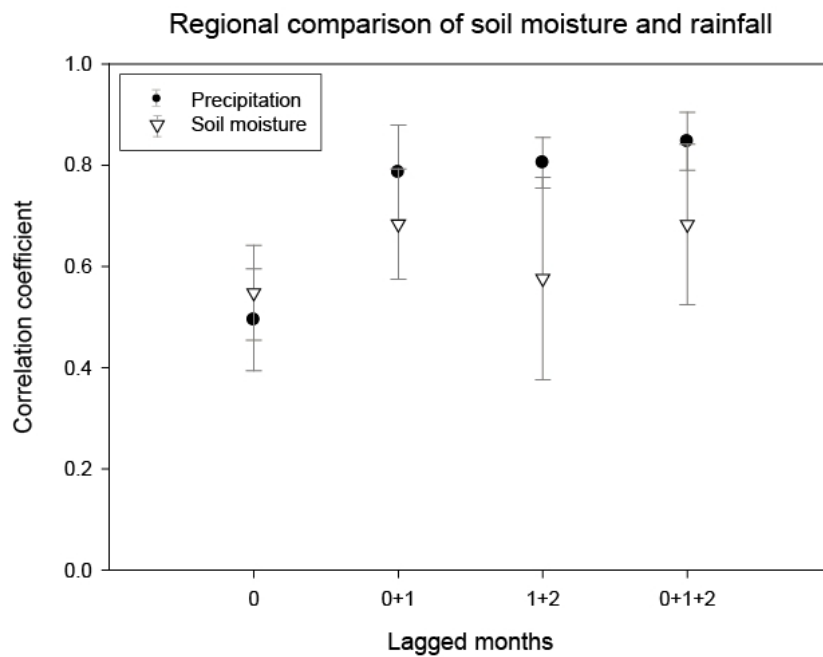
(Méndez-Barroso et al., Figure 8)



(Méndez-Barroso et al., Figure 9)



(Méndez-Barroso et al., Figure 10)



(Méndez-Barroso et al., Figure 11)

Table Captions

Table 1. Regional hydrometeorological station locations, altitudes and ecosystem classifications. The coordinate system for the locations is UTM 12N, datum WGS84.

Table 2. Missing observations periods at regional stations during 2004 to 2006. Note that the lower data gaps in the monsoon season of 2005.

Table 3. Comparison of vegetation metrics for the regional stations during the three monsoons.

Table 4. Coefficient of variation (CV) of vegetation metrics for different ecosystems during the period 2004-2006. CV is calculated as the temporal standard deviation divided by the temporal mean averaged over all stations in each ecosystem (N sites in each ecosystem).

Table 5. Comparison of iNDVI, precipitation (mm) and greenness-precipitation ratio (GPR) for the regional stations during 2005. Note that data gaps existed for stations 134 and 140.

Table 6. Linear correlation coefficients between NDVI and accumulated rainfall (mm) at different monthly lags. Precipitation was accumulated at lag 0: rainfall accumulated in the current month, 1: rainfall accumulated one month earlier, 2: two months earlier, 3: three months earlier, 0+1: accumulated rainfall in the current month plus the previous month, 1+2: two previous months, and 0+1+2: current and the two previous months.

Table 7. Linear correlation coefficients between NDVI and averaged surface soil moisture at different monthly lags. Soil moisture was averaged over lag 0: current month, 1: one month earlier, 2: two months earlier, 3: three months earlier, 0+1: current month plus the previous month, 1+2: two previous months, and 0+1+2: current plus the two previous months.

Station ID	Ecosystem	Easting [m]	Northing [m]	Altitude [m]
130	Sinaloan thornscrub	531465	3323298	720
131	Sinaloan thornscrub	532166	3317608	719
132	Sinaloan thornscrub	546347	3314298	900
133	Sinaloan thornscrub	539130	3305014	638
134	Madrean evergreen woodland	551857	3343293	1180
135	Sonoran riparian deciduous woodland	546349	3346966	1040
136	Sonoran desert scrub	532579	3353405	1079
137	Sonoran savanna grassland	571287	3312065	660
138	Sonoran savanna grassland	570690	3324453	726
139	Sonoran savanna grassland	568744	3336421	760
140	Sonoran savanna grassland	571478	3352076	1013
143	Sonoran riparian deciduous woodland	542590	3356533	960
144	Sonoran desert scrub	530134	3341169	800
146	Madrean evergreen woodland	551091	3315638	1385
147	Sinaloan thornscrub	544811	3290182	620

(Méndez-Barroso et al., Table 1)

Station ID	Start Date	End Date	Missing Data in 2004	Missing Data in 2005	Missing Data in 2006
130	06/14/2004	12/31/2006	09/12 - 10/16	–	07/08 - 08/08
131	06/14/2004	12/31/2006	09/12 - 10/16	07/30 - 08/15 12/16 - 12/31	01/01 - 01/08 03/16 - 03/27
132	06/14/2004	12/31/2006	09/12 - 10/16	03/18 - 03/29 07/30 - 08/15 12/29 - 12/31	01/01 - 01/08 03/16 - 03/27 07/27 - 09/03
133	06/14/2004	12/31/2006	09/12 - 10/16	–	07/28 - 08/10
134	06/13/2004	12/31/2007	09/11 - 10/17	03/19 - 03/30 06/06 - 06/12 10/21 - 10/22 12/29 - 12/31	01/01 - 01/07 03/15 - 03/26 07/26 - 08/24
135	06/22/2004	12/31/2006	09/11 - 10/16	01/10 - 01/20	07/26 - 08/08
136	05/07/2004	12/31/2006	09/11 - 10/26	01/10 - 01/20	07/26 - 08/08
137	05/26/2004	12/31/2006	09/11 - 10/17	03/19 - 03/20 05/03 - 10/17	07/10 - 08/18
138	05/22/2004	12/31/2006	08/04 - 08/09 09/11 - 10/17	03/19 - 03/20 10/21 - 11/17	07/26 - 08/08
139	05/22/2004	12/31/2006	09/11 - 10/26	01/10 - 01/20 10/21 - 11/17	07/26 - 08/08
140	05/22/2004	12/31/2006	09/11 - 10/26	01/10 - 01/20 03/19 - 03/20 10/21 - 11/17 11/17 - 12/31	01/01 - 03/15 07/26 - 08/28
143	05/13/2004	12/31/2006	09/11 - 10/26	–	07/26 - 08/08
144	05/22/2004	12/31/2006	09/12 - 10/16	–	07/06 - 08/08
146	05/14/2004	12/31/2006	09/12 - 09/22	07/30 - 08/15 12/29 - 12/31	01/01 - 01/08 03/16 - 03/27 07/07 - 09/03 10/08 - 10/24
147	07/17/2004	12/31/2006	07/17- 07/23	06/13 - 07/27 12/30 - 12/31	–

(Méndez-Barroso et al., Table 2)

Station ID	Year	iNDVI []	NDVI _{max} []	NDVI _{min} []	ΔNDVI []	Duration of Greenness [days]	Days to NDVI _{max} [days]
130	2004	5.72	0.66	0.22	0.44	208	32
	2005	5.70	0.62	0.21	0.41	256	48
	2006	6.36	0.64	0.21	0.43	256	64
131	2004	5.18	0.61	0.23	0.38	176	32
	2005	6.47	0.70	0.23	0.47	272	64
	2006	6.27	0.68	0.22	0.46	240	64
132	2004	5.86	0.75	0.28	0.47	176	32
	2005	8.56	0.80	0.27	0.53	288	64
	2006	8.68	0.80	0.25	0.55	272	80
133	2004	3.71	0.52	0.21	0.31	144	32
	2005	6.10	0.70	0.22	0.48	272	32
	2006	6.74	0.62	0.20	0.42	288	96
134	2004	4.91	0.49	0.27	0.22	192	64
	2005	6.07	0.53	0.25	0.28	272	48
	2006	6.18	0.58	0.24	0.34	256	80
135	2004	4.53	0.58	0.30	0.28	224	32
	2005	6.18	0.73	0.23	0.50	240	48
	2006	6.46	0.71	0.23	0.48	240	80
136	2004	7.57	0.60	0.24	0.36	272	64
	2005	7.19	0.73	0.23	0.50	304	80
	2006	6.53	0.71	0.21	0.50	272	64
137	2004	2.74	0.52	0.19	0.33	128	48
	2005	4.93	0.56	0.21	0.35	256	48
	2006	6.10	0.63	0.19	0.44	240	48
138	2004	2.91	0.42	0.23	0.19	144	32
	2005	4.93	0.58	0.21	0.37	240	32
	2006	6.21	0.67	0.19	0.48	224	48
139	2004	2.93	0.39	0.19	0.20	144	48
	2005	4.02	0.45	0.19	0.26	224	48
	2006	5.91	0.65	0.19	0.46	224	48
140	2004	4.78	0.60	0.23	0.37	176	32
	2005	5.49	0.56	0.23	0.33	256	48
	2006	7.08	0.69	0.21	0.48	272	64
143	2004	3.61	0.58	0.28	0.30	144	32
	2005	5.28	0.58	0.24	0.34	224	80
	2006	6.31	0.69	0.20	0.49	304	96
144	2004	5.85	0.60	0.26	0.34	208	48
	2005	6.79	0.72	0.23	0.49	256	48
	2006	6.87	0.68	0.24	0.44	240	96
146	2004	6.78	0.59	0.32	0.27	240	32
	2005	7.48	0.64	0.28	0.36	272	48
	2006	8.69	0.78	0.36	0.42	272	80
147	2004	5.48	0.54	0.19	0.35	240	32
	2005	6.29	0.66	0.20	0.46	336	112
	2006	7.02	0.66	0.19	0.47	288	96

(Méndez-Barroso et al., Table 3)

Ecosystem	Coefficient of Variation (CV)						
	N	iNDVI	NDVI _{max}	NDVI _{min}	ΔNDVI	Duration of Greenness	Days to NDVI _{max}
Madrean evergreen woodland	2	0.19	0.17	0.15	0.22	0.13	0.33
Sinaloan thornscrub	5	0.20	0.12	0.12	0.14	0.21	0.47
Sonoran savanna grassland	4	0.30	0.17	0.09	0.28	0.24	0.20
Sonoran desert scrub	2	0.09	0.35	0.35	0.30	0.41	0.46
Sonoran riparian deciduous forest	2	0.21	0.26	0.30	0.31	0.41	0.50

(Méndez-Barroso et al., Table 4)

Station ID	iNDVI []	Precipitation [mm]	GPR [cm⁻¹]
130	5.70	251.21	2.27
131	6.47	300.74	2.15
132	8.55	300.74	2.85
133	6.10	212.34	2.87
135	6.18	322.58	1.92
136	7.19	335.50	2.14
138	4.93	245.36	2.01
139	4.02	200.40	2.01
143	5.28	262.89	2.01
144	6.79	364.49	1.86
146	8.98	432.05	2.08
147	6.30	284.50	2.21

(Méndez-Barroso et al., Table 5)

Station ID	NDVI and Precipitation Correlation Coefficients						
	Monthly Lags						
	0	1	2	3	0+1	1+2	0+1+2
130	0.442	0.836	0.387	0.172	0.784	0.749	0.843
131	0.465	0.824	0.704	0.247	0.727	0.872	0.874
132	0.494	0.770	0.553	0.199	0.721	0.741	0.805
133	0.477	0.885	0.537	-0.004	0.807	0.876	0.885
135	0.559	0.800	0.407	0.032	0.831	0.745	0.847
136	0.580	0.828	0.361	0.127	0.900	0.790	0.859
143	0.495	0.781	0.532	0.151	0.819	0.822	0.903
144	0.314	0.812	0.415	0.432	0.735	0.805	0.789
146	0.429	0.800	0.571	0.340	0.608	0.844	0.736
147	0.691	0.868	0.347	-0.072	0.927	0.802	0.928

(Méndez-Barroso et al., Table 6)

Station ID	NDVI and Soil Moisture Correlation Coefficients						
	Monthly Lags						
	0	1	2	3	0+1	1+2	0+1+2
130	0.450	<i>0.706</i>	0.344	0.080	0.675	0.612	0.700
131	0.406	<i>0.828</i>	0.631	0.153	0.672	0.818	0.803
132	0.435	0.627	0.557	0.381	0.572	<i>0.631</i>	0.616
133	0.673	0.720	0.274	-0.200	<i>0.781</i>	0.584	0.752
135	<i>0.582</i>	0.381	-0.174	-0.421	0.537	0.120	0.347
136	0.548	0.454	0.093	-0.040	<i>0.554</i>	0.381	0.528
143	0.683	0.778	0.381	-0.008	0.877	0.677	<i>0.881</i>
144	0.572	0.766	0.351	0.154	<i>0.769</i>	0.635	0.754
146	0.542	0.790	0.505	0.229	0.717	0.765	<i>0.819</i>
147	0.589	0.655	0.293	-0.063	<i>0.684</i>	0.541	0.629

(Méndez-Barroso et al., Table 7)

APPENDIX 9: DESERT SURVIVAL PRIMER

Desert Survival Primer: Safety from the Heat

Prevention of Heat Stroke and Dehydration in Desert Conditions:

- Loose-fitting and light colored clothing
- Long-sleeves shirts and pants
- Sunglasses
- Sunscreen
- Large brimmed hat
- Sufficient water!!! (at least a gallon of water for ea. person) and Gatorade – or some other way of replacing electrolytes
- Avoid tea, coffee, soda and alcohol as these can lead to dehydration
- Schedule vigorous activity and sports for cooler times of the day
- First aid / survival kit
- Sharp knife

Hot Weather Conditions

During hot weather, walk through the desert slowly and rest for 10 minutes every hour. Begin early in the morning or late in the day. Water and body temperature are critical to survival. A person requires about a gallon of water each day. Be sure extra drinking water is available as it may be the difference between life and death.

To reduce water loss, keep the mouth closed, breathe through the nose and avoid conversation. Do not drink alcohol. It causes dehydration. Digestion consumes water so don't eat food if there is not a sufficient amount of water available. Don't ration water in hot weather. When you are thirsty, drink. Conserve water as best as possible and look for more.

In the summer, ground temperatures can be 30 degrees hotter than the surrounding air temperature, so, when resting, sit at least 12 inches above the ground on a stool or a branch.

Body temperature is absorbed in three ways: from direct sunlight, hot air and heat reflected from the ground. Stay in the shade and wear clothing, including shirt, hat and sunglasses. Clothing helps retain sweat by slowing evaporation and prolonging the cooling effect. Travel at night or early in the day if possible.

Water sources can be located at the base of rock cliffs or in the gravel wash from mountain valleys, especially after a recent rain. Water may be found by digging three to six feet at the outside edge of a sharp bend in a dry stream bed. If wet sand is found, dig down into it to find seeping water. Green vegetation, tree clusters and other "indicator" shrubbery, such as cottonwood, sycamore, willow or tamarisk trees, may indicate the presence of water. Animal paths and flocks of birds also may lead you to water.

Cactus fruit and flowers may be eaten when food or water is scarce. Split open the base of cactus stalks and chew on the pith...but don't swallow it. Carry chunks of pith to alleviate thirst while walking. Other desert plants are not edible

Heat Exhaustion

Heat exhaustion is a milder form of heat-related illness that can develop after several days of exposure to high temperatures and inadequate or unbalanced replacement of fluids. Those most prone to heat exhaustion are elderly people, people with high blood pressure, and people working or exercising in a hot environment.

Signs of Heat Exhaustion

Warning signs of heat exhaustion include:

- Heavy sweating
- Paleness
- Muscle cramps
- Tiredness
- Weakness
- Dizziness
- Headache
- Nausea or vomiting
- Fainting

The skin may be cool and moist. The victim's pulse rate will be fast and weak, and breathing will be fast and shallow. If heat exhaustion is untreated, it may progress to heat stroke. Seek medical attention immediately if:

- Symptoms are severe, or
- The victim has heart problems or high blood pressure.

Otherwise, help the victim to cool off, and seek medical attention if symptoms worsen or last longer than 1 hour.

Heat Exhaustion: What to Do

Cooling measures that may be effective include:

- Cool, non-alcoholic beverages, as directed by your physician
- Rest
- Cool shower, bath, or sponge bath
- An air-conditioned environment
- Lightweight clothing

Dehydration can be a serious heat-related disease, as well as being a dangerous side-effect of diarrhea, vomiting and fever. Children and persons over the age of 60 are particularly susceptible to dehydration.

Dehydration

Under normal conditions, we all lose body water daily through sweat, tears, urine and stool. In a healthy person, this water is replaced by drinking fluids and eating foods that contain water. When a person becomes so sick with fever, diarrhea, or vomiting or if an individual is overexposed to the sun, dehydration occurs. This is caused when the body loses water content and essential body salts such as sodium, potassium, calcium bicarbonate and phosphate. Occasionally, dehydration can be caused by drugs, such as diuretics, which deplete body fluids and electrolytes. Whatever the cause, dehydration should be treated as soon as possible.

Symptoms of Dehydration

The following are the most common symptoms of dehydration, although each individual may experience symptoms differently. Symptoms may include:

- Thirst
- Less-frequent urination
- Dry skin
- Fatigue
- Light-headedness
- Dizziness
- Confusion
- Dry mouth and mucous membranes
- Increased heart rate and breathing

Dehydration: What to do

In cases of mild dehydration, simple rehydration is recommended by drinking fluids. Many sports drinks on the market effectively restore body fluids, electrolytes, and salt balance. For moderate dehydration, intravenous fluids may be required, although if caught early enough, simple rehydration may be effective. Cases of serious dehydration should be treated as a medical emergency, and hospitalization, along with intravenous fluids, is necessary. Immediate action should be taken.

Heat Stroke

Our bodies produce a tremendous amount of internal heat and we normally cool ourselves by sweating and radiating heat through the skin. However, in certain circumstances, such as extreme heat, high humidity or vigorous activity in the hot sun, this cooling system may begin to fail, allowing heat to build up to dangerous levels. If a person becomes dehydrated and cannot sweat enough to cool their body, their internal temperature may rise to dangerously high levels, causing heat stroke.

Symptoms of Heat Stroke

The following are the most common symptoms of heat stroke, although each individual may experience symptoms differently. Symptoms may include:

- Headache
- Agitation
- Strange behavior
- Difficulty breathing
- High body temperature
- Dizziness
- Disorientation, agitation or confusion
- Sluggishness or fatigue
- Seizure
- Coma
- Dry skin that is flushed but not sweaty
- High body temperature
- Loss of consciousness
- Rapid heart beat
- Hallucinations

Heat Stroke: What to Do

It is important for the person to be treated immediately as heat stroke can cause permanent damage (organ damage) or death. There are some immediate first aid measures you can take while waiting for help to arrive.

- ***First and foremost, cool the victim.*** Get the victim to a shady area or indoors.
- Get the person indoors.
- Remove clothing and gently apply cool water to the skin followed by fanning to stimulate sweating (for example you may spray the victim with cool water from a garden hose).
- Apply ice packs to the groin and armpits.
- Have the person lie down in a cool area with their feet slightly elevated
- Monitor body temperature with a thermometer and continue cooling efforts until the body temperature drops to 101-102 degrees.
- Always notify emergency services (such as - 911) immediately. If their arrival is delayed, they can give you further instructions for treatment of the victim.

Intravenous fluids are often necessary to compensate for fluid or electrolyte loss. Bed rest is generally advised and body temperature may fluctuate abnormally for weeks after heat stroke.

References:

http://www.medicinenet.com/heat_exhaustion/article.htm
<http://www.medicinenet.com/dehydration/article.htm>
http://www.medicinenet.com/heat_stroke/article.htm

Desert Survival Primer: Emergency Situations

In an emergency situation follow ABC's:

- Accept the situation. Do not blame yourself or others.
- “Brew a cup of tea.” As in start a fire, complete something familiar, a calming chore.
- Consider options. Take stock of items on hand, i.e., water reserves, first-aid kit, etc.
- Decide on a plan that best ensures safety.
- Execute the plan and stick with it unless new conditions warrant.

Desert Survival Priorities

Water

Learn to locate water through areas of green vegetation, flights of birds, converging animal trails and digging in the outside bends of dry creek beds. Burros and other animals are excellent at finding water and digging it up in creek.

Fire

Fire can be used to signal, cook food and purify water. Fire also provides psychological comfort.

Shelter

Aside from your clothes, additional shelter may be needed. In desert areas, shelter from the sun is usually the main consideration, but cold, rain, hail, even snow can also be factors. It is important to keep the skin temperature under 92 degrees F, to keep from sweating away precious water. Draping a sleeping bag over a bush for shade, while allowing for breezes, may be the best bet. Try not to sit on the hot ground, even if it means tearing the seats out of your brand new 4x4. Try to make shelter visible to searchers. Build shelter in a safe place, such as out of creek beds which can flash flood.

Food

In hot climates, however, food is not as important as other factors. If water is in short supply it is important not to eat *anything* because it increases your water needs to digest

Text by David Alloway from <http://www.desertusa.com/mag99/mar/stories/desertsur.html>

Other

IF YOU BECOME LOST

If you become lost while hiking on foot or traveling by vehicle, stay put! Sit down for a while and take stock of the situation. Stay with your vehicle if you came in one. Most lost or stranded victims would be rescued sooner if they resisted the urge to walk for help. It is better to conserve energy and prepare distress signals.

If you feel you can retrace your steps, mark your spot and leave a note. Then backtrack by following footprints or vehicle tracks. Consult a map and try to identify landmarks and other surroundings. Don't take shortcuts. Go to a high point and look around. Always move downstream or down country, but travel the ridges instead of washes or valleys.

Move with a purpose. Don't wander aimlessly. If you aren't absolutely sure you can follow your tracks or prints, stay put!

Reference:

<http://www.phoenix.gov/fire/desert.html>

Desert Survival Primer: Snake Bites

Snake Bites

The danger of snake bites:

Each year, nearly 8,000 people receive poisonous snake bites in the United States. Even a bite from a so-called "harmless" snake can cause infection or allergic reaction in some people. People who frequent wilderness areas, camp, hike, picnic, or live in snake-inhabited areas should be aware of the potential dangers posed by venomous snakes.

What snakes cause poisonous bites?

Any of the following snakes cause poisonous bites:

- Rattlesnake
- Copperhead
- Cottonmouth Water Moccasin
- Coral Snake

What are the symptoms of poisonous bites?

While each individual may experience symptoms differently, the following are the most common symptoms of poisonous snake bites:

- Bloody wound discharge
- Fang marks in the skin and swelling at the site of the bite
- Severe localized pain
- Diarrhea
- Burning
- Convulsions
- Fainting
- Dizziness
- Weakness
- Blurred vision
- Excessive sweating
- Fever
- Increased thirst
- Loss of muscle coordination
- Nausea and vomiting
- Numbness and tingling
- Rapid pulse

How are snake bites treated?

Call for emergency assistance immediately if someone has been bitten by a snake. Responding quickly in this type of emergency is crucial. While waiting for emergency assistance:

- Wash the bite with soap and water.
- Immobilize the bitten area and keep it lower than the heart.
- Cover the area with a clean, cool compress or a moist dressing to minimize swelling and discomfort.
- Monitor vital signs.

If a victim is unable to reach medical care within 30 minutes, the American Red Cross recommends:

- Apply a bandage, wrapped two to four inches above the bite, to help slow the venom. This should not cut off the flow of blood from a vein or artery - the band should be loose enough to slip a finger under it.
- A suction device can be placed over the bite to help draw venom out of the wound without making cuts. These devices are often included in commercial snake bite kits.

Most often, physicians use antivenin -- an antidote to snake venom -- to treat serious snake bites. Antivenin is derived from antibodies created in a horse's blood serum when the animal is injected with snake venom. Because antivenin is obtained from horses, snake bite victims sensitive to horse products must be carefully managed.

Preventing snake bites:

Some bites, such as those inflicted when you accidentally step on a snake in the woods, are nearly impossible to prevent. However, there are precautions that can reduce your chances of being bitten by a snake. These include:

- Leave snakes alone. Many people are bitten because they try to kill a snake or get too close to it.
- Stay out of tall grass unless you wear thick leather boots and remain on hiking paths as much as possible.
- Keep hands and feet out of areas you cannot see. Do not pick up rocks or firewood unless you are out of a snake's striking distance.
- Be cautious and alert when climbing rocks.

References:

http://www.umm.edu/non_trauma/snake.htm

Desert Survival Primer: Scorpion Stings

Scorpion Stings

The danger of scorpion stings:

Of the more than 1,000 species of scorpions worldwide, only 30 carry a toxin that may be fatal in humans. In the U.S., the rate is very low: one death from a scorpion sting occurs on average every two to three years. In Mexico, there are a reported 1,000–2,000 deaths per year. Because of their size and ability to travel in shoes and luggage, scorpions are found in many parts all over the world, having arrived as stowaways. Scorpions are nocturnal, typically emerging only at night. They are commonly found in cupboards, closets, in shoes, and under beds. Scorpions sting with a poisoned hook on the tail, which is raised prior to an attack.

Scorpions sting; they do not bite, although they can pinch. All scorpions are venomous, but most are harmless to humans. In general, the smaller the species, the more dangerous it is for humans (of course, it is hard to tell juveniles of a large species from adults of a small species). Bark Scorpions are the main problem because their stings can be deadly, and this scorpion is found in

Mexico and the southwestern United States. However, the stings of other species are not serious and usually result in localized pain with some swelling and tenderness. Some people, however, are allergic to scorpion venom and may show more serious reactions.

What are the symptoms of a scorpion sting?

Being infected by scorpion venom results in a local reaction that, while painful, it is easily treated with analgesics, antihistamines, ice, and supportive care. Most scorpion venom destroys red blood cells, producing localized discoloration at the sting site and painful swelling. Symptoms include:

- Moderate to severe pain
- Numbness, or tingling in the area around the sting
- Nausea or vomiting is not uncommon

In more serious stings, pain and tingling may be followed by:

- Marked changes in blood pressure (high or low)
- High fever
- Difficulty breathing
- Restlessness
- Rotary or roving eye movements
- Involuntary muscle spasms
- Difficulty swallowing, excessive salivation
- Blurred vision

Shock or respiratory arrest may ensue without prompt medical intervention.

Bark Scorpion venom is a neurotoxin, and causes little swelling and discoloration. Symptoms of Bark Scorpion venom include:

- Restlessness
- Convulsions
- Staggering gait
- Thick tongue sensation
- Slurred speech
- Drooling, excessive
- Sensitivity of skin
- Muscle twitches
- Abdominal pain and cramps
- Respiratory depression

These symptoms usually subside within 48 hours, but should be treated by a doctor.

What is the treatment for scorpion stings?

- Clean the location of the sting using soapy water, and dry the area gently.
- Elevate the injured limb at or above the heart.
- Icing may limit pain to the wound.
- Analgesics such as Tylenol or Ibuprofen may be taken for minor pain. Intravenous or intramuscular injections of meperidine (Demerol) or morphine may be used if the pain is severe.
- Calcium gluconate (10 ml of 10% solution) may be given intravenously for muscle spasms.
- Valium may be given intravenously for anxiety and restlessness.

As to antivenom, this is available in most Mexican hospitals for more serious stings. There is always the possibility of a severe allergic reaction to the antivenom; thus, it must be administered by a physician in a hospital setting. The antivenom is primarily used for severe reactions to the venom of the *Centruoides Exilicauda* scorpion, a small, light brown, inch-long creature also known as a “Bark Scorpion.” This scorpion is found in Mexico and the southwestern United States.

How can I Avoid Getting Stung By a Scorpion?

- Wear shoes when walking outside at night. If scorpions are suspected indoors, wear shoes inside at night as well.
- Wear leather gloves when moving rocks, boards, and other debris.
- Shake out shoes or slippers before they are worn, and check beds before they are used.
- Shake out damp towels, washcloths, and dishrags before use.
- When camping, shake out sleeping bags, clothes, and anything else that has been in contact with the ground before use.
- If you are afraid of scorpions getting into your bed, put the legs of your bed into glass containers. Scorpions are unable to gain traction on glass surfaces. Also, make sure your bedding doesn't touch the floor.

References:

<http://www.medtogo.com/scorpion-stings.html>

<http://www.birdandhike.com/Wildlife/Invert/Scorpion/Scorp/Scorp.htm>

http://www.cdpr.ca.gov/cfdocs/apps/schoolipm/managing_pests/gdebook/scorpion.pdf

http://www.associatedcontent.com/article/18030/facts_and_information_on_scorpions.html?page=3&cat=5

Desert Survival Primer: Sunburns and Sun Safety

Sunburns

Excessive UVA and UVB energy from the sun causes the skin to burn, which can lead to pain and discomfort that will interfere with a fun vacation. The darker your skin is naturally, the more you are protected, but even very dark-skinned people can get sunburned. People with fair skin or many moles must be especially careful, as they are at an increased risk for developing skin cancer.

Don't be fooled by the clouds overhead or the cool breeze. UV light easily penetrates most cloud coverage, and a cool breeze can fool you into thinking you're not getting much sun.

Important note: if you have sensitive skin, avoid sunscreens with PABA, a common ingredient that can cause irritation; instead try a formulation with titanium dioxide (a non-irritating, non-chemical compound).

The Dangers of Sunburns:

- Premature and accelerated skin aging: age spots, wrinkles
- Aggravation of existing or underlying skin disorders: eczema, rosacea, psoriasis
- Dehydration
- Photosensitivity / photoreactions
- Second-degree burns
- Secondary infection
- Shock (such as from massive fluid loss)
- Death

Long-term complications may include:

- Pre-cancerous growths
- Skin cancer

Additional studies show UV rays' connection to:

- Cataracts, corneal burns, macular degeneration, and other ocular disorders

What is the Treatment for Sunburns?

Sunburns accompanied by dizziness, fever, severe blistering, and other symptoms are considered serious and require medical attention. Less severe burns can be painful, itchy, and make your skin feel tight. Take a cool (not cold) bath or apply cool compresses to relieve the pain. Ibuprofen (Motrin), aspirin, or acetaminophen (Tylenol) can help, if you have no contraindications for their use. Apply an aloe vera gel or a topical moisturizing cream to reduce the burning and drying that comes with bad sunburn. If you have a bad burn that is very itchy, you may get some relief from 1% hydrocortisone cream or topical sunburn relief products such as Solarcaine.

How can I Prevent Myself from Getting a Sunburn?

Following careful guidelines can help you reduce your risk. The best way to prevent sunburn is to always wear sunscreen with SPF protection. The higher the SPF, the more protection you get. To calculate the amount of protection you will get from sunscreen, multiply the amount of time it normally takes you to get sunburned by the SPF of the sunscreen.

Therefore, if you normally burn in 20 minutes and you wear SPF 20 sunscreen, you will be protected for 20 minutes x 20 SPF, or 400 minutes (6.67 hours).

Despite this formulation, weather conditions, sweating, and activity can reduce the effectiveness any sunscreen, so be sure to reapply after two or three hours.

You can also take additional measures, such as wearing protective clothing and sunglasses, staying in the shade, and avoiding sun during its most powerful hours from 11am to 3pm. Excessive and repeated sun exposure can also damage the cornea of the eye and lead to early cataract formation.

References:

<http://www.medtogo.com/sunburn-sun-safety.html>

<http://www.get-healthyfit.com/allergy/the-dangers-of-sunburn-are-far-more-than-cosmetic.html>

Desert Survival Primer: Traveler's Diarrhea

Traveler's Diarrhea

What Is It?

Traveler's Diarrhea (TD) is defined as three to four loose stools in a 24-hour period. Diarrhea when traveling to a foreign country is common, with a reported 40 percent of travelers affected who stay at least one week in Mexico. This rises to 60 percent if tourists stay for more than five weeks.

Recent studies have shown that 5–10 percent of travelers who experience a bout of TD do not improve with treatment and develop a chronic condition known as “irritable bowel syndrome”

(IBS). Because of the increased risk of developing IBS after TD, there is even more reason to prevent TD.

Many environmental or infectious factors can contribute to or cause diarrhea. The body's immune system responds to disease-causing bacteria by increasing fluid production, resulting in diarrhea. In most persons in high-risk areas, the illness rapidly resolves, offering short-term immunity from the most common causes of TD. Keep up your fluid and salt intake by drinking soups, broth, and soft drinks and eating saltine crackers. Most cases of simple TD resolve in about 48 hours.

What are the Associated Symptoms?

Symptoms of TD are three or four loose stools daily, nausea, vomiting, abdominal pain and cramps, low-grade fever, and exhaustion. These symptoms are generally benign—dehydration is our main concern.

Should you see bloody stools and experience fever and abdominal cramps, you probably have a more serious and invasive bacterial diarrhea known as “dysentery.” If some bacteria or their toxins enter the bloodstream, you may experience chills, sweats, and/or fever greater than 101.5° F.

Infections with shigella, salmonella, or campylobacter may result in forms of more serious diarrhea, or dysentery, that call for specific treatments and precautions. If you have blood in the stool, fever, chills or sweats associated with TD you will need to receive absorbable antibiotics for three days. Any such diarrhea that does not respond to treatment within 48 hours should be considered reason to seek medical attention.

Also, see a doctor if TD persists for longer than one month.

What Causes It?

Contaminated food and water are the sources of bacterial, viral, and even parasitic infections. Although many Mexican communities tout clean public water systems, bacteria can be found in them during the rainy season. Food is an even more important source of the bacteria that cause diarrhea in international visitors.

The most dangerous foods are those containing moisture that are served at room temperature, such as salads, and uncooked vegetables. Others include usually “safe” foods that are steaming hot, dry items like bread, jelly, jam, honey and syrups (with high sugar content), and any fruit or vegetable that has been peeled.

Non-infectious factors may influence the gastrointestinal tract and cause loose stools. These include:

- Alcohol consumption
- Tobacco use

- Dietary indiscretions
- Dairy foods for lactose-intolerant individuals
- Jet lag
- Fatigue
- Stress and anxiety
- Certain medications

How Can TD be Prevented?

Since contaminated foods and water are the primary source of intestinal illness while traveling, taking certain steps may help you to avoid exposure:

- First, never eat anything raw that you have not peeled yourself. All types of raw food, including salads and uncooked vegetables and fruits are often contaminated. Raw shellfish or sushi can be infected with parasites if not inspected properly. Do not eat food from street vendors.
- Second, don't use tabletop salsa as your condiment. Studies have shown that up to 75 percent of tabletop salsas left out in restaurants are contaminated with infectious e.coli.
- Third, drink only bottled, purified water that has a sealed cap. If purified water is not available, boil it for at least one minute or treat it with iodine or chlorine tablets or liquid that can be purchased at most stateside pharmacies or sporting goods stores.
- Finally, studies have shown that you can prevent TD by taking daily rifaximin (Xifaxan) or bismuth subsalicylate (Pepto-Bismol). We do not recommend that you take other common antibiotics (Ciprofloxin, Bactrim DS, or Ampicillin) for prevention, as antibiotic overuse has led to unwanted side effects and bacterial resistance, making many common antibiotics useless in diarrhea treatment.

What is the Treatment for TD?

If you don't have fever, chills, or blood in the stool, your main concern with diarrhea treatment is to avoid dehydration. This is especially true with very small children, especially infants, or with the elderly and/or debilitated. Dehydration is poorly tolerated in adults with heart conditions or on multiple medications used to treat the kidneys or the heart. If your diarrhea is significant and you are in a higher risk category, seek medical attention as a precaution.

For adults or larger children (over two years of age), ORS may be used, but it may be more cost-effective to use a soup broth or water and saltine crackers. Homemade ORS can be made with a liter of cooled, boiled water mixed with 6 teaspoons of sugar and one teaspoon of salt. If nausea and vomiting are present and the individual cannot hold down the solution, see a doctor.

If you have fever or bloody diarrhea, you need antibiotics such as ciprofloxin, levofloxin or azithromycin, which are effective in most of these cases, although antibiotic resistance is on the rise. Xifaxan is effective in treating the more common form of TD not

associated with fever or passage of bloody stools, but should not be used if you developed diarrhea while taking Xifaxan for prevention.

References:

<http://www.medtogo.com/travelers-diarrhea.html>

APPENDIX 10: MEDICAL CARE SERVICES

Emergency numbers

Ambulance: 065

Fire: 068

Police: 060

Hermosillo Doctors

CANALE, Jesus Manuel Dr. Cardiology

Hospital CIMA Internal Medicine

Clinica del Noroeste

Av. Juarez y L.D. Colosio

83000 Hermosillo, Sonora

PH: (662) 212-1857, Fax: (662) 212-1890

E-Mail: jcanale@infosel.net.mx

and: jcanale@hmo.megared.net.mx

Languages: Spanish, English-2

DE LEON CABALLERO, Roberto Dr. Pathology

Laboratorio de Patologia

Juarez #118-2

Hermosillo, Sonora, Mexico

Phone/Fax: (662) 217-2439

Languages: Spanish, English-2

GUDINO AGUILAR, Cesar Manuel Dr. Cardiology

Hospital Cima

Hermosillo, Sonora, Mexico

Phone: (662) 217-1357, 259-0959 Fax: (662) 259 0955

Languages: Spanish, English-2

MOJARRA ESTRADA, Jose Maria Dr. Obstetrics & Gynecology

Hospital CIMA Reproduction

Paseo Rio San Miguel #35-115 Endocrinology

83280 Hermosillo, Sonora Infertility

PH: (662) 259-0959, 259-0956; Fax: (662) 259-0943

E-Mail: jmojarra@rtn.uson.mx

Languages: Spanish, English-3

MORENO MATIELLA, Romeo Dr. Dentistry

Olivares #142

Colonia Valle Grande

Hermosillo, Sonora, Mexico

Phone: (662) 218-7790 Fax: (662) 216-6505

Languages: Spanish, English-2

HERMOSILLO DOCTORS (Cont.)

OLIVAS ROBLES LINARES, Jose Arturo Dr. Orthopedics

Av. Juarez y Luis Donaldo Colosio Traumatology

Hermosillo, Sonora, Mexico

Phone: (662) 213-6251, Fax: (662) 212-1890

E-Mail: arturoolivas@hotmail.com

Languages: Spanish, English-2

SIORDIA, Rodolfo Elias Dr. Cardiovascular Surgeon

Cirujanos Cardiovasculares del Noroeste

Hospital CIMA

Paseo Rio San Miguel #35

83280 Hermosillo, Sonora

PH: (662) 259-0959

E-Mail: resiordia@yahoo.com

Languages: Spanish, English-3, French-1

SIORDIA ZAMORANO, Arturo Dr. Cardiovascular Cardiovasculares del Noroeste Thoracic

Surgery

Hospital CIMA

Paseo Rio San Miguel #35

83280 Hermosillo, Sonora

PH/Fax: (631) 312-2810 (Nogales) (662) 259-0967 Hermosillo

E-Mail: Siordia@dakotacom.net

Languages: Spanish, English-3, French-1

SOLIS DA COSTA, Oscar Arturo Dr. Ear, Nose & Throat

Juarez y Gaston Madrid Head & Neck Surgery

Hermosillo, Sonora, Mexico

Phone/Fax: (662) 212-1653

E-Mail: solisotorrino@yahoo.com.mx

Languages: Spanish, English-2

SOUFFLE VILLA, Francisco Jesus Marcos Dr. Plastic & Reconstructive Juarez #120

Norte Surgery

Colonia Modelo

83190 Hermosillo, Sonora

PH: (662) 214-8188, Fax: (662) 214-6609 cel.(044 662) 256-6319

E-Mail: soufflé_cirujano@prodigy.net.mx

Languages: Spanish, English-2

Hermosillo Hospitals**CENTRO MEDICO DEL NOROESTE**

Av. Luis Donaldo Colosio 23 Oriente
esquina con Manuel Gonzalez
Colonia Centro
Hermosillo, Sonora
Tel. (662) 217-4521 or 213-6250

HOSPITAL CIMA

Paseo Rio San Miguel
Hermosillo, Sonora
Tel. (662) 259-0900, 259-0959,
Emergency Ward (662) 259-0911
Fax (662) 259-0999
E-Mail: cimahillo@terra.com.mx

HOSPITAL LICONA

Luis Donaldo Colosio #42
esquina con Jesus Garcia
Hermosillo, Sonora
Tel. (662) 217-4828, Fax 213-6616
E-Mail: slicona@prodigy.net.mx

HOSPITAL GENERAL DEL ESTADO

Blvd. Luis Encinas
Hermosillo, Sonora
Tel. (662) 259-2500, 213-2556

HOSPITAL INFANTIL DIF (Children's Hospital)

Reforma 355 Norte
Hermosillo, Sonora
Tel. (662) 289-0600

HOSPITAL SAN JOSE

Blvd. Morelos #340
Entre Blvd. Lopez Portillo y Ave. 7
Colonia Bachoco 83148
Tel. (662) 109-0500

SALUD EN CASA
Local Air Ambulance
Hospital Cima
Paseo Rio San Miguel
Hermosillo, Sonora
Tel. (662) 208-3885
259 0911
Cel: (0446621) 44 1477

APPENDIX 11: DRIVING TIPS

Among the many vehicle types, Sports utility vehicles or SUVs are more prone to rolling over. In fact, SUVs are three times more likely to roll over compared to passenger cars. Moreover, 36% of rollover accidents involving SUVs result in fatalities. This is actually the highest rate in all vehicle categories. To curb this alarming rate, JD Power and Associates offered some helpful safety tips that SUV drivers will find useful.

- Drive at safe speed, especially on curved roads; keep steering smooth, avoid sudden turns.
- Allow extra distance for braking, be cautious of wet pavement
- Secure interior cargo behind rear seat when possible, store on roof only when necessary
- Keep tires properly inflated, check tire pressure at least monthly
- Use caution when towing, avoid sudden turns
- Check around vehicle for low-lying objects before entering

SEAT BELTS!!

APPENDIX 12: SAFETY CONSIDERATIONS WHEN DRIVING ON RURAL ROADS

Introduction

Secondary roads in remote and/or rural areas may present hazards that drivers accustomed to travel on urban and suburban roadways may not be aware of. This document describes hazards particular to unpaved and rural roads and recommends safety procedures to follow.

Characteristics of rural or forest roads

Extra caution is required when driving on “country roads” because they are often not designed for efficient high-speed travel like urban roadways. The following safety hazards are more likely to be found on rural roads:

- Lack of signs or accurate maps
- Blind curves
- Narrow width (not sufficient for vehicles to pass safely)
- No shoulder or guard rails
- Soft surface (uncompacted gravel or dirt)
- Rough or damaged road surface
- Obstacles on road (slow-moving vehicles, animals, debris)
- Unusually steep hills or sharp curves

Since help may often be difficult to reach or unavailable in the event of an accident, it is particularly important to exercise caution when driving in remote areas. Never exceed posted speed limits and remember that some circumstances require driving well below the posted speed. Beyond exercising normal driver safety, travel on rural roads may also warrant specific additional precautions due to the hazards listed above. These hazards and the recommended ways to deal with them are listed below.

Navigation

Description: Rural roads may not be clearly signed. New or unmapped roads are common in areas where logging or mining activities occur.

Hazard: One can easily become lost and possibly end up on difficult or dangerous roads when traveling in rural areas.

Cautions:

- Carry a compass and/or GPS when traveling to remote areas on rural roads.
- Obtain the most current USFS or BLM maps if traveling on federal lands.
- Always double check directions or maps before venturing onto rough or little-used dirt roads.
- Fill fuel tank before leaving populated areas. Fuel stations may be unavailable for long distances. Carry extra fuel in an approved gas can if you will be a long way from populated areas.

- Check the air in the spare before you go. Be sure you have a jack and usable flashlight.
- Carry water, food, and emergency supplies.
- Don't count on cell phone service. Be sure someone knows where you have gone and when you are expected back so they can notify authorities if you don't return or check in within a reasonable amount of time after your expected return time.

Blind curves and dips

Description: Mountain roads are often too narrow for 2 vehicles to pass easily and have many sharp curves that prevent seeing approaching traffic. Rural and desert roads may follow the topography of the landscape, resulting in many dips and rises that create blind spots in the road ahead. Agricultural or prescribed forest burning may produce smoke on roads.

Hazard: Approaching vehicles, livestock or wild animals on the road, or slow-moving vehicles may be encountered without warning. Visibility may be suddenly reduced due to smoke.

Cautions:

- When approaching a blind curve or dip/rise on a narrow road, slow down and keep to the right. Watch for dust indicating on-coming traffic and sound your horn to warn approaching vehicles if lack of visibility warrants.
- Stay as far right as possible when entering a blind curve.
- Dips in the road may be due to creeks where animals congregate on or near the road. Approach carefully if in a free-range area, or in twilight or darkness.
- If you see smoke plumes crossing the road ahead, slow down when approaching because visibility can decrease rapidly and there may be workers or vehicles along the road.

Obstacles

Description: Off-road vehicles such as tractors or bulldozers may drive on rural roads or be left parked on forest roads. Livestock or wildlife may be encountered on roads. Fallen trees or landslide debris may not be removed quickly from rural or forest roads.

Hazard: Slow moving vehicles or stationary obstacles may require sudden stops. Animals may move onto road unexpectedly, or block it entirely. Collisions with large animals (deer, cows, sheep) can result in major vehicle damage and serious injury.

Cautions:

- Reduce speed on roads with blind curves or dips in case you need to stop suddenly.
- Be aware that farm vehicles and construction equipment may be wider than passenger vehicles. Pass with extra caution unless they pull over.
- When driving in free-range areas, on forest roads near dawn or dusk, or if you see wildlife near the road, slow down and watch carefully for animals on or approaching the road. *Note: in some free-range areas livestock owners are not legally liable for any damage caused by their animals on a roadway.*
- If a small animal (e.g. rabbit, coyote) runs out into the road in front of you, do not try to swerve around it or slam on the brakes. Animals move rapidly and unpredictably and may be confused by any changes in your approach.

- When passing large animals near the edge of the road, go slowly as they may suddenly move onto the road. If a group of animals is crossing the road, wait until they have all moved to a safe distance before proceeding. For example, don't try to creep through a slow moving flock of sheep or between a group of indecisive deer crossing the road because they may become startled and run right into your vehicle.

Passing other vehicles

Description: Some roads may be too narrow to pass oncoming vehicles safely.

Hazard: Trying to pass oncoming vehicles at speed could result in a collision or one vehicle being forced off the road.

Cautions:

- When an oncoming vehicle is encountered, pull over to give adequate passing room. Watch out for steep drop offs or loose surface on the shoulder. If no safe shoulder is available at your location, stop and wait for the other vehicle to pull over.
- When there is no shoulder available for either vehicle to pull over safely, stop. One vehicle should back up until a safe spot is reached. By custom the vehicle closest to the safe shoulder will reverse or, on a steep hill, the vehicle traveling downhill.
- Do not expect logging trucks, cars with trailers, or other large vehicles to make room for you. Pull over early when you see them coming.

Steep grades

Description: the steepness of most roads is limited for safety, however, rural or logging roads may exceed this limit putting unusual demands on vehicle brakes.

Hazard: Excessive use of brakes can result in overheating and eventual failure. Skidding may occur more easily, especially when towing.

Cautions:

- When descending a long or particularly steep grade shift the vehicle into a low gear to reduce the need to use the brakes. This applies to both manual and automatic transmission vehicles.
- On more level stretches of a long grade, avoid using brakes to let them cool.
- If towing, or if the road may have sharp curves, maintain a lower speed than normal to allow stopping without skidding.

Washboards

Description: these corrugations in the road surface are commonly found on hills or curves, but may occur anywhere on dirt or gravel surface roads that have not been regularly maintained.

Hazard: Due to the reduced traction created by the rough surface, washboards make it difficult to steer and may result in sudden loss of control or drifting sideways. Many drivers have skidded into roadside ditches or rolled their vehicles over after losing control on washboards.

Cautions:

- SLOW DOWN! Although the vehicle may appear to handle more smoothly at higher speeds when driving on washboards, this is due to reduced contact with the road surface and therefore less control.
- Brake BEFORE entering curves, downhills, or other potentially washboarded stretches of road. Once you are on the washboards, braking may reduce your ability to control the vehicle. Shifting into a lower gear than normal will help reduce the need to brake suddenly.
- Putting your vehicle in 4WD (if available) before going uphill on a washboarded road can help with navigation.
- Steer gently when on washboards. Trying to make sharp turns or corrections will be ineffective and may result in loss of control.

Loose surface

Description: unpaved roads may range from hard-packed dirt or gravel that is as solid as asphalt to soft sand, fine dust, or deep uncompacted gravel.

Hazard: The primary hazard is loss of traction which may result in getting stuck or losing control of the vehicle. Secondary hazards are reduced visibility and/or engine damage due to heavy dust, windshield damage due to flying stones, and damage to the vehicle's undercarriage.

Cautions:

- Reduce speed and avoid sharp turns, to avoid skidding. If your vehicle starts to skid, brake gently and keep the steering wheel straight as you would on wet or icy roads. Engage four wheel drive (4WD) if available, even if the road is level.
- Leave extra distance between your vehicle and those ahead of you to avoid dust and flying rocks. Slow down when approaching oncoming vehicles in preparation for a loss of visibility.
- Be aware of changing road surface. If you enter an area of soft sand or gravel, steer gently and avoid braking or accelerating suddenly. Remember that if you drive down a hill with loose surface you may have trouble climbing back up.
- Stay off of shoulders which may be less compacted than the road. Use extra caution when pulling off the road.
- If your vehicle has low clearance, watch for rocks or other obstacles protruding from the road surface.
- Air and oil filters can clog rapidly due to excessive road dust, causing reduced performance and eventual engine damage. Have them changed more often when traveling on unpaved roads. If you experience a rapid loss of power when driving in very dusty conditions, try cleaning the air filter by shaking surface dust off of it. Dirt and debris can also clog the radiator surface, resulting in overheating. Brush or hose off the radiator surface (after letting engine cool) as needed.
- Watch the weather closely before setting off on dirt roads. Even a few drops of rain can turn some surfaces, such as clays, from hard packed dirt to impassable slippery mud.

Ruts

Description: Unpaved roads often develop deep ruts due to tire wear or erosion.

Hazard: Lower clearance vehicles may become “high-centered” when the wheels go into ruts. This can cause the vehicle to become stuck or damage the undercarriage.

Cautions:

- Try to keep one or both tires out of wheel ruts by driving on edge or in center of road.
- When crossing ruts, approach at an angle (not perpendicular) to reduce the effective steepness of the rut.
- If vehicle undercarriage makes contact with the road, stop and check underneath for fluid leaks or damage before proceeding. If vehicle becomes stuck, have all passengers get out and remove any heavy cargo before trying to reverse (or possibly go forward if you have 4WD) slowly.

Washouts/Flooding

Description: Unmaintained roads may become partially damaged during floods or heavy rainstorms. Damaged areas may or may not be signed. Flood waters may cross roads at low points.

Hazard: Attempting to cross damaged or flooded sections of road may run risk of getting stuck or sliding off road down a steep slope.

Cautions:

- If undamaged portion of road is not clearly wide enough for vehicle to pass, have someone get out and watch or, if alone, pull vehicle close to washout and compare wheelbase width before crossing.
- If it is necessary to cross the washed-out area, first check how solid the surface is before attempting.
- Do not attempt to cross a wash-out if a sideways slide could result in the vehicle slipping down a steep slope. Be extra cautious if there is running water present.
- Never enter running water unless you can tell how deep it is and you are sure it is not rising. Always avoid crossing moving water that is deep enough to touch the vehicle’s body. If you get stuck, exit the vehicle on the upstream side only. Don’t stop while crossing a washout or flooded area.

Reference:

<http://safety.dri.edu/FieldSafety/Guidelines/DrivingRuralRoads.doc>

<http://www.jdpower.com/articles/article.aspx?ID=109>

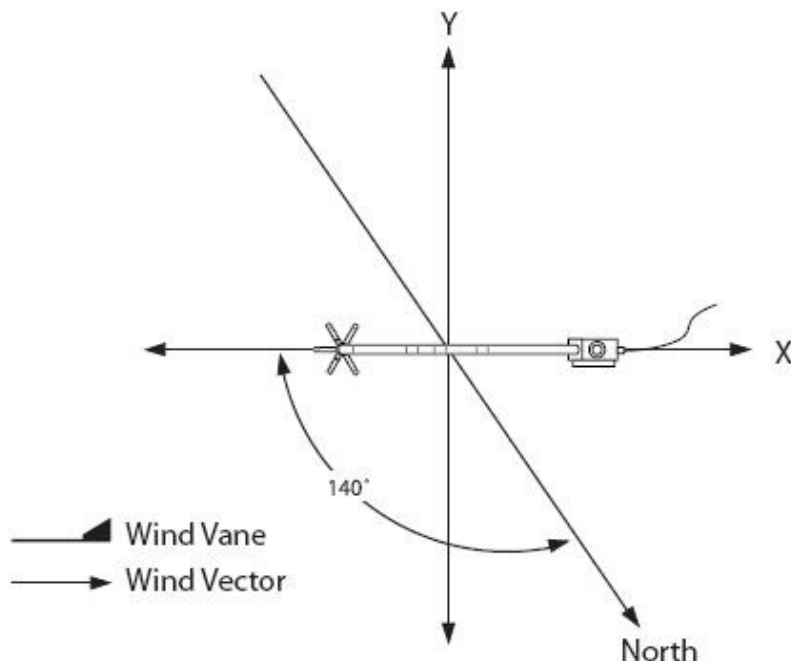
Appendix 13: CSAT3 Azimuth

The example programs report the wind direction in both the CSAT3 coordinate system (a right-handed coordinate system) and in the compass coordinate system (a screwball left-handed coordinate system). The CSAT3 coordinate system is relative to the CSAT3 itself and does not depend on the CSAT3's orientation (azimuth of the negative x-axis). The compass coordinate system is fixed to the earth. In order for the programs to compute the correct compass wind direction, the azimuth of the CSAT3 negative x-axis must be entered into the program. The program default value for the CSAT3_AZIMUTH is 0. This assumes that the prevailing wind is from the North, e.g. the CSAT is mounted such that the negative x-axis points to the North.

As described in the CSAT3 installation section, orient the CSAT3 so that it is pointing into the prevailing wind direction. If you have done so, the CSAT3 negative x-axis will point into the prevailing wind direction. Enter this prevailing wind direction for the constant CSAT3_AZIMUTH.

Don't forget to account for the magnetic declination at the site; see below for details.

Figures X and Y show the orientation of a CSAT3 with a compass bearing of 140 degrees, e.g. the negative x-axis is pointing into 140 degrees. If the wind is blowing into the CSAT3, from the negative x-axis to the positive x-axis (from the transducers to the block), the horizontal wind vector angle (*wind_dir_csat3*) is 0 degrees (wind vector) and the compass wind direction (*wnd_dir_compass*) is 140 degrees (wind vane).



The

orientation of the

CSAT3 negative x-axis is found by reading a magnetic compass and applying the site-specific correction for magnetic declination; where the magnetic declination is the number of degrees between True North and Magnetic North. Magnetic declination for a specific site can be obtained from a USGS map, local airport, or through a NOAA web calculator. A general map showing magnetic declination for the Conterminous United States in 2004 is shown in Figure Z.

Declination angles are always subtracted from the compass reading to find True North. A declination angle East of True North is reported as a positive value and is subtracted from 360 (0) degrees to find True North as shown in Figure Z-1. A declination angle West of True North is reported as a negative value and is also subtracted from 0 (360) degrees to find True North as shown in Figure Z-2.

For example, the declination for Longmount, CO (10 June 2006) is 9.67 degrees, thus True North is 360 degrees minus 9.67 degrees or 350.33 degrees as read on a compass. Likewise, the declination for McHenry, IL (10 June 2006) is -2.68 degrees, and True North is 0 degrees minus -2.68 degrees, or 2.68 degrees as read on a compass.

For our two possible tower locations, the declination is approximately ... as computed from <http://www.ngdc.noaa.gov/geomagmodels/struts/calcDeclination>.

APPENDIX 14: EQUIPMENT LISTS

Personal Equipment

- Travel Documents / Cards
 - . Passport
 - . Health Insurance Card
 - . Credit Cards
 - . Driver's License
 - . Phone Card
- Clothes for a Few Days
(Wash the clothing at the house)
 - . Pants
 - . Shorts
 - . Shirts
 - . Light Long Sleeved Collared Shirt
 - . Underwear
 - . Socks
 - . Hiking Boots
 - . Tennis Shoes
 - . Sandals/Flip-flops
 - . Raincoat/Poncho
- Accessories
 - . Hat
 - . Bandana
 - . Sunglasses
 - . Watch
 - . Belt
- Toiletries
 - . Sunscreen
 - . Bug Repellent
 - . Lip Balm
 - . Shampoo/Conditioner
 - . Body Soap

- . Deodorant
- . Toothpaste/Toothbrush
- . Toilet Paper
- . Shaving Kit
- . Medicine – Personal, Pain, Upset Stomach
- . Laundry Detergent
- . Towel
- . Contact Lens Care Supplies

- House Gear
 - . Pillow
 - . Sheet
 - . Sleeping Bag
 - . Lunch Box
 - . Utensils
 - . Cup
 - . Entertainment (books, cards, CD player)
 - . Camera
- Field Gear
 - . Water Bottle/CamelPack
 - . Emergency Whistle
 - . Small Mirror
 - . Pocketknife/Leatherman
 - . Work Gloves
 - . Backpack

First Aide Kits

- Pre-made kit 2
- Snakebite kits 4
- Large Home Kit 1
 - . Bactine 1 btl

- . Alcohol 1 btl
- . Peroxide 1 btl
- . Iodine 1 btl
- . Aspirin 1 btl
- . Various gauze
- . Various bandages
- . Immodium 1 box
- . Benedryl 1 box
- . Pepto Bismol 1 btl
- . Tums 1 btl
- . Tweezers 1
- . ACE Bandage 3
- . Thermometer 1
- . Eye Wash 1
- . Antibiotic Ointment 1 tube
- . Butterfly Clips 1 box
- . Instant Cold Packs 3
- . Tape 1
- . Medical Gloves 1 box

Vehicle Equipment

- Tool Set (3 total, 1 per vehicle)
 - . Philips Screwdriver
 - . Flathead Screwdriver
 - . Pliers
 - . Needle-nose pliers
 - . Adjustable wrench
 - . Side-cut pliers
 - . Claw Hammer
 - . Shovel
 - . Pick
 - . Duct Tape

- . Electrical Tape
- . Zip/Cable Ties
- . Bubble Level
- . Socket/Wrench/Allen Set
- . Hammer
- . Bailing Wire
- Gloves
- Vehicle Repair
 - . Vehicle Water
 - . Motor Oil
 - . Fix-a-Flat
 - . Radio
 - . Roadside Emergency Kit
 - i. Tow Rope
 - ii. First Aid Kit
 - iii. Battery Charger Cables
 - iv. Air Compressor
 - v. Air Gauge
 - vi. Mini Tool Kit
 - vii. Glow Stick
 - viii. Flashlight (w/ batteries)
 - ix. Zip Ties
 - x. Safety Vest
 - xi. Emergency Poncho
 - xii. Cone
 - xiii. Blanket
 - xiv. Gloves
- Triangle Reflector

Experiment 1: Isotopic Partitioning of Evapotranspiration – Rayon Tower

- Markers/Pens/Pencils (1 pk. ea.)
- GPS Unit (1)
- Chronometer (1)
- Field Notebook (1)
- Soil Auger (1)
- 25 ml Screw-capped Vials (65)*
- Extra Vegetation Vials (144)*
- Labels (a few rolls)
- Hand Pruners (3 in set)
- Parafilm (1 box)*
- Vapor Trapping System (1)*
- 12 Volt Battery (1)
- Aluminum Foil (1 box)
- Cooler (1 medium sized)
- Ziploc Bags (1 box, gal. size)
- Metal File (1)*
- Scissors (1)
- Glass Vapor Traps (120)*
- Liquid Nitrogen (40 l)*in MEX
- Ethanol*
- Dewar Flask with Lid (1)*
- Thermometer (1)*
- Valves (several)*
- Tubing*
- Handheld Porometer (1)*
- AA Batteries for GPS (8)

**Enrico Yepez will bring*

Experiment 2: Tree Sampling for Sapflow Allometric Relations

- Bow Saw (1)
- 8” Increment Borer (1)
- Tape Measure 50 ft. (2)
- DHB (diameter) Tape (3)*
- Box of Transparencies (1)*

**Enrico Yepez will bring*

Experiment 3: Daily Soil Moisture and Temperature Sampling Plots – Rayon Tower

- Markers/Pens/Pencils (1 pk. ea.)
- GPS Unit (1)
- Field Notebook (2)
- Hand-held Theta Probes (4)
- Extra Tines (bag)
- Multimeter (1)
- Hammer (2)
- Infrared Thermometer (2)
- Soil Thermometers (10)
- Flags (200)
- Stakes (100, 1’)
- Map & Coordinates of Station Locations
- Radios
- Digital Camera
- AA Batteries (12) for GPS
- 9V Batteries (12) for multimeter/hydroprobes

- 76 A Batteries extra for thermometers
- Eyeglass screwdriver for thermometers (1)

Experiment 4: Eddy Covariance Tower Installation/Operation – Cucurpe

Tools Required for Tower

Installation:

- Shovels
- Open end wrenches: 5/16”, 3/8”, 7/16”, 1/2”, (2) 9/16”, 15/16”
- Adjustable/Crescent wrench
- Magnetic compass
- Tape measure (25’)
- Nut driver (3/8”)
- Level (36” to 48”)
- Small Sledgehammer
- Pliers
- Cable Ties
- Climbing harness
- Haul rope (50’)
- Non-stretch line
- Wire rope cutters
- Materials for Guy Wires
- 120’ Aircraft Cable 3/16”
- (3) Turnbuckles 1/2” x 17”
- (3) Turnbuckles

- (24) Wire Cable U-bolt Clamps 3/16"
- (12) Wire Cable Thimbles 3/16"
- (3) 5/8"-11 x 4" Coarse Hex Cap Bolts
- (3) 5/8"-11 Coarse Nuts
- (3) 3/4" x 30" Dbl. Head Earth Auger Anchor
- Metal bar to screw in anchors
- Cement (MEX)
- Materials for B18 Base
- (4) Wood Stakes 12"
- Pick or digging bar
- Concrete form materials (optional) (2" x 4" lumber, stakes, saw, hammer, nails, etc.)
- Cement, Sand, Agg. (MEX)

Additional Tools for Instrumentation Installation:

- Lock and key for enclosure
- Magnetic declination angle
- Straight bit (flathead) screwdrivers (small, medium, large)
- Phillips-head screwdrivers (small & medium)
- Small diagonal side-cuts
- Needle-nose pliers
- Wire strippers
- Pocket knife
- Calculator

- Volt/Ohm meter
- Electrical tape
- Datalogger prompt sheet
- Station manuals
- Socket wrench and 7/16" deep well socket
- Pliers
- Felt-tipped marking pens
- Claw hammer
- Channel-lock pliers
- 3/8" nut driver
- 1/4" washers (spacers for U-bolts)
- 5/64" Allen hex wrench
- Enclosure Sealing and Desiccant Kit
- Hose Clamps (2)

Instrumentation Equipment:

- CR5000 Measurement and Control System Datalogger
- Datalogger Enclosure and mounting hardware
- CSAT3 3-D Sonic Anemometer and Electrical Box
- LI-7500 Open Path CO₂/H₂O Analyzer and Electrical Box
- HMP45AC Humidity and Temperature Probe with Shield
- (4) CS616 Water Content Reflectometers

- CMP3 Pyranometer, radiation shield and mount
- Setra 278 Barometer
- CNR2 Net Radiometer and mounting arm
- (2) Hukseflux HFP01SC Soil Heat Flux Sensors
- (4) 4 Probe Type-E Averaging Soil Thermocouples
- Crossbars and crossarms (3?)
- Tripods
- Tower Grounding Kit
- Enclosure sealing and desiccant kit

Equipment for EC Tower Power Supply:

- (2) 65 watt solar panels
- (2) Solar panel mounts
- Solar panel wiring
- (2) SunXtender deep cycle battery
- SunSaver 10 amp solar charge controller
- Tower Grounding Kit (wire, rod & connectors)
- Battery cables (to datalogger and between both batteries)
- Battery Boxes (2)

Experiment 5: Hydrometeorological Station Installation (10) including Calibration/Soil Sampling

- Data Loggers *in MEX
- Laptop (1)
- Tipping Bucket Rain Gauges*in MEX
- Solar Panels*in MEX
- Pick (2)
- Shovel (2)
- Allen wrench (1)
- Soil Moisture Hydro Probes (1)
- Field Notebook (2)
- AA Batteries for GPS (8)
- Cement
- Water for cement
- U-bolts, washers, rectangular plates (20)

Calibration of Rain Gauge Tipping Buckets:

- Field Notebooks (2)
- Calibration Kit (1)
- Burette (2)
- Water for Calibration
- Chronometer (2)
- Allen Wrenches (2)
- Laptop (2)
- AA Batteries for GPS (8)

Surface Soil Sampling:

- Picks
- Shovels
- Measuring tapes or ruler
- Sieves
- Soil notebook or field spreadsheets
- Digital camera
- GPS device
- 4 mil (mm?) thick soil sample storage bags (1 for each location)
- Clinometer and compass

Experiment 6: Flux Measurements using DF Scintillometer Installation and Operation – Rio San Miguel

- GPS Unit (1)
- Field Notebook (1)
- Scintillometers *in MEX
- AA Batteries for GPS (8)

Site Setup Equipment:

- Scintillometer set (1 transmitter, 1 receiver, 2 sun shields, 2 telescopes, and 2 cables)*
- Data logger / Data logger container*

- Laptop (data logger cables)*
- 2 Radios
- 2 GPS units
- 2 Tool kits (including the following: Flathead screwdriver, Phillips screwdriver, Allen set(metric and standard) , 2 adjustable wrenches, wire, wire cutters, scissors, voltmeter, desiccants, lens cleaner, cotton swabs, distilled water, replacement screws, and replacement cable)*
- 2 Batteries*
- 2 Battery covers*
- 2 Solar panels*
- 2 Charge controllers*
- Weather station equipment*
- 2 Backpacks (4 if available)*

Scintillometer Alignment and Power Setting Instruction / Site Maintenance Equipment:

- Scintillometer telescopes, with the same serial code as the scintillometer being visited
- Laptop (data logger cables)
- 2 Radios
- 2 GPS units
- 2 Tool kits (including the following: Flathead

screwdriver, Phillips screwdriver, Allen set(metric and standard) , 2 adjustable wrenches, wire, wire cutters, scissors, voltmeter, desiccants, lens cleaner, cotton swabs, distilled water, replacement screws, and replacement cable)

- Replacement battery (2 if available)
- 2 Backpacks (4 if available)

Experiment 7: Water Source Characterization using Major Anions and Isotopes

- GeoPump*
- 125 ml. Plastic bottles*
- 10 ml. Plastic vials*
- pH and EC meter*
- Labeling tape*
- Markers*
- Cooler*
- Buckets*
- Screen*
- Wire*
- Screen scissors*
- Mineral Oil*
- Syringes*
- Samplers*
- 1 lt. Plastic Bottles*
- Autosamplers*

*Lissette de La Cruz will provide

Experiment 8: Soil Surveying

- Picks
- Shovels
- Measuring tapes or ruler
- Sieves
- Soil notebook or field spreadsheets
- Digital camera
- GPS device
- 4 mil (mm?) thick soil sample storage bags (1 for each location)
- Measuring tape
- Munsell color chart
- Knife
- Bottle with HCl
- Bottle with water
- Compass and clinometers
- 4 mil (mm?) thick soil sample storage bags
- Pedon storage containers
- Glass to scratch for parent material test
- parafilm

**Harrison / Zarate will provide more supplies*

OTHER SUPPLIES:

- CR-2032 Batteries (15)
- Tent/Tarp (1)
- BBQ Grill (1)
- 6' Foot Bubble Level (1)
- Duct Tape (2)
- Datalogger Posts *in MEX
- Red Gas Cans (2)
- Electrical Tape (2)
- Moisture Meter User Manual
- Moisture Meter Data Link
- Flathead Screwdriver
- Philips Screwdriver
- Data Logger Spare Equipment
- Data Logger Mounting Brackets
- Data Logger Boxes
- Rain Gauge Manual
- Rain Gauge Mounting Brackets
- Rain Gauge Posts 7' *in MEX
- Large Topographic Maps
- Soil Permits
- HOBO Base Stations (USB)
- Cable SC30B for Laptop
- Tables (2)
- Chairs (4)
- AC/DC Converter
- Battery Charger
- Water Bottles (2)
- Ziploc Bags (# boxes)
- Radios (set of long range)
- Backpacks (3)
- Toolbox/kit (3)

APPENDIX 15: LIST OF PARTICIPANTS

New Mexico Institute of Mining and Technology - Socorro, NM

Enrique Vivoni

Associate Professor of Hydrology
Research Hydrologist

Bruce Harrison

Associate Professor of Geology

Soni Yatheendradas

Post-doctoral Research Associate in Hydrology

Laura Alvarez

Graduate Student of Hydrology

Luis Mendez

Graduate Student of Hydrology

Agustin Morua

Graduate Student in Environmental Engineering

Alexis Martinez

Undergraduate Student in Environmental Engineering

Kim Bandy

Undergraduate Student in Biology

James Craft

Undergraduate Student in Environmental Science

K. Thomas Dotson

Undergraduate Student of Materials Engineering

University of New Mexico – Albuquerque, NM

Enrico Yepez

Post-doctoral Research Associate in Biology

University of Arizona – Tucson, AZ**Tom Meixner**

Associate Professor, Hydrochemistry
Department of Hydrology and Water Resources

Lissette De La Cruz

Graduate Student in Hydrology
Department of Hydrology and Water Resources

University of California, San Diego – San Diego, CA**Jan Kleissl**

Assistant Professor
Dept of Mechanical and Aerospace Engineering

Universidad de Sonora, Hermosillo, MX**Christopher Watts**

Professor of Physics

Juan Sainz

Professor of Civil Engineering

Marco Antonio Molina Ramirez

Undergraduate in Civil Engineering

Jessica Gutiérrez Burboa

Undergraduate in Civil Engineering

Instituto Tecnológico de Sonora, Ciudad Obregón, Sonora, MX**Jaime Garatuza**

Professor of Hydrology

Benjamín Rivera Félix

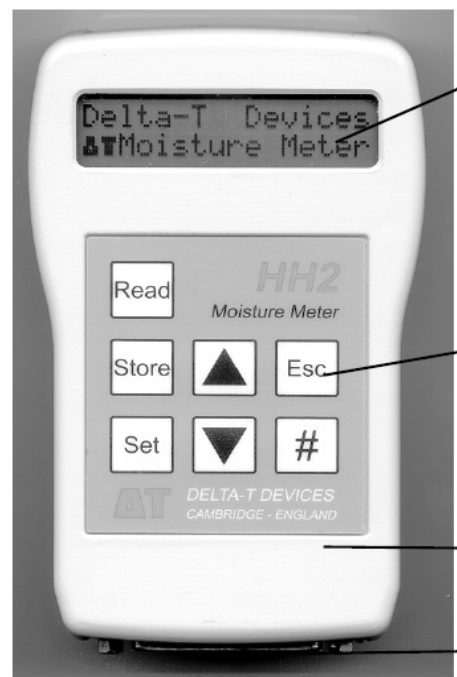
Undergraduate in Environmental Engineering

Jocelyn Benítez

Undergraduate in Environmental Engineering

APPENDIX 16: MOISTURE METER MANUAL

Moisture Meter Parts



LCD with 2 rows of 16 characters - used to display menus and readings

Keypad	
Read	take readings
Store	save reading
Set	select menu or select option
Esc	wake meter or reject option & go back
▲ ▼	scroll
# #	average

Splash proof case

25-pin D Connector for sensor connection or PC connection



Battery compartment - takes one PP3 battery

How the Moisture Meter takes readings

Analogue sensors (SM200, ML1, ML2, ML2x, EQ2, PR2, PR1)

The Moisture Meter applies power to the sensor and measures the output signal voltage returned.

It displays this directly, in mV, and/or converts into other units, depending on the type of sensor and information available. (Equitensiometer results can only be displayed in mV.)

The meter converts the mV reading into soil moisture units using a linearisation table and soil-specific parameters.

Linearisation tables are pre-installed for sensors, and for Organic and Mineral soil parameters.

For greatest accuracy you can enter your own soil type parameters - but these have to be determined experimentally. This is outside the scope of this manual.

For mm Deficit you need to supply Field Capacity and Root Depth for each soil type and crop.

The date and time is saved with each reading. Before saving readings you may enter a unique Plot, Sample or Device identity (ID) label.

Digital Sensor (WET)

The Moisture Meter applies power to the sensor, receives readings as serial data, processes these (as described in the WET sensor Application Note available from Delta-T), and calculates bulk and pore conductivity, bulk permittivity and temperature as required. Using installed soil calibrations the HH2 calculates water content. Given the root depth and field capacity it can also calculate mm Deficit.

Sleep and Waking the Meter

To conserve the battery, the meter will “go to sleep” when it is not used for 1 minute. The display will go blank and the meter will power down to reduce its power consumption.

To make the HH2 sleep, press **Esc** once to return to the banner "Delta-T Devices Moisture Meter" then press **Esc** one more time to make it sleep.

The meter will “wake up” when **Esc** is pressed or when RS232 messages are received from the PC or when the battery is reconnected.

Averaging

Press **#** to shows the previous average – and press **#** twice to update it with the current reading. Averages are not stored – sorry. Write it down if you need it.

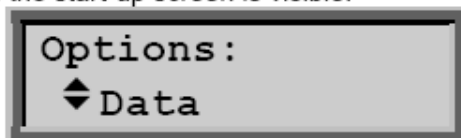
For details see Averaging on page 14.

Navigating Options and Readings

Press **Esc** to wake the HH2 and examine the Navigation Map overleaf. There are two main routes - round the Read Cycle, and down (and up) the Options Menus. Individual options or values are set at the bottom level of each menu path. See also the Options Summary at the back of each sensor chapter.

Not all options are available with all devices. A table of permitted options, ranges and default values are shown in each sensor chapter.

To display the main **Options** menu press the **Set** key when the readings are visible on the display, or when the start-up screen is visible.



Press **Set** to select an option - this may be another, lower menu.

Press **Esc** to reject an option and backtrack up to the previous menu.

When the **◆** and **▼** symbols are displayed, press the **up** **▲** and **down** **▼** keys to scroll through the options in any given menu.

To save **Readings** - press **Store**.

To save **Options** - press **Set**.

Press **Read** and **Store** to take and save readings.

Options Menu

The **◆** symbol indicates that other options are available.

Data: Add label for Plot ID, Sample, Device ID, Root Depth, Sensor Depth or delete all data.

Device: Select the sensor e.g. PR1 for a Profile Probe.

Soil Type: Choose one for each sensor if you want results in engineering units. The default is Mineral.

Soil Set-Up: Define parameters associated with each soil type.

Units: Select which engineering units are used - e.g. %vol or $m^3.m^{-3}$.

Display: Select readings to be taken and displayed - e.g. mV and %Vol.

Date and Time: The clock can be set via the keypad or from the PC

Status: Displays: % memory used, % battery life remaining & number of readings in memory. Also version numbers of firmware and any installed tables.

Remote: Select this when connecting to a PC.

APPENDIX 17: GPS START-UP MANUAL

Operating the eTrex Vista

1 Installing the Batteries

The eTrex Vista operates on two AA batteries (not included), which are placed in the back of the unit. Rechargeable Alkaline, NiMH, NiCad or Lithium batteries may be used, but cannot be charged in the unit.

Stored data will not be lost when changing the batteries.

To install the batteries:

1. Remove the battery cover from the back of the unit by turning the D-ring 1/4 turn counter-clockwise and pulling out.
2. Insert the batteries observing proper polarity as shown at the right.
3. Reinstall the battery cover by turning the D-ring 1/4 turn clockwise.



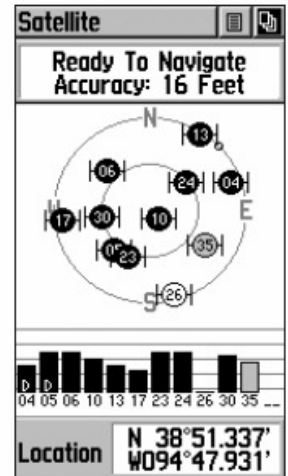
Operating the eTrex Vista

3 Start Up Sequence

To turn the unit On:

1. Press and hold the **POWER** button.
2. Press the **PAGE** button to acknowledge the copyright.
3. Carefully read the warning message and press the **PAGE** button to acknowledge and proceed to the Satellite Page.

The first time you use the unit it may take up to 5 minutes to establish a position. After that, it should take only 15 to 45 seconds. When the Vista has acquired enough satellite signals to determine your location, a “Ready To Navigate” message and your location coordinates are shown.



Satellite Page:
displaying
Satellite Position,
Signal Strength,
and your Location

2 Using the Button Functions

The ZOOM IN and OUT buttons:

- When on the Map Page, press to Zoom in and out.
- When on the Satellite Page, press to adjust the screen contrast.

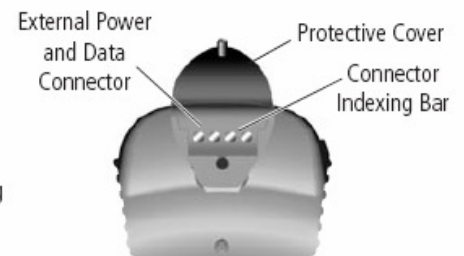
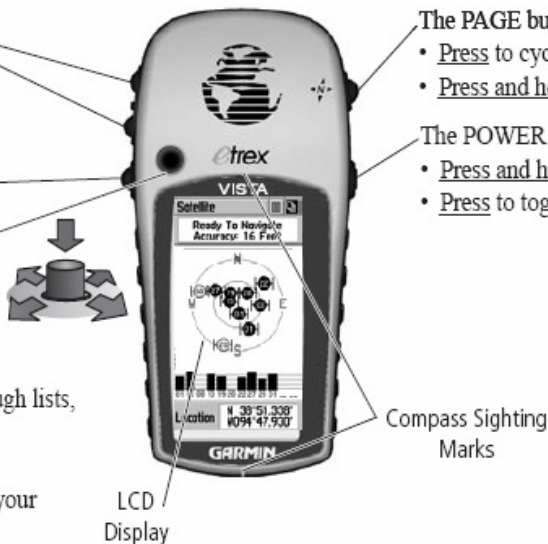
The FIND button:

- Press to access the Find Menu.

The THUMB STICK:

(When moved or pressed in, this button ‘clicks’)

- Press to enter highlighted options or confirm messages.
- Move Up/Down or Right/Left to move through lists, highlight fields, on-screen buttons, icons, enter data or move the map panning arrow.
- Press in and hold for two seconds to mark your current location as a waypoint.



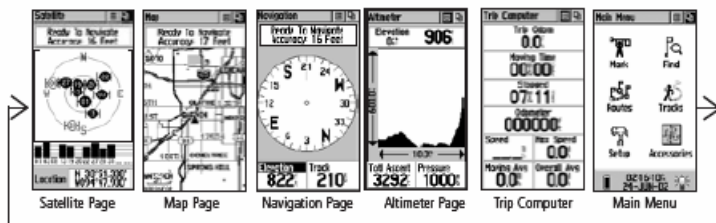
NOTE: While designed to be held and operated in the left hand, the unit can be used with the right hand, if preferred.

The Main Pages, Setting the Time Zone

Compass Calibration

4 Previewing the Main Pages

All of the information you need to operate the eTrex Vista is found on the five Main Pages (or display screens). To preview these pages, press the PAGE button to cycle from one page to the next. The five pages are shown in order below.



Satellite Page - Provides a visual reference of satellites being tracked.
Map Page - Displays your movements and nearby map features.
Navigation Page - Provides guidance to your destination.
Altimeter Page - Provides current elevation and ascent/descent info.
Trip Computer - Provides a variety of trip and navigation data.
Main Menu - A directory of advanced features and settings.

5 Setting the Time Zone

If the Vista is “Ready to Navigate” (Step 3) but the time shown is not correct, you may need to change the Time Zone selection.

To change the Time Zone:

1. Use the **PAGE** button to access the Main Menu.
2. Use the **THUMB STICK** to highlight the Setup icon and then press to display the Setup Menu.
3. Use the **THUMB STICK** to highlight the Time icon and then press to display the Time Page.
4. Use the **THUMB STICK** to highlight the ‘Time Zone’ field then press to display the list of time zone options.
5. Highlight a time zone and then press the **THUMB STICK**.
6. The correct time is displayed at the bottom of the page.

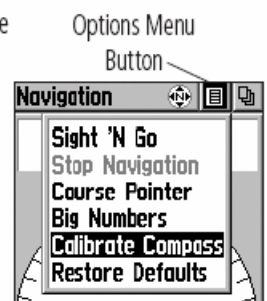


6 Calibrating the Compass

The eTrex Vista’s Electronic Compass must be calibrated (outdoors away from metal objects) whenever new batteries have been installed, and before using the unit for navigation.

To calibrate the compass:

1. Use the **PAGE** button to access the Navigation Page.
2. Use the **THUMB STICK** to highlight the Options Menu on-screen button and then press to display the menu.
3. Highlight the ‘Calibrate Compass’ option and then press the **THUMB STICK** to display the Calibration Page. The information screen explains: “To Calibrate Compass”, “Slowly Turn Two Full Circles In The Same Direction While Holding the Vista Level”.
4. Press the **THUMB STICK** to activate the ‘Start’ button. The screen will prompt you to “Turn Slowly”. Keep the unit level and begin to rotate it in your hand. A ‘Just Right’ message will display when you are turning at the proper rate. If you turn it too slowly or too rapidly, a “Too Slow” or “Too Fast” message appears.
5. When the “Calibration Successful” message appears, use the **THUMB STICK** to highlight the ‘OK’ button. If a “Calibration Failed” message appears, press the **THUMB STICK** to restart the calibration.



NOTE: The eTrex Vista must be held level during compass calibration and during use. The more the unit is tilted on either axis, the less accurate the compass readings will be.

Basic Navigation

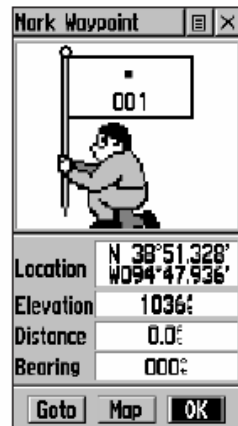
Basic Navigation

Starting to Navigate

Basic navigation with your eTrex Vista requires only three steps: mark, move, and return. Mark your location as a waypoint, move a distance away, and then return after choosing one of several methods to help you find your way.

To mark a waypoint:

1. Press in and hold the **THUMB STICK** for two seconds to display the Mark Waypoint Page. Your current location is marked as a waypoint and automatically assigned a three digit number.
2. The 'OK' button is highlighted so press the **THUMB STICK** to save the Waypoint.

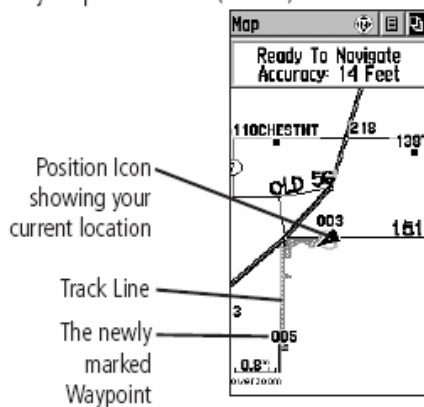


To return to a waypoint using Goto:

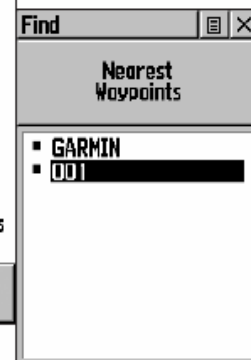
1. Press the **FIND** button to display the Find Menu.
2. Use the **THUMB STICK** to highlight 'Waypoints' and then press.
3. Use the **THUMB STICK** to highlight 'Nearest' and then press.
4. Use the **THUMB STICK** to highlight the waypoint and then press to display the Information Page.
5. With the on-screen 'Goto' button highlighted, press the **THUMB STICK** to activate the Goto navigation feature.

To move about with the Map Page:

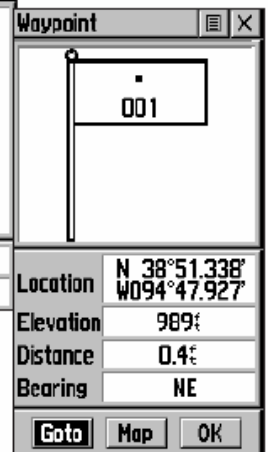
1. Use the **PAGE** button to access the Map Page and view the new waypoint.
Press the **ZOOM IN** button to get a more detailed view of the map.
2. Walk or drive around for a few minutes, make a right or left turn, then continue for a few more minutes and then stop.
The 'position icon' shows your location and the dotted line shows your path of travel (a Track).



Find Menu



Waypoints List



Waypoint Information Page

Basic Navigation

Basic Navigation

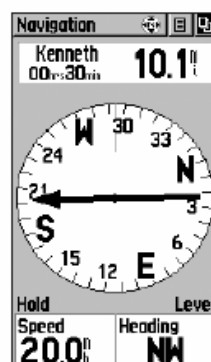
Returning to Waypoint with a Goto

To finish your return:

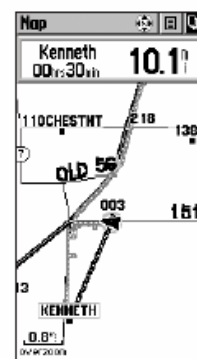
1. The Navigation Page displays the 'Bearing Pointer' indicating the direction to go. Because you can't always travel in a straight line, refer to the Bearing Pointer from time to time. When possible, turn in the direction the Bearing Pointer directs.
2. Use the **PAGE** button to move to the Map Page to see your location marked by the Position Icon and a straight dark line leading to the waypoint.

Move back and forth between the Map Page and the Navigation page to check your progress and verify your bearing.

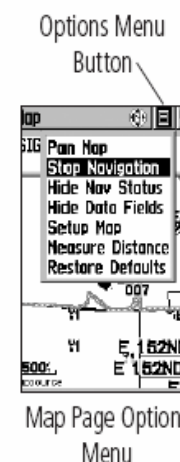
3. To stop navigating, highlight the Options Menu button on either page, press the **THUMB STICK**, select 'Stop Navigation', and then press the **THUMB STICK**.



A Goto on the Navigation Page



Map Page on a Goto



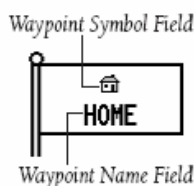
Map Page Options Menu

Changing the Waypoint Name or Symbol

You can personalize a Waypoint by changing the Name field and map Symbol field to make them easier to recognize.

To change the Waypoint symbol or name:

- Use the **THUMB STICK** to highlight the Waypoint symbol field and then press to display the symbol list. Use the **THUMB STICK** to move up and down the list to highlight a symbol and then press to place the symbol in the symbol field.
- Use the **THUMB STICK** to highlight the Waypoint name field and then press to display the keyboard. Use the **THUMB STICK** to highlight the desired characters and then press. Repeat the process until you are through, highlight 'OK', and then press the **THUMB STICK** to save the name and close the keyboard.



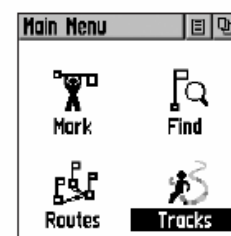
The Data Entry Keyboard

Clearing the Track Log and Elevation Plot

After you have navigated a few times over the same area, the map display may become difficult to read, cluttered by the recorded tracks. Clear the Track Log to clean the screen and clear the Elevation Plot of the Track Log shown on the Altimeter Page.

To clear the Track Log:

1. Use the **PAGE** button to access the Main Menu and highlight 'Tracks'.
2. Press the **THUMB STICK** to display the Tracks Page.
3. Use the **THUMB STICK** to highlight the 'Clear' button and then press to display the 'Yes/No' prompt.
4. Highlight 'Yes' and press the **THUMB STICK** to clear the Track Log and the Pressure or Elevation Plot.



Highlight 'Clear' and press the **THUMB STICK**.



Track Log Page